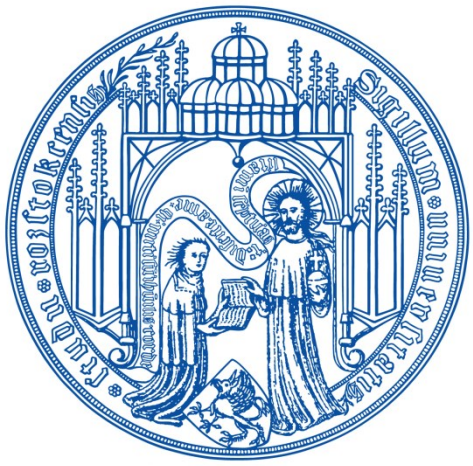

Carbon Dioxide as a C–1 Building Block in Monomers and Polymers

Dissertation

zur

Erlangung des akademischen Grades

– doctor rerum naturalium (Dr. rer. nat.) –

der Mathematisch-Naturwissenschaftlichen Fakultät

der Universität Rostock

vorgelegt von

Matthias Reckers

geb. am 03.03.1986 in Recklinghausen

aus Rostock

Rostock, 03.05.2016

urn:nbn:de:gbv:28-diss2017-0169-5

Die vorliegende Arbeit wurde unter der Leitung von Herrn Dr. Thomas Werner in der Zeit von November 2011 bis Mai 2016 am Leibniz-Institut für Katalyse e.V. an der Universität Rostock angefertigt.

Tag der Einreichung: 03.05.2016

Tag der öffentlichen Verteidigung: 15.11.2016

Erster Gutachter: Prof. Dr. Matthias Beller
Leibniz-Institut für Katalyse e.V.
an der Universität Rostock

Zweiter Gutachter: Prof. Dr. Matthias Bauer
Fakultät für Naturwissenschaften
Universität Paderborn

Erklärung

Ich versichere hiermit des Eides, dass ich die vorliegende Arbeit selbständig und ohne fremde Hilfe verfasst habe, keine außer der den von mir angegebenen Hilfsmitteln und Quellen dazu verwendet habe und die den benutzten Werken inhaltlich und wörtlich entnommenen Stellen als solche kenntlich gemacht habe.

Diese Dissertation wurde bisher an keiner anderen Hochschule oder Universität vorgelegt.

Matthias Reckers

Rostock, den 03.05.2016

“The country which is in advance of the rest of the world in chemistry will also be foremost in wealth and in general prosperity.”

— William Ramsay (*1852 – † 1916)

TABLE OF CONTENTS

LIST OF FIGURES

LIST OF SCHEMES

LIST OF TABLES

ABBREVIATIONS

Ac	acetyl
Alk	alkyl
aq	aqueous
Ar	aryl
bp	boiling point
^{t}Bu	*tert*-butyl
°C	degree Celsius
c	concentration
calc	calculated
cat	catalyst
CCS	carbon capture and storage
CCU	carbon capture and utilization
CH	cyclohexane
CHO	cyclohexene oxide
CMP	coordinated microporous polymer
cocat	cocatalyst
δ	chemical shift
Đ	dispersity
d	doublet
DABCO	1,4-diazabicyclo[2.2.2]octane
DEG	diglycidyl ether
DEPT	distortionless enhancement by polarization transfer
dest	distilled
DMAP	4-dimethylaminopyridine
DMF	dimethylformamide
DMSO	dimethylsulfoxide
DP	degree of polymerization
DSC	differential scanning calorimetry
E	electrophile
E_a	activation energy
EA	elemental analysis
EI	electron ionization
equiv	equivalent
ESI	electrospray ionization
Et	ethyl
Et_2O	diethyl ether
EtOAc	ethyl acetate
FA	formaldehyde
FID	flame ionization detector
FLP	frustrated *Lewis* pair
FPS	frames per second
FT	fourier transformation
g	gram
GC	gas chromatography
GHE	greenhouse effect
GHG	greenhouse gas
GPC	gel permeation chromatography
h	hour
H	enthalpy
HMI	4(5)-(hydroxymethyl) imidazole
HPPO	hydrogen peroxide propylene oxide

HRMS	high-resolution mass spectrometry
Hz	hertz
IL	ionic liquid
IPR	1,3-bis(2,6-diisopropyl-phenyl)imidazolium
IR	infrared
J	coupling constant
λ	wavelength
LCA	life cycle assessment
m	multiplet; meter
M	molecular weight
MALDI	matrix assisted laser desorption ionization
Me	methyl
MeCN	acetonitrile
MEK	methyl ethyl ketone
MHz	megahertz
min	minute
M_n	number average molecular weight
mol%	mole fraction
MS	mass spectrometry
M_w	weight average molecular weight
m/z	mass to charge ratio
ND	not determined
NHC	*N*-heterocyclic carbene
NIPU	non-isocyanate polyurethane
NMI	*N*-methyl-imidazole
NMP	*N*-methyl-2-pyrrolidone
NMR	nuclear magnetic resonance
Nu	nucleophile
p	pressure
PEG	polyethylene glycol
PFA	paraformaldehyde
PPG	polypropylene glycol
Ph	phenyl
PHU	poly(hydroxyurethane)
PIR	polyisocyanurate
POM	polyoxymethylene
ppm	part(s) per million
^{i}Pr	*iso*-propyl
PTSA	*p*-toluenesulfonic acid
PU	polyurethane
q	quartet
R_f	retention factor
s	singlet
SiO_2	silica gel
t	time
t	triplet
T	temperature
TBAB	tetrabutylammonium bromide
TBAC	tetrabutylammonium chloride
TBAI	tetrabutylammonium iodide
T_d	decomposition temperature
TEA	triethanol amine
T_g	glass transition temperature
TGA	thermogravimetric analysis
THF	tetrahydrofuran
TLC	thin-layer chromatography
T_m	melting point

1 INTRODUCTION

Since the beginning of industrialization the consumption of energy and resources has rapidly increased.[1] In particular, nonrenewable resources like the hydrocarbon energy carrier coal, gas and oil were needed to fill these demands.[2] As a consequence, the CO_2 level in the atmosphere has risen significantly.[3] Due to the fact that carbon dioxide absorbs and emits radiation within the thermal infrared range, it is today a main cause of the greenhouse effect (GHE).[4] For this reason, there is a urgent need to reduce the accumulation of CO_2 in the atmosphere.[5]

Therefore, the impact of CO_2 emissions on global warming and the various CO_2 management strategies are topics of current social, political as well as scientific discussions.[6] With **c**arbon **c**apture and **u**tilization (CCU) there is a reconsideration of the frequently discussed **c**arbon **c**apture and **s**torage (CCS) strategy, regarding CO_2 rather as an economical and abundant raw material than as waste.[7] This combination of a strategy that contributes to climate change mitigation and at the same time turns waste CO_2 emissions into products such as chemicals and fuels attracted worldwide attention. One of the great advantages of CCU compared to CCS is that the utilization of CO_2 is normally a profitable activity as products can be sold, which in turn makes it highly attractive for the chemical industry. Subsequently, the conversion of the CO_2 into value added products is widely studied in current academic and industrial research with the ambitious goal of a sustainable chemical economy.[8]

Nonetheless, one of the biggest obstacles for scientists is still the inherent thermodynamic stability of CO_2.[9] In fact, CO_2 is the highest oxidized form of carbon and therefore relatively inert. Consequently, it needs to be activated to make a utilization possible. This activation can be achieved by finding suitable additional substances which lower the required energy for the chemical reaction. These substances, if used in sub stoichiometric amounts and not consumed during the reaction, are called catalysts.[10] The utilization of catalysts is generally a further improvement of a reaction to more sustainability since it often reduces the amount of generated waste and needed energy.[11] Resembling nature, the research area of CO_2 conversion catalysis is dominated by the use of heterogeneous or homogeneous transition metal-based catalysts.[12] A

relatively young research area in organic chemistry and in the field of CO_2 utilization is the organocatalysis. Here, catalysts consisting exclusively of nonmetal elements are employed. Although, it has been shown that the activation of substrates through metal complexes are more efficient compared with organo-based catalytic mediators the organocatalysis offers several advantages.[13] For instance, they are generally inexpensive and non-toxic molecules, which inherent a good stability and inertness towards moisture and air.[14] Especially from an environmental point of view, they can be regarded as a greener and desirable catalyst class. In this respect, organo-based catalysts are of growing interest and importance in the area of CO_2 catalysis and conversion developing "carbon-neutral" processes to produce sustainable chemicals, fuels and materials.[15]

Significant classes of organocatalysts for the conversion of CO_2, are *N*-heterocyclic bases,[16] *N*-heterocyclic carbenes,[17] organic salts,[18] ionic liquids[19] and phenolic compounds.[20] In particular, the catalyzed synthesis of cyclic carbonates and the incorporation of CO_2 into polymeric materials are the focus of recent developments.[21] In fact, one of the more successful processes for CO_2 utilization for material synthesis is the catalytic production of cyclic carbonates.[22] They are used as electrolytes in batteries, polar aprotic solvents, as reactive intermediates for the synthesis of fine chemicals and as prepolymers.[23] The application as prepolymers is especially appealing, since they are used as a substitute for the toxic isocyanate compound in the conventional polyurethane production to form non-isocyanate polyurethanes.[24]

A scarcely researched area is the catalyzed polymerization of CO_2 and formaldehyde to form polycarbonates. Since this reaction would allow polymers derived solely from renewable resources with a high CO_2 content of up to 60% it can be regarded as a "Dream Polymer".[25]

In this context, this work is a good example for the interest of politics, industry and academics in this topic, since it was mainly enabled by the initiative "Technologies for Sustainability and Climate Protection – Chemical Processes and Use of CO_2" of the German government. The goal of this program is to bring these different partners together and combine the diverse excellences for the main goal of a sustainable chemical industry leading to a more sustainable society.[26]

2 FUNDAMENTALS

2.1 Properties of Carbon Dioxide

Carbon dioxide has two strong vibrational bands in the IR spectrum at 2349 cm^{-1} and 667 cm^{-1}. Because it absorbs and subsequently emits IR radiation in the atmosphere it causes global warming. Therefore, it is considered as a greenhouse gas (GHG) (Figure 1).[4a, 27]

Under atmospheric pressure CO_2 appears as a gaseous form and sublimates at –78.5 °C or below. The triple point occurs at 216.6 K at a pressure of 5.2 bar.[28] Only above this pressure can the liquid form of CO_2 be observed. A supercritical fluid occurs at 304.1 K and 73.8 bar.[29]

As stated, CO_2 is the highest oxidized form of carbon and therefore a stable and inert compound. In fact, the standard enthalpy of formation is with –394 $KJ \cdot mol^{-1}$ strongly negative.[30] Additionally, reactions are often endergonic.[31] This relatively inertness of CO_2 is the main reason why the utilization of carbon dioxide is a challenging task. Especially the activation of carbon dioxide is a crucial part to overcome the activation energy (E_a) and to enable the utilization as a C–1 building block.

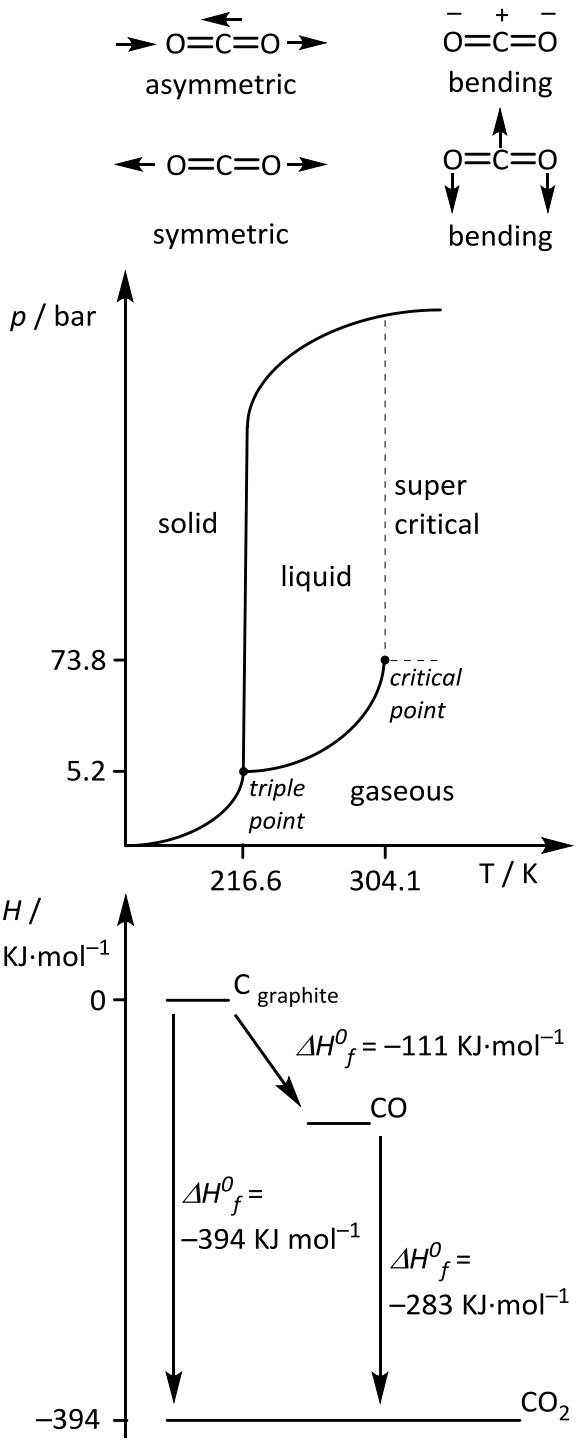

Figure 1. Vibrational bands of CO_2 (top); phase diagram (middle); enthalpy diagram (bottom).

2.2 Activation of Carbon Dioxide

Carbon dioxide is thermodynamically and kinetically stable. Nonetheless, due to the high electron deficiency of the carbon atom it can be seen as an electrophilic reagent. Therefore, it reacts with basic compounds or in general with nucleophilic compounds (Scheme 1).

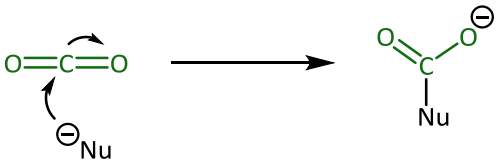

Scheme 1. Nucleophilic attack on CO_2.

In fact, reactions with CO_2 often take place by formation of a carboxyl group through nucleophilic attack or the building of cyclic compounds through cycloaddition. The activation of CO_2 and / or the substrates can be accomplished by using metal or non-metal catalysts.[32] Here, the catalyst reduces the activation energy (E_a) to reach the transition state, thereby enabling or enhancing the reaction. In an idealized process for the chemical transformation of CO_2 it can be divided into two possible reaction ways. First, the conversion of CO_2 in an exothermic reaction. The driving forces of these reactions are high energy reactants (e.g. epoxides) which lead to low energy products (Figure 2, left). Second, are endothermic reactions using reactants which are lower in the energy level leading to high energy products (Figure 2, right). For endothermic reactions, energy needs to be provided in the form of heat, light or electricity.[32-33]

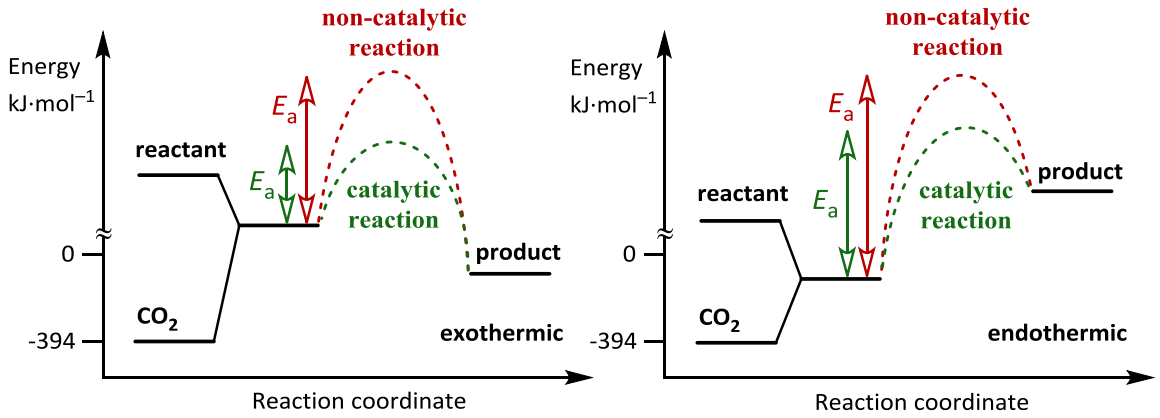

Figure 2. Catalytic and non-catalytic reaction of CO_2 (exothermic, left; endothermic, right).[32-33]

In general, the overall energy of the process has to be carefully taken into account to develop a sustainable process. This is due to the fact, that even for exothermic reactions of CO_2 the transformations are often endergonic.[7a]

2.3 Utilization of Carbon Dioxide

The utilization of CO_2 as a green carbonyl source is already well known and established through several reactions in academics and industries (Figure 3).[7a, 32, 34] They can be categorized by the formed products. Examples are reactions with amines and CO_2 to form carbamates **1**,[35] formamides **2**,[7a] isocyanates **3**,[36] oxazolidinones **4**[37] and polyurethanes **5**.[38] Moreover, the synthesis of carboxylic acids like formic acid (**6**),[39] acetic acid (**7**),[40] naphtoic acid (**8**) and salicylic acid (**15**) is possible.[41]

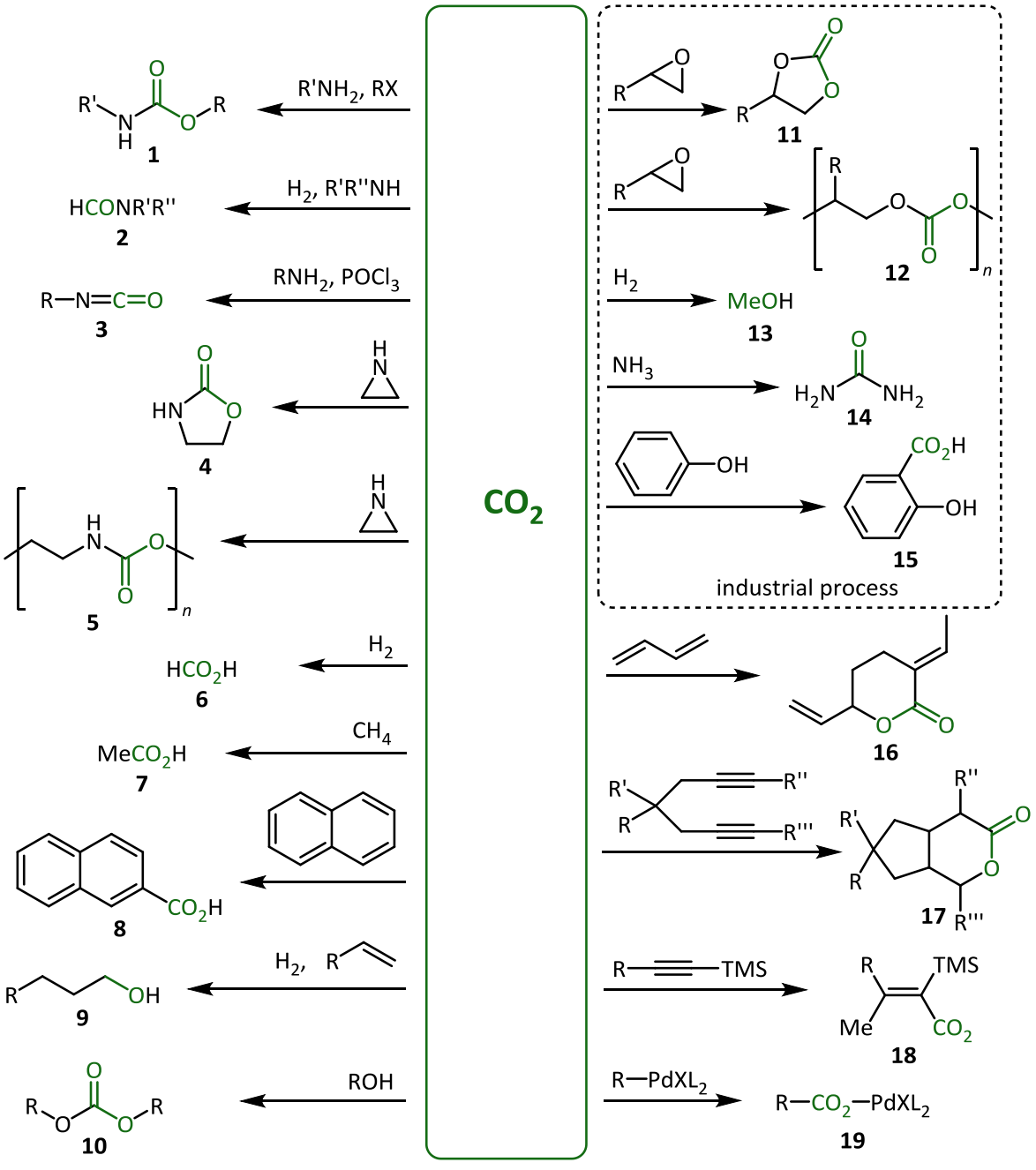

Figure 3. Selection of reactions using CO_2 as a C–1 building block.[7a, 32, 34]

The formation of methanol (**13**) by direct hydrogenation[42] of CO_2 and the formation of alcohols with longer chains **9** derived from alkenes are reported.[43] Also the reaction with alcohols to form carbonate ester **10** is possible.[7a] Additionally, carbonylation reactions of alkenes and alkynes to form **16**–**18** are known.[44] Furthermore, the formation of metal complexes **19** were reported.[32, 45] Due to the promise of high profitable products by utilizing CO_2 as a nontoxic, nonflammable, sustainable, abundant and inexpensive resource, a few compounds are already industrialized. The chemicals produced on an industrial scale are mainly cyclic carbonates **11**, polycarbonates **12**, methanol (**13**), urea (**14**) and salicylic acid (**15**). Namely, small molecules like urea (**14**) which is used as fertilizer (184 mio. $t \cdot a^{-1}$)[46] and methanol (**13**)[47] as replacement for fossil fuels have currently the highest market share. Nevertheless, there is an emerging demand for eco-friendly produced cyclic carbonates **11** and polycarbonates **12**. As mentioned before, are cyclic carbonates **11** used as electrolytes in batteries, as polar aprotic solvents and as reactive intermediates for the syntheses of fine chemicals **20**–**27** and polymers **28** and **29** (Figure 4).[23] Of particular interest is also the use of polyfunctional cyclic carbonates as precursors for polymers to obtain isocyanate-free polyurethanes.[48]

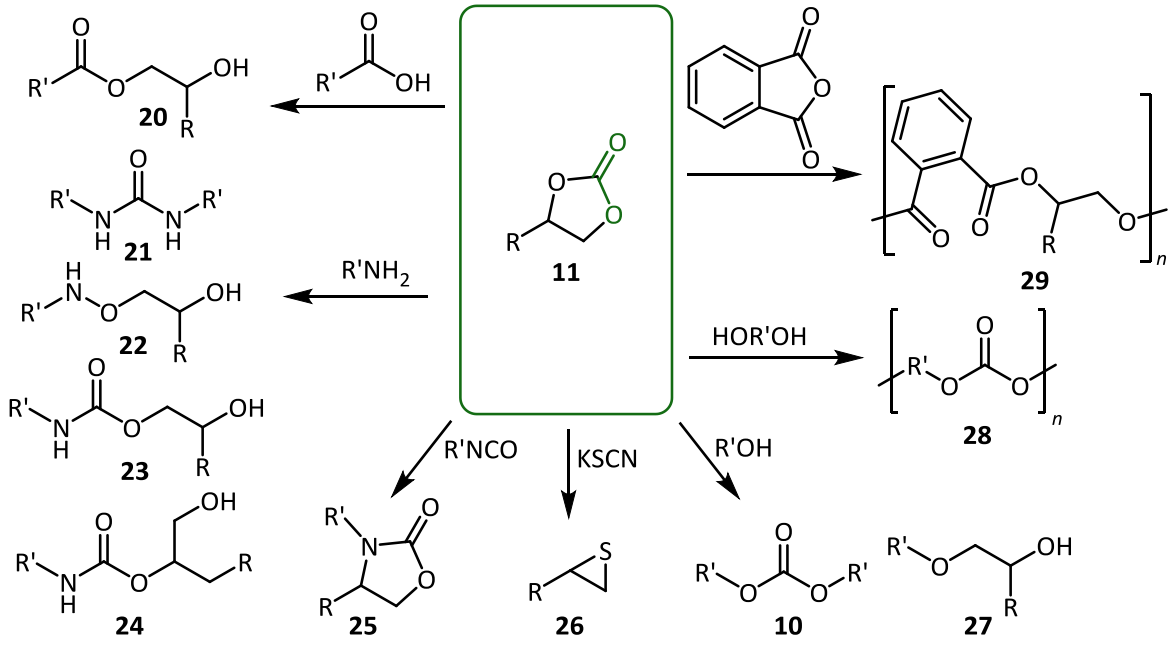

Figure 4. Examples of reactions using cyclic carbonates **11**.[23]

In addition, various applications for polycarbonates **12** can be found. They are used as an alternative for glass and other construction materials, as materials for compact discs and several optical media, in the automotive industry, for medical equipment and for numerous niche applications.[49]

2.3.1 Cyclic Carbonates

Recently, cyclic carbonates **11** are in focus of academic research due to their unique physical and toxicological properties as solvents, electrolytes[50] and as starting compound for the synthesis of fine chemicals.[51] Especially, the employment of organic carbonates like propylene carbonate or butylene carbonate offers various benefits, since they display some outstanding properties as solvents. In addition to their high solvency, they inherent a negligible vapor pressure, show excellent thermal and chemical stabilities, are odorless and display low toxicity.[21, 32, 52] The synthesis of cyclic carbonates **11** as well as polycarbonates **12** can be obtained by applying the "phosgene process" (Scheme 2).[53] As the term indicates, phosgene (**30**) is used as a C–1 building block in a reaction with diols **31**. Since phosgene (**30**) is known to be highly toxic and was even used as a chemical weapon in World War I, this reaction needs to be carried out under high safety regulations.[54] From an ecological and economical point of view it is highly advantageous to substitute this reaction component.

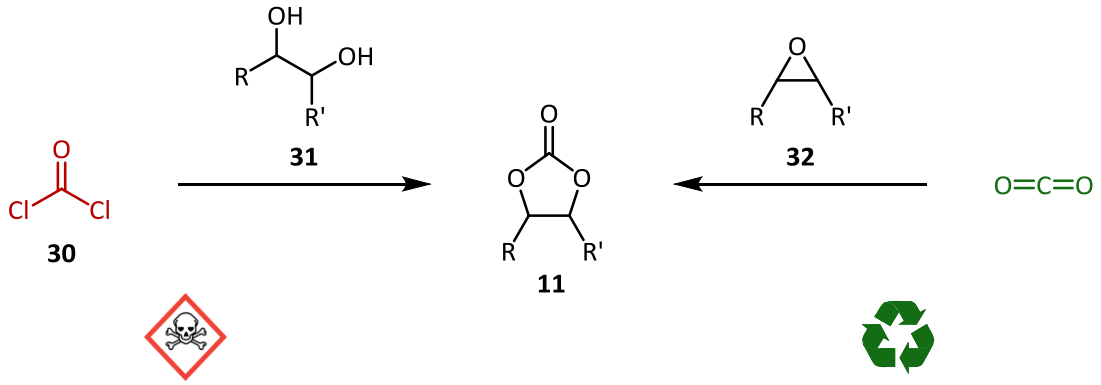

Scheme 2. Synthesis of cyclic carbonates **11** using phosgene (**30**) or CO_2 as a C–1 source.

In this context, the synthesis of cyclic carbonates **11** is a paradigm for the implementation of green chemistry as a main idea of finding sustainable reaction routes.[55] In fact, one possible way to substitute phosgene (**30**) is the use of carbon dioxide as a C–1 building block (Scheme 2). In other words, a highly toxic gas can be replaced by a hazard free and abundant gas. Here, CO_2 as a relatively inert compound reacts with epoxides as a highly energetic compound to produce cyclic carbonates **11**. In addition to the substitution of phosgene (**30**), the cycloaddition of CO_2 and epoxides **32** is also one hundred percent atom economic.[56] To enable this reaction different types of catalysts are employed.[57]

2.3.1.1 Catalyst Design & Mechanism

The catalytic reactions of CO_2 to cyclic carbonates **11** can be separated by the possible ways of activation (Scheme 3). One way is the direct activation of CO_2 by the catalyst. Another way is the activation of a high energy reactant like an epoxide **32**. Furthermore, it is also possible that both activation modes are taking place simultaneously.[13]

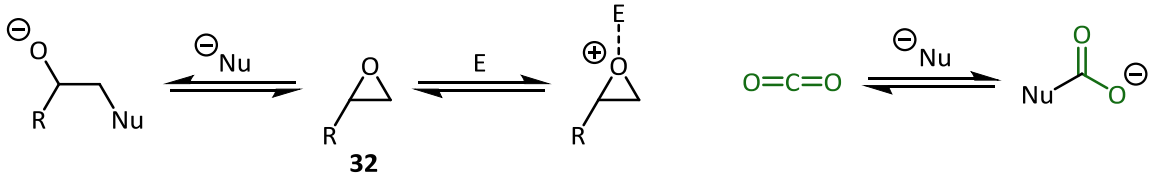

Scheme 3. Possible activations of epoxides **32** and carbon dioxide.

For the reaction of epoxides **32** to cyclic carbonates **11**, the activation of the high energetic epoxide is often described (Scheme 4).[58] For this reaction path, a few general properties of the used catalyst can be determined. First, the catalyst needs to provide a *Lewis* or *Brønsted* acid (E) which activates the epoxide **32**.[9a, 59] Second, it has to provide a good nucleophile (Nu) to open the epoxide **32**. Third, the nucleophile needs to be at the same time a good leaving group. This is due to the fact that with the forming of the five membered ring, the nucleophile has to leave the alkoxide and thereby regenerates the catalyst.[60]

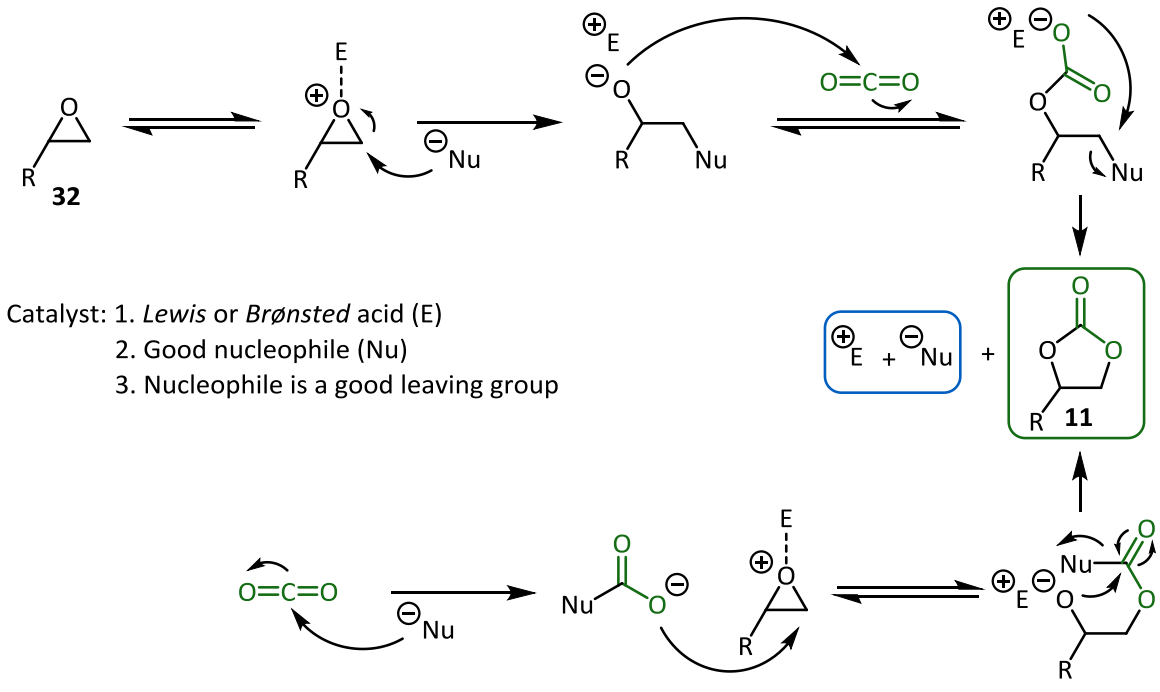

Scheme 4. Possible mechanism for the synthesis of cyclic carbonates **11**.

A lot of research on the catalyst design and on the reaction mechanism for the conversion of epoxides **32** to cyclic carbonates **11** has been done in the last decade (Chapter 2.3.1.2 and 2.3.1.2). As a result, highly active catalysts emerged from these efforts. The most important catalysts can be subdivided into non-metallic and metallic compounds. It is possible to further distinguish the metal based catalysts by the group of the periodic table they belong to. There are catalysts using elements from the alkali group, alkaline earth group, boron group and from transition metal groups (Figure 5).

As organocatalysts, nitrogen based heterocycles like organic bases and *N*-heterocyclic carbenes (NHCs) can be used. Also organic salts and ionic liquids (ILs)[61] are known to catalyze this reaction. Finally, polyphenolic and polyalcoholic compounds show catalytic activity in the synthesis of cyclic carbonates **11**.

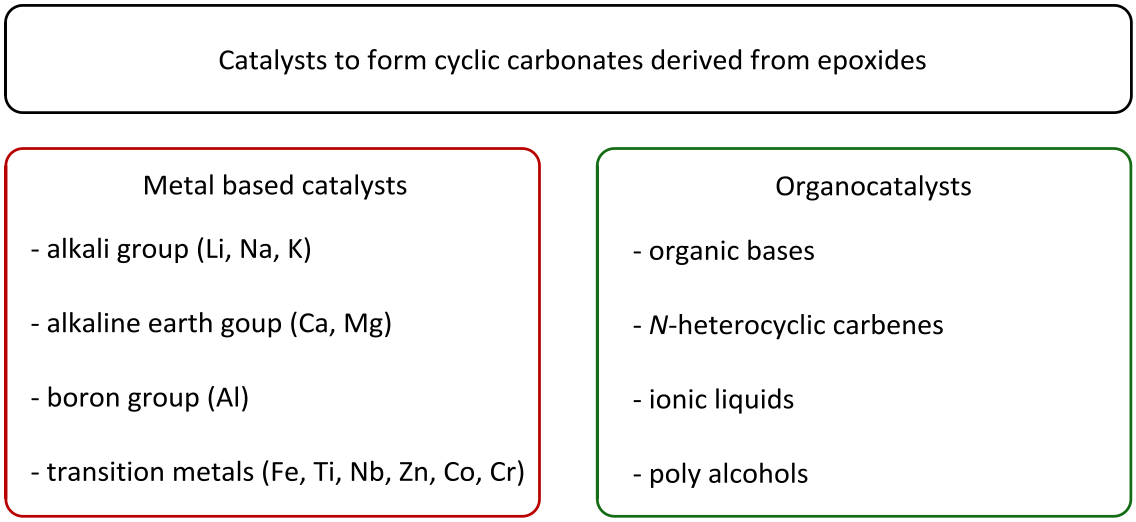

Figure 5. Overview of important classes of catalysts for the synthesis of cyclic carbonates **11**.

Furthermore, a lot of synergistic effects of combinations of the different classes are recently discussed and reported.[12a] One example is the use of metal complexes in combination with ionic liquids. Here, high activities were observed. Recent examples employ hydrogen bond-promoted ionic liquids which show good activity due the functional groups of the cations and anions (Chapter 2.3.1.2.1 and 2.3.1.2.2). Furthermore, supported ionic liquids show synergistic effects of functional groups (in cations or supports) and the anions.[56] The different catalyst classes and structure activity relations are described more detailed in the following chapters.

2.3.1.2 Metal Catalysts

There are various metal complexes which catalyze the reaction of epoxides **11** to cyclic carbonates **32**. The high activity of the complexes is due to the strong *Lewis* acidity of the metal.[62] However, to reach high conversions the employment of a cocatalyst is indispensable.[63] The reaction is often sensitive to air and moisture[64] and the syntheses of the complexes and the ligands need some effort beforehand.[65] Furthermore, the use of metals somehow contradicts the idea of a most possible green and sustainable reaction to utilize CO_2 as an ecologically benign C–1 source. If metals are used it should be limited to the employment of abundant metals which are not listed as endangered elements.[66] Since this work mainly focuses on an organocatalytic approach only a few representative catalysts are introduced and discussed. Examples for catalysts using non endangered elements are mainly Al, Fe, Ti, Na, K and Ca salts and complexes. Already 1978, an aluminum porphyrin complex **33** solved in *N*-methyl-imidazole (NMI, **37**) was shown to convert propylene oxide (PO, **32a**) to the cyclic carbonate **11a** in low yields (Table 1, entry 1).[67] More recently, *Kleij et al.* developed a catalyst system using Iron complex **34** in combination with tetrabutylammonium iodide (TBAI, **38a**).[68] However, conversion of the epoxide **32a** was only observed in combination with high amounts of the cocatalyst (Table 1, entries 2 and 3). The group of *North et al.* employed a bimetallic aluminum complex **35** in combination with tetrabutylammonium bromide (TBAB, **38b**) and obtained high yields of PO **32a** (Table 1, entry 4).[69]

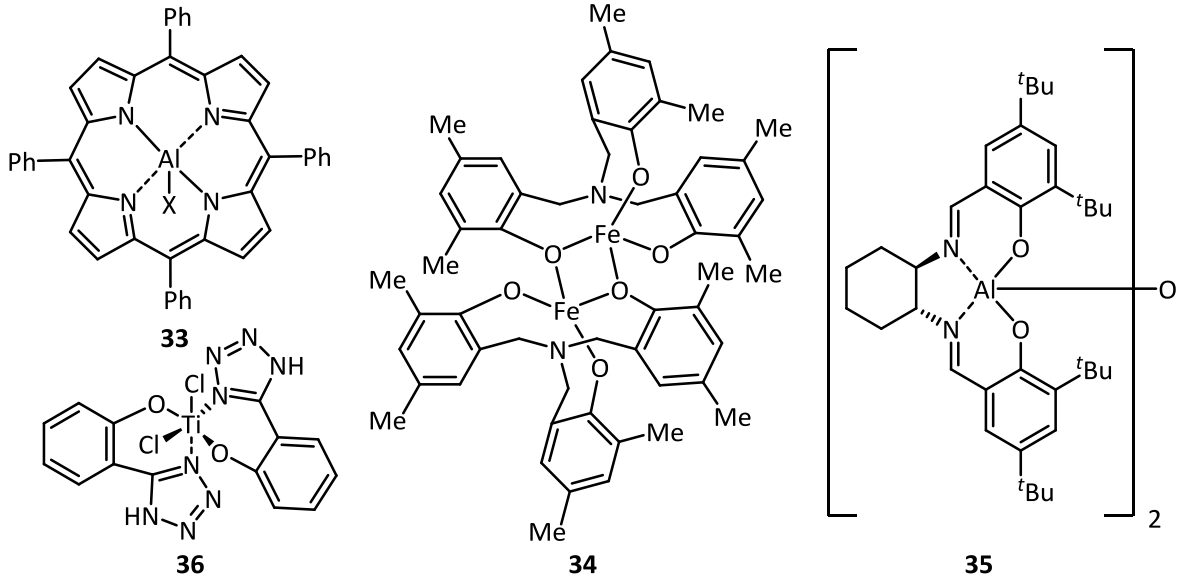

Figure 6. Selected metal catalysts **33**–**36** for the synthesis of cyclic carbonates **11**.[67-70]

Additionally, *Go et al.* reported the high activity of the titanium bis-tetrazole complex **36** and TBAI **38a** for the conversion of PO **32a** (Table 1, entry 5).[70]

Table 1. Reported conversion of PO **32a** using selected metal complexes.[67-70]

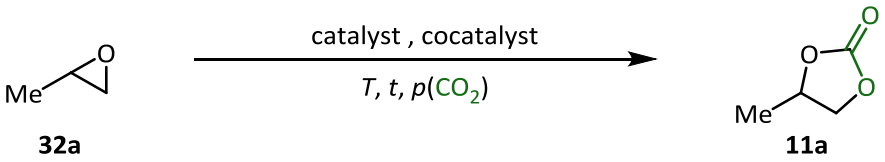

32a **11a**

Entry	Cat.	mol%	Cocat.		mol%	T / °C	$p(CO_2)$ / bar	t / h	Yield / %
1[67]	**33**	5.0	NMI	**37**	8.0	25	1	96	39
2[68]	**34**	0.5	TBAI	**38a**	5.0	25	2	18	74[a,b]
3[68]	**34**	1.25	-	-	-	45	10	18	0[a,b]
4[69]	**35**	2.5	TBAB	**38b**	2.5	26	1	3	62[a]
5[70]	**36**	0.1	TBAI	**38a**	0.1	75	22	4.5	86[a]

[a] Determined by ^{1}H NMR. [b] 5 mL NMP.

As mentioned, are alkali and alkaline earth metals also catalytic active for the conversion of epoxides **32** to the corresponding cyclic carbonates **11**. Since they are non-toxic, highly available and also inexpensive, they are highly attractive for the utilization as catalysts. Nonetheless, high conversions are only obtained by adding salts as cocatalysts.[71]

2.3.1.2.1 Potassium Iodide and Functionalized Cocatalysts

For the alkali and alkaline earth metals, potassium iodide (KI, **40**) shows the highest activity. Typically, conversions of over 90% within 4 h can be reached using cocatalyst and harsh reaction conditions.[60, 72] Interestingly, the group of *Werner et al.* used as two component catalyst systems triethanol amine (TEA, **39**) with KI **40** and 4(5)-(Hydroxy-methyl)imidazole (HMI, **41**) with KI **40**. Excellent yields of 97%–98% of **32a** were reached using 2 mol% of the catalysts, at 90 °C, 10 bar CO_2 pressure and a reaction time of 3 h.

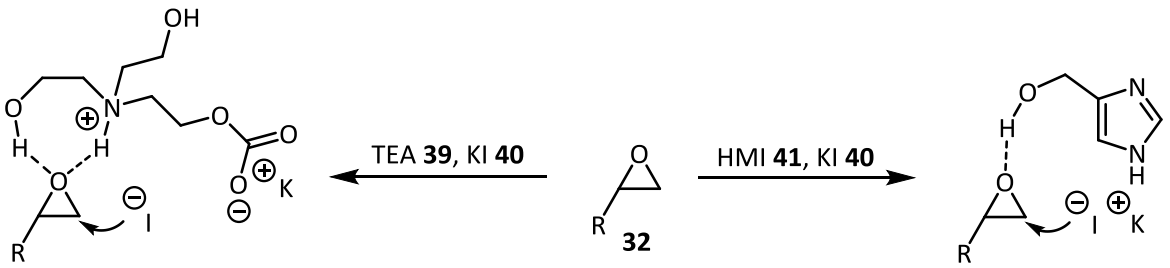

Figure 7. Proposed activation of epoxides **32** via hydrogen bonding.[73]

The high catalytic activity is explained by the hydroxyl groups of TEA **39** and HMI **41**. It is proposed that they activate the epoxide **32** by hydrogen bond building and thereby enhancing the nucleophilic attack of the halogen (Figure 7).[73] Several organic cocatalysts are known to enhance the catalytic activity for the conversion of epoxides **32**.[13] As a result, it was discovered that a good motif for potential catalysts and cocatalysts are functional groups with the ability to form hydrogen bonds.[74] In particular, the use of cocatalysts containing hydroxyl groups showed high conversions.[63a] *Han et al.* used density functional theory modelling to quantify the lowering of the reaction barrier using hydroxyl containing cocatalysts.[75] The calculations showed that the reaction pathway is not altered but that the hydroxyl groups participate in the cycloaddition through intermolecular hydrogen bonds. Exemplarily, it was shown that the energy barrier of the epoxide ring opening step was lowered significantly by the use of glycerol as a cocatalyst. As a result, they confirmed with their calculations that the use of hydroxyl containing coatalysts have positive effects on the catalytic activity.

2.3.1.3 Metal Free Catalysts

As previously shown (Chapter 2.3.1.2) are halogen salts used as cocatalysts in combination with metal complexes (Table 1). In fact, they also show catalytic activity without the metal catalysts. Consequently, catalysts for the synthesis of cyclic carbonates based on non-metallic substances are already utilized.[76] As mentioned, nitrogen based heterocycles, NHCs, organic salts, ILs and alcohols can be employed.[13]

The focus will be especially on mono- and bifunctional ionic liquids and related catalysts. Particularly ammonium- and phosphonium salts show good catalytic activity. Often described examples are the utilization of tetrabutylammonium and tetra-butylphosphonium halides. Indeed, they are frequently used as benchmark catalysts and were applied under several reaction conditions (Table 2). One example is the utilization of TBAB **38b** for the conversion of ethylene oxide (**32b**) at 200 °C, 34 bar CO_2 pressure, using 1 mol% TBAB **38b** and obtaining a yield of 97% after only half an hour (Table 2, entry 1).[77] Other examples are the conversion of PO **32a** by *Wang et al.* using 1 mol% TBAB **38b** and tetrabutylammonium chloride (TBAC, **38c**) at 100 °C for 2 h and obtaining 56% and 72% of the carbonate (Table 2, entries 2 and 3).[57b] Furthermore, the group of *Werner et al.* tested also TBAI **38a** and the homologous phosphonium salts **42a**–**42c**

(Table 2, entries 4–7).[78] They noted that the yield increased from I^- < Br^- < Cl^- in accordance to the nucleophilicity.[79]

Table 2. Reported conversions of epoxides **32a** and **32b** using different organic salts.

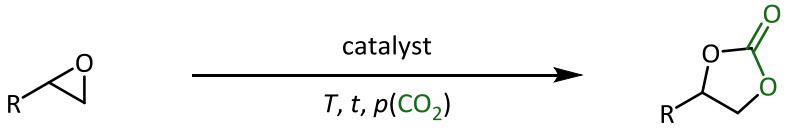

32a, R = Me
32b, R = H

11a, R = Me
11b, R = H

Entry	Reactant	Catalyst		mol%	T / °C	$p(CO_2)$ / bar	t / h	Yield / %[a]
1[77]	**32a**	$[Bu_4N]Br$	**38b**	1	200	34	0.5	97
2[57b]	**32b**	$[Bu_4N]Br$	**38b**	1	100	30	2	56
3[57b]	**32b**	$[Bu_4N]Cl$	**38c**	1	100	30	2	72
4[78]	**32b**	$[Bu_4N]I$	**38a**	2	90	10	2	19
5[78]	**32b**	$[Bu_4P]I$	**42a**	2	90	10	2	19
6[78]	**32b**	$[Bu_4P]Br$	**42b**	2	90	10	2	25
7[78]	**32b**	$[Bu_4P]Cl$	**42c**	2	90	10	2	36

[a] Determined by GC.

2.3.1.3.1 Organocatalytic Bifunctional One Component Catalysts

The concept to improve the catalytic activity by using hydrogen bond donating cocatalysts was used for the organocatalytic conversion of epoxides **32** to the corresponding carbonates **11**. Especially interesting is the concept to avoid the need of a cocatalyst and instead directly employ a hydroxyl functionalized catalyst as a one component system.

Reported examples are often conducted under different reaction conditions which made comparisons difficult. One group applied an ammonium salt **43** with an acid group and reached a yield of >95% **11a** (Table 3, entry 1).[74c] In another report, the group of *Sun et al.* employed functionalized imidazolium salts which showed higher activity due to a hydroxyl group (Table 3, entry 2).[80] As a result, the bromide salt **44** led to a conversion of 90%. The same group also used the hydroxyl functionalized ammonium bromide salt **45b** which showed high catalytic activity (Table 3, entry 3). The group of *Werner et al.* did additional research on these ammonium **45** and analog phosphonium salts **46** as bifunctional organocatalysts and observed high catalytic activity. As a result, the synthesized bifunctional ammonium[78] and phosphonium[79] salts and ILs[80] showed superior activities compared to their monofunctional analogs (Table 3, entries 4 and 5).

Table 3. Reported conversions of epoxide **32a** using bifunctional organocatalysts **43**–**46**.

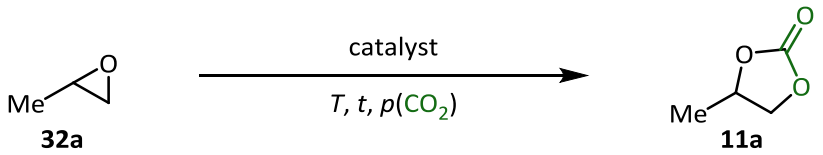

Entry	Catalyst		mol%	*T* / °C	*p*(CO_2) / bar	*t* / h	Yield / %[a]
1[74c]	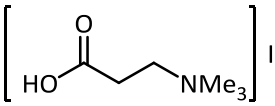	**43**	2.5	140	80	8	95
2[80]	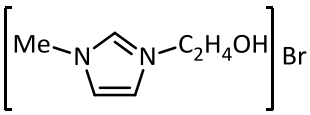	**44**	1.6	125	7	1	90
3[80]	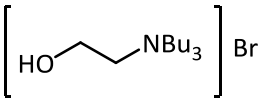	**45b**	3.2	125	7	1	96
4[78]	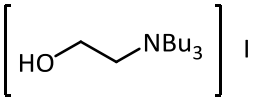	**45a**	2	90	10	2	96
5[79]	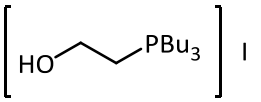	**46a**	2	90	10	2	95

[a] Determined by GC.

The mechanism is proposed to take place in three steps.[74d, 78, 81] The energy barrier of the epoxide ring opening step is lowered by hydrogen bonding of the catalyst **46**. The halide attacks the epoxide **32** and opens the ring to form the stabilized alkoxide **47**. The CO_2 is attacked by the alkoxide to form **48** and finally an intramolecular substitution reaction leads to the cyclic carbonate **11** and regenerates the catalyst **46** (Figure 8).

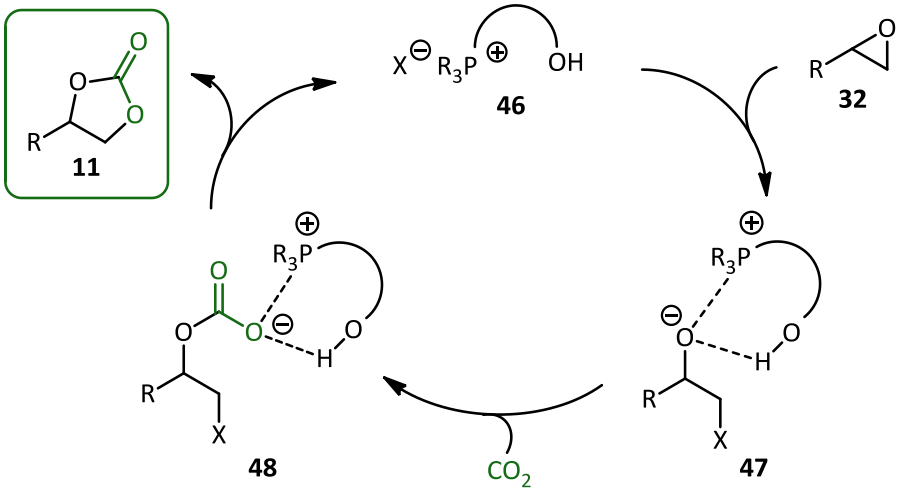

Figure 8. Proposed mechanism using a bifunctional organocatalysts **46**.[78]

2.3.2 Polyfunctional Cyclic Carbonates

The synthesis of polyfunctional cyclic carbonates is interesting, because they can be used as reactants for the synthesis of isocyanate free polyurethanes. Surprisingly, most studies have focused on the conversion of monofunctional terminal epoxides **32** to form cyclic carbonates **11**. As a consequence, research on the reaction of epoxides containing two or more epoxide moieties is limited. However, there are some examples using mostly metal catalysts to convert these reactants.

Table 4. Selected conversions of bisepoxides **49** to cyclic carbonates **50**.

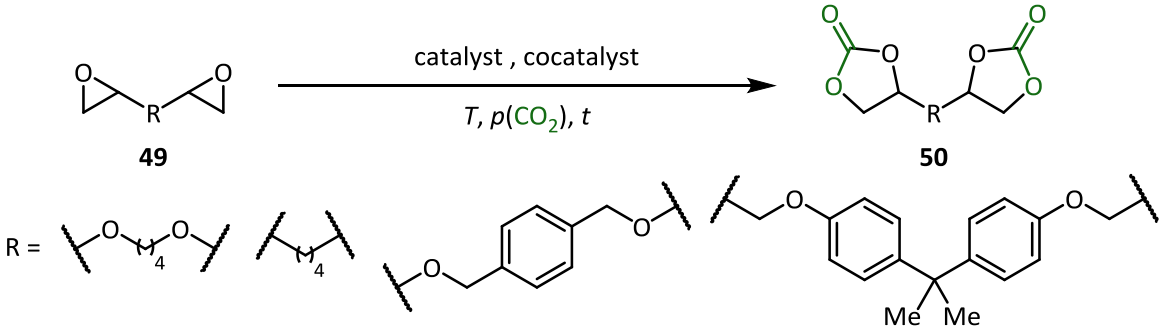

49 **50**

49a or **50a** **49b** or **50b** **49c** or **50c** **49d** or **50d**

Entry	Product	Catalyst		mol%	T / °C	$p(CO_2)$ / bar	t / h	Yield / %
1[82]	**49a**	NaI PPh_3	**51** **52**	1.2 1.6	100	1	72	74
2[83]	**49b**	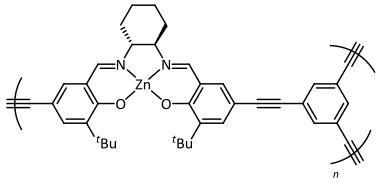	**53**	0.2	120	30	1	93
		$[Bu_4N]Br$	**38b**	3.6				
3[84]	**49b**	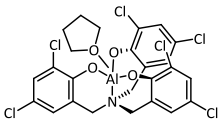	**54**	0.05	70	10	18	73
		$[Bu_4N]I$	**38a**	0.25				
4[85]	**49b**	LiBr	**55**	5.0	100	1	30	65[a]
5[82]	**49c**	NaI PPh_3	**51** **52**	1.2 1.6	100	1	72	59
6[82]	**49d**	NaI PPh_3	**51** **52**	1.2 1.6	100	1	72	75[b]
7[86]	**49d**	$[Cy_2H_2N]I$	**56**	5.0	45	1	48	99[c]

[a] 20 mL NMP. [b] 50 mL Diglyme. [c] 4 mL NMP.

One of the earliest studies in this field was conducted by the group of *Endo* and coworkers.[82] They converted several bisepoxides **49a–49d** using sodium iodide (**51**) / PPh_3 **52** and LiBr **55** at high temperatures. Additionally, long reaction times were needed and the cyclic carbonates **50a–50d** were obtained in moderate yields (Table 4, entries 1, 4, 5 and 6).[82, 85] A more recent example is the conversion of 1,4-di(oxiran-2-yl)butane (**49b**). The group of *Zou et al.* used a zinc-coordinated microporous polymer (**53**, Zn-CMP) in combination with TBAB **38b**, obtaining 93% of the desired product **49b** (Table 4, entry 2).[83] The group of *Kleij et al.* converted the same epoxide **49b** using an aluminum amino triphenolate complex **54** / TBAI **38a** system and obtained by full conversion a yield of 73% (Table 4, entry 3).[84] Here, the difference between conversion and yield can probably be explained by the formation of the monocarbonylated product, which was however not further explained by the author. In another study 2,2'-(((propane-2,2-diylbis(4,1-phenylene))bis(oxy))bis(methylene))bis (oxirane) (**49d**) was converted by *Endo* and coworkers. A yield of >99% was obtained using 5 mol% of an ammonium iodide salt containing two cyclohexyl moieties **56** (Table 4, entry 7).[86] The group of *Endo et al.* also converted a reactant with three epoxides **57**.[87] They used a high catalyst loading of 5 mol% LiBr (**55**) at 100 °C, atmospheric CO_2 pressure, in NMP and a reaction time of 5 h.

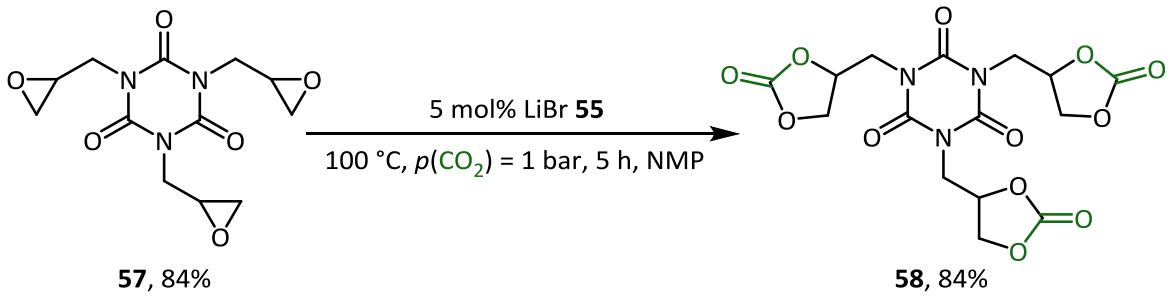

57, 84% **58**, 84%

Scheme 5. Reported conversion of the tricyclic epoxide **57**.[87]

Furthermore, *Wilkes* and coworkers converted the epoxidized soybean oil to the corresponding cyclic carbonate by using 5 mol% TBAB **38b** as a catalyst at 110 °C.[88] *Mülhaupt* converted limonene oxide, epoxidized soybean and linseed oil at 120–140 °C by employing silica supported 4-pyrrolidinopyridinium iodide / TBAB **38b** as a catalyst system.[89] Alternatively, *Zhang et al.* used a nanolamellar zinc-cobalt double metal cyanide complex (Zn-Co(III) DMCC) to convert bisepoxides **49**.[90] Additionally, they discovered that propylene carbonate (**11a**) was the best solvent for this reaction and therefore converted PO **32a** and several bisepoxides **49** at the same time. Conversions of

up to 82.9% of the bisepoxide **49** and 93.2% of the PO **32a** were observed using reaction temperature of 120 °C for 9 h at 5 bar CO_2 pressure. Also the group of *Wang et al.* converted a series of bisepoxides **49** using an Iron complex in combination with TBAB **38b**.[91] Good conversions were observed using 0.1 mol% of the catalysts and cocatalyst at 100 °C and a reaction time of 4 h.

According to recent literature, the complete conversion of polyfunctional epoxides **49** and **57** often required solvents, relatively long reaction times and in general harsh reaction conditions (Table 4). Additionally, often metal complexes in combination with a cocatalyst were needed. The used complexes and ligands often had to be synthesized with some efforts beforehand.

2.3.2.1 Stereochemistry

Additionally, it is to mention that the used bisepoxides **49** are normally available as a mixture of stereoisomers. This is further explained by the example of 2,2'-(((propane-2,2-diylbis (4,1-phenylene))bis(oxy))bis(methylene))bis(oxirane) (common name: bisphenol A diglycidyl ether) (**49d**) (Figure 9). The (*R,R*)-form and the (*S,S*)-form of the mixture are building a racemate. The (*R,S*) form can be seen as an achiral *meso* form. Subsequently, the obtained polyfunctional cyclic carbonates are also mixtures of stereoisomers.

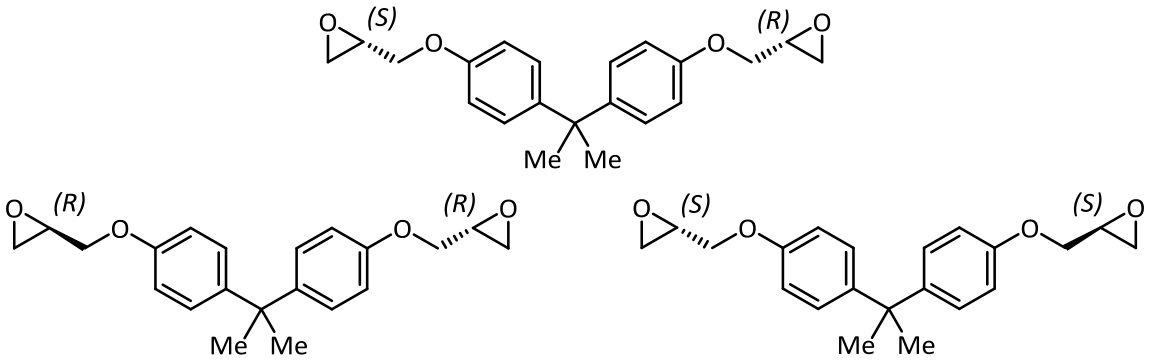

Figure 9. Stereochemistry of bisphenol A digylcidyl ether (**49d**).

In a following reaction the synthesized cyclic dicarbonates (**50**) were used as reactants in a polymerization reaction with amines. In fact, the importance of polyfunctional carbonates is due to this possible further use as polymerization reactants.[24, 92] Therefore, the polymerization of polyfunctional cyclic carbonates with polyfunctional amines to obtain isocyanate-free polyurethanes is currently a highly researched topic.[24]

2.3.3 Polyurethanes

2.3.3.1 Conventional Polyurethane Synthesis

Since the discovery of polyurethane (PU, **61**) of *Bayer* and his coworkers in 1937[93] it became one of the most important classes of polymeric materials.[94] Actually, PU polymers account for nearly 5% of the world wide polymer production and will presumably exceed 18 $kt \cdot a^{-1}$ in 2016.[95] Linear PUs **61** are generally prepared by the polyaddition reaction of diols **60** with diisocyanates **59** in the presence of a catalyst (Scheme 6).[96]

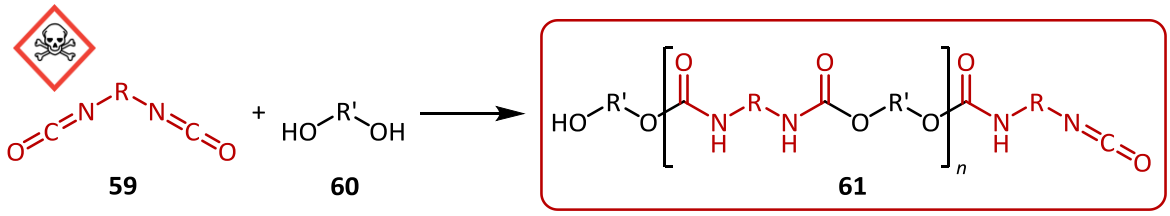

Scheme 6. Classic PU **61** synthesis.

The great success of these polymers can be explained by the large variety of product properties which can be obtained by using these inexpensive precursors.[95] However, one major drawback is the high toxicity of the isocyanates **59** (and the needed phosgene to obtain isocyanates) which subsequently leads to the need of expensive security measures.[97] In fact, the use of isocyanates **59** for chemical companies become more and more cost intensive through new EU and government regulations like REACH.[98] Therefore, it is highly advantageous to find less toxic substitutes for isocyanates **59** to facilitate the synthesis of isocyanate-free polyurethanes (NIPU).[99]

2.3.3.2 Non-Isocyanate Polyurethanes

The most employed isocyanate-free routes to obtain NIPUs are the polyaddition of cyclic dicarbonates **50** and diamines **62**,[100] the polycondensation of linear dicarbonates **50** and diamines **62**,[101] the polycondensation of carbamates **1** and diols **60**[101c, 102] and the ring opening polymerization of cyclic carbamates **4** (Scheme 7).[103] The most popular synthetic alternative for isocyanate to synthesize isocyanate-free polyurethanes is the polyaddition of cylic dicarbonates **50** and diamines **62**.[24] This is due to the fact that they show low toxicity, are biodegradable and that they are highly reactivity towards amines. Additionally, no volatile by-products[104] are released during the reaction and the resulting

NIPUs show better thermal stability than conventional PUs.[105] The better thermal stability can be explained by the absence of thermally unstable biurets and allophanates.[106]

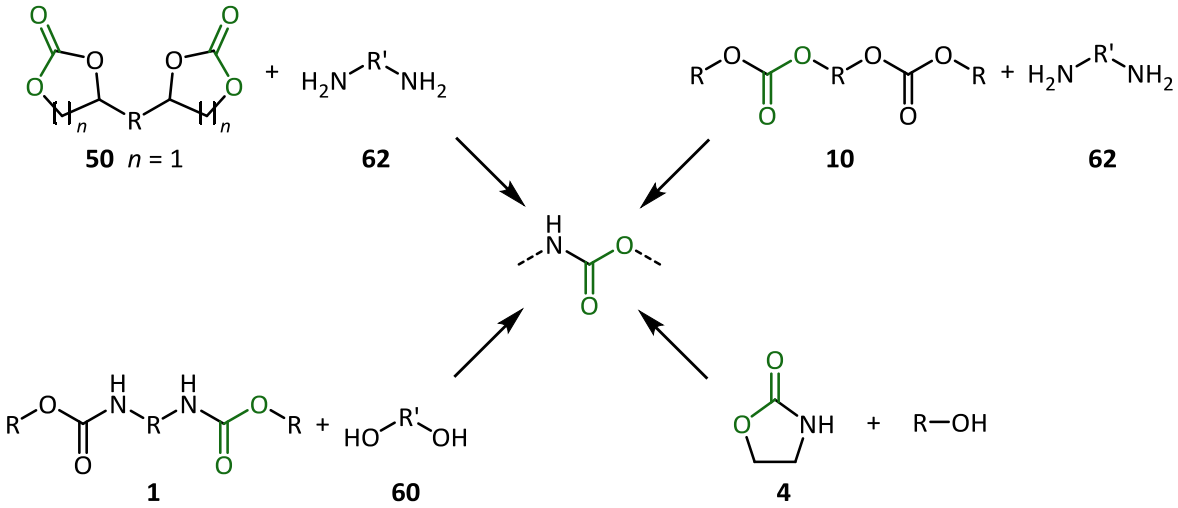

Scheme 7. Isocyanate-free routes to synthesize PUs.[96a]

During the polyaddition the cyclic carbonate **50** can open in two ways, leading to isomers with primary or secondary alcohols (Scheme 8 and Scheme 9).[85, 107] Because of the formation of alcoholic groups, these NIPUs **64** are also often mentioned as poly (hydroxyurethane)s (PHU) in recent literature.[108]

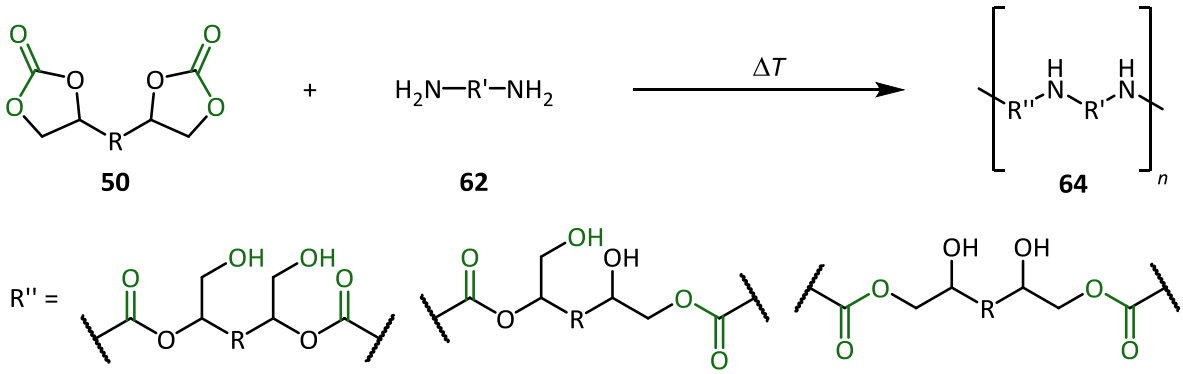

Scheme 8. Polyaddition of cyclic dicarbonates **50** and diamines **62**.

In a model reaction employing a monofunctional carbonate **11** and an amine *Endo* and coworkers investigated this ring opening step. They conducted molecular orbitals calculations to demonstrate plausible pathways of the reaction and determined the heat of formation values. As a result, the comparison of the heat formation values revealed a preferable formation of the product with the secondary hydroxyl group **23** (Scheme 9).[85] In accordance to these calculations, experiments verified the predominant formation of

product **23**. Only a few investigations have dealt with the synthesis of isocyanate-free PUs utilizing 5-and 6-membered cyclic carbonates.

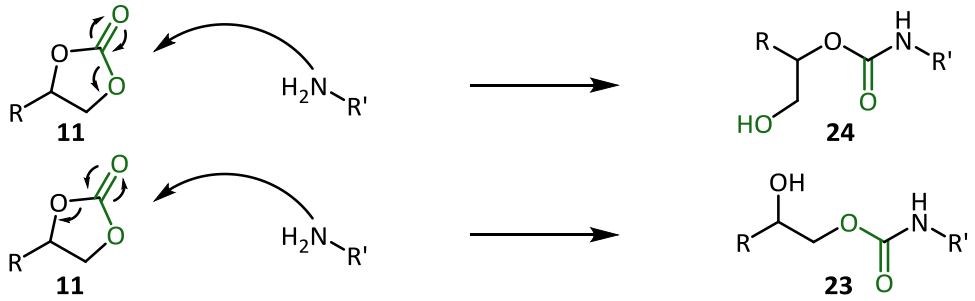

Scheme 9. Cycloaddition of **11** leading to primary **24** and or secondary alcohols **23**.

Early works for the synthesis of NIPUs derived from cyclic carbonates **50** and diamines **62** were done by *Endo*[82] and *Fedtke*.[109] The reaction was carried out in DMSO for 24 at 100 °C by using mainly 4,4'-(((propane-2,2-diylbis(4,1-phenylene))bis(oxy))bis (methylene))bis(1,3-dioxolan-2one) (**50d**) and several amines **62a**–**62d**. As a result, molecular weights of M_n = 13000–28000 g·mol^{-1} were obtained (Table 5, entry 1).[82]

Table 5. Reported polymerizations of cyclic dicarbonates **50** and aliphatic amines **62**.

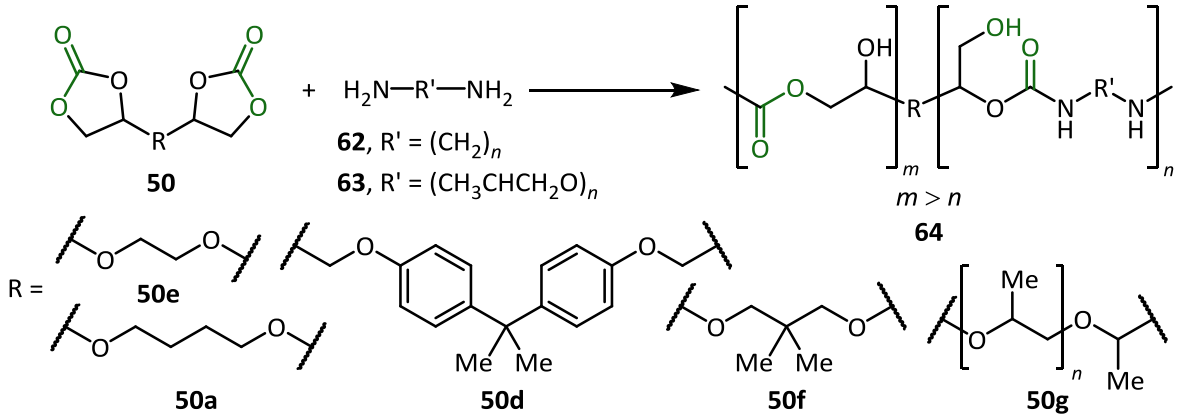

Entry	Reactant	Amine **62** or **63** / *n*		*T* / °C	*t* / h	M_n / 10^3 g·mol^{-1}	Conversion / %
1[82]	**50d**	2, 3, 6, 12	**62a–62d**	100	24	13.0–28.0	ND[a]
2[110]	**50d**	12	**62d**	70	6	19.3–37.0	84–96[b]
3[91]	**50e**	2, 3, 6	**62a–62c**	60 / 80[c]	2	25.4–30.2	ND
4[90]	**50a**	6	**62c**	60	5	6.74	84[d]
5[90]	**50f**	6	**62c**	60	5	7.10	84[d]
6[111]	**50g**	2-3	**63**	80	16	6.03–15.7	65–80[e]

[a] DMSO as solvent. [b] 5 mol% Salt, DMSO as solvent. [c] 60 °C for 20 min, then 80 °C for 2 h. [d] NMP as solvent. [e] Reaction of 5 mol% salt.

Interestingly, *Endo* and coworkers also used different additives to promote the polymerization reaction of **50d** and 1,12-diamindodecane (**62d**).[110] After 6 h at 70 °C a conversion of 84–96% was reached and molecular masses of 19300–37000 g·mol^{-1} were measured (Table 5, entry 2). Additionally, several different bifunctional carbonates **50** were converted at lower temperatures. The reaction mixture was first heated to 60 °C for a short time and then the reaction was continued at 80 °C for 2 h. Molar masses of 25400–30200 g·mol^{-1} were reached (Table 5, entry 3). The group of *Zhang* and coworkers converted the cyclic dicarbonates **50a** and **50f** at 60 °C for 6 h in NMP.[90] A conversion of 84% and low molar masses of around 7000 g·mol^{-1} (Table 5, entries 4 and 5) were obtained. Additionally, they used an oligomeric polyether diamine **63** and dicarbonates **50** to obtain conversions of 65–80% after 16 h at 80 °C. Molecular masses of 6030-15700 g·mol^{-1} were reached (Table 5, entry 6). Interestingly, the utilization of salts (e.g.: LiX and TBAC)[110-111] (Table 5, entries 2 and 6) and organic bases (e.g.: TBD)[112] seem to lead to higher conversions of the reactant. The reported synthesis methods for NIPUs derived from cyclic carbonates led to low to moderate molecular weights.

In general, NIPUs have better porosity, water absorption, thermal and chemical resistance than PUs.[100] Applications can be found as foams,[113] thermosetting coatings,[114] UV stable coatings[115], insulating materials[116] and monolithic floorings.[24] Additionally, they can be seen as an approach for the synthesis of environmentally beneficial prepolymers. This is due to the fact that no diisocyanate **59** is needed to obtain the polymer and the hydroxyl groups of the NIPUs can further react in subsequent polymerization reactions.[117]

2.3.4 Polycarbonates

2.3.4.1 Conventional Polycarbonate Synthesis

The first linear polycarbonate was patented in 1953 by *Hermann Schnell* (Bayer).[118] Since then, the reactants and methods for the production of polycarbonates on an industrial scale do not differ much. In fact, the mostly used and marketed polycarbonate **65** is still produced by the reaction of bisphenol A (**60a**) and phosgene (**30**) (Scheme 10).[119]

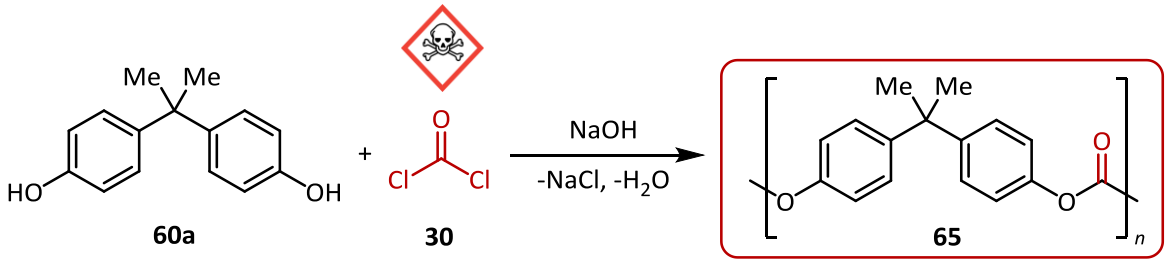

Scheme 10. Conventional synthesis of polycarbonate **65** using phosgene (**30**).

In addition to the toxic phosgene (**30**), the strong base sodium hydroxide is needed for the reaction.[120] Obviously, the substitution of phosgene (**30**) and sodium hydroxide for the polycarbonate synthesis are highly desirable.

2.3.4.2 Copolymerization of Epoxides and CO_2

One promising approach is the utilization of CO_2 as a chemical building block to produce polycarbonates **12** and thereby mitigating the use of fossil resources (Scheme 11).[121] In this research area significant progress has been made recently.[122]

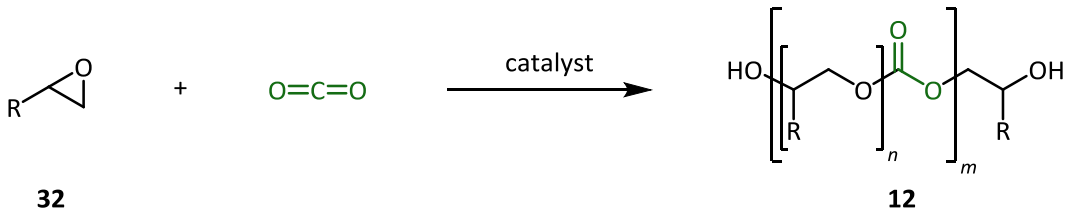

32 **12**

Scheme 11. Copolymerization of epoxides **32** and CO_2.[123]

The fast progress was mainly initiated through the Federal Ministry of Education and Research (BMBF), supporting cooperation between industrial and research partners. Namely, research programs like “Dream Reaction” and “Dream Production”[124] from Bayer in Germany were initiated by the funding.[125] The idea behind this programs is to implement this new technology into existing technologies and production facilities.[126]

In fact, the obtained polyether polycarbonate polyols should be implementable into long known existing polymerization reactions. This is possible by copolymerization of **12** with diisocyanate **59** (Figure 10). Actually, a successfully operating miniplant for the production of polyurethane foams was already build and a production line with an annual capacity of 5000 t·a^{-1} will commence operation in 2016.[127]

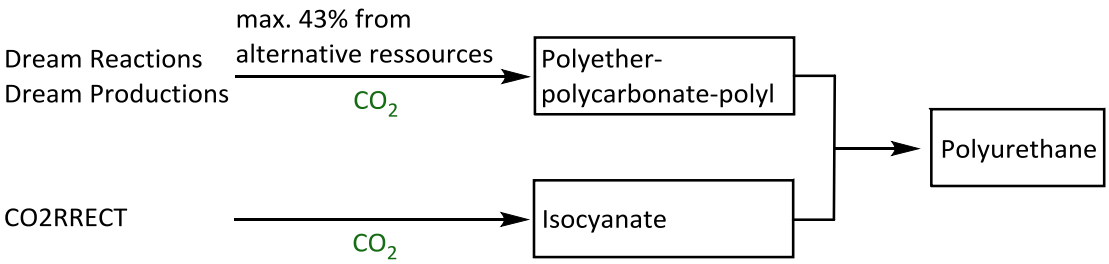

Figure 10. PU synthesis employing CO_2 as a C–1 building block.

Additionally, the possibility of better isocyanate routes is tested in another research program (CO2RRECT). Here, the ecological efficient production of H_2 and CO from CO_2 is investigated which is needed for the synthesis of isocyanates. The obtained polyether-polycarbonate polyols can at a maximum of 43 wt% be produced from CO_2. Especially propylene (**66**), which is needed to obtain PO **32a** is obtained mainly from petroleum and natural gas. As a fact, major sources of propylene (**66**) are oil refining and natural gas processing operations. Especially, naphtha cracking intended to produce ethylene is here a main factor (Figure 11).

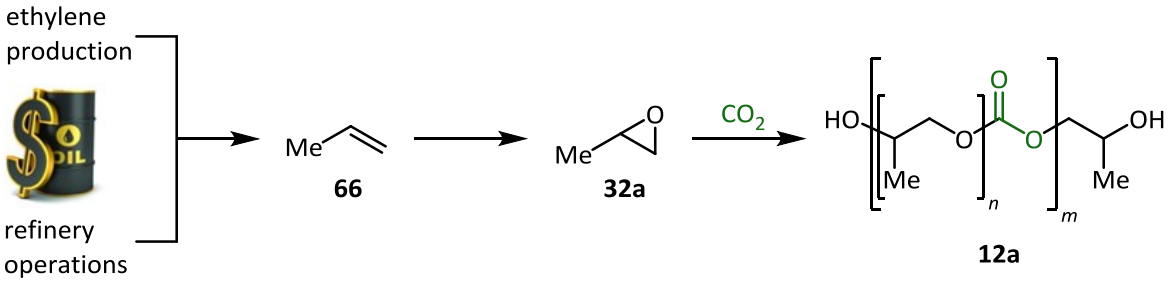

Figure 11. Production of polypropylene carbonate (**12a**) using propylene oxide (**32a**) and CO_2.

The industrial production of PO **32a** from propylene (**66**) is primary done through the hydrochlorination[128] or hydrogen peroxide propylene oxide oxidation (HPPO) process (Scheme 12).[129] In particular, the chlorhydrin technology uses environmentally hazardous substances. Here, highly toxic chlorine gas and propylene gas (**66**) are mixed with an excess of water to produce propylene chlorhydrin. Furthermore, the process

produces a lot of waste, since the dehydrochlorination of propylene chlorohydrin with caustic or lime leads to an equivalent amount of salt. Therefore, to handle the large occurring waste stream extensive effluent treatment is needed.

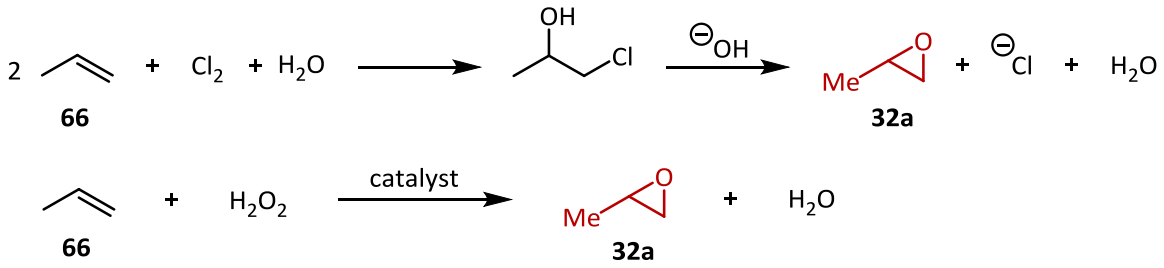

Scheme 12. Hydrochlorination (top) and HPPO (bottom) process to produce PO **32a**.[128-129]

In fact, *Bardow* and coworkers showed in a life cycle assessment (LCA) for the polyol production, that the highest environmental impact originates from the PO **32a** production.[130] They also conclude that PO **32a** should be substituted as a carbon feedstock. To overcome the limitation on PO **32a**, which is produced from fossil resources in a hazardous way, current research focuses on raw materials which can be obtained from alternative sources. One potential alternative is the utilization of formaldehyde (FA, **67**) in a copolymerization reaction with CO_2.

2.3.4.3 Copolymerization of Formaldehyde and CO_2

The copolymerization of aldehydes and CO_2 allows it to obtain polymers with a high content of incorporated CO_2. Especially, the most basic reactant of this class, formaldehyde (FA, **67**) has a huge potential to be employed for polymerization reactions. However, FA **67** is more complicated than many simple carbon compounds, because it adopts several different forms. For instance, gaseous FA is highly reactive and tends to polymerize with itself which makes it a challenging reactant.

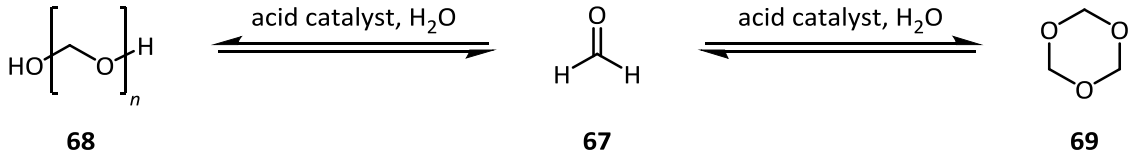

Figure 12. Reactants for the copolymerization with CO_2.[131]

To enable the utilization of this reactant several more stable forms can be used as FA sources. One alternative is the utilization of paraformaldehyde (PFA, **68**) which can be regarded as a linear oligomeric polyoxymethylene (POM). It is easy to handle and

decomposes through heating to gaseous FA. Furthermore, trioxane (**69**) the stable cyclic trimer of FA **67** can be used as an FA source. [131a] For the decomposition of trioxane (**69**) acidic conditions are needed.[132] Additionally, FA solutions in water (formalin) and THF can be used. In water FA **67** forms the hydrate methanediol and also various repolymerization products should occur. To suppress the polymerization and oxidation process it is stabilized with methanol. For water free applications it is possible to use a THF-FA solution (*Schlosser* solution). It can be obtained by depolymerization of PFA **68** and channeling the gaseous FA **67** in THF.[133] However, this solution is unstable and repolymerization occurs after a short time. To conclude, the reactants PFA **68**, trioxane **69** and FA **67** solutions like formalin and the *Schlosser* solution can be used as FA sources for the reaction of FA **67** and CO_2 to form polycarbonates.

Beside the theoretical polymerization of CO_2 itself, FA **67** allows with nearly 60 wt% the highest theoretical possible CO_2 content for a polycarbonate **71** (Figure 13). In comparison, the polymerization of CO_2 and PO **32a** leads to CO_2 contents of only 27% **12a** for a composition of two PO **32a** and one CO_2.[134] The copolymerization of epoxides **32** and CO_2 can lead to cyclic carbonates **11** as side products.[135]

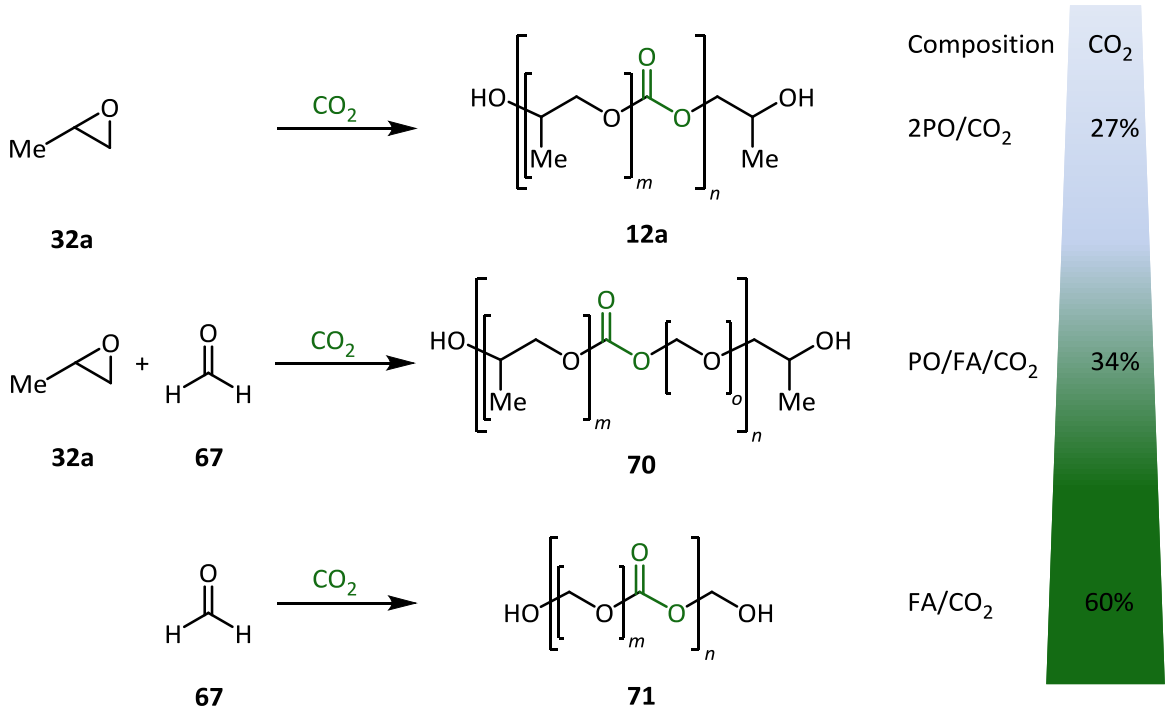

Figure 13. Comparison of polymerizations using CO_2 and the respective possible CO_2 content.

The importance of this possible CO_2 content is explained by the fact, that for every CO_2 which is incorporated in these polymers the needed amount of fossil resources like

petroleum and gas is reduced for a similar amount. Additionally, this process also has the potential to produce polycarbonates from up to 100% of renewable resources. This is due to the fact that FA **67** is normally produced from methanol in a catalytic process. Although, most of the produced methanol derives from fossil fuels it is already possible to produce methanol from biomass.[136] In a subsequent reaction the obtained polymethylene polyether polyols **71** can then be used in further polymerization reactions and thereby be implemented into already existing technologies.[137]

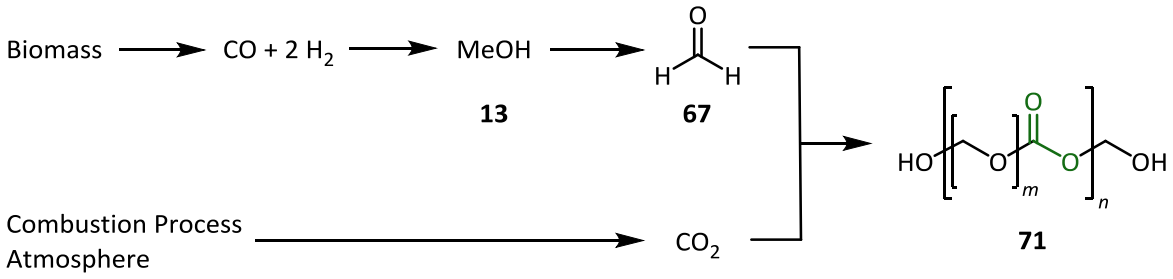

Scheme 13. Polycarbonates **71** from renewable resources.

Because of the high CO_2 content the polymers are expected to have good fire resistance abilities. Surprisingly, little research was done in the field of FA **67** copolymerization so far. In a more recent publication the copolymerization of FA **67**, epoxide **32** and CO_2 is described.[138] As a catalyst, a bimetallic cobalt-zinc complex was applied which was previously developed for the polymerization of epoxides with CO_2 and polyalcohols (Scheme 14).[122a, 123, 139] The catalyst enabled to polymerize PFA **68** and PO **32a** to form **72** and also the polymerization with CO_2 to obtain **70** (Scheme 14). Molecular weights of M_n = 2400 g·mol^{-1} and M_w = 3900 g·mol^{-1} were reached.

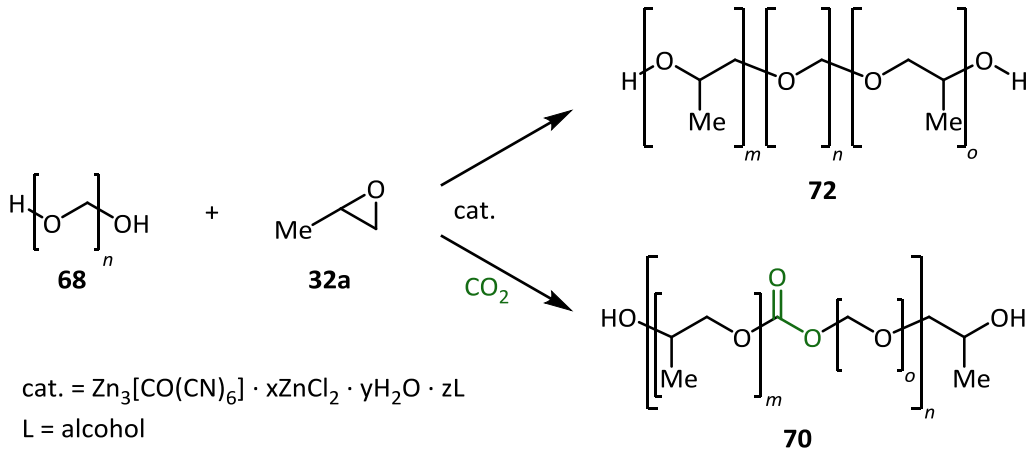

68 **32a** **72** **70**

Scheme 14. Copolymerization of PFA **68** and PO **32a** using a DMC catalyst.[138]

The copolymerization was described as living ring opening polymerization. Furthermore, the authors highlight that the nearly insoluble paraformaldehyde (PFA, **68**) was utilized to create a soluble, room temperature liquid and stable triblock polymer. For the direct copolymerization of FA **67** and CO_2 only two consecutive publications from the group of *Sharma*[140] and *Chiang*[141] are known (Table 6).

Table 6. Selected results for the copolymerization of CO_2 and FA **67**.[140-141]

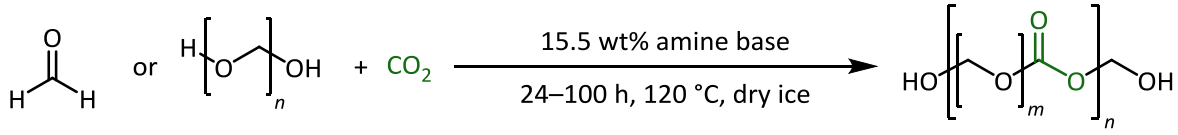

67 **68** **71**

Entry	Reactant		Catalyst		t / h	Yield / g	M_w / g·mol^{-1}
1[a]	Formalin	**67**	DABCO	**73**	100	5.1	22000 1000
2[b]	Formalin	**67**	DABCO	**73**	100	3.7	2800
3[a]	Formalin	**67**	DMAP	**74**	100	6.2	22000 14000
4[a]	Formalin	**67**	DMAP	**74**	24	1.2	20000 19500
5[c]	PFA	**68**	DMAP	**74**	48	6.5	85000 23000 22000

[a] 40 mL Formalin (37 wt%) (**67**), 15.5 wt% Catalyst **73** or **74**, yields determined by GPC using an internal standard. [b] 4.29 mol% DABCO **73**, 10 mL formalin (35 wt%) **67**, conversion calc from yield and EA. [c] 15.5 wt% DMAP **74**, 15.0 g PFA **68**, 40 mL dioxane.

They used amine bases **73** and **74** as catalysts, dry ice as the CO_2 source and mainly employed PFA **68** and formalin as the FA source (Scheme 6, entries 1–5). As a result, *Chiang* obtained molar masses of up to 2800 g·mol^{-1}. Applying very similar reaction conditions, *Sharma* reported a mass average molar mass of 22000 g·mol^{-1} (22%) (compare Table 6, entries 1 and 2). Additionally, DMAP **74** was used as a catalyst and molar masses of up to M_w = 85.000 g·mol^{-1} (16%) were measured (Table 6 entries 3–5). The formation of maximal 6.5 g of the polycarbonate **71** was observed (Table 6, entries 5). An IR band at $\tilde{\nu}$ = 1750 cm^{-1} was measured which was assigned to the carbonyl group of the incorporated CO_2. The conversions were determined by elemental analyses (EA) or by gel permeation chromatography (GPC). Since these methods are not entirely suitable for quantifications the stated yields are therefore to be regarded as tendencies. It is important to note that *Sharma* reported molar masses eight times higher than *Chiang* using very similar reaction conditions (Table 6, compare entries 1 and 2). In regard to the reachable molar masses the two reports seem to contradict each other.

The reaction was proposed to occur through anionic polymerization and a mechanism was suggested (Scheme 15).[141] In the first step, the amine **73** initiates the catalytic reaction by a nucleophilic attack on carbon dioxide. Then, propagation takes place were FA **67** copolymerizes with the activated CO_2. Finally, termination follows and the active catalyst is restored.

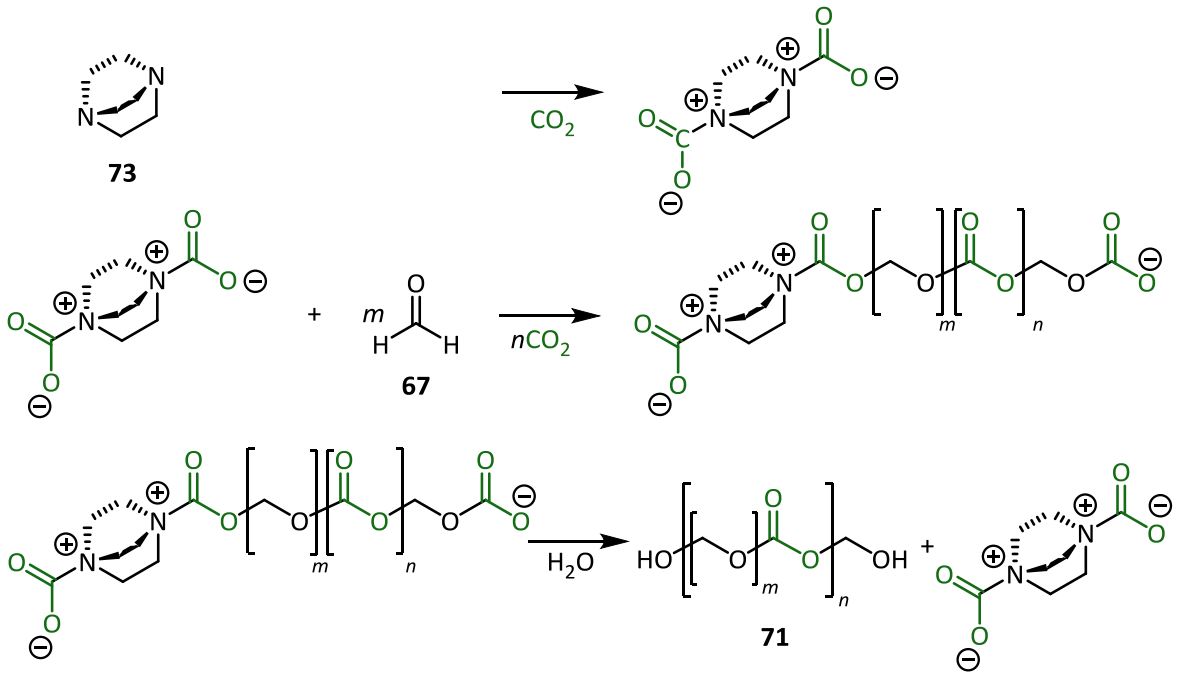

Scheme 15. Proposed reaction for the amine catalyzed polymerization of FA **67** and CO_2.[141]

In a more recent patent a catalyst system consisting of a *Lewis* acid metal component and a basic component is described to enable the copolymerization of FA **67** and CO_2.[142] The *Lewis* acid component is described to either occur as free metal ion or as a complexed metal ion. The *Lewis* basic component is described to have a preferred pK_b-value of ≥ 1.5 to ≤ 8. Reaction temperatures between 60–180 °C and reaction times of 0.5–48 h were preferred. An example was given were PFA **68** was copolymerized with CO_2 using Cs_2CO_3 and dibutyl tinlaurate as catalysts solved in dioxane. After stirring the reaction mixture for 16 h at 120 h a colorless oil was obtained. A molecular weight of M_n = 407 g·mol^{-1} was measured by using gel permeation chromatography (GPC). Furthermore, nuclear magnetic resonance (NMR) and electrospray ionization mass spectrometry (ESI-MS) showed that the obtained polymer consists of a not alternating FA/CO_2 copolymer structure.

3 OBJECTIVES

The main objective of this thesis is the utilization of carbon dioxide as an abundant, nontoxic and cheap C–1 building block for the synthesis of monomeric and polymeric compounds. In fact, CO_2 has the potential to substitute the toxic C–1 source phosgene and thereby promising more sustainable processes and products.

In the first part, the conversion of polyfunctional epoxides **49** to the corresponding cyclic carbonates **50** and the synthesis of non-isocyanate polyurethanes (NIPU, **64**) are investigated. In the second part, the copolymerization ability of formaldehyde (FA, **67**) and CO_2 within the framework of the project *Dream Polymers* to generate poly-carbonate **71** (Figure 14) is evaluated.

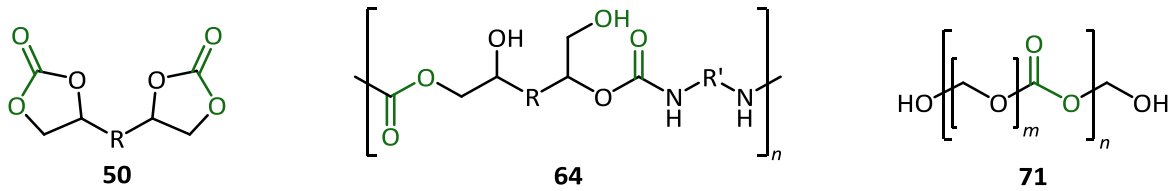

Figure 14. General structure of the target compounds.

3.1 Polyfunctional Cyclic Carbonates and NIPUs

For the organocatalyzed generation of polyfunctional cyclic carbonates **50**, the utilization of one component and two component catalyst systems and the investigation of suitable mild reaction conditions are to be evaluated. Therefore, the easily available cyclic dicarbonate 1,4-bis(oxiran-2-ylmethoxy)butane (**49a**) is to be used as the model substrate (Scheme 16).

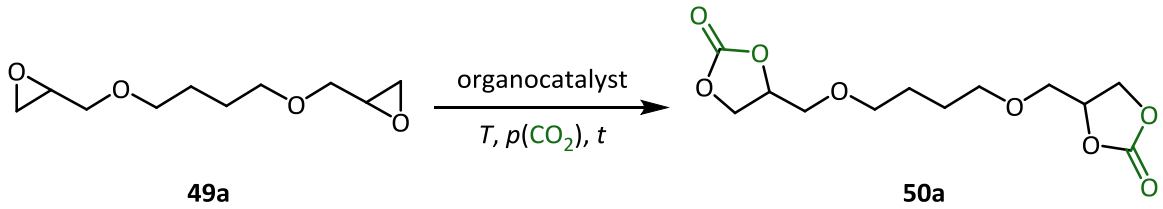

Scheme 16. Model reaction for the synthesis of polyfunctional carbonates.

Furthermore, the possible applicability of the synthesized carbonates as premonomers for polymerization reactions is to be tested. Therefore, diamines (**62**) and polyfunctional

cyclic carbonates **50** are to be utilized as premonomers to generate monodisperse non-isocyanate polyurethanes **64** (Figure 15). Additionally, a one pot procedure to form the NIPU **64** is to be applied and the influence of the organocatalysts, used to generate the polyfunctional cyclic carbonates, on the polymerization reaction is to be tested.

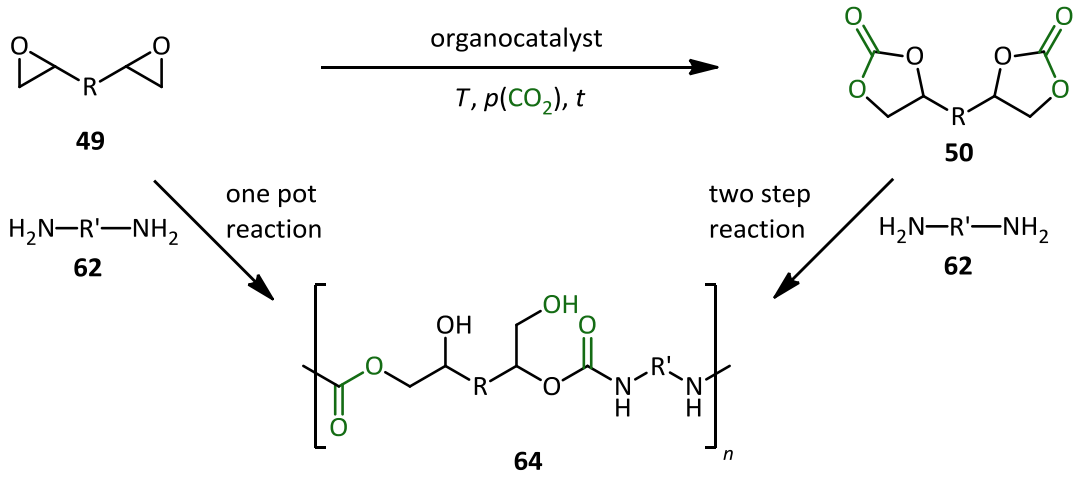

Figure 15. Organocatalytic synthesis of cyclic carbonates **50** followed by NIPU **64** synthesis.

Taking into account the large production volume of the classical polyurethane (PU) synthesis, the reaction promises a large impact for the reduction of the utilized phosgene and isocyanate required by the chemical industry.

3.2 Dream Polymers

The second objective of this thesis is the evaluation of the copolymerization ability of CO_2 as a C–1 building block with formaldehyde (FA, **67**) to produce poly(methylene carbonate) polyols. This reaction promises the synthesis of polycarbonates **69** with a comparatively high CO_2 content of up to 60 wt% and thereby significantly reduces the amount of needed fossil resources (Scheme 17).

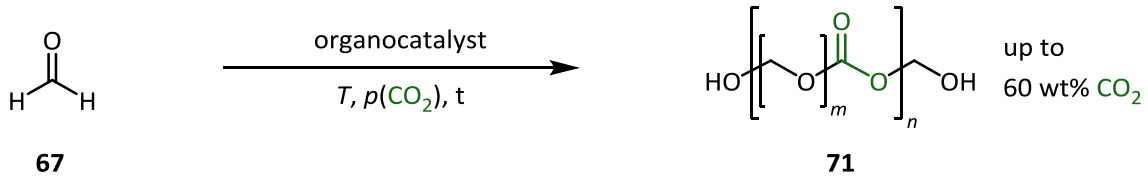

Scheme 17. Catalyzed reaction of FA sources **67–69** and CO_2.

At the beginning of this thesis only two publications described this kind of reaction.[140-141] Therefore, suitable FA **67** sources and general reaction conditions are to be evaluated. Especially, the development of selective organocatalysts to activate the relatively inert

CO_2 was focused to obtain poly(methylene carbonate) polyols **71** with defined properties. Therefore, the catalytic activity of amine bases and of amine bases in combination with imidazolium and thiazolium salts is to be tested. Furthermore, requirements for the thermal stability of the polymer were defined. To be more precise, during a heating process to 130 °C the relative mass loss of the polymer should be ≤ 5% and the decrease of the number average molecular weight (M_n) should be ≤ 15%.

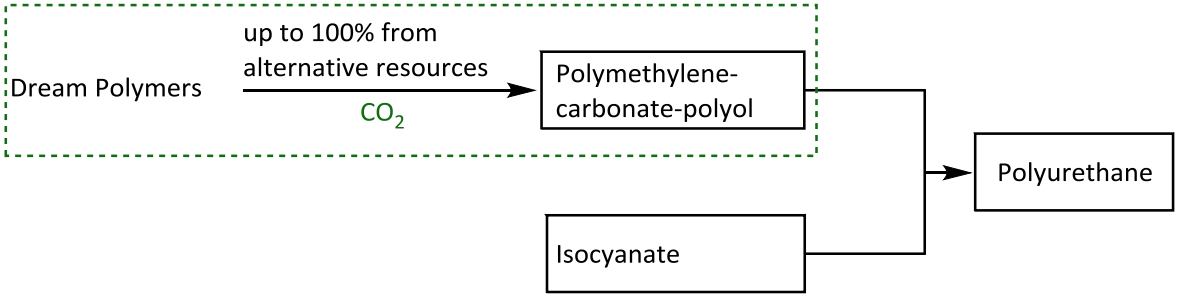

Figure 16. Project structure for the copolymerization of CO_2.

The obtained poly(methylene carbonate) polyols **71** should be implementable into existing processes to form polyurethanes, thereby generating economically and ecologically benign polymers. The work on this theme was conducted within the framework of the project *Dream Polymers* (Figure 16).

4 RESULTS

4.1 Cyclic Carbonates

The emphasis for the synthesis of cyclic carbonates was mainly on the conversion of polyfunctional epoxides **49** as reactants (Scheme 18). Furthermore, ionic liquids and two component systems, which were developed by *Werner et al.*, were used as catalysts for the reaction. This is due to the fact that these systems showed in preliminary studies high activity, are easy to handle and the workup is comparatively simple.[78-79]

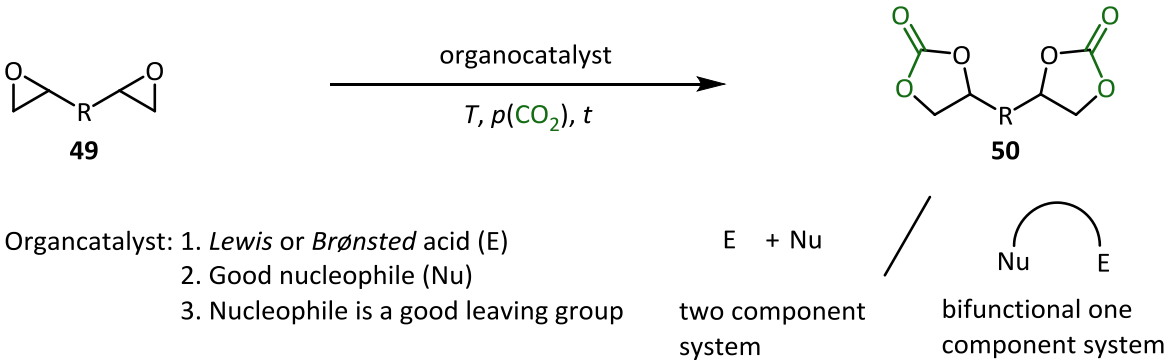

Scheme 18. Synthesis of cyclic dicarbonates **50**.

4.1.1 Catalysts and Model Reaction

The concept for the employed catalysts was to use organocatalyst systems which are known to show good catalytic activity due to an inherent electrophilic and a nucleophilic side.[73, 78-79] Here, a *Lewis* or *Brønsted* acid acts as the electrophilic and a halogen as the nucleophilic component (Scheme 18). Therefore, two component systems and bifunctional one component systems were utilized. For the bifunctional one component catalyst the amine salt **45a** and the phosphonium salt **46a** were synthesized (Scheme 19).

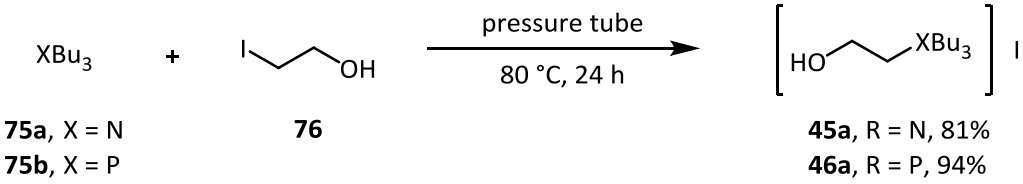

75a, X = N
75b, X = P

76

45a, R = N, 81%
46a, R = P, 94%

Scheme 19. Synthesis of **45a** and **46a**.

They were prepared readily through simple alkylation of the amine **75a** or phosphine **75b** with the halohydrin **76**. The bench stable bifunctional salt **45a** was obtained in good yield of 81% and the phosphonium salt **46a** was obtained in an excellent yield of 94% (Scheme 19).

As benchmark catalysts **38a–38c** were employed. As two component catalyst systems the additives 4(5)-(hydroxymethyl)imidazole (**41**) or triethanolamine (**39**) in combination with the commercially available potassium iodide (KI, **40**) were utilized (Figure 17).

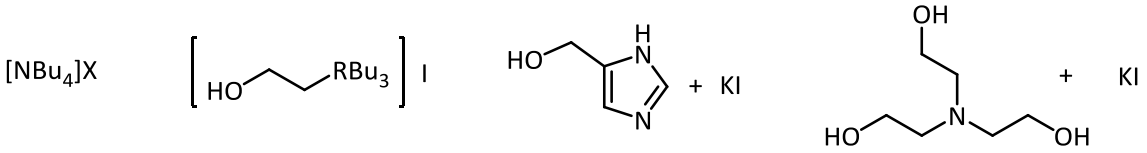

38a, X = I
38b, X = Br
38c, X = Cl

45a, R = N
46a, R = P

41 **40** **39** **40**

Figure 17. Utilized Catalysts and additives for the formation of cyclic carbonates.

As a suitable model substrate we wanted to use a bisepoxide which is available by purchase and inexpensive. Additionally, its aggregate state should be liquid at room temperature or at least be liquid at the used reaction temperature to avoid the requirement of a solvent. By avoiding the need of a solvent the reaction becomes more sustainable. Also the obtained product should be liquid at the reaction temperature to ensure a good miscibility during the reaction.

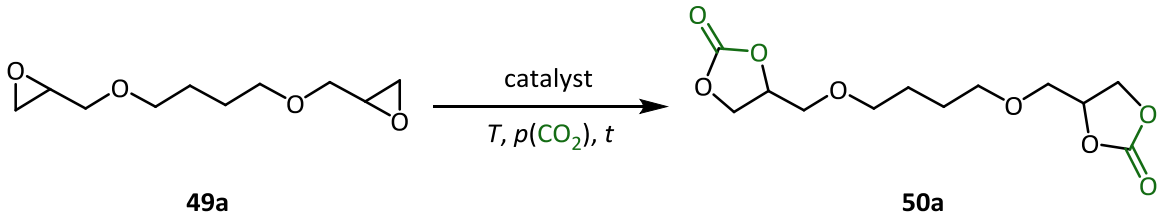

49a **50a**

Scheme 20. Conversion of the model substrate **49a**.

Furthermore, the conversion of the epoxide **49a** has to be easily determinable by ^{1}H NMR. Therefore, the carbonate signals needed to be well distinguishable from the epoxide signals in the ^{1}H NMR spectra. As a result, 1,4-bis(oxiran-2-ylmethoxy)butane (**49a**) proved to be a suitable model substrate (Scheme 20).

4.1.2 Catalyst Screening

In preliminary studies of *Werner et al.*, standard reaction conditions for the conversion of epoxides **32** to the cyclic carbonate **11** were determined.[73, 78-79] As a result, four catalyst systems performed well. The one component catalyst systems tri-*n*-butyl-(2-hydroxyethyl)ammonium iodide (**45a**) and tri-*n*-butyl-(2-hydroxyethyl) phosphonium iodide (**46a**) and the two component catalyst systems 4(5)-(hydroxyl-methyl)imidazole (**41**) / KI **40** and TEA **39** / KI **40** showed high activities. The two component systems are supposed to form the catalytic active salt in situ.

With reference to these preliminary studies of our group the reaction conditions 90 °C, 3 h and 10 bar CO_2 pressure for the conversion of the model substrate **49a** were chosen. The evaluation of the reaction was done by using ^{1}H NMR spectroscopy.

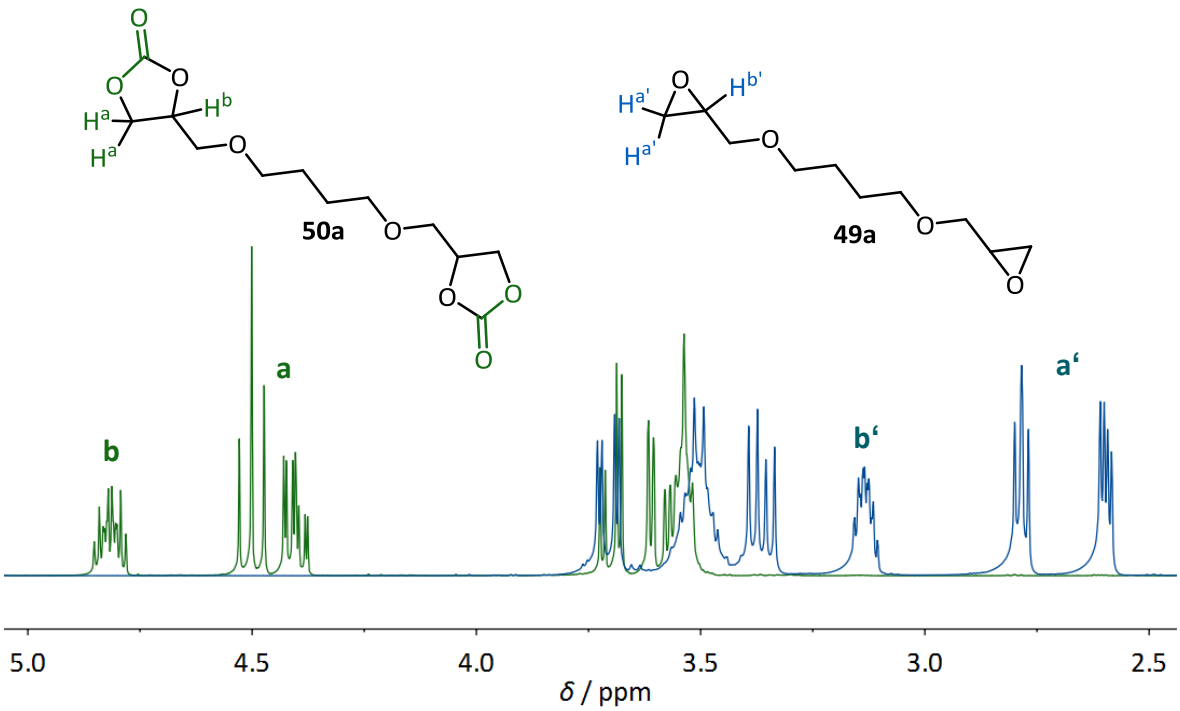

Figure 18. ^{1}H NMR of the reactant **49a** (blue) and the analog cyclic carbonate **50a** (green).

Generally, three important regions could be assigned in the ^{1}H NMR spectrum. First, a region in the range between δ = 3.3–3.8 ppm where the resonances of the product (Figure 18, blue) and reactant (Figure 18, green) overlap. Second, a downfield shifted region in the range of δ = 4.3–5.0 ppm where the resonances of the cyclic carbonates can usually be found. Third, an upfield region between δ = 2.5–3.2 ppm which could be assigned to the epoxide moieties of the reactant. Consequently, the proton signals of the

epoxide and cyclic carbonate moieties were used to determine the conversion of the reactant and thereby the performance of the four catalyst systems. It is important to note that the epoxide moieties are chemically identical and are therefore not distinguishable by ^{1}H NMR. Furthermore, the epoxide signals of the product with only one cyclic carbonate group are indistinguishable from the epoxide groups of the reactant. In fact, it is to be expected that if the conversion of the reactant is not complete, the cyclic dicarbonate **50a** and the product with only one converted epoxide group **77a** should occur.

Table 7. Conversion of **49a** at 60 °C.[a]

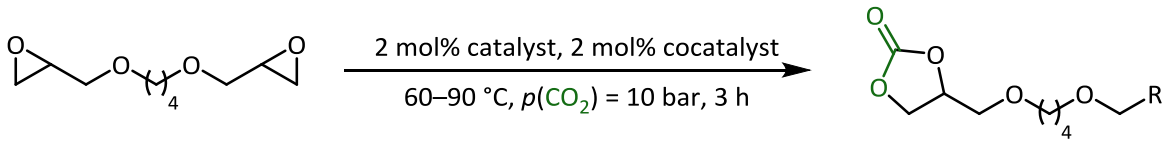

49a

50a, R = carbonate
77a, R = epoxide

Entry	Catalyst		*T* / °C	Conversion (Epoxide) / %[b]	Yield / %[c]
1	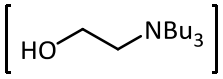	**45a**	90	>99%	98
2	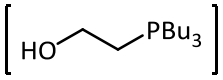	**46a**	90	>99%	98
3	HIM[d]	**41**	90	>99%	96
4	TEA[d]	**39**	90	>99%	98
5	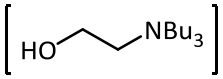	**45a**	60	60	60[e]
6	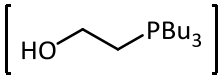	**46a**	60	54	ND
7	HIM[d]	**41**	60	55	ND
8	TEA[d]	**39**	60	28	ND
9	$[Bu_4N]Cl$	**38a**	60	20	ND
10	$[Bu_4N]Br$	**38b**	60	36	ND
11	$[Bu_4N]I$	**38a**	60	45	ND

[a] 10 mmol Bisepoxide **49a**. [b] Conversion of the epoxy groups were determined by ^{1}H NMR. [c] Isolated yield. [d] 2 mol% KI **40** as cocatalyst. [e] 28% of **50a** and 31% of monocarbonate **77a** isolated after column chromatography.

Excellent isolated yields ranging from 96% to 98% were achieved (Table 7, entries 1–4). Since all catalyst systems showed full conversion of **49a** to **50a** a change of the reaction conditions was conducted to find the most active catalyst. Subsequently, the reaction temperature was reduced from 90 °C to 60 °C (Table 7, entries 5–11). As a result, the ammonium salt **45a** exhibited with a conversion of 60% the highest activity (Table 7, entry 5). For this reaction the product with only one converted epoxide group **77a** and the cyclic dicarbonate **50a** were isolated by column chromatography. After 3 h the cyclic mono- and dicarbonates occurred with 31% of **77a** and 28% of **50a** in a ratio close to 1:1. The phosphonium salt **46a** and the two component system **41** / **40** showed with a conversion of 54% and 55% of the epoxide groups similar activity (Table 7, entries 6 and 7). Surprisingly, by applying the system TEA **39** / KI **40** only a low conversion of 28% was observed (Table 7, entry 8). Especially in comparison to the other catalysts and also in comparison to the full conversion at 90 °C this was not to be expected. It can probably be explained by a low solubility of the active catalyst salt under the reduced temperature.

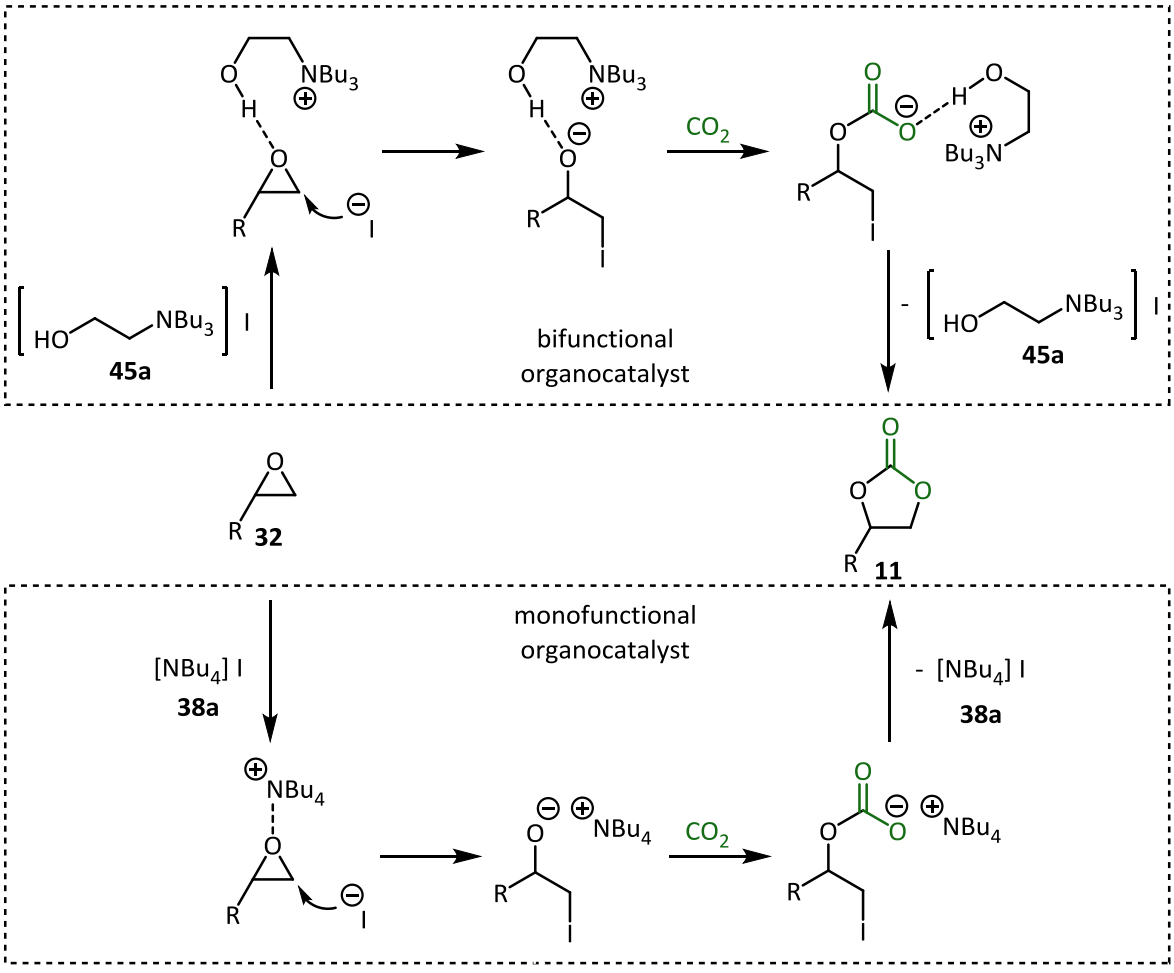

Scheme 21. Putative reaction mechanisms employing **45a** and **38a** as catalysts.[61, 73a]

For reason of comparison three simple monofunctional ammonium salts **38a**–**38c**, which were used as a reference for the bifunctional catalysts, were tested at 60 °C (Table 7, entries 9–11). As a result, the tetra-*n*-butylammonium iodide (**38a**), bromide (**38b**) and chloride (**38c**) showed lower activity, except the mentioned TEA **39** / KI **40** system, than the other catalysts. Here, conversion of the epoxide **49a** varied between 20–45% (Table 7, entries 9–11). The activity followed the order I > Br > Cl. This was unexpected, because for the conversion of monofunctional epoxides the activity was observed by our group to be the other way around.[78-79] The higher activity of the catalysts with inherent alcohol functions in comparison to the tetra-*n*-butylammonium iodide (**38a**) can be explained by an activation of the epoxide **32** through the alcohol. The alcohol forms a hydrogen bond and thereby further promotes the reaction (Scheme 21).

For further parameter screening the ammonium salt tri-*n*-butyl-(2-hydroxyethyl) ammonium iodide (**45a**) with the highest conversion of the epoxide groups at 60 °C was selected. The two component systems showed weaker performance under variation of the reaction parameters. Therefore, the one component systems seem to be more reliable.

4.1.3 Parameter Screening

To further optimize the conversion of 1,4-butanediol diglycidyl ether (**49a**), different reaction parameters were varied. The influence of the catalyst loading of tri-*n*-butyl-(2-hydroxyethyl)ammonium iodide (**45a**), reaction time, temperature and CO_2 pressure were investigated (Table 8).

Table 8. Parameter screening for the model substrate **49a**.[a]

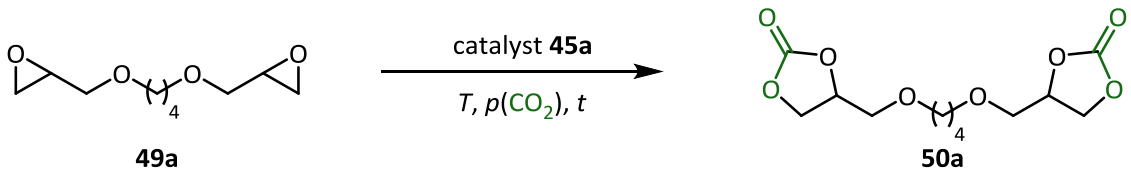

49a **50a**

Entry	Cat. **45a** / mol%	*t* / h	*T* / °C	*p*(CO_2) / bar	Conversion / %[b]
1	2	3	60	10	60
2	2	3	60	25	57
3	2	14	60	10	91
4	5	18	45	10	91
5	2	3	90	10	>99
6	2	2	90	10	96
7	1	3	90	5	93
8	1	3	90	10	93

[a] 10 mmol **49a**. [b] Conversion of the epoxy groups were determined by ^{1}H NMR.

First the influence of the pressure at 60 °C was investigated. Here, the increase of the CO_2 pressure to 25 bar led to no improvement of the conversion (Table 8, entry 2). An elongation of the reaction time to 14 h showed an increase of the conversion to 91%, but no full conversion could be achieved (Table 8, entry 3). The same conversion was obtained by lowering the reaction temperature to 45 °C and simultaneously prolonging the reaction time, using a catalyst loading of 5 mol% (Table 8, entry 4). Since no full conversion was reached at lower temperatures the parameter at 90 °C were varied. The reduction of the reaction time to 2 h showed no full conversion (Table 8, entry 6). Also the reduction of the catalyst loading to 1 mol% resulted in a lower conversion (Table 8, entries 7 and 8). As a result, the reaction conditions of 90 °C, 2 mol% tri-*n*-butyl-(2-hydroxyethyl)ammonium iodide (**45a**), 3 h and 10 bar CO_2 pressure were used to determine the scope for the conversion of polyfunctional epoxides (Table 8, entry 5).

4.1.4 Substrate Screening

The catalyst tri-*n*-butyl-(2-hydroxyethyl)ammonium iodide (**45a**) with the highest catalytic activity under the optimized reaction conditions was used to convert a variety of other epoxides. Unfortunately, the reaction conditions for the model substrate showed weaker performance for other substrates which made further investigations necessary. Although, the synthesis of 4,4'-(butane-1,4-diyl)bis(1,3-dioxolan-2-one) (**50b**) showed under the optimized reaction conditions full conversion of the bisepoxide **49b**, the conversion of the cyclic monocarbonate **77b** to the cyclic dicarbonates **50b** was not complete. An isolated yield of 82% of the cyclic dicarbonates **50b** and 16% of the cyclic monocarbonate **77b** were obtained (Scheme 22).

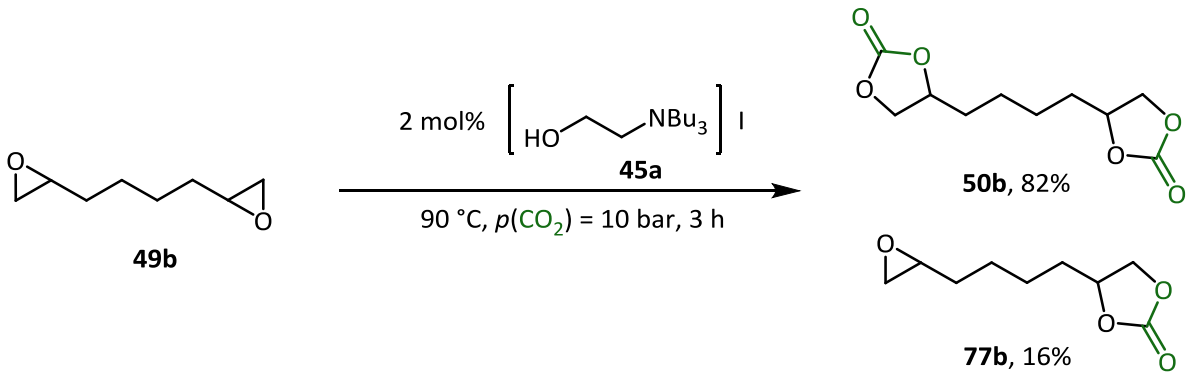

Scheme 22. Reaction of 1,4-di(oxiran-2-yl)butane (**49b**) to **50b** and **77b**.

To ensure a full conversion to the cyclic dicarbonate **50b** the reaction time was first prolonged to 6 h. Here, Full conversion to the cyclic dicarbonate **50b** could not be observed. Subsequently, the reaction time was further prolonged to 14 h. Fortunately, using a reaction time of 14 h full conversion of the epoxide groups was obtained. As a consequence, the scope of the reaction was ascertained by using the reaction conditions 90 °C, 2 mol%, 14 h and 10 bar CO_2 pressure.

Additionally, the conversion of monofunctional epoxides **32d–32f** in an upscaled reaction were tested (Table 9, entry 1). Here, good yields of the cyclic carbonate **11d–11f** were isolated. As stated, was the conversion of the model substrate **49a** after only 3 h at 90 °C complete and a yield of 98% was isolated (Table 9, entry 2). The aliphatic cyclic dicarbonate **50b** and the ether **50f** were isolated in excellent yields of 99% and 93% (Table 9, entries 4 and 5). A functionalized cyclohexane with ester groups **49h** was converted into the corresponding carbonate **50h** with a good yield of 88% (Table 9,

entry 6). Additionally, two aromatic bisepoxides **49c** and **49d** were converted. Excellent yields of 95% for the benzene derivative **50c** and 98% of the bisphenol A analog **50d** were obtained (Table 9, entries 7 and 8). The catalyst **45a** also allowed the synthesis of cyclic carbonates derived from an internal polyfunctional epoxide **78**. This was fortunate, because in internal epoxides are generally known to show a lower reactivity for the formation of cyclic carbonates.[143]

Table 9. Synthesis of cyclic carbonates.[a]

Entry	Reactant	Product		*t* / h	Yield / %[b]
1	**32d** **32e** **32f**	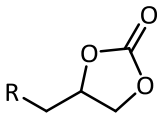	**11d** **11e** **11f**	3	90[c] 90[c] 91[c]
2	**49a**	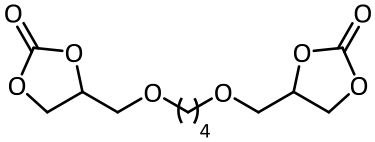	**50a**	3	98
3	**49b**	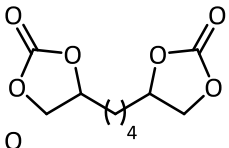	**50b**	3	82
		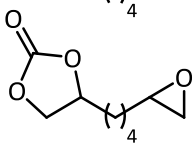	**77b**		16
4	**49b**	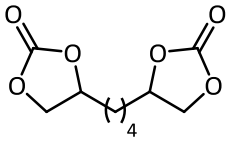	**50b**	14	99
5	**49f**	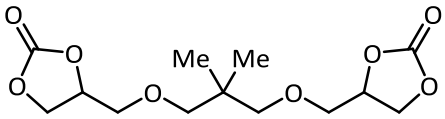	**50f**	14	93
6	**49h**	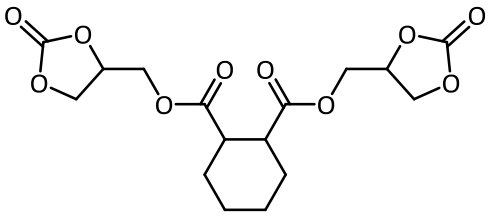	**50h**	14	88
7	**49c**	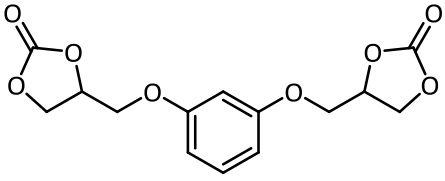	**50c**	14 14	95 94[d]

Table 9. Continued.

8	**49d**	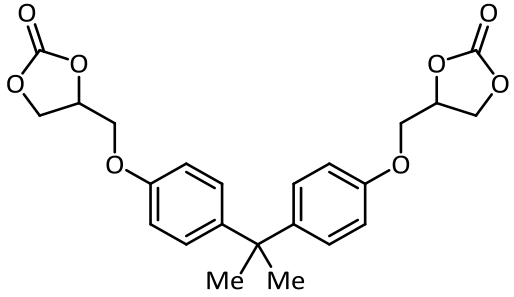	**50d**	14	98[d]
9	**78**	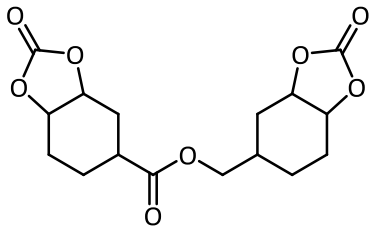	**79**	14 48	30[e] 90[f]
10	**56**	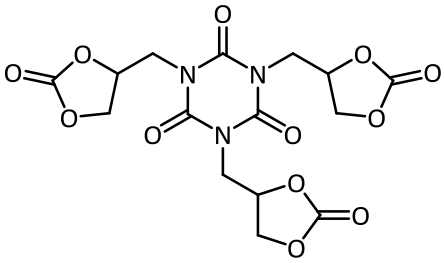	**57**	14	95[d]
11	**80**	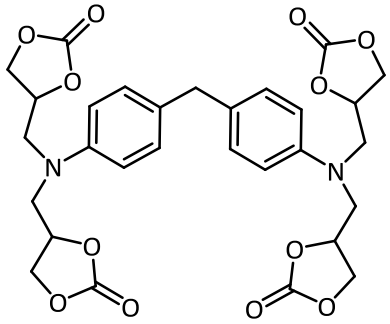	**81**	14	96[d]

[a] Reaction conditions: 10 mmol Reactant **49** and **32**, 2 mol% **45a**, T = 90 °C, $p(CO_2)$ = 10 bar, t = 3–14 h. [b] Isolated yields. [c] 70 mmol Reactant **32**. [d] 3 mL MEK. [e] Conversion of the epoxy groups were determined by ^{1}H NMR. [f] 10 mol% **45a**.

Using a prolonged reaction time and a higher catalyst loading, full conversion and a good yield of 90% for this internal carbonate **79** was obtained (Table 9, entry 9). Also substrates with more than two epoxide groups were converted to the corresponding carbonates. A substrate containing three epoxide moieties **56** was converted to the corresponding cyclic carbonate **57** in an excellent yield of 95% (Table 9, entry 10). Interestingly, the structural motif of **56** can be found in the typical PU synthesis to form polyisocyanurate foams. Subsequently, it is also a target compound for the NIPU synthesis (Chapter 4.3). Another

reactant with four epoxide moieties **80** could also be converted to **81** and a yield of 96% was obtained (Table 9, entry 11).

To conclude, the organocatalytic synthesis of polyfunctional cyclic carbonates was shown to be possible by converting 9 different polyfunctional epoxides. The reactions were conducted mostly under neat conditions. In fact, the solvent MEK was only needed for the substrates **50d**, **56** and **80** and here good to excellent yields of polyfunctional cyclic carbonates were isolated. Additionally, the conversion of a bifunctional internal epoxide **78** was possible. A great advantage was the comparatively easy workup. Often the products were simply washed with a suitable solvent or filtered over silica gel.

4.1.5 Oligomeric Cyclic Dicarbonates

It was attempted to convert oligomeric bisepoxides into the corresponding cyclic carbonates. Therefore, the oligomeric reactants polypropylene glycol diglycidyl ether with number average molecular weights of M_n = 640 g·mol^{-1} (PPG-DGE 640, **49i**) and M_n = 380 g·mol^{-1} (PPG-DGE 380, **49j**) and a polyethylene glycol diglycidyl ether with a molecular weight of M_n = 500 g·mol^{-1} (PEG-DGE 500, **49k**) were employed (Scheme 23).

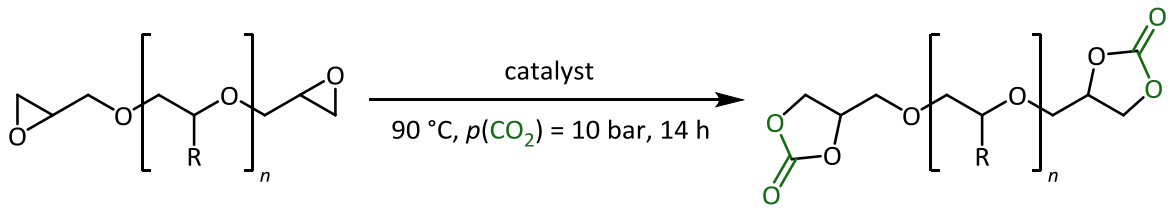

R = Me, M_n= 640 g·mol^{-1} **49i**
R = Me, M_n= 380 g·mol^{-1} **49j**
R = H, M_n= 500 g·mol^{-1} **49k**

R = Me, M_n= 728 g·mol^{-1} **50i**
R = Me, M_n= 468 g·mol^{-1} **50j**
R = H, M_n= 588 g·mol^{-1} **50k**

Scheme 23. Reaction of oligomeric bisepoxides **49i–49k** to the cyclic carbonates **50i–50k**.

For non-oligomeric substances the epoxide content of the reactant is simply given by the molecular weight. Oligomeric and polymeric compounds consist of a mixture of molecules with different molecular masses in different occurrences. The molar mass is stated as a molar mass distribution. For the used oligomers only the number average molecular weight (M_n) was given which does not allow a deduction to the exact epoxide content of the reactant. Therefore, the epoxide content of **49i–49k** was determined by ^{1}H NMR using mesitylene as a standard (Appendix, Figure 31). The calculated mol (epoxide) / g (reactant) did not differ much from the value M_n which was stated by the producer (Appendix, Table 37).

Table 10. Synthesis of oligomeric cyclic dicarbonates **50g** and **50j**.[a]

Entry	Reactant[b]		Product		Yield / %
1	PPG-DGE 640	**49i**	PPG-GC$_2$ 728	**50i**	98%
2	PPG-DGE 380	**49j**	PPG-GC$_2$ 468	**50j**	98%
3	PEG-DGE 500	**49k**	PEG-GC$_2$ 588	**50k**	99%

[a] 10 mmol Epoxide **49**. [b] Epoxide content determined by ^{1}H NMR: 3.234 mmol (epoxide)·g^{-1} (substrate) **49i**, 5.800 mmol (epoxide) g^{-1} (substrate) **49j**, 3.996 mmol (epoxide)·g^{-1} (substrate) **49k**.

With the calculated epoxide contents we performed the reaction under the standard reaction conditions of 90 °C, 14 h, a CO_2 pressure of 10 bar and without a solvent.

The salt tri-*n*-butyl-(2-hydroxyethyl)ammonium iodide (**45a**) was used as a catalyst. Here, full conversions of the epoxides were reached and the catalyst **45a** could easily be separated from the highly viscous oligomeric products by filtering the mixture over silica gel. The synthesized α,ω-diglycerol carbonates PPG-GC_2 **50i–50j** and PEG-GC_2 **50k** were obtained in excellent yields of up to 99% (Table 10). In general, oligomeric cyclic di- and polycarbonates are highly interesting for the production of block copolymers like for example non-isocyanate polyurethanes (NIPUs).

4.2 Synthesis of Non-Isocyanate Polyurethanes

The industrialized reaction to obtain polyurethanes (PU) requires a diol **60** and a diisocyanate **59** as reactants. Since isocyanates are known to be highly toxic it is favourable to find alternatives to this compound.[144] In fact, the dependency on the diisocyanate compound can be circumvented by using cyclic dicarbonates to obtain non-isocyanate polyurethanes (NIPUs).[82] Here, the cyclic dicarbonate **50** reacts with a diamine **62** compounds in a polyaddition reaction to form a linear non-isocyanate polyurethane.[145] During the polyaddition the cyclic carbonate **11** can open in two ways, leading to a primary or secondary alcohol.[146] In a proof of principle reaction the carbonate **49d** was applied in a reaction with 1,4-diaminobutane (**62f**) to form a polyurethane **64a**. No catalyst was needed and the two components were heated to 100 °C for 24 h with DMSO as a solvent (Scheme 24).

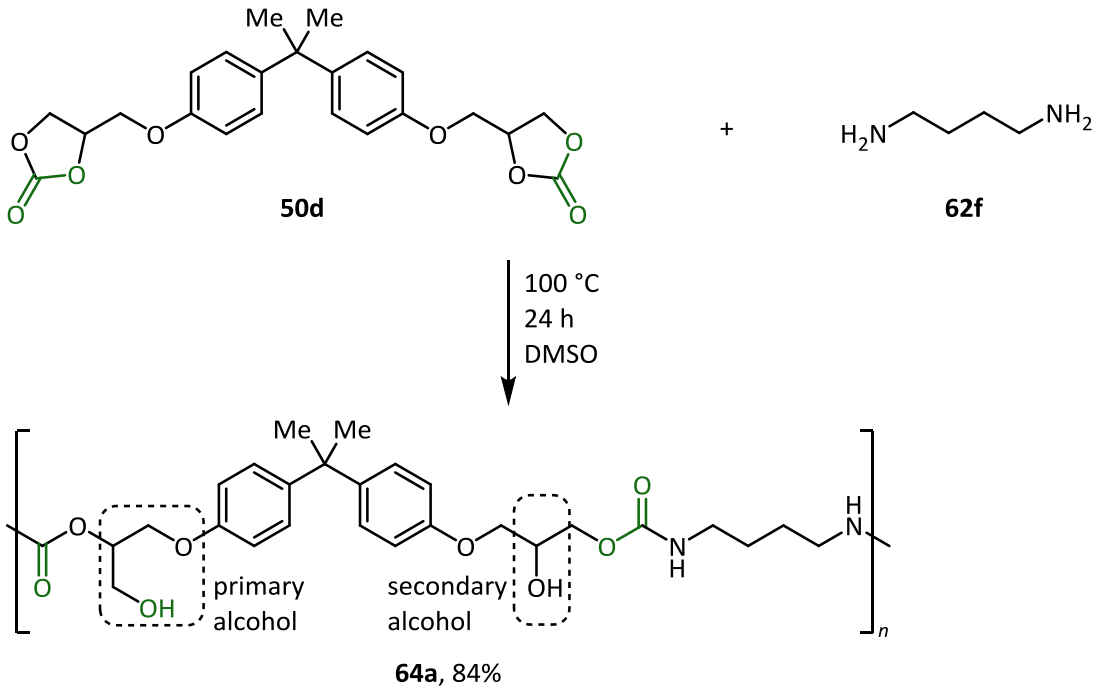

Scheme 24. NIPU **64a** synthesis using the cyclic dicarbonate **50d** and the diamine **12a**.

After the polymerization reaction the raw product was purified through precipitation in water. The cyclic carbonate **50d** and the amine **62f** were completely consumed which could be determined by ^{1}H NMR (Figure 19). Furthermore, the formation of primary and secondary alcohols could be observed with a preference to build secondary alcohols (secondary : primary alcohol 76% : 24%). The ratio was determined by comparing the integrals of the ^{1}H NMR resonances (Figure 19). Similar observations were reported for

monosubstituted five membered cyclic carbonates.[82] The polymerization occurred in a 1 : 1 ratio of the prepolymers and a yield of 84% was obtained.

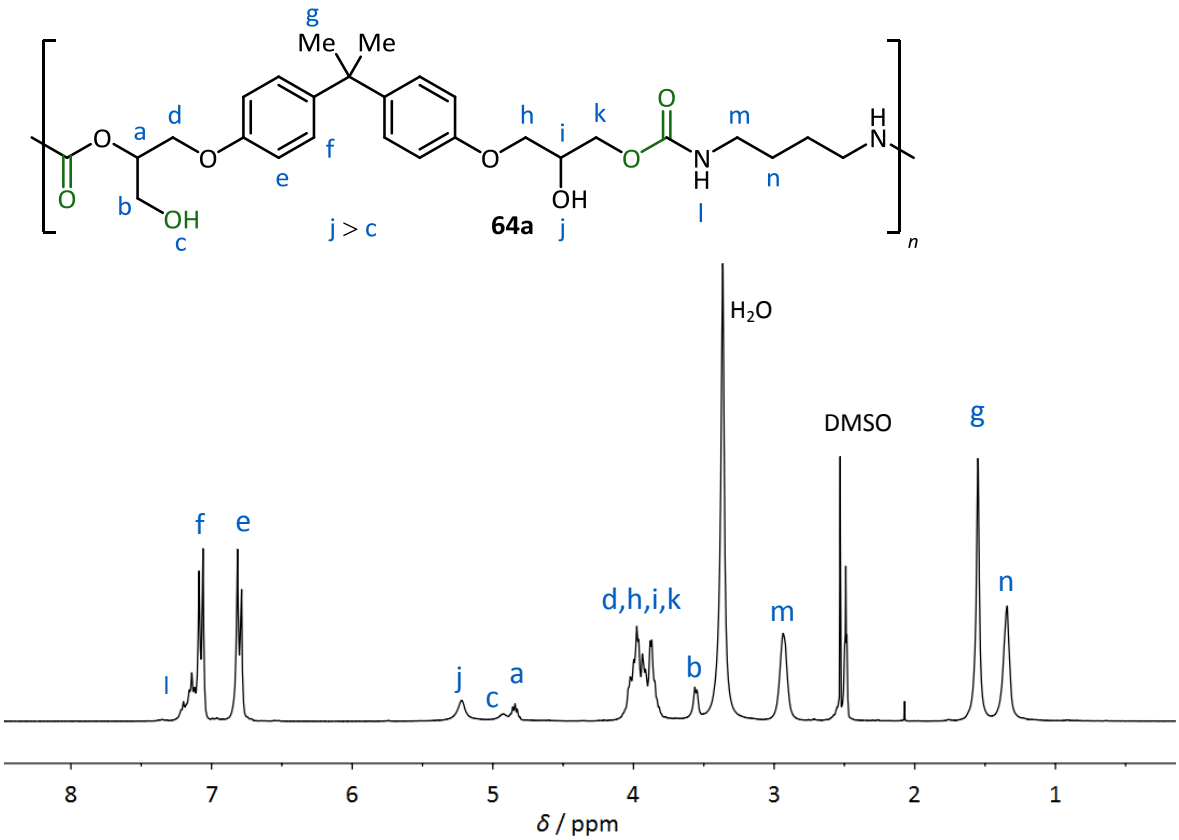

Figure 19. ^{1}H NMR of linear NIPU **64a**.

Additionally, conclusions about the structure could be obtained by using IR spectroscopy (see Appendix, Figure 32). The missing carbonyl vibration band $\tilde{\nu}$ = 1783 cm^{-1} of the cyclic carbonate **50d** in the IR spectra of the obtained linear NIPU **64a** showed that the consumption of the carbonate was complete. An IR band at $\tilde{\nu}$ = 1694 cm^{-1} and 1508 cm^{-1} could be assigned to the urethane group of the polymer **64a**.[104, 147] Furthermore, a band at $\tilde{\nu}$ = 3331 cm^{-1} belonged to the OH- and NH-group of the linear NIPU.

To determine the molar mass, gel permeation chromatography (GPC) was performed. As a result, a number average molar mass of M_n = 11940 g·mol^{-1} and a mass average molar mass of M_w = 26880 g·mol^{-1} were measured. A dispersity of $Đ$ = 2.25 was obtained (Table 11, entry 1).

Furthermore, the glass transition temperature (T_g) was measured using a DSC apparatus. Here, a T_g of 6.57 °C (onset) / 15.55 °C (middle point) was determined (Appendix, Figure 34). At higher temperatures decomposition of the polymer was observed. The

decomposition was further investigated by thermogravimetric analysis (TGA). The polymer was heated up to 500 °C (5 K·min^{-1}) and the decrease in weight of the sample was monitored. A weight loss of 5% was observed at 225 °C ($T_{d\ 5\%}$). Therefore, the obtained polymer can be regarded as thermally relatively stable.

With the intent to obtain the non-isocyanate polyurethane by starting directly from the epoxide the influence of tri-*n*-butyl-(2-hydroxyethyl)ammonium iodide (**45a**), used for converting epoxides to the corresponding cyclic carbonates, on the polymerization under the standard reaction conditions was tested (Table 11, entry 2). The obtained polymer **64a** showed a molar mass of M_n = 12110 g·mol^{-1} and M_w = 25560 g·mol^{-1} and a degree of polymerization of DP_n = 23.4. The glass transition differed with a T_g of 12.77 °C (onset) / 23.51 °C (middle point) slightly from the obtained polymer without the addition of tri-*n*-butyl-(2-hydroxyethyl)ammonium iodide (**45a**) (Appendix, Figure 34).

Table 11. Comparison of NIPU **64a** and **82** obtained through different reaction procedures.[a]

Entry	Cat.[b]	Reactant	Solvent	T / h	M_n / g·mol^{-1}	$Đ$	T_g / °C	$T_{d\ 5\%}$ / °C	Yield / %
1	-	**50d**	DMSO	24	11940	2.25	6.57	225	84[c]
2	**45a**	**50d**	DMSO	24	12100	2.12	12.77	146	93[c]
3	-	**50d**	DMSO	1	3320	1.49	-	-	55[d]
4	**45a**	**50d**	DMSO	1	3270	1.51	-	-	54[d]
5[e]	**45a**	**49d**	DMSO	24	11500	2.38	22.69	169	81[c]
6[e]	**45a**	**49d**	NMP	24	4590	1.85	25.80	-	89[c]
7[e]	**45a**	**49d**	MEK	24	2320	1.83	22.09	-	82[c]
8[f]	**45a**	**57**	DMSO	24	-	-	99.52	231	94[c]
9[e][f]	**45a**	**56**	DMSO	24	-	-	66.80	106	93[c]

[a] Reaction conditions: 3 mmol **50d**, 3 mmol **62f**, 100 °C, 3 mL solvent, pressure tube. [b] 2 mol% Catalyst **45a**. [c] Isolated yield [d] Determined by ^{1}H NMR. [e] Sequential one pot procedure: 1. 2 mol% **45a**, 3 mmol **49d**, 1 mL solvent, 90 °C, 14 h, $p(CO_2)$ = 10 bar. 2. 3 mmol Diamine **62f**, 100 °C, 24 h, 2 mL solvent. [f] 4.5 mmol **62f**.

Furthermore, the reaction was carried out with and without a catalyst at 90 °C for 1 h (Table 11, entry 3 and 4). A molecular weight of M_n = 3320 g·mol^{-1} and M_w = 4930 g·mol^{-1} without the amine salt **45a** was obtained (Table 11, entry 3). By adding 2 mol% of the catalyst **45a** a molecular weight of M_n = 3270 g·mol^{-1} and M_w = 4960 g·mol^{-1} was

measured (Table 11, entry 4). Additionally, the conversion of the carbonate **50d** was determined by ^{1}H NMR using 4,6-dimethoxypyrimidine as a standard. For the reaction without a catalyst a conversion to the cyclic carbonate of 55% was obtained. The conversion to the carbonate by employing the amine salt **45a** resulted in a conversion of 54%. Subsequently, the addition of the ammonium salt **45a** showed no negative effect on the polymerization reaction. As a consequence, a sequential one pot procedure was conducted and although it showed lower yields, the obtained molecular weights were similar to the reactions using the beforehand isolated dicarbonate **50d** (Table 11, entries 2 and 5). Since the carbonate and the polymer were solid at room temperature NMP and MEK were tested for the sequential one pot reaction (Table 11, entries 6 and 7). While using DMSO as a solvent the reaction showed little difference if used with or without an ammonium salt. The molecular weight dropped to M_n = 4590 g·mol^{-1} using NMP and further to M_n = 2320 g·mol^{-1} using MEK as a solvent. As a conclusion, DMSO was the best tested solvent for obtaining polymers with higher molecular weights. Additionally, it is possible to influence and regulate the polymerization using different solvents and thereby obtaining different molecular masses.

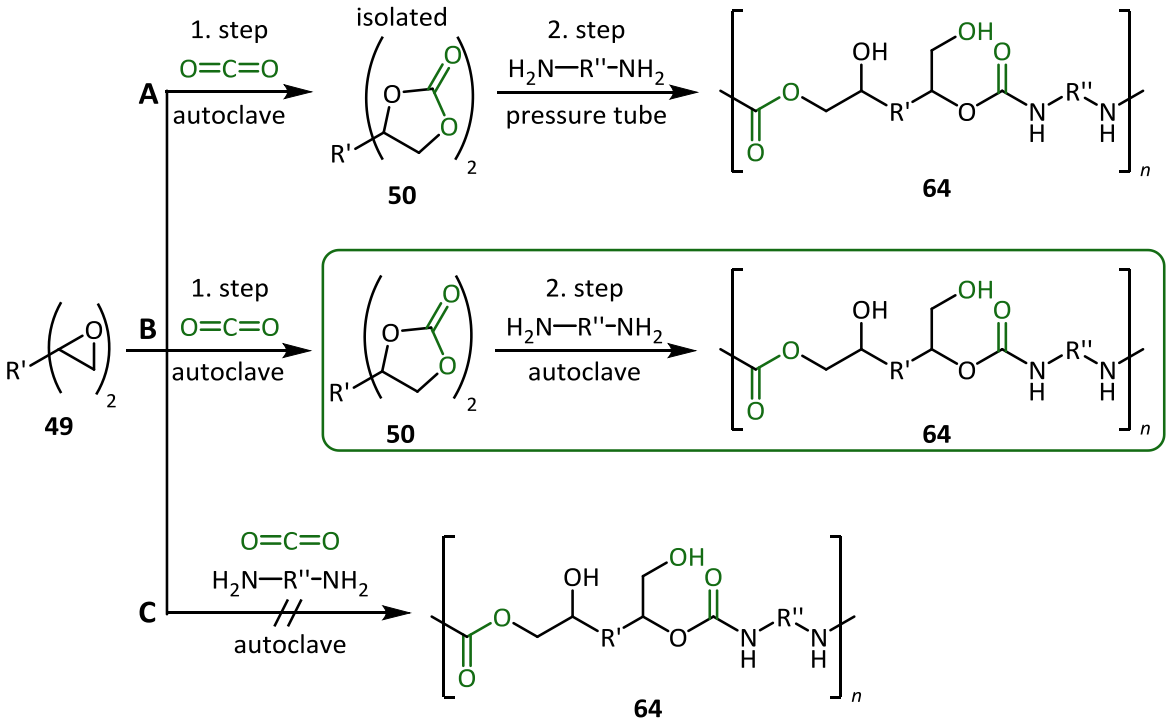

Scheme 25. Different methods tested to obtain the linear NIPUs **64**.

To summarize, the reaction of the beforehand isolated carbonate **50d** with a diamine **62f** in a pressure tube (Scheme 25, path A) and the sequential one pot reaction in an

autoclave starting from the epoxide **49d** led to the desired products (Scheme 25, path B). Additionally, we tested the method of a one pot polymerization reaction starting from the epoxide **49d** and directly adding the diamine **62f** (Scheme 25, path C). Unfortunately, this method did not lead to the desired product. No decreasing of the CO_2 pressure was observed and the reaction mixture neither showed the typical IR absorption band for a cyclic carbonate, nor the typical IR absorption band of the polymer. As a conclusion, the sequential one pot procedure to synthesize non-isocyanate polyurethanes was assessed as the best method.

Consequently, we applied the sequential one pot procedure and the procedure starting from the isolated cyclic carbonate to synthesize a cross-linked NIPU. Therefore, reactants with more than two moieties were utilized (Table 11, entries 8 and 9). As a prepolymer we used 1,3,5-tris(oxiran-2-ylmethyl)-1,3,5-triazinane-2,4,6-trione (**56**) and the corresponding cyclic carbonate 1,3,5-tris((2-oxo-1,3-dioxolan-4-yl)methyl)-1,3,5-triazinane-2,4,6-trione (**57**). The reactants inherent a typical structure element of the classical polyisocyanurate (PIR) chemistry.[148] Therefore, the expected polymer **82** has a huge potential for application e. g. as an insulation material.[116, 148]

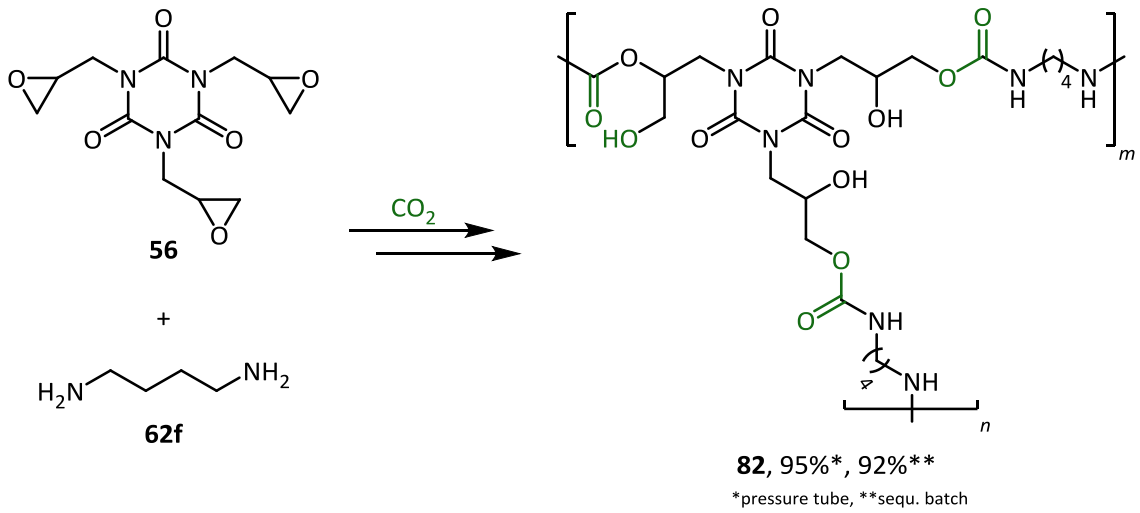

Scheme 26. Synthesis of cross-linked NIPU **82**.

First, the reaction was carried out starting from the isolated cyclic carbonate **57** in a pressure tube (Table 11, entry 8) and in a sequential one pot reaction starting from the epoxide **56** in an autoclave (Table 11, entry 9). After a short time a gel-like transparent product could be observed. The polymer **82** was insoluble in common organic solvents. Therefore, NMR and GPC studies of the polymer could not be conducted. The IR spectra

of the obtained products showed no absorption of a carbonyl band at $\tilde{\nu}$ = 1682 cm^{-1} belonging to the reactant **56** and absorptions belonging to urethane, amine and alcohol groups of the product **82** were observed (Appendix, Figure 33).

A glass transition temperature (T_g) of 99.52 °C onset (104.41 °C middle point) was measured for the reaction using the isolated cyclic carbonate (Table 11, entry 8). Furthermore, an endothermic peak in the graph of the differential scanning calorimetry heating curve indicates that part of the obtained cross-linked polymer **82** is crystalline.[149] A melting point of the cross-linked polymer at 255.53 °C was determined. Near the melting point exothermic decomposition and evaporation of the decomposition products was observed. Additionally, thermogravimetric analysis coupled with a mass spectrometry (TGA-MS) was conducted to determine the decomposition temperature ($T_{d\,5\%}$) of the polymer **82** and to observe the decomposition products. The samples were heated up to 500 °C (5 K·min^{-1}) starting from room temperature. A decomposition temperature of 231 °C ($T_{d\,5\%}$) was determined and carbon dioxide could be observed as a decomposition product (Figure 20).

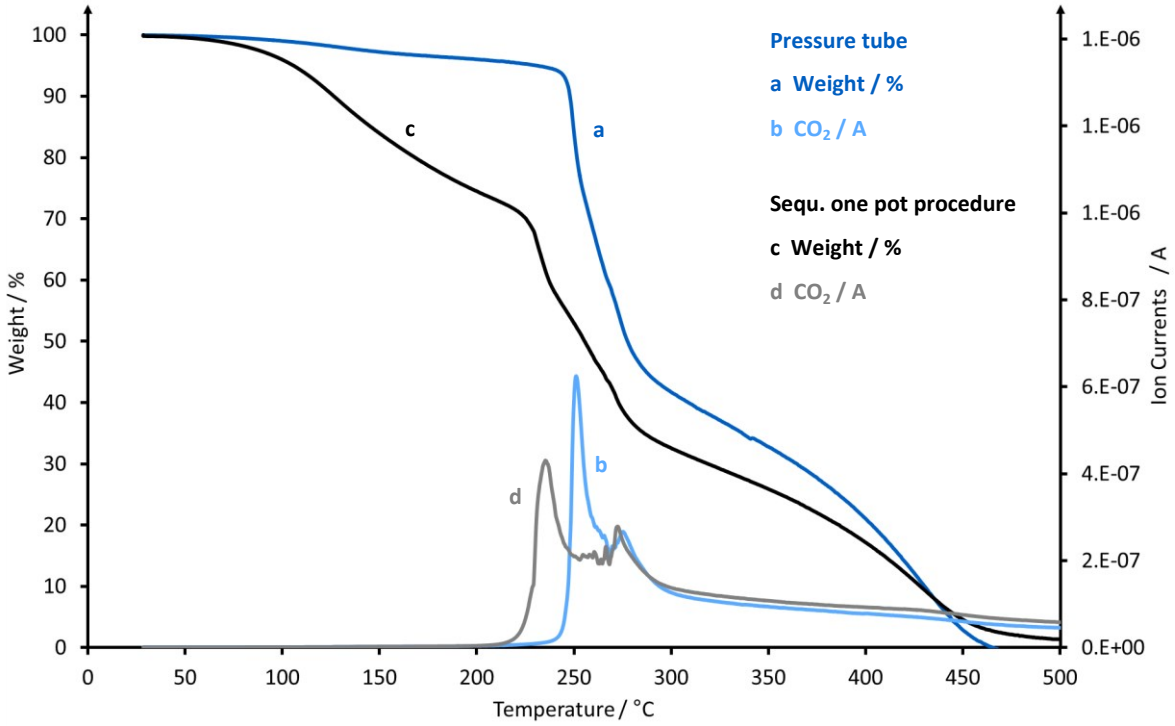

Figure 20. TGA-MS of cross-linked NIPU **82** obtained though different procedures.

The T_g-value of the product **82** of the sequential one pot reaction was with 66.8 °C onset and 78.80 °C middle point significantly lower than the T_g-values of the polymer obtained

by adding no catalyst and starting from the isolated cyclic carbonate (Table 11, entry 9 and Appendix, Figure 35). Also no enthalpy relaxation was observed. The melting point 202.29 °C and decomposition temperature were also lower (Table 11, entries 8 and 9 and Appendix, Figure 35). To conclude, the presence of the catalyst in the sequential one pot reaction led to a cross-linked polymer with a lower glass transition, melting and decomposition temperature. Therefore, it is to assume that the molecular weights of both cross-linked polymers **82** obtained through different reaction procedures also vary.
The decomposition was further investigated by using thermogravimetric analysis. A decomposition temperature of 106 °C ($T_{d\,5\%}$) was determined (Figure 20). In comparison to the linear polymer **64a** the glass transition temperature of the cross-linked polymers are higher (Table 11). This can be explained by the higher rigidity of these polymers compared to the linear NIPUs.

This reduced flexibility then results in a higher temperature for the glass transition. The thermal behavior is certainly influenced by the primary and secondary alcohols in the polymer chain of the obtained linear and cross-linked NIPUs. In fact, the influence of the hydroxyl functions on the thermal properties on the polymers is not to be underestimated.[147, 150] Additionally, the intramolecular hydrogen bonding between the alcohol and urethane functions seems to be responsible for lowering the liability of the backbone to hydrolysis.[105]

This results in a substantial increase of the chemical resistance.[151] The chemical resistance of materials containing intramolecular hydrogen bonds is known to be superior to materials without such a bond but a similar chemical structure.[152] Additionally, the linear NIPU **64a** was observed to have good optical properties like high transparency. Furthermore, the linear **64a** and the cross linked NIPU **82** were found to be luminescent when rayed with ultraviolet light (λ = 254 nm). It is to assume that the wavelength of this luminescence can be shifted to the visible light by using suitable polyfunctional cyclic carbonates and diamines.

In general, NIPUs show advantageous properties like high water absorption and thermal stability, which are superior to conventional PUs produced by polyaddition of toxic diisocyanates with diols.[105] Furthermore, the formation of hydroxyl groups can be seen as a great advantage, because they can be further functionalized. One possibility is to use the obtained PUs in consecutive block polymerization reactions.[82] It needs to be

highlighted that the polyaddition reaction of polyfunctional cyclic carbonates and diamines is a method to replace phosgene, which is needed for the synthesis of isocyanate, by CO_2. Therefore, it is a straightforward approach to develop an environmental friendly chemical processes by mitigating the need of fossil resources like petroleum, gas and coal.[100]

4.3 Dream Polymers – Polycarbonates

As stated, the utilization of CO_2 as a C–1 building block for the synthesis of polycarbonates **69** is highly attractive. Especially interesting are polymers with a high CO_2 content. This is due to the fact that the more CO_2 is incorporated lesser amount of fossil fuels are needed. Consequently, the product becomes comparatively less expensive and causes lesser impact on the environment. Furthermore, these polymers are supposed to have completely new properties like high fire resistance.[153] The expected new material properties can lead to new applications for this polymer class. Because of the theoretical possible high CO_2 content for the polymerization of formaldehyde (FA, **67**) and CO_2 this reaction is focused.

4.3.1 Formaldehyde Sources

The copolymerization of FA **67** and CO_2 is a challenging reaction, because of the reactivity of the reactants. In fact, CO_2 is relatively inert and needs to be activated, whereas gaseous FA **67** is highly reactive and adopts several forms. Therefore, the influence of different FA **67** sources as reactants was investigated (Scheme 27).

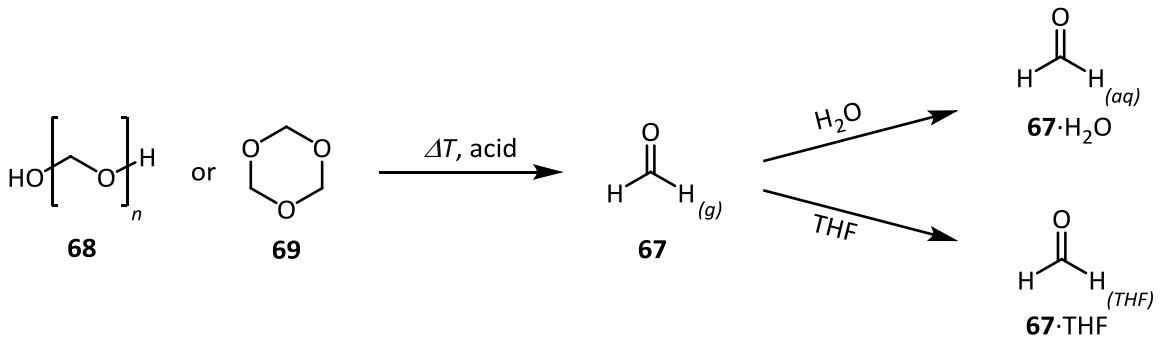

Scheme 27. Reactants **67–69** as FA sources.

In particular, the derivatives paraformaldehyde (PFA, **68**) which can be regarded as an oligomeric polyoxymethylene (POM) and trioxane (**69**), the trimer of FA **67**, are promising reactants. They are easy to handle and decompose to FA **67** through heating and/or under acidic conditions. Additionally, FA solutions in water (formalin) and THF can be used. To suppress the polymerization and oxidation process formalin **67**·H_2O is stabilized with methanol. The solution in THF is not stabilized and therefore relatively unstable. Except the FA-THF **67**·THF solution all reactants were acquired by purchase.

4.3.1.1 *Schlosser* Solution

Especially the *Schlosser* solution **67**·THF was employed to conduct the reaction under water free conditions. This is due to the fact that water may lead to chain termination of the polymeric chain.[154] The solution was produced by heating PFA **68**, THF and *p*-toluenesulfonic acid (PTSA) in flask **a** (Figure 21). The carrier gas argon (Ar) transferred the resulted FA **67** through a heated glass bridge **b** in a cooled collecting flask **c** were the solution was aggregated. In other words, a slow distillation of the solution from flask **a** to flask **c** was conducted. The gas flow was passed from flask **c** into a washing bottle. The washing bottle was equipped with a water / MeOH mixture to intercept the excess of FA **67**. The concentration of the obtained solution was determined by ^{1}H NMR using 4,6-dimethoxy pyrimidine as a standard. A concentration of 0.5 mol·L^{-1} FA **67** was obtained after 6 h, employing PTSA, an argon flow of Q(Ar) = 3–4 L·h^{-1} and a temperature of 70 °C (Appendix, Figure 31). Although, the obtained FA solutions **67**·H_2O were stored at –18 °C the FA **67** concentration dropped significantly after 24 h. Therefore, the solutions were prepared at the day of the utilization.

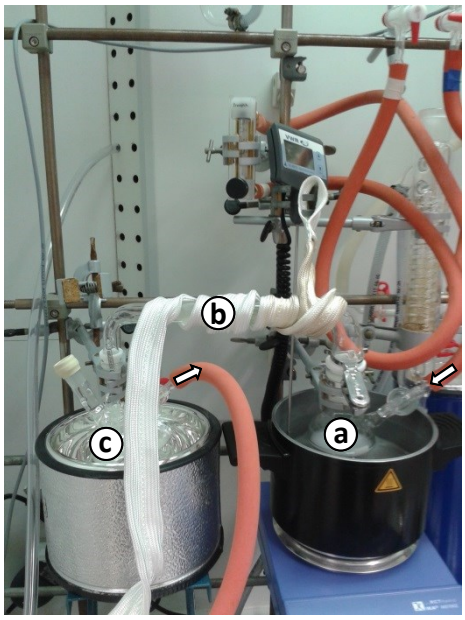

Figure 21. Setup to produce FA·THF solutions.

4.3.2 Reproduction Experiments

Little research has been conducted on the polymerization of CO_2 and FA **67**. Mainly two reports from *Sharma* and *Chiang* described this reaction so far (see Figure 6).[140-141] In reference to these two reports reproduction experiments were conducted by employing 1,4-diazabicyclo[2.2.2]octane (DABCO, **73**) and 4-dimethylaminopyridine (DMAP, **74**) as catalysts (Table 12). Highly viscous products were obtained by employing formalin as the FA **68**·H_2O source and dry ice as the CO_2 source. As a result, weight average molecular weights of M_w = 410–510 g·mol^{-1} were measured (Table 12, entries 1–3). The highest molecular weight was obtained by employing PFA **68** (Table 12, entry 4). Noteworthy, in contrast to PFA **68** which was completely insoluble in organic solvents, the obtained

products were slightly soluble in dimethylformamide (DMF) (Table 12, entry 4). IR spectroscopy showed bands at $\tilde{\nu}$ = 1770–1777 cm^{-1} which are in the region of carbonyl vibrations (Appendix, Figure 37).[155]

Table 12. Reproduction experiments.

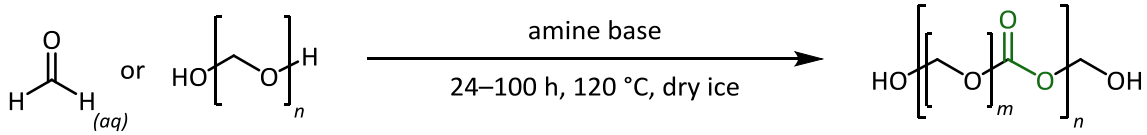

67·H_2O **68** **71**

Entry	Reactant	Catalyst	t / h	$\tilde{\nu}$ / cm^{-1}	M_n / g·mol^{-1}	M_w / g·mol^{-1}	$Đ$	Yield / g
1[a]	Formalin **67**	DABCO **73**	100	1770	480	510	1.06	1.80
2[b]	Formalin **67**	DMAP **74**	100	1775	450	470	1.04	1.89
3[b]	Formalin **67**	DMAP **74**	24	1650	400	410	1.03	1.88
4[c]	PFA **68**	DMAP **74**	48	1777	530	980	1.85	1.40

[a] 10 mL Formalin (37 wt%), 3.29 mol% DABCO **73**. [b] 10 mL Formalin (37 wt%), 15.5 wt% DMAP **74**. [c] 1.50 g PFA **68**, 15.5 wt% DMAP **74**, 4 mL dioxane.

To exclude the possibility that the carbonyl bands which were measured through IR spectroscopy belonged to a stable base-CO_2 adduct we employed the same reaction conditions without the reactant. Here, no carbonyl band was observed (Appendix, Figure 37). Therefore, the band was assigned to the carbonyl groups of the targeted product **71**.

Additionally, the ^{13}C NMR spectra of the products showed signals in the region δ = 170–175 ppm. By applying distortionless enhancement by polarization transfer measurements (DEPT) the chemical shift could be assigned to quaternary carbon atoms, thereby indicating the formation of carbonate groups.

To conclude, the reported molecular weights of up to 85000 g·mol^{-1} were experimentally not reproducible. However, IR- and NMR-spectra indicated the formation of a carbonyl group and thereby the incorporation of CO_2 in the polymeric chain of the product (Appendix, Figure 37).

4.3.3 Amine Bases

Since other purine and pyrimidine bases are reported to build base-CO_2 adducts, 1,5,7-triazabicyclo[4.4.0]dec-5-ene (TBD, **83**) was representatively employed for the polymerization reaction (Figure 22).[4a, 16b, 156]

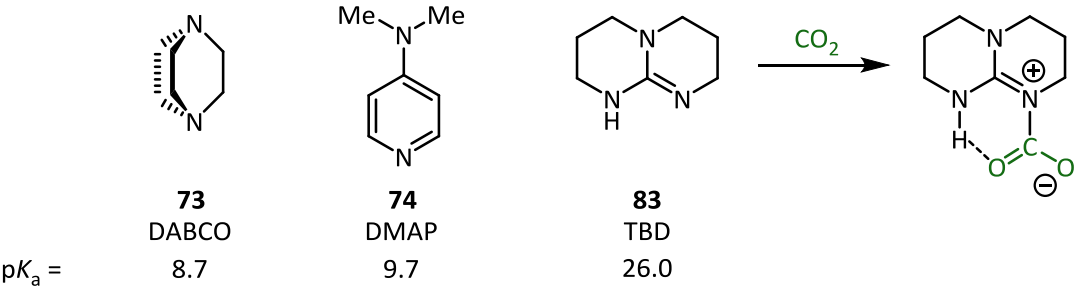

	73	**74**	**83**
	DABCO	DMAP	TBD
pK_a =	8.7	9.7	26.0

Figure 22. Selected amine bases with pK_a values and the CO_2 adduct of TBD **83**.[157]

In fact, TBD **83** possesses a high pK_a value of 26.0.[157b] As a consequence, it is a more suitable candidate to activate CO_2 by building CO_2-adducts than for example the bases DABCO **73** and DMAP **74**.[4a, 16b, 156b, 157a, 158]

Table 13. Utilization of amine bases.

Entry	Reactant		Catalyst		$\tilde{\nu}$ / cm^{-1}	M_n / g·mol^{-1}	M_w / g·mol^{-1}	$Đ$	Yield / g
1[a]	Formalin	**67**	DMAP	**74**	1766	380	570	1.50	0.94
2[a]	Formalin	**67**	DABCO	**73**	1768	500	540	1.10	0.83
3[a]	Formalin	**67**	TBD	**83**	1774	530	650	1.23	1.17
4[b]	PFA	**68**	DABCO	**73**	1771	500	510	1.02	0.34
5[b]	PFA	**68**	TBD	**83**	1767	560	630	1.13	0.29

Reaction conditions: 15 wt% catalyst, $p(CO_2)$ = 40 bar, T = 150 °C, 24 h. [a] 4.06 g Formalin (37 wt%) **67**. [b] 1.10 g PFA **68**, 4 mL dioxane.

The utilization of TBD **83** as a catalyst resulted in the product with the highest number and weight average molecular weight. Additionally, good yields were obtained (Table 13, entries 3 and 5). Therefore, TBD **83** was used for further reaction parameter screening in combination with other salts as a cocatalyst. Here, PFA **68** was used preferably for the following copolymerization reactions. This is due to the fact that formalin is an aqueous FA solution which is stabilized by methanol **13**. Both MeOH **13** and water may lead to a chain termination.[140, 154] In contrast, PFA **68** is reported to decompose at higher

temperatures. Furthermore, the basic catalysts were observed to catalyze the decomposition of PFA **68**.[140] As stated, is the formed gaseous FA highly reactive and tends to react with itself. Therefore, it is likely that self-condensation products (carbohydrates) are also formed as side products.[159]

4.3.4 Imidazolium Salts and Amine Bases

Several *N*-heterocyclic salts were employed combined with TBD **83** to catalyze the copolymerization of FA **67** and CO_2. Especially, 1,3-bis(2,6-diisopropylphenyl) imidazolium chlorid (IPr · HCl, **84a**) led to products with higher weight average molecular weights (M_w) (Scheme 28). First, the parameter screening of IPr · HCl **84a** with TBD 83 are discussed and later the influence of different salts are shown.

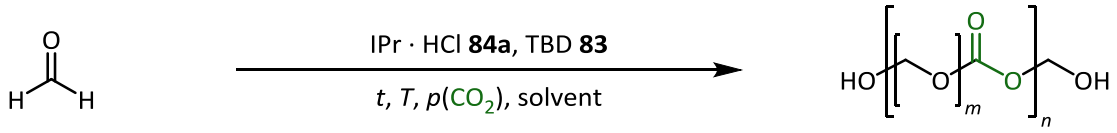

67 **71**

Scheme 28. Utilization of IPR · HCl **84a** as a catalyst for the copolymerization.

4.3.4.1 Influence of the Solvents

The influence of the solvent on the copolymerization was investigated. Therefore, polar aprotic (THF, NEt_3, NMP, MeCN, pyridine, MEK), polar protic (*n*-butanol) and nonpolar (toluene, dioxane) solvents were employed (Table 14, entries 1–9). Furthermore, the copolymerization was carried out under neat conditions (Table 14, entry 10).

Table 14. Influence of different solvents on the copolymerization.[a]

Entry	Solvent	$\tilde{\nu}$ / cm^{-1}	M_n / g·mol^{-1}	M_w / g·mol^{-1}	$Đ$	Yield / g
1	THF	1708	480	2350	4.90	1.016
2	Toluene	1700	500	1980	4.00	1.077
3	*n*-Butanol	1722	510	1300	2.55	0.956
4	Dioxane	1705	430	1250	2.91	0.891
5	NEt_3	1700	470	1170	2.49	0.979
6	NMP	1724	450	750	1.67	1.150
7	MeCN	1710	450	730	1.62	0.786

Table 14. Continued.

8	Pyridine	1707	440	680	1.55	0.976
9	MEK	1703	410	660	1.61	1.154
10	-	1779	570	770	1.35	1.094

[a] Reaction conditions: 1.00 g PFA **68**, 10 wt% IPr · HCl **84a** / TBD **83** (1:1), $p(CO_2)$ = 40 bar, T = 140 °C, 16 h, 5 mL solvent.

Furthermore, the copolymerization was carried out under neat conditions (Table 14, entry 10). The highest molecular weight was observed by employing THF as a solvent (Table 14, entry 1). Here, a weight average molecular weight of M_w = 2350 g·mol^{-1} was measured. As a consequence, THF was used for further screening reactions.

4.3.4.2 Concentration

Since the utilization of THF resulted in the product with the highest weight average molecular weight (M_w) the optimal quantity of THF was investigated. Therefore, an amount of 0–20 mL THF was employed (Table 15). The number average molecular weight (M_n) of the obtained product did not differ much. However, the highest M_w was reached by applying 5 mL THF.

Table 15. Influence of the solvent amount on the copolymerization.[a]

Entry	c / g_{PFA}·mL^{-1}	$\tilde{\nu}$ / cm^{-1}	M_n / g·mol^{-1}	M_w / g·mol^{-1}	$Đ$	Yield / g
1	-	1779	570	770	1.35	1.094
2	1	1715	470	700	1.49	1.128
3	0.2	1708	480	2350	4.90	1.016
4	0.1	1715	240	2190	9.13	1.034
5	0.07	1711	470	2080	4.43	0.999
6	0.05	1715	490	1810	3.70	0.995

[a] Reaction conditions: 1.00 g PFA **68**, 10 wt% IPr · HCl **84a** / TBD **83** (1:1), $p(CO_2)$ = 40 bar, T = 140 °C, 16 h, 0–20 mL THF.

Utilizing lower amounts of THF lead to a decreased weight average molecular weight of M_w = 700 g·mol^{-1}. Likewise, using 20 mL THF the molecular weight dropped to M_w = 1810 g·mol^{-1}. For further screening reactions 5 mL THF were applied.

4.3.4.3 Cocatalyst

Subsequently, various cocatalysts were employed in combination with IPr · HCl **84a**. More specifically, the amine bases TBD **83**, DMAP **73**, DABCO **73**, NEt_3 **85** and DBU **86** were screened (Table 16, entries 1–5). Furthermore, the activity of triphenylphosphine (PPh_3, **52**) was tested (entry 6).

Table 16. Influence of the cocatalyst on the copolymerization.[a]

Entry	Cocat.		$\tilde{\nu}$ / cm^{-1}	M_n / $g \cdot mol^{-1}$	M_w / $g \cdot mol^{-1}$	$Đ$	Yield / g
1	TBD	**83**	1708	480	2350	4.90	1.016
2	DMAP	**74**	1738	470	2200	4.68	1.104
3	DABCO	**73**	1711	280	380	1.36	1.002
4	NEt_3	**85**	1707	450	1070	2.38	0.785
5	DBU	**86**	1714	430	2200	5.12	0.935
6	PPh_3	**52**	1715	400	2060	5.15	0.950

[a] Reaction conditions: 1.00 g PFA **68**, 10 wt% IPr · HCl **84a** / cocatalyst (1:1), $p(CO_2)$ = 40 bar, T = 140 °C, 16 h, 5 mL THF.

The cocatalysts TBD **83**, DMAP **74**, DBU **85** and PPh_3 **52** led to products with molecular weights $M_w > 2000\ g \cdot mol^{-1}$ (Table 16, entries 1, 2, 5 and 6). The highest molecular weight was obtained utilizing the guanidine base TBD **83**. Here, a molecular weight of $M_w = 2350\ g \cdot mol^{-1}$ was measured using gel permeation chromatography (Table 16, entry 1).

4.3.4.4 Comparison of Formaldehyde Sources

Additionally, the influence of different FA sources was investigated. Therefore, PFA **68**, which can be regarded as a oligomeric polyoxymethylene (POM), formalin **67**·H_2O, trioxane (**69**) and a THF-FA solution (*Schlosser* solution, **67**·THF)[133] were employed (Table 17).

In particular, the *Schlosser* solution **67**·THF was employed to conduct the reaction under water free conditions. This is due to the fact that water may lead to chain termination of the polymeric chain. The used solutions were observed to be very unstable and repolymerization of FA occurred after a short time. The employment of trioxane (**69**), formalin **67**·H_2O and the *Schlosser* solution **67**·THF led to products with low molecular

weights of M_w = 310–550 g·mol^{-1} (Table 17, entries 1–3). By using PFA **68** a significantly higher molecular weight of M_w = 2350 g·mol^{-1} was obtained (Table 17, entry 4).

Table 17. Influence of different FA sources **67–69**.

Entry	Reactant	$\tilde{\nu}$ / cm^{-1}	M_n / g·mol^{-1}	M_w / g·mol^{-1}	$Đ$	Yield / g
1[a]	PFA, **68**	1708	480	2350	4.90	1.016
2[b]	Formalin, **67**·H_2O	1772	430	550	1.28	0.793
3[c]	Trioxane, **69**	-	330	370	1.12	0.301
6[d]	*Schlosser*, **67**·THF	1730	280	310	1.11	0.203

Reaction conditions: 10 wt% IPr · HCl **84a** / TBD **83** (1:1), $p(CO_2)$ = 40 bar, T = 140 °C, 16 h. [a] 1.00 g PFA **68**, 5 mL THF. [b] 2.70 g FA **67**. [c] 1.00 g Trioxane **69**, THF. [d] 5 mL FA-THF-solution **67** (0.5 mol·L^{-1}).

Since PFA **68** is the best to handle FA **67** source and the employment for the polymerization with CO_2 showed the highest molecular weight (Table 17, entry 4), it was used for further screening reactions.

4.3.4.5 Pressure Dependency

The effect of different operating pressures on the reaction was tested. It was assumed that the polymerization is dependent on the availability of CO_2 as one of the reactants. To influence this availability a CO_2 pressure between 10–50 bar was employed (Table 18).

Table 18. Influence of the CO_2 pressure on the copolymerization.[a]

Entry	p / bar	$\tilde{\nu}$ / cm^{-1}	M_n / g·mol^{-1}	M_w / g·mol^{-1}	$Đ$	Yield / g
1	10	1705	440	1420	3.23	1.022
2	20	1705	450	1870	4.16	1.069
3	30	1715	460	2220	4.83	0.950
4	40	1708	480	2350	4.90	1.016
5	50	1705	460	2210	4.80	1.201

[a] Reaction conditions: 1.00 g PFA **68**, 10 wt% IPr · HCl **84a** / TBD **83** (1:1), $p(CO_2)$ = 10–50 bar, T = 140 °C, 16 h, 5 mL THF.

As a result, the influence of the CO_2 pressure was noticeable below 30 bar (Table 18, entries 1 and 2). The weight molecular mass was reduced up to M_w = 1420 g·mol^{-1} at a CO_2 pressure of 10 bar (Table 18, entry 1). It was thereby shown that the reduced

availability of CO_2 influenced the polymerization by leading to lower molecular weights. By employing higher CO_2 pressures higher molecular weights were measured (Table 18, entry 2–5). The highest molecular weight was observed at $p(CO_2)$ = 40 bar and molecular weights of M_n = 480 g·mol^{-1} and M_w = 2350 g·mol^{-1} were ascertained (Table 18, entry 4). The highest possible CO_2 pressure of the setup of $p(CO_2)$ = 50 bar did not lead to a further improvement of the average molecular weight (Table 18, entry 5). Therefore, further screening reactions were carried out at a CO_2 pressure of 40 bar.

4.3.4.6 Temperature Dependency

The influence of the reaction temperature on the copolymerization of FA **67** and CO_2 was studied. The temperature was varied between 80–140 °C (Table 19). Here, applying temperatures below 120 °C only low molecular weights M_w = 430–540 g·mol^{-1} were obtained (Table 19, entries 1 and 2). This is due to the fact that PFA **68** needs to decompose to FA **67** to enable the copolymerization. This decomposition is only described to occur at higher temperatures.[140] Consequently, the utilization of 120 °C led to an increase of the weight average molecular weight of the product to M_w = 1850 g·mol^{-1} (Table 19, entry 3). The further increase of the reaction temperature to 140 °C led to a molecular weight for the product of M_w = 2350 °C (Table 19, entry 4).

Table 19. Influence of the temperature on the copolymerization.[a]

Entry	T / °C	$\tilde{\nu}$ / cm^{-1}	M_n / g·mol^{-1}	M_w / g·mol^{-1}	$Đ$	Yield / g
1	80	1705	510	540	1.06	1.022
2	100	1705	360	430	1.19	1.069
3	120	1715	640	1850	2.89	0.950
4	140	1708	480	2350	4.90	1.016

[a] Reaction conditions: 1.00 g PFA **68**, 10 wt% IPr · HCl **84a** / TBD **83** (1:1), $p(CO_2)$ = 40 bar, T = 80–140 °C, 16 h, 5 mL THF.

It was shown that for the copolymerization reaction temperatures higher than 100 °C are needed. This can be explained by the decomposition of PFA **68** which is mainly caused by thermic decomposition. A differential scanning calorimetry (DSC) measurement was conducted and a decomposition temperature of $T_{d\,5\%}$ = 95.14 °C was determined for PFA **68**. As a consequence, further screening reactions were carried out at higher temperatures.

4.3.4.7 Influence of the Reaction Time

Additionally, the influence of the reaction time was investigated at fixed reaction temperature of 120 °C. Reaction times of t = 6–24 h were applied (Table 20). After 6 h a molecular weight of M_w = 940 g·mol^{-1} was measured (Table 20, entry 1). Subsequently, the reaction time was prolonged and the molecular weight of the polymers increased significantly. After 14 h a molecular weight of M_w = 1410 g·mol^{-1} was determined (Table 20, entry 2). At 16 h the maximum was observed with a molecular weight of M_w = 1850 g·mol^{-1} (Table 20, entry 3). Further prolonging of the reaction time to 24 h did show a similar M_w of 1840 g·mol^{-1} and a lower M_n of 420 g·mol^{-1} (Table 20, entry 4).

Table 20. Influence of the reaction time on the copolymerization.[a]

Entry	t / h	$\tilde{\nu}$ / cm^{-1}	M_n / g·mol^{-1}	M_w / g·mol^{-1}	$Đ$	Yield / g
1	6	1711	560	940	1.68	1.200
2	14	1712	550	1410	2.56	1.210
3	16	1713	610	1850	3.03	1.229
4	24	1706	420	1840	4.38	1.120

[a] Reaction conditions: 1.00 g PFA **68**, 10 wt% IPr · HCl **84a** / TBD **83** (1:1), $p(CO_2)$ = 40 bar, T = 120 °C, 6–24 h, 5 mL THF.

As a result, the highest M_n and M_w were obtained at a reaction time of 16 h (Table 20, entry 3). Consequently, following reactions were conducted at a reaction time of 16 h.

4.3.4.8 Catalyst Loading

The influence of the catalyst amount on the copolymerization of CO_2 and PFA **68** was tested (Table 21). Therefore, catalyst loadings of 0.025–20 wt% of the imidazolium salt IPr · HCl **84a** in combination with TBD **83** were employed in a ratio of 1 : 1. A low molecular weight of M_w = 500 g·mol^{-1} was measured for the employment of 0.025 mol% of the catalyst **84a** (Table 21, entry 1). The molecular weight and the yield increased strongly up to M_w = 1760 g·mol^{-1}, employing a higher catalyst loading of 0.05 mol% and 0.1 mol% (Table 21, entries 2 and 3). The utilization of 1.0 and 5.0 mol% of **84a** did not show a further improvement regarding the molecular weight (Table 21, entries 4 and 5). The maximum was observed by employing 10 wt % IPr · HCl **84a** and TBD **83** (Table 21, entries 4 and 6).

Table 21. Influence of the catalyst loading on the copolymerization.[a]

Entry	Cat. / wt%	$\tilde{\nu}$ / cm^{-1}	M_n / g·mol^{-1}	M_w / g·mol^{-1}	$Đ$	Yield / g
1	0.025	1721	505	550	1.09	0.814
2	0.05	1718	840	1300	1.55	0.600
3	0.1	1719	620	1760	2.84	0.920
4	1.0	1704	510	1740	3.41	1.019
5	5.0	1707	430	1770	4.12	0.918
6	10	1708	480	2350	4.90	1.016
7	15	1754	430	1310	3.05	0.973
8	20	1711	420	880	2.10	1.191

[a] Reaction conditions: 1.00 g PFA **68**, 0.025–20 wt% IPr · HCl **84a** / TBD **83** (1:1), $p(CO_2)$ = 40 bar, T = 140 °C, 16 h, 5 mL THF.

Higher catalyst loadings of 15–20 wt% led to lower molecular weights (Table 21, entries 7 and 8). As a consequence, following screening reactions were carried out applying 10 wt% of the catalyst IPr · HCl **84a**.

4.3.4.9 Catalyst / Cocatalyst Ratio

Additionally, the catalyst / cocatalyst ratio was investigated. The tested compositions led to products with weight average molecular weights <2000 g·mol^{-1} (Table 22, entries 2–5). The obtained results were lower than the original conditions using 10 wt% of the base **83** and the salt **84a** (Table 22, entry 1). Since the original condition gave the highest molecular weight (Table 22, entry 1), additional screening reactions were carried out using a catalyst / cocatalyst ratio of 1 : 1.

Table 22. Influence of the catalyst / cocatalyst ratio.[a]

Entry	**84a** / wt%	**83** / wt%	$\tilde{\nu}$ / cm^{-1}	M_n / g·mol^{-1}	M_w / g·mol^{-1}	$Đ$	Yield / g
1	10	10	1708	480	2350	4.90	1.016
2	10	2	1705	560	1080	1.93	0.382
3	2	10	1715	450	1400	3.11	1.024
4	10	5	1720	390	1570	4.03	0.835
5	5	10	1715	420	1250	2.98	0.911

[a] Reaction conditions: 1.00 g PFA **68**, IPr · HCl **84a** / TBD **83**, $p(CO_2)$ = 40 bar, T = 140 °C, 16 h, 5 mL THF.

4.3.4.10 Optimized Reaction Conditions

The optimized reaction parameter for the polymerization of CO_2 and PFA **68** were identified to be: 10 wt% of IPr · HCl **84a** / TBD **83**, 140 °C, 16 h, $p(CO_2)$ = 40 bar and 5 mL THF (Scheme 29).

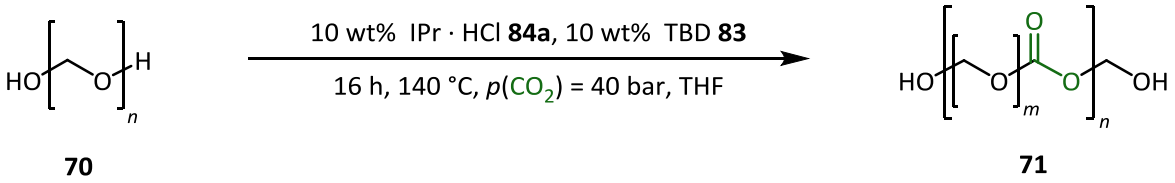

70 **71**

Scheme 29. Optimized reaction conditions.

A molecular weight of M_n = 480 g·mol^{-1} and M_w = 2350 g·mol^{-1} was obtained by applying these reaction conditions.

4.3.4.11 Structure of the Imidazolium Salt

The utilization of different imidazolium salts as catalysts for the copolymerization of FA **67** and CO_2 was tested. The optimized reaction parameters which were identified for IPr · HCl **84a** were applied (Chapter 4.4.3). The influence of the halide was investigated by employing 1,3-Bis-(2,6-diisopropylphenyl)-imidazolium iodide (**84b**) which was synthesized through ionic exchange (Scheme 30).[160]

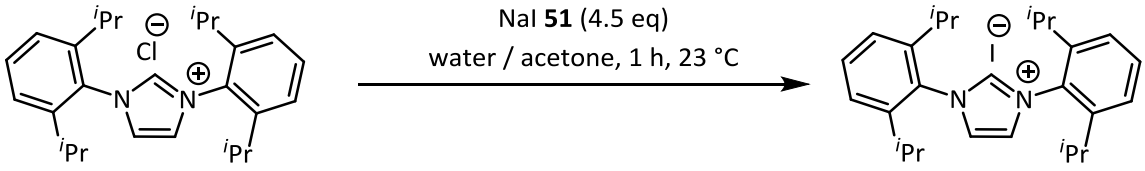

84a **84b**, 54%

Scheme 30. Synthesis of 1,3-bis(2,6-diisopropylphenyl)imidazolium iodide (**84b**).

Molecular weights >1000 g·mol^{-1} were obtained with catalysts **84b** and **87–90** (Table 23, entries 2–5 and 7–9). However, the benchmark reaction of the optimized reaction using IPr · HCl **84a** and TBD **83** led to a product with a higher molecular weight than the other imidazolium salts (Table 23, entry 1). Noteworthy, the employment of 1,3-diisopropyl-imidazolium tetrafluoroborate (**88**) led to particular monodisperse products ($Đ$ = 1.32) with a number average molecular weight of M_n = 1190 g·mol^{-1} and a weight average molecular weight of M_w = 1570 g·mol^{-1}.

Table 23. Screening of imidazolium salts.

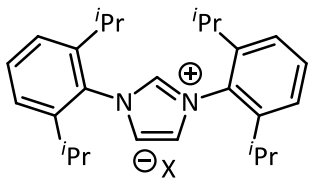

84
84a, x = Cl
84b, x = I

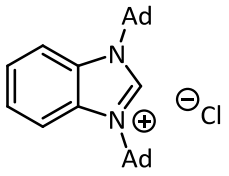

87

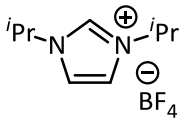

88

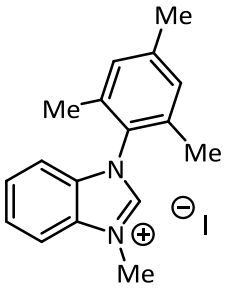

89

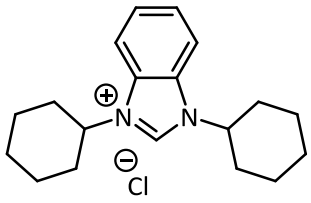

90

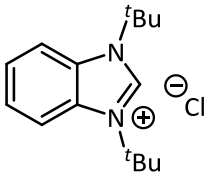

91

Entry	Cat. / wt%		$\tilde{\nu}$ / cm^{-1}	M_n / g·mol^{-1}	M_w / g·mol^{-1}	$Đ$	Yield / g
1	10	**84a**	1708	480	2350	4.90	1.016
2	1	**84a**	1704	510	1740	3.41	1.019
3	10	**84b**	1705	500	1500	3.00	1.001
4	1	**84b**	1713	560	1050	1.88	0.788
5	1	**87**	1772	890	1020	1.15	0.459
6	10	**88**	1776	340	680	2.00	1.108
7	1	**88**	1772	1190	1570	1.32	0.849
8	1	**89**	1717	615	1010	1.64	0.760
9	1	**90**	1704	880	1180	1.34	0.727
10	1	**91**	1766	770	840	1.09	0.293

1.0 g PFA **68**, 1–10 wt% cat. **84**, **87**–**91** / TBD **83** (1:1), 5 mL THF, $p(CO_2)$ = 40 bar, T = 140 °C, 16 h.

Therefore, the reaction conditions for the implementation of catalyst **88** were further investigated. The influence of the temperature, catalyst loading, CO_2 pressure and reaction time where investigated (Table 24). As a result, a catalyst loading of < 1 wt%, temperatures of < 140 °C and a CO_2 pressure of < 40 bar resulted in products with low molecular weights (Table 24, entries 2–4). Furthermore, the screening of the reaction time resulted in an optimal time of 16 h (Table 24, entries 1, 6 and 7). To conclude, 1 wt% of the catalyst **88**, 140 °C, 40 bar CO_2 pressure and 16 h reaction time showed the best result. The measured molecular weights were lower than for the IPr · HCl **84a** / TBD **83** catalyst system.

Table 24. Reaction conditions using the imidazolium salt **88** as a catalyst.[a]

Entry	T / °C	Cat. / wt%	$p(CO_2)$ / bar	t / h	$\tilde{\nu}$ / cm^{-1}	M_n / g·mol^{-1}	M_w / g·mol^{-1}	$Đ$	Yield / g
1	140	1	40	16	1772	1190	1570	1.32	0.849
2	120	1	40	16	1770	470	490	1.04	0.449
3	140	0.5	40	16	1739	580	700	1.21	0.615
4	140	1	10	16	1773	500	530	1.06	0.622
5	140	10	40	16	1776	550	710	1.29	1.108
6	140	1	40	24	1768	540	670	1.24	0.760
7	140	1	40	6	1700	550	630	1.15	0.830

[a] Reaction conditions: 1.00 g PFA **68**, 0.5–10 wt% cat. **88** / TBD **83** (1:1), $p(CO_2)$ = 10–40 bar, T = 120–140 °C, 6–24 h, 5 mL THF.

4.3.4.12 Influence of the Anion

The effect of different anions on the polymerization was tested. For the imidazole salt **92**, eight different counterions were tested (Table 25, entries 1–8). Here, only little influence on the molecular weight of the obtained polymers was observed. Also the employment of the imidazolium **92d** with BF_4^- as the anion, which showed good results for catalyst **88**, did not lead to a higher molecular weight (Table 25, entry 11). For the imidazolium salt **84** the best result was obtained by using chloride as the anion **84a** (Table 25, entries 9 and 10). The structural similar salt **93** with BF_4^- as the anion also showed poor performance (Table 25, entry 11).

Table 25. Influence of different counter ions.

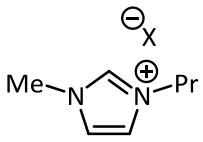

92

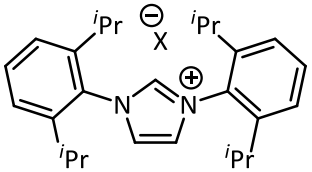

84

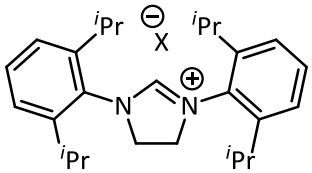

93

Entry	Cat.	X	$\tilde{\nu}$ / cm^{-1}	M_n / g·mol^{-1}	M_w / g·mol^{-1}	$Đ$	Yield / g
1	**92a**	Cl	1774	540	680	1.26	0.756
2	**92b**	Br	1773	530	660	1.25	0.732
3	**92c**	I	1776	580	740	1.28	0.904
4	**92d**	BF_4	1775	560	730	1.30	0.625

Table 25. Continued.

5	**92e**	SO_3Me	1773	510	620	1.22	0.779
6	**92f**	HSO_4	1773	530	800	1.51	0.433
7	**92g**	$FeCl_4$	1772	510	700	1.37	0.616
8	**92h**	PF_6	1773	550	730	1.33	0.782
9	**84a**	Cl	1704	510	1740	3.41	1.019
10	**84b**	I	1713	560	1050	1.88	0.788
11	**93**	BF_4	1720	480	680	1.42	0.929

1.00 g PFA **68**, 1 wt% cat. **84**, **92** or **93**, 1 wt% TBD **83**, 5 mL THF, $p(CO_2)$ = 40 bar, 140 °C, 16 h.

To conclude, the choice of the anion did not have a significant influence on the molecular weights of the obtained product. The best result was still observed employing the catalyst **84a**.

4.3.5 Thiazolium Salts and TBD

Different thiazolium salts **94–96** were tested for their catalytic activity to enable the polymerization of PFA **68** and CO_2. By applying 10 wt% thiamin hydrochloride (**94a**) in combination with TBD **83** molecular weights of M_n = 350 g·mol^{-1} and M_w = 1560 g·mol^{-1} were measured (Table 26, entry 1). Furthermore, the influence of a different counter ion for **94a** was tested. The utilization of **94b** led to a significantly lower average molecular weight of M_w = 660 g·mol^{-1} (Table 26, entry 3).

Table 26. Screening of thiazolium salts **94–96** for the copolymerization.

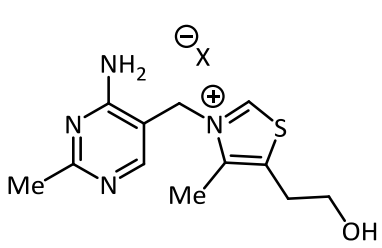

94a, X = Cl
94b, X = NO_3

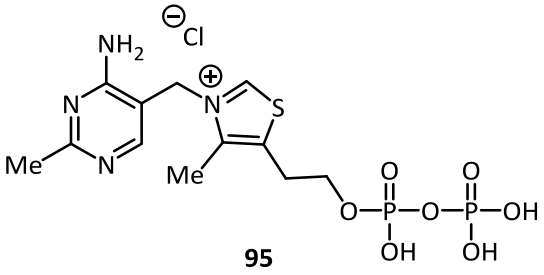

95

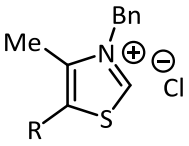

96a, R = CH_2OH
96b, R = H

Entry	Cat. / wt%		$\tilde{\nu}$ / cm^{-1}	M_n / g·mol^{-1}	M_w / g·mol^{-1}	$Đ$	Yield / g
1	10	**94a**	1770	350	1560	4.46	0.945
2	1	**94a**	1721	490	590	1.20	0.244
3	1	**94b**	1720	520	660	1.27	0.785

Table 26. Continued.

4	1	**95**	1719	510	670	1.31	0.388
5	1	**96a**	1773	1060	1300	1.23	0.762
6	10	**96a**	1700	200	2550	12.8	0.843
7	1	**96b**	1707	420	1250	2.98	0.827

1.00 g PFA **68**, 1–10 wt% cat. **94–96** / TBD **83**, 5 mL THF, $p(CO_2)$ = 40 bar, 140 °C, 16 h.

Additionally, the employment of a functionalized analog **95** led to lower molecular weights (Table 26, entry 4). Here, catalyst loadings between 0.5–10 wt% were tested. Although the use of 10 wt% of the catalyst led to the highest weight average molecular weight (M_w) of 2550 g·mol^{-1} (Table 27, entry 3), the employment of 1 wt% showed the best dispersity of $Đ$ = 1.23 and a molecular weight >1000 g·mol^{-1} (Table 27, entry 1). Consequently, the reaction time and pressure dependency were further investigated by using 1 wt% of the thiazolium salt 3-benzyl-5-(2-hydroxyethyl)-4-methylthiazolium chloride (**96a**) (Table 27, entries 5–7). As a result, the optimized reaction conditions of 1 wt% catalyst **96a**, 140 °C, 40 bar CO_2 pressure and a reaction time of 16 h led to the best results (Table 27, entry 1).

Table 27. Optimization reactions using **96a**.[a]

Entry	T / °C	Cat. / wt%	$p(CO_2)$ / bar	t / h	$\tilde{\nu}$ / cm^{-1}	M_n / g·mol^{-1}	M_w / g·mol^{-1}	$Đ$	Yield / g
1	140	1	40	16	1773	1060	1300	1.23	0.843
2	120	1	40	16	1712	550	1700	3.09	0.975
3	140	10	40	16	1700	200	2550	12.8	0.843
4	140	0.5	40	16	1722	580	740	1.28	0.816
5	140	1	10	16	1712	540	1320	2.44	0.753
6	140	1	40	24	1700	470	680	1.45	0.806
7	140	1	40	6	1700	530	680	1.28	0.830

[a] Reaction conditions: 1.00 g PFA **68**, 0.5–10 wt% cat. **96a** / TBD **83** (1:1), $p(CO_2)$ = 10–40 bar, T = 120–140 °C, 6–24 h, 5 mL THF.

To conclude, the employment of thiazolium salts did not lead to better results regarding the molecular weights of the products. The best result was still observed by using the imidazolium salt **84a**.

4.3.6 Proposed Reaction Mechanism

The reaction is proposed to take place via the CO_2 adduct of the employed imidazolium salt. In this context, the base TBD **83** is suggested to deprotonate the imidazolium salt and thereby generates the active catalyst. Additionally, TBD **83** is described to catalyze the decomposition of the mainly utilized paraformaldehyde (PFA, **68**) to generate the reactant formaldehyde (FA, **67**).[140] Since the acidic depolymerization of PFA **68** is also already known, it is likely that IPr · HCl **84a** also promotes the decomposition of PFA **68**.[130]

First, the electron rich carbon of the formed *N*-heterocyclic carbene (NHC) attacks the weak electrophilic carbon of CO_2 (Scheme 31, **A**).[161] A zwitterionic compound is generated which is structurally similar to the amine-CO_2 adduct (Scheme 31). The activated CO_2 then attacks the generate FA **67**. This is followed by propagation and the copolymer of FA **67** and CO_2 is formed.

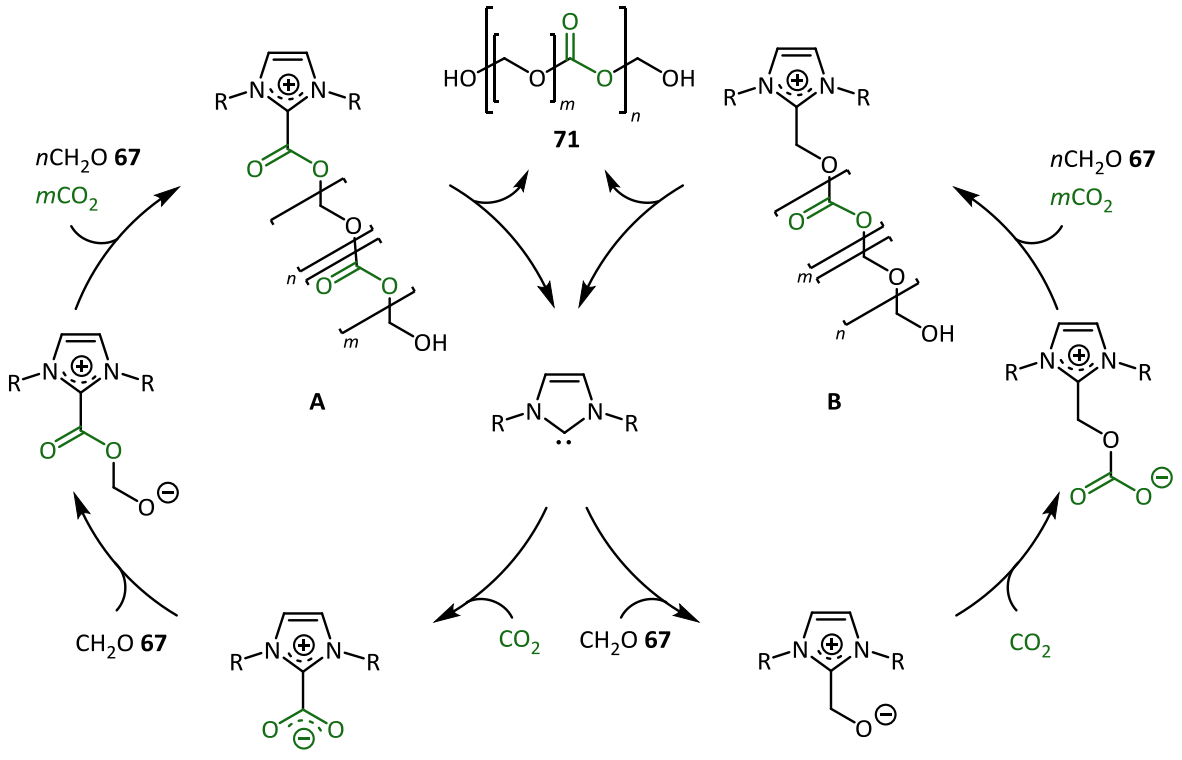

Scheme 31. Putative reaction mechanism.

Since it is reported, for a hydroxymethylation reaction were PFA **68** was employed, that NHCs can also activate aldehydes through nucleophilic attack it is also likely that the NHC attacks first the FA **67** and thereby initiating the polymerization reaction (Scheme 31, **B**).[162]

4.3.7 Imidazolium Salts without a Cocatalyst

In addition to the described catalyzed reactions of PFA **68** and CO_2 utilizing different salts and amine bases, the reaction was also conducted without the use of a cocatalyst. In particular, IPr · HCl **84a** was employed and the best reaction conditions were determined (Scheme 32).

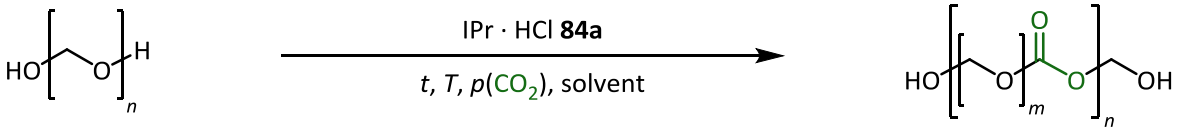

68 **71**

Scheme 32. IPr · HCl **84a** catalyzed copolymerization of PFA **68** and CO_2.

4.3.7.1 Optimization of Reaction Parameter

The optimization of the reaction parameter was carried out similar to the screening reactions of IPr · HCl **84a** in combination with TBD **83**. Therefore, the best reaction temperature, catalyst loading, operating pressure, solvent and solvent amount were tested. Hereinafter, only the results of the individual parameter are discussed. The diagrams visualizing all conducted parameter screening reactions can be found in the appendix (Figure 38).

First, the influence of the reaction time was evaluated. The obtained molecular weights were increased by employing a longer reaction time. After 16 h a weight average molecular weight of M_w = 1080 g·mol^{-1} at 120 °C was obtained (Appendix, Figure 38, a). Next, the reaction temperature was varied at a reaction time of 16 h. By increasing the reaction temperature to 140 °C a number average molecular weight of M_n = 660 g·mol^{-1} and M_w = 2970 g·mol^{-1} was measured (Appendix, Figure 38, b). Furthermore, the influence of the amount of catalyst was determined at a reaction time of 16 h and a temperature of 140 °C. (Appendix, Figure 38, c). A catalyst loading of 1–20 wt% was used. As a result, the highest molecular weight was reached by using 10 wt% of the catalyst **84a**. Furthermore, the influence of the pressure was investigated using $p(CO_2)$ = 5–50 bar. Here, a pressure of 40 bar CO_2 led to the highest molecular weights (Appendix, Figure 38, d). Additionally, the amount of the employed solvent was tested. The best result was obtained by using 5 mL THF (Appendix, Figure 38, e). To conclude, the employment of the imidazole salt IPr · HCl **84a** allowed to obtain polymers derived from

PFA **68** and CO_2. The optimized reaction parameter led to a polymer with a weight average molecular weight of M_w = 2970 g·mol^{-1}.

4.3.7.2 Influence of the Formaldehyde Source

Additionally, for the copolymerization without the base TBD **83** and only utilizing the imidazolium salt IPr · HCl **84a**, different FA sources were tested (Table 28). Only low molecular weights were obtained by using formalin (**67**·H_2O), trioxane (**69**) and the *Schlosser* solution (**67**·THF) (Table 28, entries 2–4).

Table 28. Utilization of different FA sources **67–69**.

Entry	Reactant	$\tilde{\nu}$ / cm^{-1}	M_n / g·mol^{-1}	M_w / g·mol^{-1}	$Đ$	Yield / g
1[a]	PFA, **68**	1715	660	2970	4.50	1.02
2[b]	Formalin, **67**·H_2O	1700	400	450	1.13	0.793
3[c]	Trioxane, **69**	17017	310	390	1.26	0.301
4[d]	*Schlosser,* **67**·THF	1798	280	320	1.14	0.203

Reaction conditions: 10 wt% IPr · HCl **84a**, $p(CO_2)$ = 40 bar, T = 140 °C, 16 h. [a] 1.00 g PFA **68**, 5 mL THF. [b] 2.7 g Formalin **67**·H_2O, no solvent. [c] 1.00 g Trioxane (**69**), neat conditions. [d] 5 mL FA-THF-solution **67**·THF.

Similar to the screening results utilizing TBD **83** as a cocatalyst (Chapter 4.4.3), the best result was obtained by using PFA **68**. A weight average molecular weight of M_n = 660 g·mol^{-1} and a number average molecular weight of M_w = 2970 g·mol^{-1} was determined (Table 28, entry 1).

4.3.7.3 Utilization of Different Salts

The catalytic activity of several salts were studied. More specifically, the imidazolium salts 1,3-di((3R)-adamantan-1-yl)-1H-benzo[d]imidazol-3-ium chloride (**87**) and 1,3-diisopropyl-imidazolium tetrafluoroborate (**88**), the bifunctional phosphonium salt **46c** and the thiazolium salts thiamine hydrochloride (**94a**) and 3-benzyl-5-(2-hydroxyethyl)-4-methylthiazolium chloride (**96a**) were tested under the optimized reaction conditions without a cocatalyst. Low molecular weights of M_n = 430–590 g·mol^{-1} and M_w = 510–710 g·mol^{-1} were measured (Table 29). Since the employed salts did not lead to products with higher molecular weights than the IPr · HCl **84a** salt, no further investigations were conducted.

Table 29. Screening of different salts as catalysts.

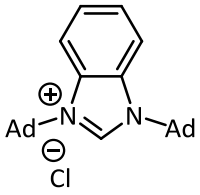

87

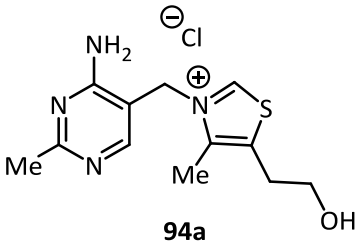

94a

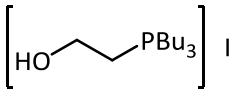

46c

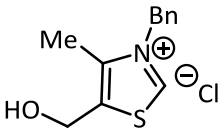

96a

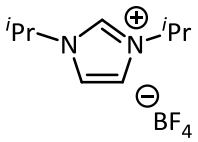

88

Entry	Cat. / wt%		$\tilde{\nu}$ / cm^{-1}	M_n / g·mol^{-1}	M_w / g·mol^{-1}	$Đ$	Yield / g
1	1	**87**	1718	500	510	1.02	0.261
2	1	**94a**	1721	490	590	1.20	0.244
3	1	**46a**	1721	590	710	1.20	0.271
4	10	**46a**	1720	430	510	1.19	0.249
5	1	**96a**	1720	490	630	1.29	0.591
6	1	**88**	1720	450	520	1.16	0.543

1.00 g PFA **68**, 1–10 wt% cat. **46a**, **87**, **88** or **96a**, 5 mL THF, $p(CO_2)$ = 40 bar, 140 °C, 16 h.

4.3.8 Comonomers

4.3.8.1 Utilizing PPG-1000 as a Comonomer

Furthermore, polypropylene glycol (**97**, PPG-1000) was employed as a bivalent alcohol. The concept was to use this alcohol with an already high molecular weight of M_n = 1000 g·mol^{-1} to obtain polymers with higher molecular weights. Therefore, different amounts of 1–50 wt% of the diol **97** were added to the reaction mixture (Table 30). The employment of 1 wt% of PPG-1000 **97** already showed a higher molecular weight of M_w = 4090 g·mol^{-1}, but a comparatively low number average molecular weight of M_n = 530 g·mol^{-1} (Table 30, entry 1). Additionally, the molecular weight was further increased using a higher amount of the diol **97**. Therefore, the amount of the diol **97** was increased to 2 wt%. This resulted in a molecular weght of M_w= 9380 g·mol^{-1} and M_n = 1800 g·mol^{-1} (Table 30, entry 2). Further increasing of the diol amount did not lead to better results (Table 30, entries 3 and 4).

Table 30. Influence of the polypropylene glycol (**97**) amount.

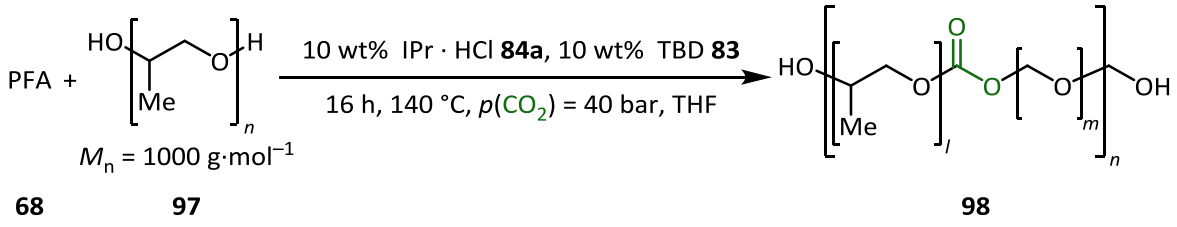

68 **97** **98**

Entry	PPG-1000 / wt%	$\tilde{\nu}$ / cm^{-1}	M_n / g·mol^{-1}	M_w / g·mol^{-1}	$Đ$	Yield / g
1	1	1704	530	4090	7.72	0.97
2	2	1705	1800	9380	5.21	1.01
3	10	1706	1750	8630	4.93	1.20
4	50	1700	1700	6600	3.88	1.40

1.00 g PFA **68**, 10 wt% IPr · HCl **84a** / TBD **83** (1:1), 1–50 wt% PPG-1000 **97**, 5 mL THF.

4.3.9 End group Protection

The product with the highest molecular weight was stabilized by adding acetic anhydride (**99**) and pyridine (**100**) directly after the polymerization to the reaction mixture.

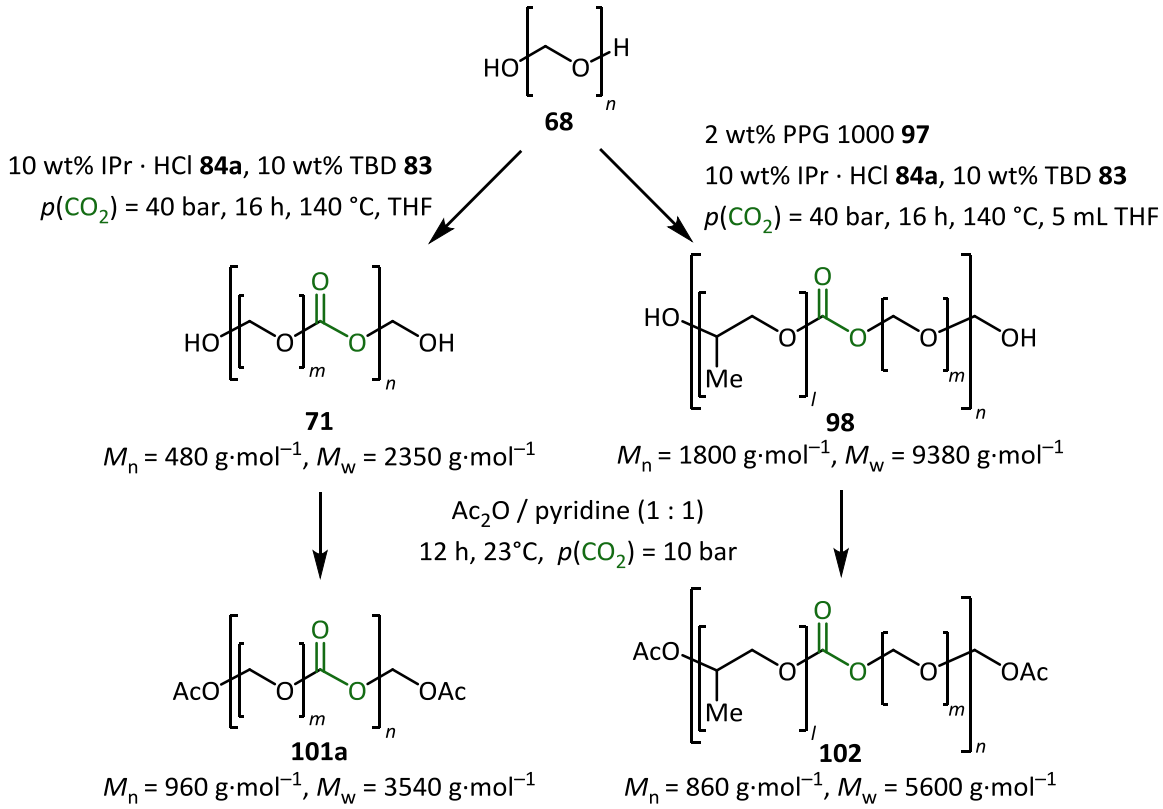

Scheme 33. End group protection.

GPC measurements were conducted and a molecular weight of M_n = 960 g·mol^{-1} and M_w = 3540 g·mol^{-1} for the polymer **101a** employing acetic anhydride (**99**) was observed (Table 30, Scheme 33). Regarding the molecular weight, this is a superior result than the molecular weight M_n = 480 g·mol^{-1} and M_w = 2350 g·mol^{-1} of the not protected polymer **71**. Here, it is highly probable that only the higher molecular weights precipitated.

Furthermore, the polyvalent alcohol PPG-1000 **97** was added and end-group protected by using acetic anhydride (**99**) and pyridine (**100**). A molecular weight of M_n = 860 g·mol^{-1} and M_w = 5600 g·mol^{-1} for **102** was measured (Scheme 33).

4.3.10 Analytical Studies

The reactions with the highest molecular weights were further investigated by conducting NMR, IR, EA, ESI, DSC, MALDI-TOF and TGA-MS measurements. The hereinafter discussed polymers are listed below (Table 31). Especially the optimized not capped polymer **71** will be discussed (Table 31, entry 1).

Table 31. Discussed polymers.

Entry	Polymer	Capped	$\tilde{\nu}$ / cm^{-1}	M_n / g·mol^{-1}	M_w / g·mol^{-1}	$Đ$	Yield / g
1	**71**	No	1707	480	2350	4.90	1.016
2[a]	**101a**	Yes	1738	960	3540	3.69	0.355
3[b]	**98**	No	1705	1800	9300	5.17	1.014
4[b, c]	**102**	Yes	1773	860	5600	6.51	0.367

Reaction conditions: 1.00 g PFA **68**, 10 wt% IPr · HCl **84a** / TBD **83** (1:1), 5 mL THF. [a] Capping: Ac_2O / pyridine (1 : 1), 23 °C, 12 h. [b] 2 wt% PPG-1000 **97**. [c] Capping: Ac_2O / pyridine (1 : 1).

4.3.10.1 IR Spectroscopy

Since carbonyl moieties are known to absorb radiation in a distinct area of $\tilde{\nu}$ = 1700–1800 cm^{-1}, IR measurements are a reliable lead for the incorporated of CO_2.[141]

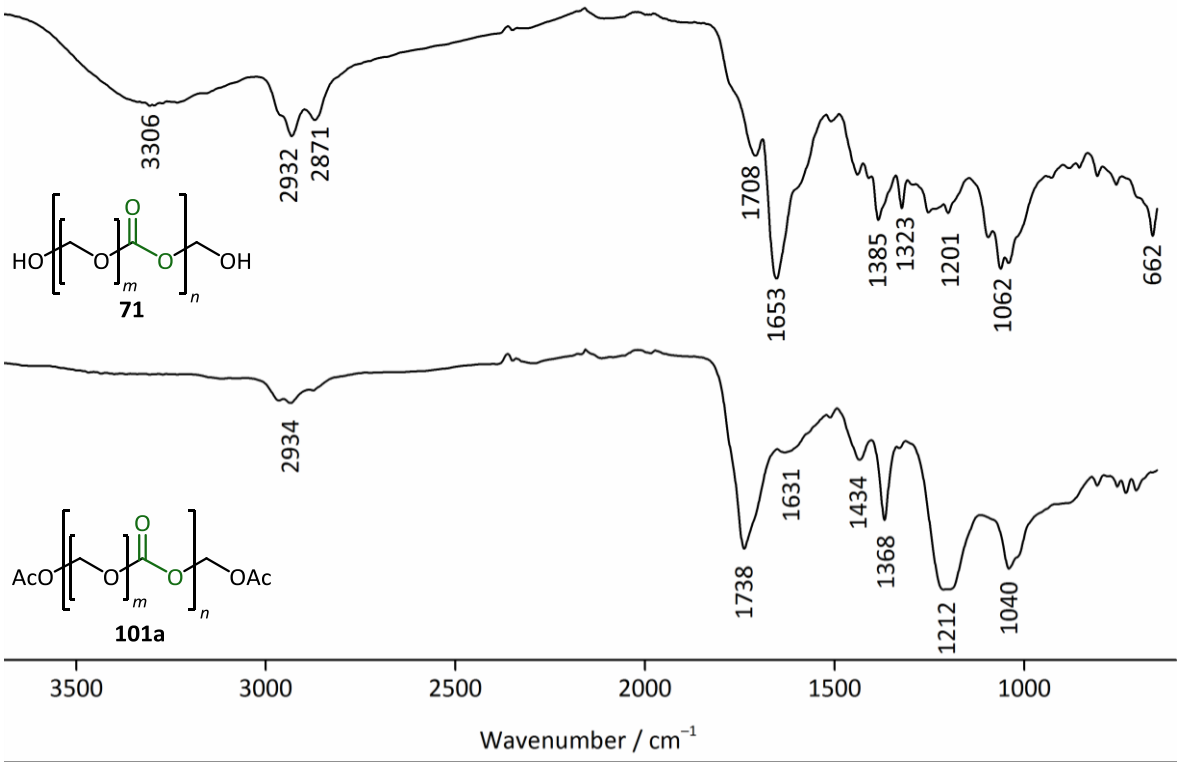

Figure 23. IR of copolymer **71** and end group protected copolymer **101a**.

For the copolymer of CO_2 and formaldehyde (FA, **67**) IR bands were observed in this area. Here, an IR Band of $\tilde{\nu}$ = 1708 cm^{-1} for the unprotected polymer **71** and a band at $\tilde{\nu}$ = 1738 cm^{-1} belonging to the end group protected polymer **101a** were observed (Figure 23).

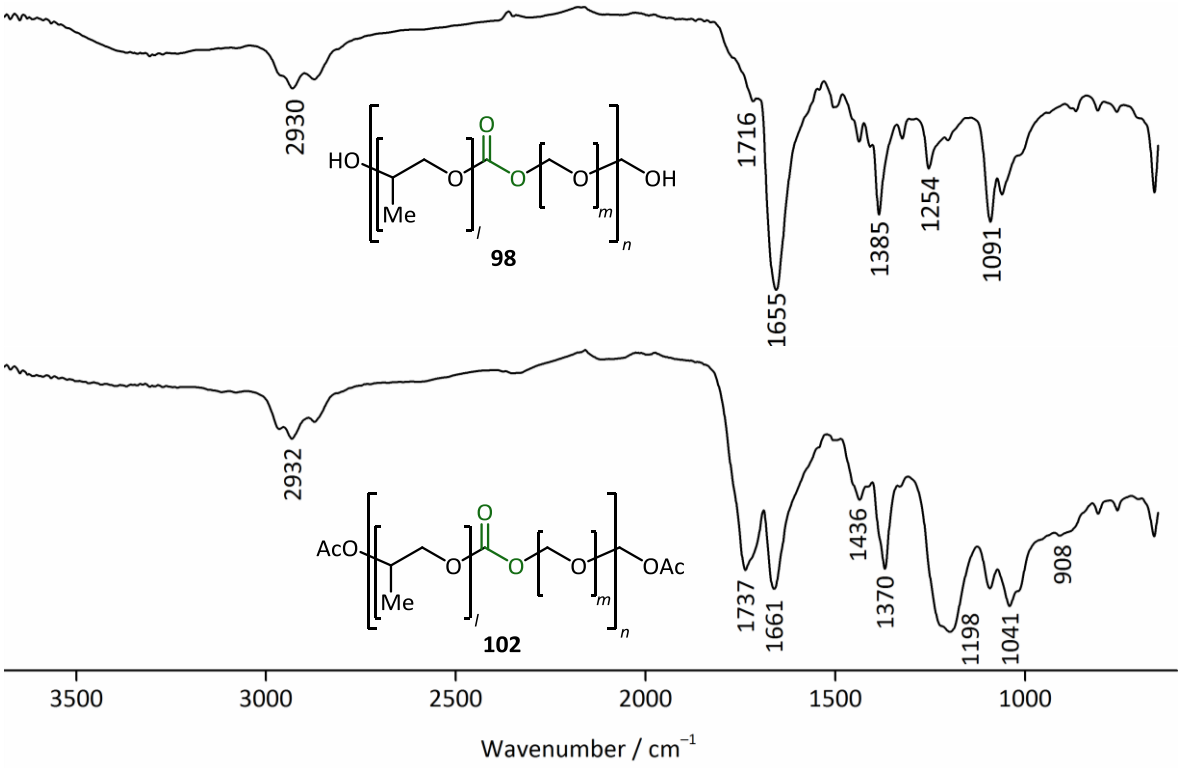

Figure 24. IR spectra of the unprotected and end group protected polymers.

Furthermore, for the obtained copolymer of CO_2, FA and the polyvalent alcohol polypropylene glycol (PPG-1000, M_n = 1000 g·mol^{-1}) IR bands of $\tilde{\nu}$ = 1716 cm^{-1} and $\tilde{\nu}$ = 1737 cm^{-1} were measured (Figure 24).

To conclude, the discussed products showed IR bands in the region $\tilde{\nu}$ = 1707–1736 cm^{-1} (Figure 24). Since these signals did not belong to the reactants, catalysts or solvents they were assigned to the carbonyl groups of the polymer.

In recent literature the reaction of paraformaldehyde (PFA, **68**) and CO_2 was already described not to take place without a catalyst.[142] Here, no carbonyl bands were observed in the IR spectra. Therefore, the utilized 1,5,7-triazabicyclo[4.4.0]dec-5-ene (TBD, **83**) and 1,3-bis(2,6-diisopropylphenyl) imidazolium chloride (IPr · HCl, **84a**) can be reagarded as catalysts to enable this copolymerization reaction.

4.3.10.2 Gel Permeation Chromatography

The obtained molecular weights were determined by conducting gel permeation chromatography (GPC). The measurements were executed in DMF under elevated temperature of 50 °C. For calibration polystyrene standards (M_p = 266–66000 g·mol^{-1}) were utilized.

The obtained graphs showed polymers with broad dispersity (Figure 25). In addition, often bimodal and multimodal peaks were obtained. The stated molecular weights were received by considering the overall signal.

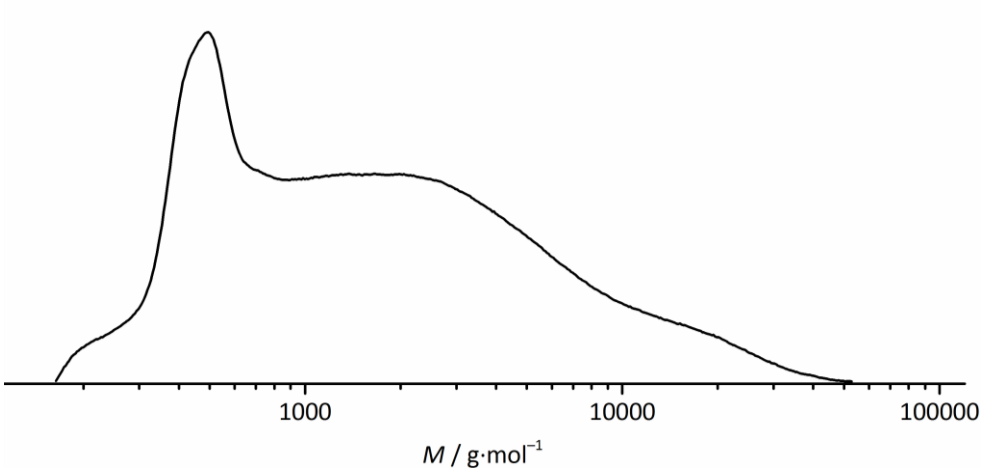

Figure 25. Example of a typical GPC signal showing the protected copolymer **101**.

The signals of the end group protected polymers were compared to the unprotected polymers more consistent. This is probably due to the fact that the protected polymers were precipitated in water, thereby generating a more homogenous polymer.

4.3.10.3 Elemental Analysis

Elemental analysis were conducted for the optimized unprotected polymer which was obtained using IPr · HCl **84a** / TBD **83** as a catalyst system (Table 31, entry 1). The carbon and hydrogen content was ascertained. The data was compared with the carbon and hydrogen content of a control experiment where argon instead of CO_2 pressure was applied. As a result, the carbon and hydrogen contents of the polymer applying CO_2 pressure were lower than the product obtained from the blind testing (Table 32). In fact, the incorporation of CO_2 into the polymer should lead to a decrease of the carbon and hydrogen content since the overall oxygen content increases.

Table 32. EA measurements.

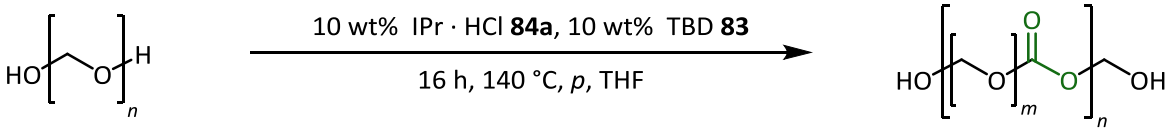

68 **71**

Entry	Gas	*p* / bar	H / %[a]	C / %[a]
1	Ar	15	54.68	6.606
2	CO_2	40	49.88	6.069

[a] Determined by EA.

To conclude, the observation of a lower hydrogen and carbon content for the polycarbonate compared to the blind testing is in agreement with the incorporation of CO_2 into the polymeric chain.

4.3.10.4 NMR

Nuclear magnetic resonance (NMR) experiments were conducted to obtain more detailed information about the structure of the polymer. In contrast to the reactant, which was completely insoluble in all common solvents, the obtained products were very slightly soluble in DMF and DMSO. Therefore, high temperature NMR experiments (T = 50 °C) were conducted to increase the solubility and enable the successful execution of the measurements.

The signals in the ^{1}H NMR spectra were observed to be mostly accumulated or very broad. This is typical for polymers since the ^{1}H atoms of the different chain length have only slightly different adjacencies and are chemically very similar. More revealing than the ^{1}H NMR spectrum is the ^{13}C NMR spectrum of the polymer. This is due to the fact that the ^{13}C NMR spectrum should verify the incorporation of CO_2 into the polymeric chain. Unfortunately, the signal intensity of the quaternary carbon atom of the incorporated CO_2 is very low.[163] Therefore, the measurement was conducted at a high frequency (500 MHz) and for a longer time (6144 scans) at an elevated temperature to increase the signal intensity. As a result, good signal intensities for the ^{13}C NMR and distortionless enhancement by polarization transfer (DEPT) measurements were reached (Figure 26 and Figure 27).

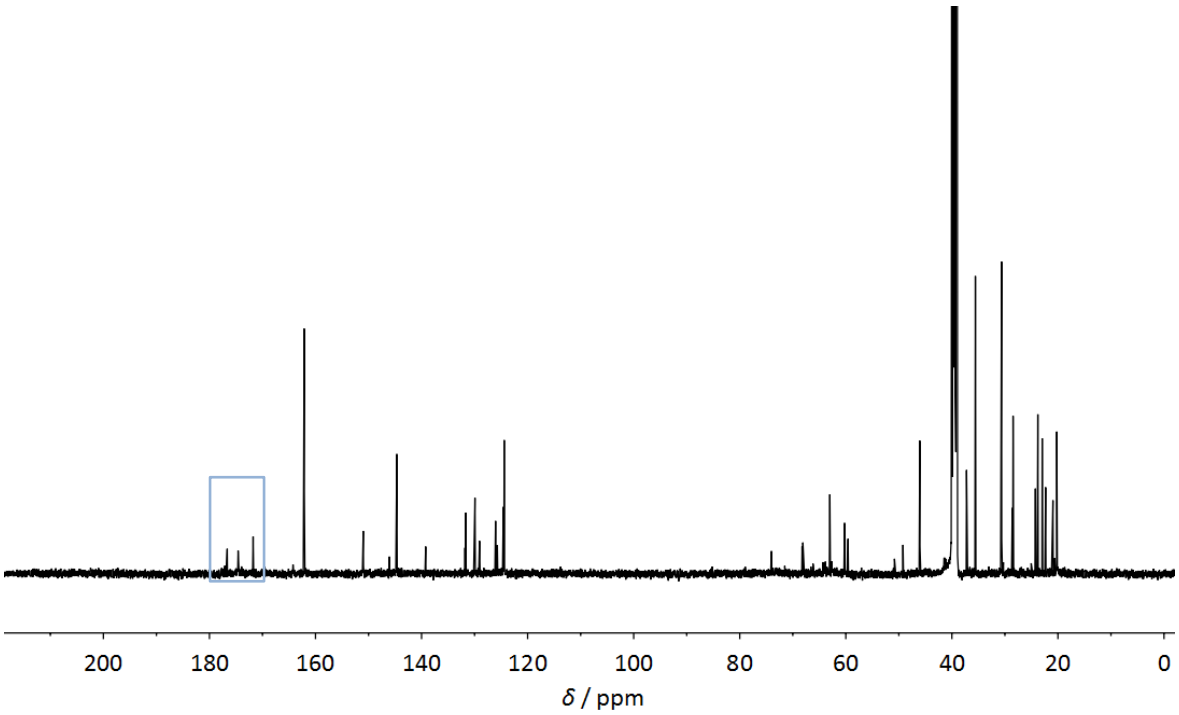

Figure 26. ^{13}C NMR and DEPT spectra of **71**.

The signals in the region $\delta = 170–180$ ppm are supposedly belonging to the quaternary carbon atoms of the incorporated CO_2 of the polymer (Figure 26, blue area). A further lead to this assumption showed the DEPT spectrum. Here, the mentioned signals in the ^{13}C did not occur, which is proof that the signals belong to quaternary carbon atoms (Figure 27, bottom spectrum, blue area).

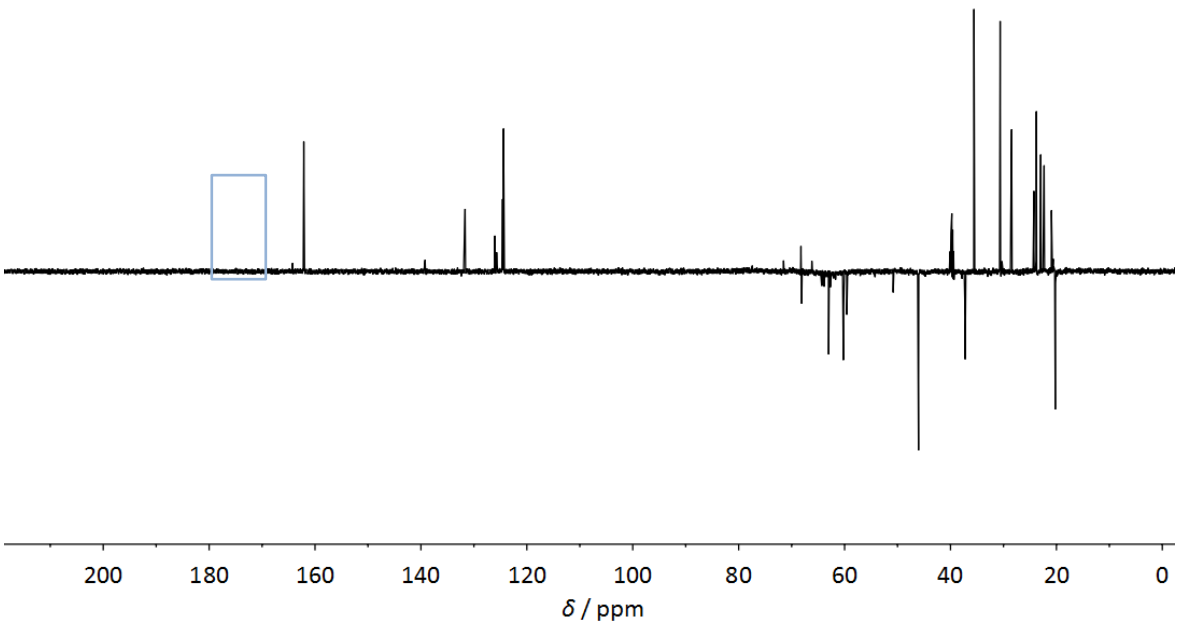

Figure 27. ^{13}C NMR and DEPT spectra of **71**.

As a result, the signals of the quaternary carbon atoms of the obtained product are an indication for the CO_2 incorporation into the polymeric chain of the expected product. However, it is important to mention that the distribution of signals is uncommonly narrow for a polymer. Additionally, the high number of signals in the upfield region of the spectra leads to the consideration that maybe formose products are formed as side products.

4.3.10.5 TGA-MS and DSC

The thermal stability and behavior of the obtained products were determined. Therefore, TGA and DSC measurements were conducted. The aim was to obtain polycarbonates **71** which are thermally stable. In particular, the relative mass loss and the decrease of the number average molar weights are to be considered. The decomposition products were analyzed using mass spectrometry (MS). The reactions using IPr · HCl **84a** and TBD **83**, which showed the best results in the screening reactions, were further investigated regarding the composition of the obtained polymers (Scheme 34).

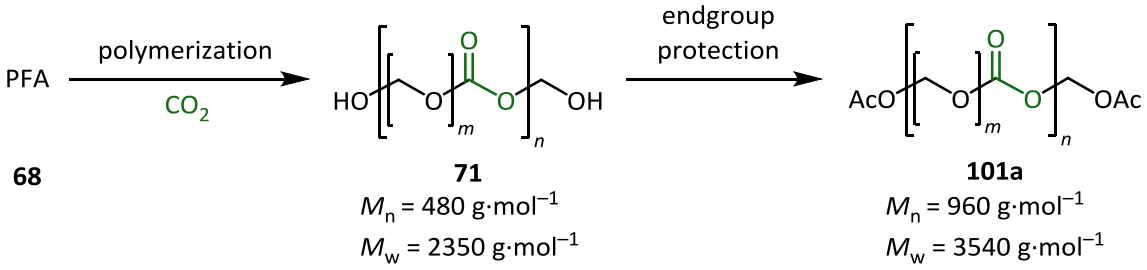

Scheme 34. Analyzed polymers **71** and **101a**.

Here, DSC and TGA-MS measurements are especially helpful for determining the thermal stability and behavior of the polymer and also for the CO_2 incorporation. Following requirements for the thermal stability of the polymer were defined beforehand:

Relative mass loss:

The relative mass loss of the obtained product during the heating process of the TGA measurement to 130 °C should be ≤ 5%.

Decrease of M_n:

The decreasing of the number average molecular mass during the heating process to 130 °C should be ≤ 15%.

The end group protected polymer **101a** was analyzed and compared with the not protected polymer **71** and with the reactant PFA **68**. Therefore, the weight losses were

measured. Decomposition of PFA **68** started at 80 °C and complete decomposition was already reached at 145 °C (Figure 28, yellow). Furthermore, the protected polymer **101a** (Figure 28, black) was more stable than the unprotected polymer **71** (Figure 28, red).

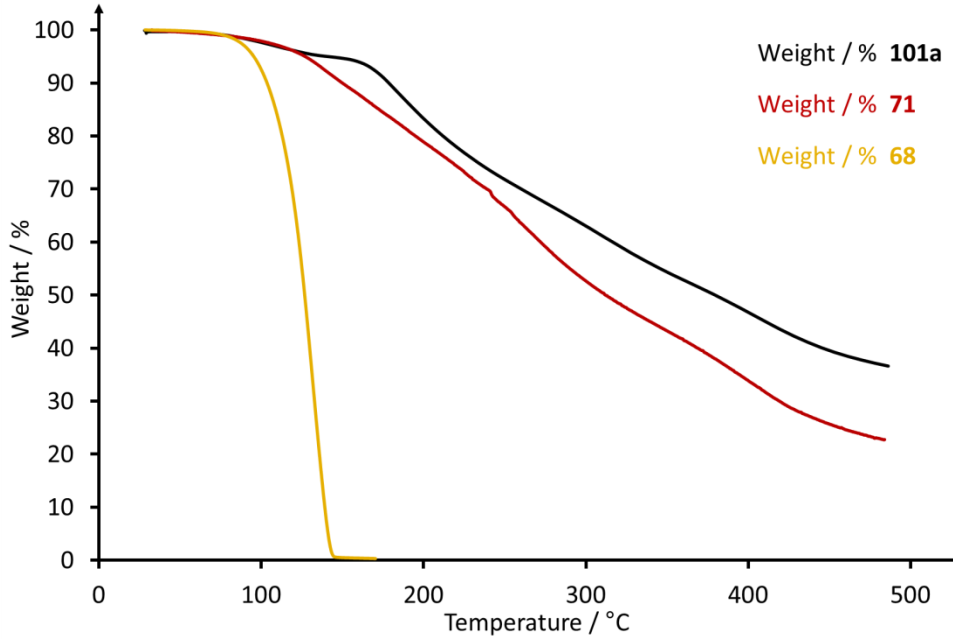

Figure 28. TGA-MS: Loss of mass during heating of **101a** (black), **71** (red) and PFA **68** (yellow).

The end group protected polymer **101a** will be further discussed regarding the different decomposition products which occurred during the heating or rather decomposition.

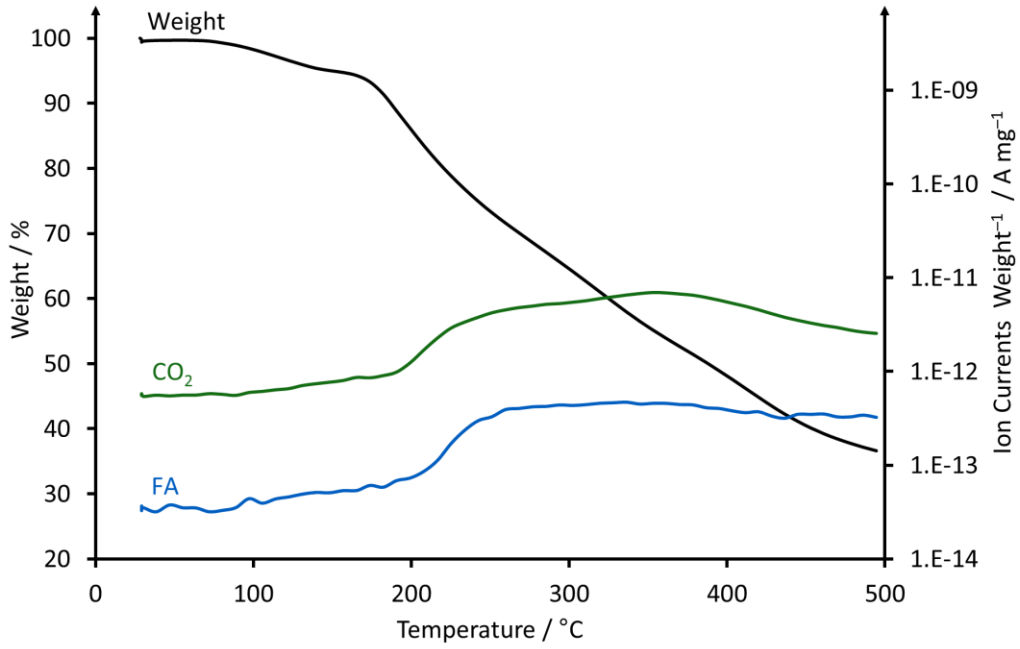

Figure 29. TGA-MS: Loss of mass and decomposition of **101a**.

The main decomposition was observed in the temperature range of 160–500 °C (Figure 28, black). A total mass loss of 65.1% was observed during the heating. At 130 °C the weight loss of the polymer reached 4% and thereby in the region of the specification. The resulting decomposition products were further analyzed by mass spectrometry. Therefore, the ion current of the molecular masses of carbon dioxide (green) and FA **67** (blue) were recorded (Figure 29 and Appendix, Figure 39). The intensities of both molecular masses increased simultaneously at a temperature of approximately 200 °C. This can be seen as a lead that FA **67** and CO_2 are part of the polymer. In other words, it is a hint for the implementation for CO_2.

Additionally, DSC measurements were conducted to support the TGA measurements. Therefore two measurements were conducted. The polymer was heated up to T_{max} = 130 °C and 500 °C and the pans were weighed before and after the heating. The measured weight losses were in accordance to the TGA measurements (Table 33). Furthermore, the sample which was heated to 130 °C was measured after the heating with GPC. The decrease of the number average molecular weight was with 1.3% within the specifications. Additionally, the glass transition temperature (T_g) was ascertained. To conclude, the end-capped product was within the beforehand defined range for the thermal stability of the polymer.

Table 33. Thermal measurement and weight losses of **101a**.

Entry	Method	T_{max} / °C[a]	Weight Loss / Δ%
1	TGA	500	65.1
2	TGA	130	4.01
3	DSC	500	62.7
4	DSC	130	4.03

[a] Heating rate: 5 K·min^{-1}.

Furthermore, the glass transition (T_g) and decomposition temperatures ($T_{d\,5\%}$) of the reactant **68** and the polymers **71** and **107** were determined.

In comparison to the polymers **71** and **107** the thermal stability of PFA **68** was far lower. No glass transition was observed and decomposition started already at a low temperature which is in accordance with the former studies.[164] A $T_{d\,5\%}$ = 95% was determined which

supports the concept that under the applied reaction conditions the reactant decomposes to FA **67** which then can reacts with CO_2. Additionally, PFA **68** was observed to decompose completely to FA **67** and no other non-volatile decomposition products remained (Table 34).

For the unprotected compound **71** a T_g = –31.22 °C and a $T_{d\,5\%}$ = 127 °C was measured. For the capped product a T_g = 3.42 °C and a $T_{d\,5\%}$ = 157 °C was ascertained.

Table 34. Glass transition and decomposition temperatures.

Entry	Polymer	T_g / °C	$T_{d\,5\%}$ / °C	Weight Loss (500 °C) / Δ%
1	**68**	-	95	>99
1	**71**	–31.22	127	77
2	**101a**	3.42	157	65

[a] Determined by DSC. [b] Determined by TGA.

The glass transition and the decomposition temperatures for the end group protected polymer were observed to be higher. In fact, only the protected polymer showed the required thermal stability.

4.3.10.6 MALDI-TOF

For the polymer **71** and **101a** matrix assisted laser desorption / ionization (MALDI) measurements were conducted. This method allows obtaining mass spectra without the conventional fragmentation which occurs for example by conducting electron ionization (EI) measurements. Therefore, it is a good method for the investigation of polymers. The polymers **71** and **101a** were mixed with the matrix material dithranol Li and a pulsed Nd:YAG laser was applied to irradiate the sample.

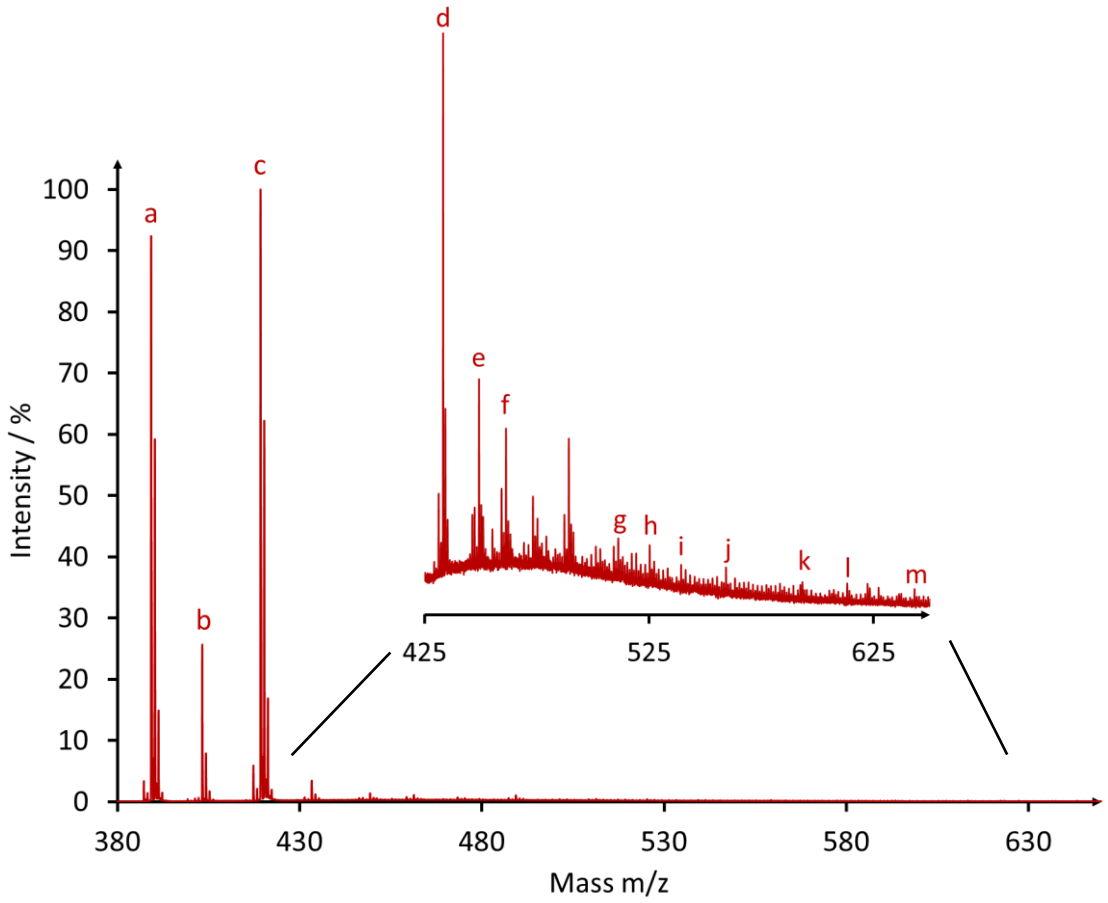

Figure 30. MALDI-TOF spectrum of **71**.

From the spectra several measured molecular masses could be assigned to the copolymers. Particularly, the mass differences of formaldehyde (FA, **67**) with a molecular mass of $M = 30\ \mathrm{g{\cdot}mol^{-1}}$ and of CO_2 with a molecular mass of $M = 44\ \mathrm{g{\cdot}mol^{-1}}$ were emphasized. Examples are **a** to **c** for FA **67** (Table 35, entries 1 and 3) and **a** to **d** for CO_2 (Table 35, entries 1 and 4).

Table 35. Assigned measured masses of polymer **71**.

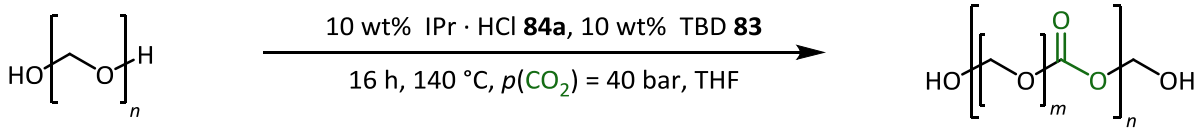

68 **71**

Entry	Signal	Mass / m/z[a]	**71** *m*FA	**71** CO_2
1	**a**	389.30	5	5
2	**b**	403.26	6	4
3	**c**	419.26	5	6
4	**d**	433.29	6	5
5	**e**	449.30	5	7
6	**f**	463.30	6	6
9	**g**	511.36	3	12
10	**h**	525.32	4	11
11	**i**	541.33	3	13
12	**j**	555.34	4	12
13	**k**	583.36	6	10
14	**l**	613.35	6	11
15	**m**	643.32	6	12

[a] Determined by MALDI-TOF.

The same measurement was conducted for the end-capped polymer **101a**. The expected end-capped products on one and both sides were observed. The determined molecular masses were assigned to the most probable molecules.

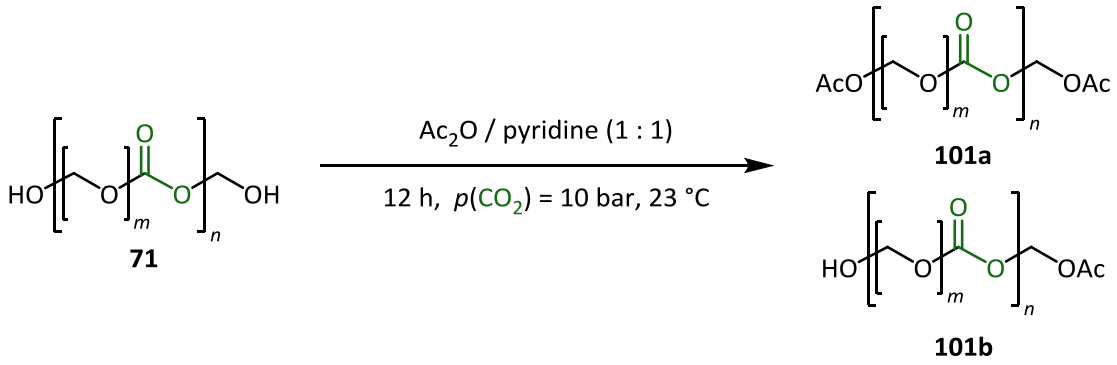

71 **101a** **101b**

Scheme 35. End group capping of **69**.

The capped polymer on both sides **101a** and the capped polymer only on one side **101b** were observed.

Table 36. Assigned masses of polymer **101a**.

Entry	Mass / *m/z*[a]	**101a** / **101b**	*n*CO_2	*m*FA
1	389.31	**101b**	2	8
2	403.33	**101b**	3	7
3	417.34	**101a**	1	9
	"	**101b**	5	5
4	461.35	**101a**	2	9
5	"	**101b**	6	5

[a] Determined by MALDI-TOF.

4.3.10.7 ESI

Electrospray ionization (ESI) experiments were conducted for the polymer **69**. The observed molecular weights were assigned to the most probable structures. The signals discussed for the MALDI-TOF measurement were also observed in the ESI spectra. It thereby confirms the MALDI-TOF measurement.

5 SUMMARY

5.1 Polyfunctional Cyclic Carbonates and NIPUs

With the objective to utilize CO_2 as a C–1 building block, several monofunctional and bifunctional catalysts were tested for the conversion of the model substrate bisepoxide 1,4-bis(oxiran-2-ylmethoxy)butane (**49a**) to the corresponding cyclic dicarbonate **50a**. From the employed compounds the bifunctional one component catalyst tri-*n*-butyl-(2-hydroxyethyl)ammonium iodide (**45a**) showed the highest activity. Optimized reaction conditions of 2 mol% **45a**, 90 °C, $p(CO_2)$ = 10 bar and 14 h were determined (Scheme 36). At lower temperatures the monocarbonylated product was observed and could be isolated in some cases.

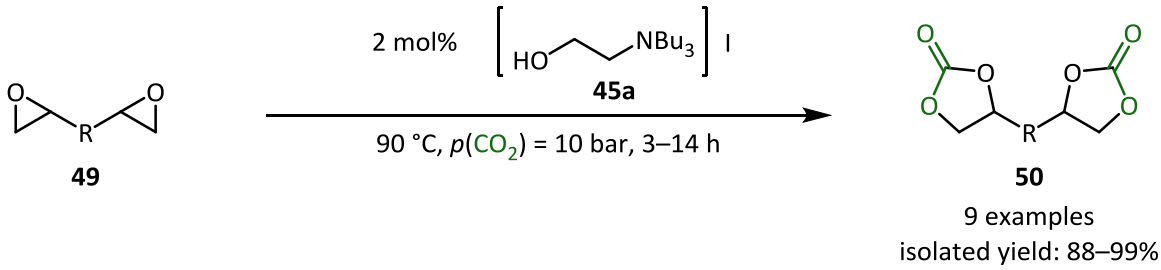

Scheme 36. Optimized reaction conditions for the conversion of bisepoxides **49**.

Under the optimized reaction conditions bisepoxides containing ether, ester, aliphatic and aromatic groups were converted to the corresponding cyclic dicarbonates **50**, including three oligomeric bisepoxides. Here, good to excellent isolated yields of 88–99% were obtained. Additionally, a cyclic tricarbonate and a compound with four cyclic carbonate moieties were synthesized in excellent yields. Furthermore, it was possible to convert an internal bisepoxide to the corresponding carbonate in a good yield. Great advantages of this method are the mostly applied solvent-free conditions and the comparatively easy workup. The products were simply washed with a suitable solvent or filtered over silica gel.

Subsequently, a synthesized bifunctional cyclic carbonates and a trifunctional cyclic carbonate were employed for polymerization reactions to form monodisperse non-isocyanate polyurethanes (NIPUs). Therefore, polyaddition reactions utilizing an aliphatic

diamine were performed. The expected linear and cross-linked polymers were obtained in good yields. A tendency to form the secondary alcohol (≈ 3 : 1 secondary : primary alcohol) was observed for the linear NIPU.

It was shown that the target compound **64** can be obtained through a sequential one pot procedure (Scheme 37). As a result, a yield of 81% for the linear NIPU and a molecular weight of M_n = 11500 g·mol^{-1} were obtained. Furthermore, an isolated yield of 93% of the cross-linked polymer was achieved.

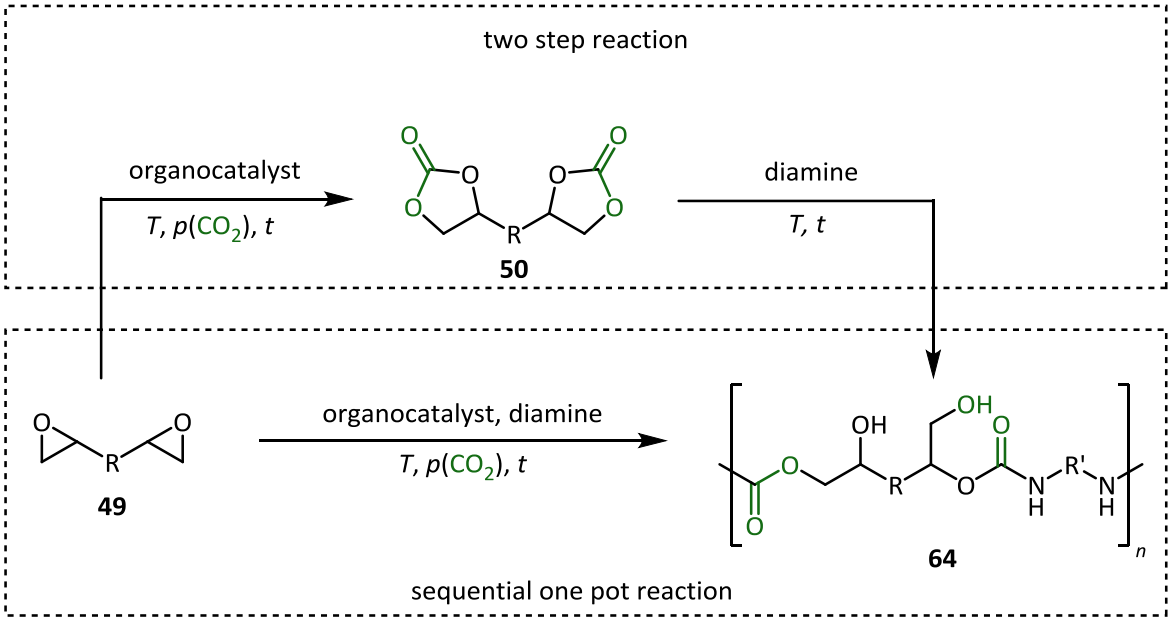

Scheme 37. Employed methods for the synthesis of linear NIPUs.

Additionally, the thermal properties of the polymers were ascertained by conducting TGA-MS and DSC measurements. For the linear NIPU a glass transition temperature of T_g = 22.69 °C and a decomposition temperature of $T_{d\,5\%}$ = 169 °C were measured. The cross- linked polymer showed a significantly higher decomposition temperature. Furthermore, the DSC measurement revealed that the cross-linked NIPU is partly crystalline. The different thermal behaviour can be explained by the higher rigidity of the cross-linked polymer compared to the linear NIPU.

To conclude, the procedure of a sequential one pot reaction was shown to be an effective way to form linear and cross-linked NIPUs in good to excellent yields.

5.2 Dream Polymers

A second objective of this thesis is the evaluation of the copolymerization ability of formaldehyde (FA, **67**) and CO_2 within the framework of the project *Dream Polymers* to generate polycarbonates (Scheme 38). Because of the high reactivity of FA **67** it was employed in its trimeric, polymeric or solved form. Furthermore, several imidazolium and thiazolium salts were screened in combination with amine bases for their catalytic activity. Based on the observed molecular weights optimized standard reaction conditions were ascertained.

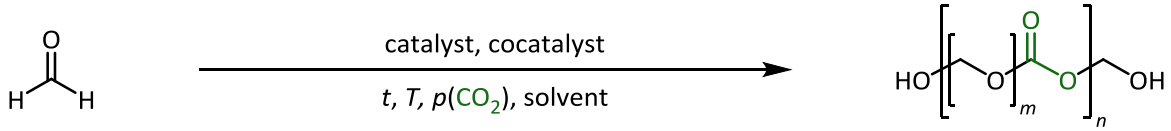

67 **71**

Scheme 38. Copolymerization of **67** and CO_2 to form **71**.

The highest molecular weights were observed utilizing the reactant paraformaldehyde (PFA, **68**) and the catalysts TBD **83** and IPr · HCl **84a**. Under the optimized reaction conditions of 16 h, 140 °C and $p(CO_2)$ = 40 bar a molecular weight of M_w = 2350 g·mol^{-1} was obtained (Scheme 39). The product with the highest molecular weight **71** was stabilized by adding acetic anhydride and pyridine directly after the polymerization to the reaction mixture in the autoclave to form the putative product **101a**.

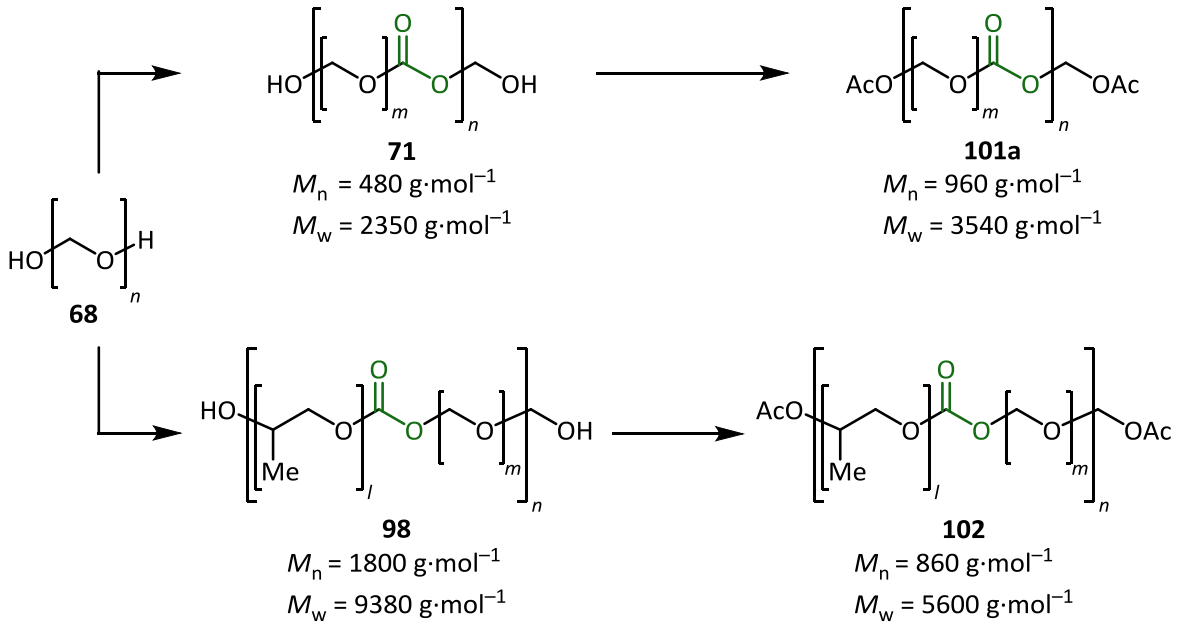

71
M_n = 480 g·mol^{-1}
M_w = 2350 g·mol^{-1}

101a
M_n = 960 g·mol^{-1}
M_w = 3540 g·mol^{-1}

68

98
M_n = 1800 g·mol^{-1}
M_w = 9380 g·mol^{-1}

102
M_n = 860 g·mol^{-1}
M_w = 5600 g·mol^{-1}

Scheme 39. Obtained Dream Polymers.

Furthermore, a polyvalent alcohol with a defined molecular weight of M_n = 1000 g·mol^{-1} was employed. The concept was to use this alcohol to obtain polymers with higher molecular weights compared to the received average molecular weight of **71**. Additionally, the obtained product **98** was also protected by adding acetic anhydride and pyridine to form **102**. The isolated products reached weight average molecular weights of up to M_w = 9380 g·mol^{-1}.

To determine the structure and the physical properties of the obtained products ^{1}H NMR, ^{13}C NMR, IR, EA, DSC, TGA-MS and MALDI-TOF experiments were conducted. Here, it is important to note that the formation of formose products during the reaction is possible and that the low solubility and low signal intensity of the obtained products made the investigations a challenging task. As a result, the applied analytical methods indicate the formation of an carbonyl group containing oligomer during the reaction.

APPENDIX

6 EXPERIMENTAL SECTION

6.1 Analytical Methods

NMR spectroscopy: ^{1}H NMR spectra were recorded with a *Bruker AV 300* (300 MHz), *Bruker AV 400* (400 MHz) and a *Bruker AV 500* (500 MHz). Broadband proton decoupled ^{13}C NMR spectra were recorded with a *Bruker AV 300* (75 MHz) and a *Bruker AV 400* (100 MHz). Measurements at elevated temperatures (50 °C) were recorded with a *Bruker AV 500* (500 MHz). The assignments of the signals were done by using DEPT spectra. For ^{1}H and ^{13}C NMR spectra the remaining solvent signal was used as an internal standard. Broadband pro glass transition, melting and decomposition of cross-linked NIPU **82**. ton decoupled ^{31}P NMR spectra were measured with a *Bruker AV 400* (162 MHz for phosphorus) and referenced against a phosphoric acid standard (85%, aq). Shifts δ were stated in ppm, the coupling constants *J* are given as a frequency in hertz (Hz). Signals are abbreviated as: s (singlet), d (doublet), t (triplet), q (quartet), sept (septet), m (multiplet).

IR spectroscopy: Infrared spectra were recorded with a Fourier transform infrared spectrometer *Nicolet iS10 MIR* from *Thermo Fisher Scientific*. All measurements were recorded by using attenuated total reflection technology. Absorbance bands are shown in wave numbers (cm^{-1}). Intensities are abbreviated: vs (very strong), s (strong), m (medium), w (weak), br (broad).

Mass spectrometry: High resolution mass spectra were measured with a *MAT 95XP* mass spectrometer from *Thermo Fisher Scientific*. The ionization of the samples was done by electron ionization (EI). Furthermore, a *HPLC System 1200* combined with an *ESI-TOF-MS 6210* from *Agilent* was used. The ionization of the samples was done by ESI. GC-MS spectra were measured with an *Agilent 7890A GC System* using a mass detector *5975C inert XL MSD* from *Agilent*. The ionization was done by using electron impact ionization (EI) with an ionization potential of 70 eV. The relative intensities were expressed as a percentage relative to the main peak.

MALDI-TOF-MS: Matrix assisted laser desorption / ionization – time of flight – mass spectrometry (MALDI-TOF-MS) was conducted with a *4700 Proteomics Analyzer* from *Applied Biosystems*. A pulsed (20000 FPS) ND:YAG laser with a wavelength of λ = 355 nm was employed. As the matrix material a concentrated solution of dithranol and LiCl in acetone was applied.

Elemental analysis: CHN elemental analyses were performed with a *TruSpec CHNS Micro* from *Leco*. The halogen content was determined utilizing potentiometric titration with a *TitraLab 870* from *Radiometer Analytical SAS*. The phosphorus content was determined using an acid (HNO_3–$Mg(NO_3)_2$)-digestion method in a quartz pan.

Melting point: Melting points (mp) were measured in a glass capillary tube with a *Melting Point Apparatus SMP3* from *Stuart*.

TGA-MS: Thermogravimetric analyses were performed with a TGA system from *Setaram*. The system was coupled with a quadrupole mass spectrometer from *Pfeiffer Vacuum*. A heating rate of 5 $K \cdot min^{-1}$ was applied. The inert gas argon or nitrogen were used as carrier gases (20 $mL \cdot min^{-1}$).

Gel permeation chromatography (GPC): Gel permeation chromatograms were measured with a *1260 Infinity GPC/SEC System* from *Agilent Technologies*. The setup consisted of a *SECcurity Isocratic Pump*, SECcurity 2-Canal-Inline-Degaser*, SECcurity GPC-Column thermostat TCC6000, SECcurity Fraction Collector* and *SECcurity Differential Refractometer detector.* The measurements were performed at a constant temperature of 50 °C using three columns with a polyester copolymer network as the stationary phase (PSS GRAM 30 Å, 10 µm particle size, 8.0 × 50 mm; PSS GRAM 30 Å, 10 µm particle size, 8.0 × 300 mm; PSS GRAM 1000 Å particle size, 8.0 × 300 mm). As the mobile phase a DMF lithium bromide solution (1.5 $g \cdot L^{-1}$) with a flow rate of 1 $mL \cdot min^{-1}$ was applied. For calibration polystyrene standards from *ReadyCal* (PSS-pskitr1l-05, M_p = 266–66000 $g \cdot mol^{-1}$) were used.

Differential scanning calorimetry (DSC): Thermal properties were determined with a differential scanning calorimetry *DSC 1 STARe System* (400 W) from *Mettler Toledo*. A *FRS5* sensor and the dynamic temperature system IntraCooler *TC100 RC* from *HUBER* were used. For all measurements sample pans with pin and lid were employed. As reference an empty sample pan was used. The lid was penetrated with a needle and the pan was closed through cold welding. The measurements were performed at atmospheric

pressure under inert conditions. For each sample, one full heating and cooling cycle was measured prior to the actual measurements. All samples were analyzed by using a constant heating and cooling rate of 10 K·min^{-1} in a temperature range from –80 °C to 110 °C and 0 °C to 450 °C.

6.2 Chromatography

Flash column chromatography: For flash column chromatography silica gel from *Macherey-Nagel* (60 M, grain diameter 0.040 to 0.063 mm) was used. The particularly used eluents are stated.

Thin layer chromatography: Thin layer chromatography (TLC) was done by using ready-to-use films from *Merck* (silica gel type 60, F_{254}). The particular R_f-values of the products were stated with the eluents. The R_f -values of non-UV active substances were determined through staining. Therefore, a vanillin reagent was used (0.5 g vanillin were solved in 80 mL sulfuric acid and 20 mL ethanol and stirred for 14 h under air).[165] For complete staining the thin layer films were heated.

6.3 Solvents and Chemicals

Solvents: Following solvents were acquired by purchase from *Acros*, *Sigma-Aldrich*, *Roth* or *Fluka* and used without further purification: acetone, *n*-butanol, CH_2Cl_2, dioxane, DMF, DMSO, Et_2O, EtOH, MeOH, MeCN, MEK and NMP.

Toluene was first dried over sodium wire using benzophenone as indicator and then distilled.[166] Pyridine was distilled and stored under inert gas. THF was purified with a *PureSolv MD 7 Solvent Purification System* from *Innovative Technology*.

Chemicals: EtOAc, Ac_2O and 2,2'-(((2,2-dimethylpropane-1,3diyl)bis(oxy))bis (methylene)) bis(oxirane) (*ABCR*, 95%) were distilled and stored under inert gas. All other chemicals were used without further purification.

Acetic anhydride (*Merck*, 98%), 3-benzyl-4-methylthiazolium chloride (*TCI*, 98%), 3-benzyl-5-(2-hydroxyethyl)-4-methylthiazolium chloride (*Sigma-Aldrich*, 98%), 1,3-bis(2,6-diiso-propylphenyl)-4,5-dihydroimidazolium tetrafluoroborate (*Sigma-Aldrich*, 95%), 1,3-bis-(2,6-diisopropylphenyl) imidazolium chloride (*TCI*, 98%), 1,3-bis(oxiran-2-ylmethoxy)-benzene (*Sigma-Aldrich*, 94%), 1,4-bis(oxiran-2-ylmethoxy)butane (*Sigma-Aldrich*, 95%),

bis(oxiran-2-ylmethyl) cyclohexane-1,2-dicarboxylate (*Sigma-Aldrich*, 88%), carbon dioxide (*Linde*, ≥99.998%), cyclohexene oxide (*Alfa Aesar*, 98%), 1,3-di(1-adamantyl)-benzimidazolium chloride (*Abcr*, 97%), 1,4-diazabicyclo[2.2.2]octane (*Roth*, 98%), 1,8-diazabicyclo[5.4.0]undec-7-ene (*Alfa Aesar*, 99%), 1,3-dicyclohexylbenzimidazolium chloride (*Abcr*, 97%), 1,3-dicyclohexylimidazolium tetrafluoroborate (*Sigma-Aldrich*, 97%), 1,3-diisopropylimidazolium tetrafluoroborate (*TCI*, 96%), 4-dimethylaminopyridine (*Sigma-Aldrich*, 97%), 1,4-di(oxiran-2-yl)butane (*Sigma-Aldrich*, 97%), 1,3-di-*tert*-butyl-benzimidazolium chloride (*Abcr*, 97%), 2,3-epoxypropyl-*iso*-butylether (*Sigma-Aldrich*, 99%), 2,3-epoxypropyl-*tert*-butylether (*Sigma-Aldrich*, 99%), 2,3-epoxypropyl-*iso*-propyl-ether (*Sigma-Aldrich*, 99%), 1-ethyl-3-methylimidazolium bromide (*Acros*, 98%), 1-ethyl-3-methylimidazolium chloride (*Acros*, 97%), 1-ethyl-3-methylimidazolium hexafluoro-phosphate (*Alfa Aesar*, 98%), 1-ethyl-3-methylimidazolium hydrogen sulfate (*TCI*, 98%), 1-ethyl-3-methylimidazolium iodide (*Alfa Aesar*, 97%), 1-ethyl-3-methylimidazolium methansulfonate (*TCI*, 98%), 1-ethyl-3-methylimidazolium tetrachloroferrate (*TCI*, 98%), 1-ethyl-3-methylimidazolium tetrafluoroborate (*Alfa Aesar*, 98%), formalin (*Sigma-Aldrich*, 37% w/w aqueous solution, 7% methanol as stabilizer), 4(5)-(hydroxyl-methyl)imidazole (*Sigma-Aldrich*, 99%), 3-mesityl-1-methyl-1H-benzimidazolium chloride (*Sigma-Aldrich*, 95%), 4,4'-methylenebis(*N*,*N*-bis(oxiran-2-ylmethyl)aniline) (*Sigma-Aldrich*, 99%), (7-oxabicyclo[4.1.0]heptan-3-yl)methyl 7-oxabicyclo[4.1.0]heptane-3-carboxylate (*Sigma-Aldrich*, 99%), paraformaldehyde (*Sigma-Aldrich*, 95%), phenyl-isocyanate (*Alfa Aesar*, 98%), polyethylene glycol diglycidyl ether M_n = 580 g·mol^{-1} (*Sigma-Aldrich*, 99%), polypropylene glycol M_n = 1000 g·mol^{-1} (*BMS*, 99%), polypropylene glycol diglycidyl ether M_n = 380 g·mol^{-1} (*Sigma-Aldrich*, 99%), polypropylene glycol diglycidyl ether M_n = 640 g·mol^{-1} (*Sigma-Aldrich*, 99%), potassium iodide (*Sigma-Aldrich*, 99%), 2,2'-(((propane-2,2-diylbis(4,1-phenylene))bis(oxy))bis(methylene))bis(oxirane) (*Sigma-Aldrich*, 95%), pyridine (*Acros*, 99%), tetrabutylammonium bromide (*Sigma-Aldrich*, 99%), tetrabutylammonium chloride (*Sigma-Aldrich*, 97%), tetrabutylammonium iodide (*Sigma-Aldrich*, 99%), thiamine hydrochloride (*Roth*, 98%), thiamine nitrate (*TCI*, 98%), thiamine pyrophosphate (*TCI*, 98%), 1,5,7-triazabicyclo[4.4.0]dec-5-ene (*Sigma-Aldrich*, 98%), triethanolamine (*Acros*, 99%), 1,3,5-trioxane (*Sigma-Aldrich*, 99%), triphenylphosphine (*Alfa Aesar*, 99%), 1,3,5-tris(oxiran-2-ylmethyl)-1,3,5-triazinane-2,4,6-trione (*Sigma-Aldrich*, 99%).

6.4 General Procedures (GP)

High pressure experiments: All experiments under high pressure were performed in stained steel reactors from *Parr Instrument GmbH*. As a high throughput setup the *Multiple Reactor System 5000* from *Parr Instrument GmbH* was used.

General Procedures – Cyclic Carbonates

GP-I: Parameter screening

A 45 cm^3 stainless steel autoclave was charged with catalyst (**38a**–**38c**, **45a**, **46a** or **40**, 0.01–0.05 equiv). For catalyst **40** a cocatalyst (**39** or **41**, 0.02 equiv) was added. The model substrate 1,4-bis(oxiran-2-ylmethoxy)butane (**49a**, 1.0 equiv) was employed. The reactor was purged once with CO_2 and subsequently pressurized to 0.5–2.5 MPa at 23 °C until the equilibrium was reached. The reaction mixture was heated to 45–90 °C under constant pressure and was stirred for 2–18 h. The reactor was cooled to ≤20 °C on an ice bath and CO_2 was released slowly. Conversion of the epoxide groups were determined by ^{1}H NMR with a *Bruker AV 300* (300 MHz).

GP-II: Syntheses of cyclic carbonates

A 45 cm^3 stainless steel autoclave was charged with tri-*n*-butyl-(2-hydroxyethyl)ammonium iodide (**45a**, 0.02–0.1 equiv) and epoxide (**32**, **49**, **56**, **78** or **80**, 1.0 equiv). The reactor was purged once with CO_2 and subsequently pressurized to 1.0 MPa at 23 °C until the equilibrium was reached. The reaction mixture was heated to 90 °C under constant pressure and was stirred for 3–48 h. The reactor was cooled to ≤20 °C on an ice bath and CO_2 was released slowly. The reaction mixture was filtered over SiO_2 (CH_2Cl_2) or purified by column chromatography (CH:EtOAc). All volatiles were removed under reduced pressure.

General Procedures – Non-isocyanate polyurethanes (NIPUs)

GP-III: Syntheses of NIPUs

A 10 cm^3 pressure tube was charged with tri-*n*-butyl-(2-hydroxyethyl)ammonium iodide (**45a**, 0.02 equiv), polyfunctional cylic carbonate (**50d** or **57**, 1.0 equiv), 1,4-diaminobutane (**62f**, 1.0–1.5 equiv) and DMSO (1 mL · $mmol^{-1}$ carbonate). The pressure tube was heated to 100 °C for 24 h. Subsequently, the pressure tube was cooled to ambient temperature and the reaction mixture was poured into water (10 mL · $mmol^{-1}$ carbonate). The precipitate was filtered off and washed with water (70 mL · $mmol^{-1}$ carbonate) or

with DMSO (70 mL · mmol^{-1} carbonate) and water (70 mL · mmol^{-1} carbonate). All volatiles were removed under reduced pressure.

GP-IV: Sequential one pot procedure for the syntheses of NIPUs

A 45 cm^3 stainless steel autoclave was charged with tri-*n*-butyl-(2-hydroxyethyl) ammonium iodide (**45a**, 0.02 equiv), polyfunctional epoxide (**50d** or **57**, 1.0 equiv) and DMSO (0.33 mL·mmol^{-1} epoxide). The reactor was purged once with CO_2 and pressurized with CO_2 to 1.0 MPa at 23 °C until the equilibrium was reached. After heating to the desired reaction temperature of 90 °C the pressure was kept constant and the reaction mixture was stirred for 14 h. The reactor was cooled to ambient temperature and CO_2 was released slowly. Subsequently, 1,4-diaminobutane (**62f**, 1.0–1.5 equiv) and DMSO (0.66 mL· mmol^{-1} epoxide) was added to the reaction mixture and the autoclave was heated to 100 °C for 24 h under argon. The reaction mixture was poured into water (10 mL·mmol^{-1} (epoxide)). The precipitate was filtered off and washed with water (70 mL·mmol^{-1} (epoxide)) or with DMSO (70 mL·mmol^{-1} (epoxide)) and water (70 mL·mmol^{-1} (epoxide)). All volatiles were removed under reduced pressure.

General Procedures – *Dream Polymers*

***Schlosser* solution:**[133] The *Schlosser* solution was produced by codistillation of THF and paraformaldehyde (PFA, **68**). Therefore, PFA (**68**, 1.5 g) and *p*-toluenesulfonic acid (PTSA, 0.25 g) were placed in a three necked flask and THF (50 mL) was added. The mixture was heated to 70 °C for approximately 6 h and an argon flow of *Q*(Ar) = 3–4 L·h^{-1} was applied. The solvent was collected in a cooled flask. To intercept the excess gas the stream was introduced in a washing bottle containing a water / methanol mixture. ^{1}H NMR-measurements (*Bruker AV 300*) revealed concentrations of FA **67** in the range of 0.2–0.5 mol·L^{-1}.

GP-V: Syntheses of poly(methylene carbonate) using imidazolium salt **84a** and TBD **83**

A 45 mL steel autoclave was charged with 1,3-bis-(2,6-diisopropylphenyl)-imidazolium chloride (**84a**, 10 wt%), TBD (**83**, 10 wt%), PFA (**68**, 1.0 g) and THF (5 mL). The reactor was purged once with CO_2 and pressurized with CO_2 to 4.0 MPa at 23 °C until the equilibrium was reached. After heating to the desired reaction temperature of 80–140 °C the reaction mixture was stirred for 6–24 h. The reactor was cooled to ambient temperature and CO_2 was released slowly. All volatiles were removed under reduced pressure.

GP-VI: Synthesis ofpoly (methylene carbonate) using imidazolium salt **84a** A 45 mL steel autoclave was charged with 1,3-bis-(2,6-diisopropylphenyl)-imidazolium chloride (**84a**, 10 wt%), PFA (**68**, 1.0 g) and THF (5 mL). The reactor was purged once with CO_2 and pressurized with CO_2 to 4.0 MPa at 23 °C until the equilibrium was reached. After heating to the desired reaction temperature of 80–140 °C the reaction mixture was stirred for 6–24 h. The reactor was cooled to ambient temperature and CO_2 was released slowly. All volatiles were removed under reduced pressure.

GP-VII: Parameter screening using imidazolium salt **84a** and TBD **83**

A 45 mL steel autoclave was charged with 1,3-bis-(2,6-diisopropylphenyl)-imidazolium chloride (**84a**, 0.025–20 wt%), TBD (**83**, 0.025–20 wt%), PFA (**68**, 1.0 g) THF (0–20 mL). The reactor was purged once with CO_2 and pressurized with CO_2 to 1.0–5.0 MPa at 23 °C until the equilibrium was reached. After heating to the desired reaction temperature of 80–140 °C the reaction mixture was stirred for 6–24 h. The reactor was cooled to ambient temperature and CO_2 was released slowly. All volatiles were removed under reduced pressure.

General Procedures – Grafting

GP-VIII: Syntheses of polycarbonates employing PPG-1000 **97**

A 45 mL steel autoclave was charged with 1,3-bis-(2,6-diisopropylphenyl)-imidazolium chloride (**84a**, 10 wt%), TBD (**83**, 10 wt%), PFA (**68**, 1.0 g), PPG-1000 (**97**, 1–50 wt%) and THF (5 mL). The reactor was purged once with CO_2 and pressurized with CO_2 to 4.0 MPa at 23 °C until the equilibrium was reached. After heating to the desired reaction temperature of 140 °C the reaction mixture was stirred for 16 h. The reactor was cooled to ambient temperature and CO_2 was released slowly. All volatiles were removed under reduced pressure.

General Procedures – Capping

GP-IX: End group protected poly(methylene carbonate)

A 45 mL steel autoclave was charged with 1,3-bis-(2,6-diisopropylphenyl)-imidazolium chloride (**84a**, 10 wt%), TBD (**83**, 10 wt%), PFA (**68**, 1.0 g) and THF (5 mL). The reactor was purged once with CO_2 and pressurized with CO_2 to 4.0 MPa at 23 °C until the equilibrium was reached. After heating to the desired reaction temperature of 140 °C the reaction mixture was stirred for 16 h. The reactor was cooled to ambient temperature and CO_2

was released slowly. After adding pyridine (**100**, 5 mL) and Ac_2O (**99**, 3 mL) the reactor was pressurized with argon (Ar) and the reaction mixture was stirred for 12 h at 23 °C. Ar was released slowly and the reaction mixture was poured into ice water (20 mL). The precipitate was filtered off and washed with water (40 mL). All volatiles were removed under reduced pressure.

GP-X: End group protected polycarbonates employing PPG-1000 **97**

A 45 mL steel autoclave was charged with 1,3-bis-(2,6-diisopropylphenyl)-imidazolium chloride (**84a**, 10 wt%), TBD (**83**, 10 wt%), PFA (**68**, 1.0 g), PPG-1000 (**97**, 2 wt%) and THF (5 mL). The reactor was purged once with CO_2 and pressurized with CO_2 to 4.0 MPa at 23 °C until the equilibrium was reached. After heating to the desired reaction temperature of 140 °C the reaction mixture was stirred for 16 h. The reactor was cooled to ambient temperature and CO_2 was released slowly. After adding pyridine (**100**, 5 mL) and Ac_2O (**99**, 3 mL) the reactor was pressurized with argon (Ar) and the reaction mixture was stirred for 12 h at 23 °C. Next, Ar was released slowly and the reaction mixture was poured into ice water (20 mL). The precipitate was filtered off and washed with water (40 mL). All volatiles were removed under reduced pressure.

6.5 Procedures and Spectroscopic Data

6.5.1 Monomeric Compounds

Tri-*n*-butyl-(2-hydroxyethyl)ammonium iodide (45a)[78]

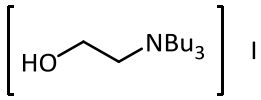

$C_{14}H_{32}INO$
M = 357.32 g·mol^{-1}

A 20 cm^3 pressure tube was charged with tri-*n*-butylamine (**75a**, 1.85 g, 10.0 mmol) and 2-iodoethanol (**76**, 1.72 g, 10.0 mmol) was added. The reaction mixture was heated to 80 °C for 24 h. The obtained product was washed with Et_2O (3×50 mL). All volatiles were removed under reduced pressure. The product **45a** was obtained as a pale yellow solid (2.91 g, 8.15 mmol, 81%).

Melting point: T_m = 60 °C.

^{1}H NMR (300 MHz, DMSO-d_6): δ = 1.00 (t, J = 7.3 Hz, 9H), 1.37–1.49 (m, 6H), 1.63–1.74 (m, 6H), 3.37-3.42 (m, 6H), 3.58–3.61 (m, 2H), 4.07–4.12 (m, 2H), 4.37 (t, J = 6.1 Hz, 1H) ppm.

^{13}C{^{1}H} NMR (75 MHz, DMSO-d_6): δ = 13.63 (3×CH_3), 19.63 (3×CH_2), 24.04 (3×CH_2), 55.21 (CH_2), 59.61 (3×CH_2), 60.45 (CH_2) ppm.

IR (ATR): $\tilde{\nu}$ = 3315 (s, br), 2960 (vs), 2873 (s), 1463 (vs), 1380 (m), 1320 (w), 1247 (w), 1167 (w), 1087 (vs), 1063 (m), 1000 (m), 943 (m), 906 (s), 870 (m) 797 (w), 737 (s), 667 (w) cm^{-1}.

MS (EI, 70 eV): *m/z* (%) = 184 (42), 173 (4) [M^+ – C_4H_9I], 155 (5), 142 (100), 130 (72), 128 (47), 116 (4), 112 (2), 100 (67), 98 (6), 88 (30), 86 (14), 74 (13), 58 (11), 57 (83) [$C_4H_9^+$], 44 (95), 41 (98), 36 (32).

HRMS (ESI): *m/z* calc. for $C_{14}H_{32}NO$: 230.2478; found: 230.2479 [M^+ – I].

EA: calc. (%) for $C_{13}H_{32}INO$: C 47.06, H 9.03, N 3.92; found: C 46.62, H 9.36, N 3.96.

Halide Titration: calc. (%) for $C_{13}H_{32}INO$: I 35.52; found: I 35.73.

Tri-*n*-butyl-(2-hydroxyethyl)phosphonium iodide (46a)[79]

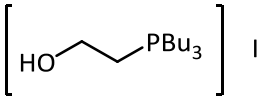

$C_{14}H_{32}IOP$
M = 374.29 g·mol^{-1}

A 20 cm^3 pressure tube was charged with tri-*n*-butylphosphine (**75b**, 2.13 g, 10.5 mmol) and 2-iodoethanol (**76**, 1.72 g, 10.0 mmol) was added. The reaction mixture was heated to 80 °C for 24 h. The obtained product was washed with Et_2O (3×50 mL). All volatiles were removed under reduced pressure. The product **46a** was obtained as a colorless solid (3.71 g, 9.91 mmol, 94%).

Melting point: T_m = 43 °C.

^{1}H NMR (300 MHz, $CDCl_3$): δ = 0.96 (t, J = 7.0 Hz, 9H), 1.52–1.60 (m, 12H), 2.31–2.41 (m, 6H), 2.73 (dt, J = 11.7 Hz, J = 5.9 Hz, 2H), 4.06 (dt, J = 20.6 Hz, J = 5.5 Hz, 2H), 4.30 (s, br, 1H) ppm.

^{13}C{^{1}H} NMR (75 MHz, $CDCl_3$): δ = 13.41 (s, 3×CH_3), 19.83 (d, J = 47.3 Hz, 3×CH_2), 22.85 (d, J = 49.2 Hz, CH_2), 23.65 (d, J = 4.8 Hz, 3×CH_2), 23.83 (d, J = 15.6 Hz, 3×CH_2), 54.68 (d, J = 7.1 Hz, CH_2) ppm.

^{31}P{^{1}H} NMR (121.5 MHz, $CDCl_3$): δ = 33.86 ppm.

IR (ATR): $\tilde{\nu}$ = 3314 (s, br), 2960 (vs), 2929 (vs), 2873 (vs), 1461 (s), 1414 (m), 1383 (m), 1310 (w), 1321 (m), 1207 (w), 1073 (vs), 1008 (m), 968 (m), 916 (m), 869 (m), 796 (m), 739 (m), 718 (m) cm^{-1}.

MS (EI, 70 eV): *m/z* (%) = 247 (6) [M^+ – I], 229 (12), 217 (3), 202 (40) [M^+ – C_2H_5O], 190 (2) [M^+ – C_4H_9], 173 (78), 160 (9), 146 (29), 131 (31), 127 (33), 118 (47), 104 (67), 92 (22), 89 (14), 78 (11), 76 (100), 62 (83), 57 (10), 55 (23), 48 (5), 45 (4), 41 (25), 36 (14).

HRMS (ESI): *m/z* calc. for $C_{14}H_{32}OP$: 247.2185 found: 247.2187 [M^+ – I].

EA: calc. (%) for $C_{14}H_{32}IOP$: C 44.93, H 8.62; found: C 44.39, H 8.85.

Halide Titration: calc. (%) for $C_{14}H_{32}IOP$: I 33.91; found: I 33.94.

Phopsphor calc.: (%) for $C_{13}H_{32}IOP$: P 8.28; found: P 8.58.

1,3-Bis-(2,6-diisopropylphenyl)-imidazolium iodide (84b)[160]

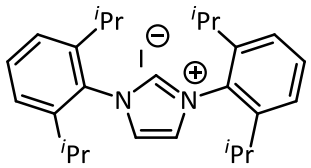

$C_{27}H_{37}IN_2$
M = 516.51 g·mol^{-1}

A solution of 1,3-bis-(2,6-diisopropylphenyl)-imidazolium chloride (**84a**, 1.00 g, 2.35 mmol) in water (30 mL) and sodium iodide (**51**, 1.71 g, 11.4 mmol) in acetone (35 mL) was prepared. The sodium iodide solution was added to the IPr · HCl solution resulting in an immediate precipitation of a yellow solid. After 1 h of stirring the solid was filtrated and washed with a minimal volume of water / acetone (1 / 1). The product **84b** was obtained as a yellow solid (0.651 g, 1.26 mmol, 54%).

Melting point: T_m = 218 °C.

^{1}H NMR (300 MHz, DMSO-d_6): δ = 1.30 (d, J = 6.8 Hz, 12H), 1.40 (d, J = 6.8 Hz, 12H), 2.49 (sept, J = 6.8 Hz, 4H), 7.67 (d, J = 7.8 Hz, 4H), 7.78–7.89 (m, 2H), 8.71 (d, J = 1.5 Hz, 2H), 10.30 (t, J = 1.5 Hz, 1H) ppm.

^{13}C{^{1}H} NMR (100 MHz, DMSO-d_6): δ = 23.07 (4×CH_3), 24.08 (4×CH_3), 28.60 (4×CH), 124.59 (2×CH), 126.16 (4×CH), 129.97 (2×C), 131.82 (2×CH), 139.20 (CH), 144.76 (4×C) ppm.

IR (ATR): $\tilde{\nu}$ = 2965 (s), 2097 (s), 1981 (w), 1813 (w), 1621 (w), 1532 (m), 1454 (w), 1388 (w), 1255 (w), 1201 (w), 1177 (w), 1104 (w), 1056 (m), 910 (m), 810 (s), 760 (s) cm^{-1}.

MS (EI, 70 eV): *m/z* (%) = 389 (13) [M^+ – I], 373 (25), 357 (18), 289 (5), 281 (7), 211 (6), 201 (35), 188 (38), 184 (12), 170 (18), 165 (8), 158 (14), 146 (27), 144 (15), 133 (4), 127 (13), 117 (10), 115 (14), 97 (5), 83 (5), 91 (19), 78 (16), 63 (19), 44 (100).

HRMS (ESI): *m/z* calc. for $C_{27}H_{37}IN_2$: 389.2951; found: 389.2956 [M^+].

EA: calc. (%) for $C_{27}H_{37}IN_2$: C 62.79, H 7.22, N 5.42; found: C 62.73, H 7.14, N 5.58.

Halide Titration: calc. (%) for $C_{27}H_{37}IN_2$: I 24.57; found: I 24.52.

4-(Isobutoxymethyl)-1,3-dioxolan-2-one (11d)[167]

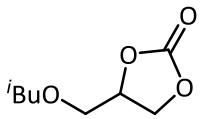

$C_8H_{14}O_4$
M = 174.19 g·mol^{-1}

According to **GP-II**, 2,3-epoxypropyl-*iso*-butylether (**32d**, 8.26 g, 63.5 mmol), 2-hydroxyethyl-tributylammonium iodide (**45a**, 453 mg, 1.26 mmol) and CO_2 were converted for 3 h. The reaction mixture was filtered over silica with CH_2Cl_2 and volatiles were removed under reduced pressure. The product **11d** was obtained as a yellow oil (9.96 g, 57.2 mmol, 90%).

^{1}H NMR (300 MHz, $CDCl_3$): δ = 0.90 (d, J = 6.7 Hz, 6H), 1.87 (sept, J = 6.7 Hz, 1H), 3.28 (d, J = 5.5 Hz, 2H), 3.60 (dd, J = 3.6 Hz, J = 11.0 Hz, 1H), 3.68 (dd, J = 3.6, J = 11.0 Hz, 1H), 4.42 (d, J = 6.7 Hz, 1H), 4.50 (m, 1H), 4.77–4.81 (m, 1H) ppm.

^{13}C{^{1}H} NMR (75 MHz, $CDCl_3$): δ = 19.09 (2×CH_3), 28.34 (CH), 66.26 (CH_2), 69.76 (CH_2), 75.08 (CH), 78.78 (CH_2), 154.99 (C=O) ppm.

IR (ATR): $\tilde{\nu}$ = 2958 (w), 2874 (w), 1786 (vs), 1479 (w), 1393 (w), 1164 (m), 1044 (s), 954 (w), 773 (m), 714 (m) cm^{-1}.

MS (EI, 70 eV): *m/z* (%) = 88 (9), 87 (14) [$M^+ - C_3H_3O_3$], 58 (13), 57 (100) [$C_4H_9^+$].

HRMS (ESI): *m/z* calc. for $C_8H_{15}O_4$: 175.0965; found: 175.0964 [M^++H].

4-(*tert*-Butoxymethyl)-1,3-dioxolan-2-one (11e)[168]

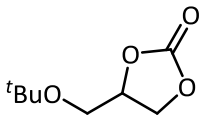

$C_8H_{14}O_4$
M = 174.19 g·mol^{-1}

According to **GP-II**, 3-Epoxypropyl-*tert*-butylether (**32e**, 8.48 g, 65.1 mmol), 2-hydroxy-ethyl-tributylammonium iodide (**45a**, 454 mg, 1.27 mmol) and CO_2 were converted for 3 h. The reaction mixture was filtered over silica with CH_2Cl_2 and volatiles were removed under reduced pressure. The product **11e** was obtained as a yellow oil (10.16 g, 58.31 mmol, 90%).

^{1}H NMR (300 MHz, $CDCl_3$): δ = 1.20 (s, 9H), 3.54 (dd, *J* = 3.6 Hz, *J* = 10.3 Hz, 1H), 3.62 (dd, *J* = 3.6 Hz, *J* = 10.3 Hz, 1H), 4.37–4.41 (m, 1H), 4.45–4.51 (m, 1H), 4.74–4.81 (m, 1H) ppm.

^{13}C{^{1}H} NMR (75 MHz, $CDCl_3$): δ = 27.27 (3×CH_3), 61.25 (CH), 66.56 (CH_2), 73.88 (CH), 75.10 (CH_2), 154.99 (C=O) ppm.

IR (ATR): $\tilde{\nu}$ = 2975 (w), 1786 (vs), 1390 (w), 1365 (m), 1163 (s), 1087 (m), 1053 (s), 883 (m), 773 (m), 714 (w) cm^{-1}.

MS (EI, 70 eV): *m/z* (%) = 159 (16) [$M^+ - CH_3$], 59 (19) [$C_3H_7O^+$], 57 (100) [$C_4H_9^+$].

4-(Isopropyloxymethyl)-1,3-dioxolan-2-one (11f)[169]

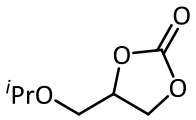

$C_7H_{12}O_4$
M = 160.17 g·mol^{-1}

According to **GP-II**, 2,3-Epoxypropyl-*iso*-propylether (**32f**, 8.43 g, 72.6 mmol), 2-hydroxyethyl-tributylammonium iodide (**45a**, 518 mg, 1.45 mmol) and CO_2 were converted for 3 h. The reaction mixture was filtered over silica with CH_2Cl_2 and volatiles were removed under reduced pressure. The product **11f** was obtained as a yellow oil (10.59 g, 66.12 mmol, 91%).

^{1}H NMR (300 MHz, $CDCl_3$): δ = 0.90 (dd, *J* = 6.1 Hz, *J* = 3.1 Hz, 6H), 3.59–3.71 (m, 3H), 4.37–4.42 (m, 1H), 4.47–4.52 (m, 1H), 4.76–4.83 (m, 1H) ppm.

^{13}C{^{1}H} NMR (75 MHz, $CDCl_3$, 23 °C): δ = 21.79 (CH_3), 21.89 (CH_3), 66.45 (CH_2), 67.11 (CH_2), 72.99 (CH), 75.08 (CH_2), 155.02 (C=O) ppm.

IR (ATR): $\tilde{\nu}$ = 2975 (w), 1784 (vs), 1391 (w), 1370 (w), 1336 (w), 1166 (m), 1053 (s), 937 (w), 773 (m), 714 (m) cm^{-1}.

MS (EI, 70 eV): *m/z* (%) = 145 (9) [$M^+ - CH_3$], 130 (13) [$C_5H_6O_4^+$], 88 (65) [$C_3H_4O_3^+$], 73 (100) [$C_4H_9O^+$], 59 (36), 58 (27), 57 (80) [$C_3H_5O^+$], 55 (15).

HRMS (ESI): *m/z* calc. for $C_7H_{13}O_4$: 161.0808; found: 161.0808 [M^+ + H].

4,4'-((Butane-1,4-diylbis(oxy))bis(methylene))bis(1,3-dioxolan-2-one) (50a)[90]

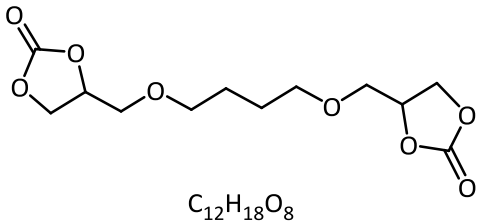

$C_{12}H_{18}O_8$
M = 290.27 g·mol^{-1}

According to **GP-II**, 1,4-bis(oxiran-2-ylmethoxy)butane (**49a**, 2.13 g, 10.5 mmol), 2-hydroxyethyl-tributylammonium iodide (**45a**, 72 mg, 0.20 mmol) and CO_2 were converted to the desired cyclic carbonate after 3 h. The product **50a** was obtained as a colorless solid (2.99 g, 10.3 mmol, 98%, 1:1 mixture of diastereoisomers).

Melting point: T_m = 68 °C.

^{1}H NMR (300 MHz, mixture of stereoisomers, $CDCl_3$): δ = 1.63–1.67 (m, 4H), 3.52–3.72 (m, 8H), 3.40–4.43 (m, 2H), 4.53 (t, J = 8.3 Hz, 2H), 4.78–4.85 (m, 2H) ppm.

^{13}C{^{1}H} NMR (75 MHz, mixture of stereoisomers, $CDCl_3$): δ = 26.00 (CH_2), 26.02 (CH_2), 66.16 (2×CH_2), 69.58 (CH_2), 69.61 (CH_2), 71.56 (CH_2), 71.61 (CH_2), 75.14 (2×CH), 155.03 (2×C=O) ppm.

IR (ATR): $\tilde{\nu}$ = 2940 (w), 2899 (w), 2870 (w), 1780 (vs), 1477 (m), 1450 (w), 1396 (s), 1360 (m), 1331 (w), 1248 (w), 1170 (s), 1131 (s), 1045 (s), 1003 (s), 767 (m), 713 (m) cm^{-1}.

MS (EI, 70 eV): *m/z* (%) = 203 (2) [$M^+ - C_3H_3O_3$], 189 (12) [$M^+ - C_4H_5O_3$], 173 (69) [$M^+ - C_4H_5O_4$], 144 (2), 119 (24), 111 (2), 87 (13) [$C_3H_3O_3^+$], 81 (3), 79 (1), 71 (64), 63 (3), 57 (100), 43 (47), 39 (11).

HRMS (ESI): *m/z* calc. for $C_{12}H_{19}O_8$: 291.1074; found: 291.1073 [M^+ + H].

EA: calc. (%) for $C_{12}H_{18}O_8$: C 49.65, H 6.25; found: C 50.08, H 6.38.

4-((4-(Oxiran-2-ylmethoxy)butoxy)methyl)-1,3-dioxolan-2-one (77a)

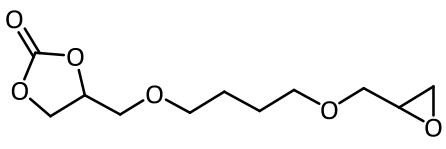

$C_{11}H_{18}O_6$
M = 246.26 g·mol^{-1}

According to **GP-II**, 1,4-bis(oxiran-2-ylmethoxy)butane (**49a**, 2.13 g, 10.6 mmol), 2-hydroxyethyl-tributylammonium iodide (**45a**, 72 mg, 0.20 mmol) and CO_2 were

converted for 3 h at 60 °C. After purification with column chromatography (SiO_2, CH:EtOAc = 3:1, 1:1) the complete carboxylated product **50a** was obtained as a white solid (864 mg, 2.98 mmol, 28%) and the product **77a** was obtained as a colorless oil (806 mg, 3.27 mmol, 31%).

R_f (SiO_2, CH:EtOAc = 1:1) = 0.22.

^{1}H NMR (300 MHz, mixture of stereoisomers, $CDCl_3$): δ = 1.63–1.65 (m, 4H), 2.60 (dd, *J* = 5.0 Hz, *J* = 2.7 Hz, 1H), 2.77–2.91 (m, 1H), 3.06–3.25 (m, 1H), 3.34 (dd, *J* = 11.5 Hz, *J* = 5.9 Hz, 1H), 3.44–3.79 (m, 7H), 4.38 (dd, *J* = 11.5 Hz, *J* = 5.9 Hz, 1H), 4.49 (t, *J* = 8.3 Hz, 1H), 4.74–4.89 (m, 1H) ppm.

^{13}C{^{1}H} NMR (75 MHz, mixture of stereoisomers, $CDCl_3$): δ = 26.11 (CH_2), 26.14 (CH_2), 44.17 (2×CH_2), 50.81 (2×CH), 66.20 (2×CH_2), 69.57 (4×CH_2), 71.04 (2×CH_2), 71.38 (2×CH_2), 71.71 (2×CH_2), 75.01 (2×CH), 154.92 (2×C=O) ppm.

IR (ATR): $\tilde{\nu}$ = 2867 (w), 1788 (vs), 1480 (w), 1472 (w), 1477 (m), 1393 (w), 1361 (w), 1337 (w), 1252 (w), 1167 (m), 1100 (s), 1047 (vs), 954 (w), 909 (w), 851 (m), 772 (m) cm^{-1}.

MS (EI, 70 eV): *m/z* (%) = 189 (1) [$M^+ - C_3H_5O$], 173 (4) [$M^+ - C_8H_{13}O_4$], 144 (5), 129 (17), 114 (16), 111 (1) [$C_3H_3O_3^+$], 100 (8), 87 (16), 81 (2), 73 (10) [$C_8H_{13}O_4^+$], 71 (94), 63 (4), 57 (91) [$C_3H_5O^+$], 43 (82), 29 (100).

HRMS (ESI): *m/z* calc. for $C_{11}H_{18}O_6Na$: 269.0996; found: 269.0995 [M^+ + Na].

EA: calc. (%) for $C_{11}H_{18}O_6$: C 53.65, H 7.73; found: C 53.68, H 7.18.

4,4'-(Butane-1,4-diyl)bis(1,3-dioxolan-2-one) (50b)[83]

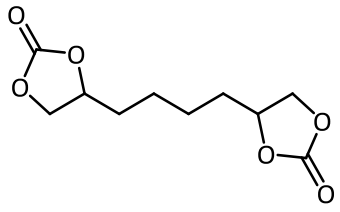

$C_{10}H_{14}O_6$
M = 230.22 g·mol^{-1}

According to **GP-II**, 1,4-di(oxiran-2-yl)butane (**49b**, 1.47 g, 10.3 mmol), 2-hydroxyethyl-tributylammonium iodide (**45a**, 75 mg, 0.21 mmol) and CO_2 were converted for 14 h. After purification with column chromatography (SiO_2, CH:EtOAc = 2:1, 1:2) the product **50b** was obtained as a colorless solid (2.34 g, 10.2 mmol, 99%, 1:1 mixture of diastereoisomers).

R_f (SiO_2, CH:EtOAc = 1:1) = 0.06.

Melting point: T_m = 28 °C.

^{1}H NMR (300 MHz, mixture of stereoisomers, $CDCl_3$): δ = 1.38–1.67 (m, 4H), 1.67–1.98 (m, 4H), 4.08 (dd, *J* = 8.4 Hz, *J* = 7.1 Hz, 2H), 4.55 (t, *J* = 8.2 Hz, 2H), 4.66–4.90 (m, 2H) ppm.

^{13}C{^{1}H} NMR (75 MHz, mixture of stereoisomers, $CDCl_3$): δ = 24.09 (CH_2), 24.14 (CH_2), 33.56 (CH_2), 33.63 (CH_2), 69.25 (2×CH_2), 76.64 (2×CH), 154.88 (2×C=O) ppm.

IR (ATR): $\tilde{\nu}$ = 2938 (w), 2866 (w), 1776 (s), 1553 (w), 1483 (w), 1471 (w), 1387 (m), 1161 (s), 1095 (w), 1051 (vs), 869 (w), 860 (w), 773 (m), 716 (m) cm^{-1}.

MS (EI, 70 eV): *m/z* (%) = 129 (11) [$M^+ - C_6H_9O_3$], 124 (1), 116 (2), 109 (5), 103 (1), 98 (1), 95 (8), 87 (13) [$C_3H_3O_3^+$], 82 (21), 71 (15), 67 (49), 58 (30), 54 (40), 43 (100), 39 (23).

HRMS (ESI): *m/z* calc. for $C_{10}H_{15}O_6$: 231.0863; found: 231.0857 [M^+ + H].

EA: calc. (%) for $C_{10}H_{14}O_6$: C 52.17, H 6.13; found: C 52.23, H 6.19.

4-(4-(Oxiran-2-yl)butyl)-1,3-dioxolan-2-one (77b)

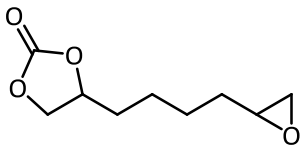

$C_9H_{14}O_4$
M = 186.07 g·mol^{-1}

According to **GP-II**, 4,4'-(butane-1,4-diyl)bis(1,3-dioxolan-2-one) (**49b**, 1.47 g, 10.3 mmol), 2-hydroxyethyltributylammonium iodide (**45a**, 75 mg, 0.21 mmol) and CO_2 were converted for 3 h. After purification with column chromatography (SiO_2, CH:EtOAc = 2:1, 1:2) the complete carboxylated product **50b** was obtained as a colorless solid (1.94 g, 8.43 mmol, 82%) and the product **77b** was obtained as a colorless oil (319 mg, 1.71 mmol, 16%).

R_f(SiO_2, CH:EtOAc = 1:1) = 0.25.

^{1}H NMR (300 MHz, mixture of stereoisomers, $CDCl_3$): δ = 1.39–1.91 (m, 8H), 2.45–2.48 (m, 1H), 2.75 (dd, *J* = 4.9 Hz, *J* = 4.0 Hz, 1H), 2.86–3.26 (m, 1H), 4.07 (dd, *J* = 8.4 Hz, *J* = 7.2 Hz, 1H), 4.53 (t, *J* = 8.1 Hz, 1H), 4.65–4.82 (m, 1H) ppm.

$^{13}C\{^1H\}$ NMR (75 MHz, mixture of stereoisomers, $CDCl_3$): δ = 24.19 (CH_2), 24.23 (CH_2), 25.58 (CH_2), 25.61 (CH_2), 32.03 (CH_2), 32.11 (CH_2), 33.72 (CH_2), 33.79 (CH_2), 46.89 (CH_2), 46.92 (CH_2), 51.95 (2×CH), 69.29 (CH_2), 69.28 (CH_2), 76.80 (2×CH), 154.94 (2×C=O) ppm.

IR (ATR): $\tilde{\nu}$ = 2933 (w), 2866 (w), 1786 (s), 1553 (w), 1483 (w), 1471 (w), 1387 (m), 1372 (w), 1166 (s), 1095 (w), 1055 (s), 914 (w), 833 (w), 860 (w), 773 (m), 716 (m) cm^{-1}.

MS (EI, 70 eV): *m/z* (%) = 143 (5) [$M^+ - C_2H_3O$], 129 (4) [$M^+ - C_6H_9O_3$], 124 (1), 116 (2), 109 (5), 103 (1), 99 (1), 95 (8), 87 (5) [$C_3H_3O_3^+$], 81 (71), 79 (48), 71 (55), 67 (62), 58 (21), 54 (49), 43 (100) [$C_2H_3O^+$], 39 (48).

HRMS (ESI): *m/z* calc. for $C_9H_{14}O_4Na$: 209.0784; found: 209.0782 [M^+ + Na].

EA: calc. (%) for $C_9H_{14}O_4$: C 58.05, H 7.58; found: C 58.25, H 7.93.

4,4'-((1,3-Phenylenebis(oxy))bis(methylene))bis(1,3-dioxolan-2-one) (50c)[91]

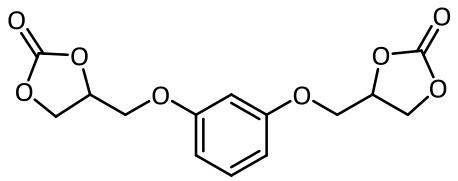

$C_{14}H_{14}O_8$
M = 310.26 g·mol^{-1}

According to **GP-II**, 1,3-bis(oxiran-2-ylmethoxy)benzene (**49c**, 2.36 g, 10.6 mmol), 2-hydroxyethyl-tributylammonium iodide (**45a**, 72 mg, 0.20 mmol) and CO_2 were converted for 14 h. The reaction mixture was filtered through a pad of silica with CH_2Cl_2 and all volatiles were removed under reduced pressure. The product **50c** was obtained as a yellow solid (3.13 g, 10.1 mmol, 95%).

Melting point: T_m = 85 °C.

^1H NMR (300 MHz, mixture of stereoisomers, $CDCl_3$): δ = 4.10 (dd, *J* = 10.8 Hz, *J* = 3.5 Hz, 2H), 4.23 (ddd, *J* = 10.8 Hz, *J* = 3.4 Hz, *J* = 0.9 Hz, 2H), 4.46–4.56 (m, 2H), 4.61 (dd, *J* = 8.5 Hz, *J* = 8.5 Hz, 2H), 4.92–5.19 (m, 2H), 6.43–6.68 (m, 3H), 7.09–7.26 (m, 1H) ppm.

$^{13}C\{^1H\}$ NMR (75 MHz, mixture of stereoisomers, $CDCl_3$): δ = 66.04 (2×CH_2), 67.00 (CH_2), 67.05 (CH_2), 74.17 (CH), 101.90 (CH), 101.99 (CH), 107.87 (2×CH), 130.33 (CH), 154.73 (2×C=O), 158.99 (2×C) ppm.

IR (ATR): $\tilde{\nu}$ = 2990 (w), 2929 (w), 2878 (w), 1781 (vs), 1593 (s), 1491 (m), 1452 (m), 1397 (w), 1289 (w), 1266 (w), 1154 (s, br), 1085 (m), 1048 (vs), 956 (m), 837 (w), 767 (m), 735 (w) cm^{-1}.

MS (EI, 70 eV): *m/z* (%) = 310 (56) [M^+], 223 (6) [$M^+ - C_3H_3O_4$], 210 (10), 193 (4) [$M^+ - C_4H_5O_4$], 147 (8), 137 (18), 123 (34), 117 (1) [$C_4H_5O_4^+$], 110 (100), 92 (28), 87 (2) [$C_3H_3O_4^+$], 82 (23), 77 (20), 64 (20), 57 (34), 44 (14).

HRMS (ESI): *m/z* calc. for $C_{14}H_{15}O_8$: 311.0761; found: 311.0761 [M^+ + H].

EA: calc. (%) for $C_{14}H_{14}O_8$: C 54.20, H 4.55; found: C 54.14, H 4.49.

4,4'-(((Propane-2,2-diylbis(4,1-phenylene))bis(oxy))bis(methylene))bis(1,3-dioxolan-2-one) (50d)[86]

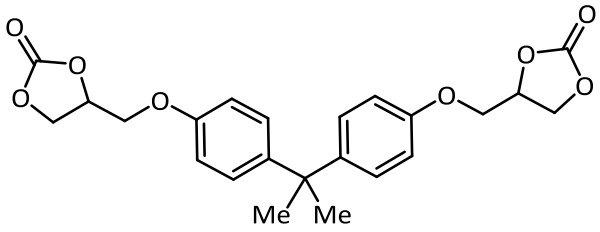

$C_{23}H_{24}O_8$
M = 428.44 g·mol^{-1}

According to **GP-II**, 2,2'-(((propane-2,2-diylbis(4,1-phenylene))bis(oxy))bis(methylene)) bis(oxirane) (**49d**, 3.42 g, 10.0 mmol), 2-hydroxyethyl-tributylammonium iodide (**45a**, 72 mg, 0.20 mmol) and CO_2 were converted for 14 h in MEK (3 mL). The reaction mixture was filtered through a pad of silica with CH_2Cl_2 and all volatiles were removed under reduced pressure. The product **50d** was obtained as a colorless solid (4.21 g, 9.83 mmol, 98%).

Melting point: T_m = 163 °C.

^{1}H NMR (300 MHz, mixture of stereoisomers, $CDCl_3$): δ = 1.64 (s, 6H), 4.13 (dd, *J* = 10.6, 3.6 Hz, 2H), 4.22 (dd, *J* = 10.6 Hz, 4.3 Hz, 2H), 4.53 (dd, *J* = 8.5 Hz, *J* = 5.9 Hz, 2H), 4.66 (dd, *J* = 8.4 Hz, *J* = 8.4 Hz, 2H), 4.98–5.06 (m, 2H), 6.81 (d, *J* = 8.9 Hz, 4H), 7.15 (d, *J* = 8.9 Hz, 4H) ppm.

^{13}C{^{1}H} NMR (75 MHz, mixture of stereoisomers, $CDCl_3$): δ = 30.94 (2×CH_3), 41.82 (C), 66.21 (2×CH_2), 66.88 (2×CH), 74.06 (2×CH_2), 114.03 (4×CH), 127.91 (4×CH), 144.33 (2×C), 154.61 (2×C), 155.63 (2×C=O) ppm.

IR (ATR): $\tilde{\nu}$ = 2990 (w), 2929 (w), 2878 (w), 1783 (vs), 1604 (m), 1509 (s), 1476 (s), 1460 (m), 1419 (m), 1367 (w), 1281 (w), 1173 (s), 1105 (s), 995 (s), 821 (m), 771 (m) cm^{-1}.

MS (EI, 70 eV): *m/z* (%) = 428 (5) [M^+], 413 (44), 369 (1), 355 (2), 281 (4), 253 (3), 234 (3), 219 (4), 207 (25), 191 (3), 165 (6), 133 (4), 119 (6), 117 (1), 57 (2), 43 (100), 40 (63).

HRMS (ESI): *m/z* calc. for $C_{23}H_{25}O_8$: 429.1544; found: 429.1543 [M^+ + H].

EA: calc. (%) for $C_{23}H_{24}O_8$: C 64.48, H 5.65; found: C 64.44, H 5.26.

4,4'-(((2,2-Dimethylpropane-1,3-diyl)bis(oxy))bis(methylene))bis(1,3-dioxolan-2-one) (50f)[91]

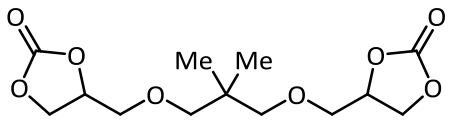

$C_{13}H_{20}O_8$
M = 304.30 g·mol^{-1}

According to **GP-II**, 2,2'-(((2,2-dimethylpropane-1,3-diyl)bis(oxy))bis(methylene)) bis(oxirane) (**49f**, 2.16 g, 10.0 mmol), 2-hydroxyethyl-tributylammonium iodide (**45a**, 72 mg, 0.20 mmol) and CO_2 were converted for 14 h. After purification with column chromatography (SiO_2, CH:EtOAc = 2:1, 1:1) the product **50f** was obtained as a colorless solid (2.84 g, 9.33 mmol, 93%, 1:1 mixture of diastereoisomers).

R_f (SiO_2, CH:EtOAc = 1:1) = 0.29.

Melting point: T_m = 34 °C.

^{1}H NMR (300 MHz, mixture of stereoisomers, $CDCl_3$): δ = 0.88 (s, 6H), 3.22–3.34 (m, 4H), 3.57 (dd, J = 11.2 Hz, J = 3.4 Hz, 2H), 3.71 (dd, J = 11.2 Hz, J = 2.8 Hz, 2H), 4.35–4.53 (m, 4H), 4.79–4.85 (m, 2H) ppm.

^{13}C{^{1}H} NMR (75 MHz, mixture of stereoisomers, $CDCl_3$): δ = 21.89 (2×CH_3), 36.32 (C), 66.14 (2×CH_2), 70.07 (CH_2), 70.39 (CH_2), 75.26 (2×CH), 76.67 (CH_2), 76.91 (CH_2), 155.15 (2×C=O) ppm.

IR (ATR): $\tilde{\nu}$ = 2968 (w), 2904 (w), 2871 (w), 1781 (vs), 1490 (m), 1398 (m), 1243 (w), 1164 (s), 1133 (s), 1102 (s), 1075 (m), 1038 (s), 961 (m), 846 (w), 764 (m) cm^{-1}.

MS (EI, 70 eV): *m/z* (%) = 217 (2) [$M^+ - C_3H_3O_3$], 203 (13) [$M^+ - C_4H_5O_3$], 187 (4) [$M^+ - C_9H_{15}O_4$] 185 (6), 172 (4), 159 (1), 145 (2), 141 (1), 125 (4), 119 (19), 111 (13), 101 (3)

[$C_4H_5O_3^+$], 99 (14), 87 (34) [$C_3H_3O_3^+$], 85 (25), 99 (14), 87 (34), 85 (25), 73 (18), 71 (16), 69 (54), 57 (100), 44 (25), 39 (16).

HRMS (ESI): *m/z* calc. for $C_{13}H_{20}O_8Na$: 327.1050; found: 327.1055 [M^+ + Na].

EA: calc. (%) for $C_{13}H_{20}O_8$: C 51.31, H 6.63; found: C 51.54, H 6.43.

Bis((2-oxo-1,3-dioxolan-4-yl)methyl) cyclohexane-1,2-dicarboxylate (50h)[170]

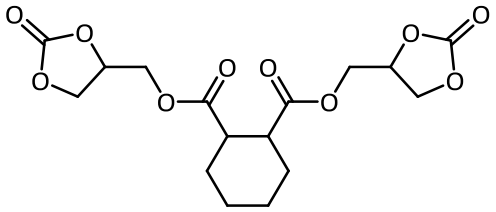

$C_{16}H_{20}O_{10}$
M = 372.33 g·mol^{-1}

According to **GP-II**, bis(oxiran-2-ylmethyl) cyclohexane-1,2-dicarboxylate (**49h**, 3.72 g, 10.0 mmol), 2-hydroxyethyl-tributylammonium iodide (**45a**, 72 mg, 0.20 mmol) and CO_2 were converted for 14 h. After purification with column chromatography (SiO_2, CH:EtOAc = 2:1, 1:2) the product **50h** was obtained as a colorless oil (3.28 g, 8.82 mmol, 88%).

R_f (SiO_2, CH:EtOAc = 1:1) = 0.12.

^{1}H NMR (300 MHz, mixture of stereoisomers, $CDCl_3$): δ = 1.43–1.60 (m, 4H), 1.80–1.87 (m, 2H), 1.96–2.01 (m, 2H), 2.86–2.99 (m, 2H), 4.21–4.46 (m, 6H), 4.52–4.60 (m, 2H), 4.92–4.96 (m, 2H) ppm.

^{13}C{^{1}H} NMR (101 MHz, mixture of stereoisomers, $CDCl_3$): δ = 23.34 (CH_2), 23.56 (CH_2), 23.75 (CH_2), 25.77 (CH_2), 26.06 (CH_2), 26.13 (CH_2), 26.37 (CH_2), 42.35 (CH), 42.38 (CH), 62.84 (CH_2), 62.95 (CH_2), 63.22 (CH_2), 63.33 (CH_2), 65.84 (CH_2), 65.90 (CH_2), 65.92 (CH_2), 65.94 (CH_2), 73.84 (CH), 73.85 (CH), 73.88 (CH), 73.91 (CH), 154.45 (C=O), 154.49 (C=O), 172.97 (C=O), 173.03 (C=O), 173.07 (C=O) ppm.

IR (ATR): $\tilde{\nu}$ = 2941 (w), 1786 (vs), 1729 (vs), 1481 (w), 1452 (w), 1393 (m), 1337 (m), 1302 (w), 1158 (vs), 1129 (m), 1089 (m), 1048 (s), 865 (w), 856 (w), 767 (w), 713 (w) cm^{-1}.

MS (EI, 70 eV): *m/z* (%) = 255 (62) [$M^+ - C_4H_5O_4$], 241 (1), 227 (53) [$M^+ - C_5H_5O_5$], 212 (6), 207 (11), 187 (3), 173 (9), 160 (4), 136 (4), 119 (9), 109 (17), 81 (100), 67 (29), 57 (16), 55 (22), 44 (98), 40 (12).

HRMS (ESI): *m/z* calc. for $C_{16}H_{20}O_{10}Na$: 395.0949; found: 395.0952 [M^+ + Na].

EA: calc. (%) for $C_{16}H_{20}O_{10}$: C 51.61, H 5.41; found: C 51.30, H 5.55.

1,3,5-Tris((2-oxo-1,3-dioxolan-4-yl)methyl)-1,3,5-triazinane-2,4,6-trione (57)[87]

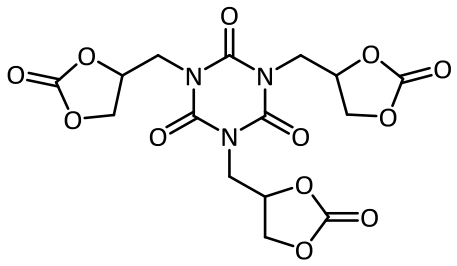

$C_{15}H_{15}N_3O_{12}$
M = 429.29 g·mol^{-1}

According to **GP-II**, 1,3,5-tris(oxiran-2-ylmethyl)-1,3,5-triazinane-2,4,6-trione (**56**, 2.97 g, 10.0 mmol), 2-hydroxyethyl-tributylammonium iodide (**45a**, 72 mg, 0.20 mmol) and CO_2 were converted for 14 h in MEK (3 mL). The reaction mixture was filtered and washed with CH_2Cl_2. volatiles were removed under reduced pressure. The product **57** was obtained as a colorless solid (4.07 g, 9.48 mmol, 95%).

Melting point: T_m = 261 °C.

^{1}H NMR (300 MHz, mixture of stereoisomers, DMSO-d_6): δ = 3.99–4.13 (m, 3H), 4.13–4.28 (m, 3H), 4.27–4.46 (m, 3H), 4.56 (t, J = 8.3 Hz, 3H), 4.86–5.08 (m, 3H) ppm.

^{13}C{^{1}H} NMR (75 MHz, mixture of stereoisomers, DMSO-d_6): δ = 43.75 (3×CH_2), 67.47 (3×CH_2), 73.80 (CH), 73.85 (CH), 73.91 (CH), 149.25 (3×C=O), 154.38 (3×C=O) ppm.

IR (ATR): $\tilde{\nu}$ = 1787 (s), 1685 (vs), 1455 (s), 1405 (m), 1327 (w), 1167 (s), 1167 (s), 1101 (w), 1072 (m), 1038 (m), 989 (w), 937 (w), 910 (w), 871 (w) 851 (w), 767 (s), 716 (m) cm^{-1}.

MS (EI, 70 eV): *m/z* (%) = 429 (4) [M^+], 355 (6), 281 (3), 256 (3), 246 (3), 221 (4), 217 (3), 125 (2), 188 (3), 178 (4), 167 (4), 149 (13), 112 (6), 97 (5), 91 (32), 83 (7), 78 (13), 63 (15), 57 (9), 49 (5), 44 (100).

HRMS (ESI): *m/z* calc. for $C_{15}H_{16}N_3O_{12}$: 430.0729; found: 430.0736 [M^+ + H].

EA: calc. (%) for $C_{15}H_{15}N_3O_{12}$: C 41.97, H 3.52, N 9.79; found: C 41.63, H 3.29, N 9.70.

(2-Oxohexahydrobenzo[1,3]dioxol-5-yl)methyl 2-oxohexahydrobenzo[d][1,3]dioxole-5-carboxylate (79)

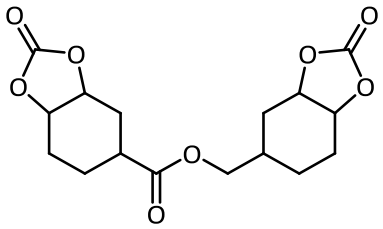

$C_{16}H_{20}O_8$
M = 340.33 g·mol^{-1}

According to **GP-II**, (7-oxabicyclo[4.1.0]heptane-3-yl)methyl 7-oxabicyclo[4.1.0]heptane-3-carboxylate (**78**, 2.52 g, 10.0 mmol), 2-hydroxyethyl-tributylammonium iodide (**45a**, 357 mg, 1.00 mmol) and CO_2 were converted for 48 h. The reaction mixture was filtered on silica with CH_2Cl_2 and volatiles were removed under reduced pressure. The product **79** was obtained as a colorless oil (3.05 g, 8.96 mmol, 90%).

^{1}H NMR (300 MHz, mixture of stereoisomers, DMSO-d_6): δ = 1.02–1.25 (m, 1H), 1.41–2.78 (m, 13H), 3.82–4.09 (m, 2H), 4.48–5.26 (m, 4H) ppm.

^{13}C{^{1}H} NMR (75 MHz, mixture of stereoisomers, DMSO-d_6): δ = 21.02 (CH_2), 21.48 (CH_2), 21.61 (CH_2), 21.76 (CH_2), 24.27 (CH_2), 24.50 (CH_2), 25.03 (CH_2), 25.59 (CH_2), 27.36 (CH_2), 27.74 (CH_2), 28.78 (CH_2), 29.04 (CH), 29.07 (CH), 29.91 (CH_2), 31.48 (CH_2), 35.16 (CH_2), 36.36 (CH_2), 36.43 (CH_2), 38.67 (CH_2), 38.95 (CH_2), 39.22 (CH_2), 39.50 (CH_2), 39.78 (CH_2), 40.23 (CH), 40.33 (CH), 67.54 (CH), 67.69 (CH), 74.36 (CH_2), 74.57 (CH_2), 74.79 (CH_2), 74.92 (CH_2), 74.95 (CH_2), 74.98 (CH_2), 75.57 (CH_2), 75.59 (CH_2), 154.47 (C=O), 154.52 (C=O), 154.64 (C=O), 154.69 (C=O), 173.39 (C=O), 173.42 (C=O), 173.80 (C=O), 173.83 (C=O) ppm.

IR (ATR): $\tilde{\nu}$ = 2945 (w), 2899 (w), 1787 (vs), 1724 (s), 1452 (w), 1436 (w), 1358 (w), 1306 (w), 1260 (w), 1170 (s), 1144 (s), 1027 (vs), 975 (w), 899 (w), 777 (m), 732 (m), 699 (w) cm^{-1}.

MS (EI, 70 eV): *m/z* (%) = 296 (22) [M^+ – CO_2], 268 (5), 252 (4) [M^+ – C_2O_4], 240 (6), 227 (7), 187 (15), 173 (10), 169 (35), 155 (48) [$C_8H_{11}O_3^+$], 142 (59), 128 (45), 125 (88), 114 (19), 110 (99), 97 (99), 85 (75), 82 (100), 73 (15), 67 (96), 54 (53), 44 (62), 39 (73).

HRMS (ESI): *m/z* calc. for $C_{16}H_{20}O_8Na$: 363.1050; found: 363.1055 [M^+ + Na].

EA: calc. (%) for $C_{16}H_{20}O_8$: C 56.47, H 5.92; found: C 56.33, H 6.21.

4,4',4'',4'''-(((Methylenebis(4,1-phenylene))bis(azanetriyl))tetrakis(methylene))tetrakis (1,3-dioxolan-2-one) (81)

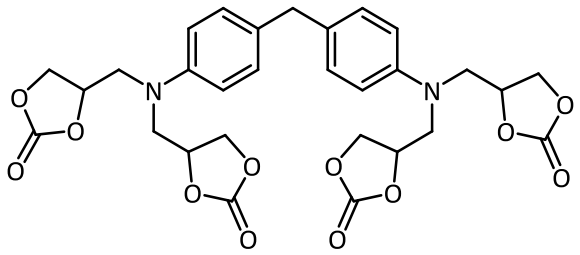

$C_{29}H_{30}N_2O_{12}$
M = 598.56 g·mol^{-1}

According to **GP-II**, 4,4'-methylenebis(N,N-bis(oxiran-2-ylmethyl)aniline) (**80**, 4.23 g, 10.0 mmol), 2-hydroxyethyl-tributylammonium iodide (**45a**, 72 mg, 0.20 mmol) and CO_2 were converted for 14 h in MEK (3 mL). The reaction mixture was filtered over silica with CH_2Cl_2 and all volatiles were removed under reduced pressure. The product **81** was obtained as a colorless solid (5.77 g, 9.64 mmol, 96%).

Melting point: T_m = 90 °C.

^{1}H NMR (300 MHz, mixture of stereoisomers, $CDCl_3$): δ = 3.70–3.78 (m, 10H), 4.14 (ddd, J = 8.7 Hz, 7.2 Hz, 1.9 Hz, 4H), 4.55 (td, J = 8.7 Hz, 7.2 Hz, 4H), 4.89–5.00 (m, 4H), 6.75–6.81 (m, 4H), 7.02 (d, J = 8.2 Hz, 4H) ppm.

^{13}C{^{1}H} NMR (75 MHz, mixture of stereoisomers, $CDCl_3$): δ = 39.05 (CH_2), 52.43 (CH_2), 53.43 (CH_2), 67.16 (CH_2), 75.01 (CH), 75.02 (CH), 112.66 (CH), 113.01 (CH), 129.27 (CH), 129.30 (CH), 130.72 (C), 144.69 (C), 145.22 (C), 154.72 (C=O), 154.73 (C=O) ppm.

IR (ATR): $\tilde{\nu}$ = 2979 (w), 2939 (w), 2880 (w), 1780 (vs), 1611 (w), 1514 (m), 1479 (w), 1393 (m), 1301 (w), 1242 (w), 1164 (s), 1077 (s), 986 (w), 937 (w), 850 (w), 801 (w), 769 (m) 745 (w), 680 (w) cm^{-1}.

MS (EI, 70 eV): *m/z* (%) = 511 (7) [$M^+ - C_3H_3O_3$], 467 (39), 423 (100), 410 (18) [$M^+ - C_7H_8O_6$], 393 (10), 381 (15), 379 (26), 367 (24), 351 (13), 337 (11) [$M^+ - C_9H_9O_9$], 329 (11), 323 (31), 311 (13), 279 (26), 262 (16), 237 (17), 223 (23), 206 (9), 165 (11), 142 (78), 130 (10), 118 (56), 100 (27), 56 (40), 41 (14).

HRMS (ESI): *m/z* calc. for $C_{29}H_{31}N_2O_{12}$: 599.1872; found: 599.1874 [M^+ + H].

EA: calc. (%) for $C_{29}H_{30}N_2O_{12}$: C 58.19, H 5.05, N 4.68; found: C 57.62, H 5.33, N 4.90.

6.5.2 Polymeric Compounds

PPG-GC$_2$ 728 (50i)[111]

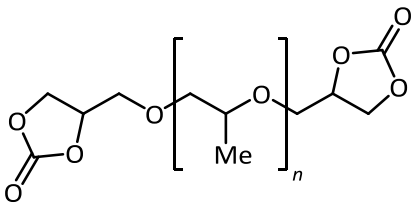

According to **GP-II**, polypropylene glycol diglycidyl ether 640 (**49i**, 6.55 g, 10.6 mmol), 2-hydroxyethyl-tributylammonium iodide (**45a**, 72 mg, 0.20 mmol) and CO_2 were converted for 14 h. The reaction mixture was filtered on silica with CH_2Cl_2 and volatiles were removed under reduced pressure. The product **50i** was obtained as a yellow oil (7.31 g, 10.3 mmol, 98%).

^{1}H NMR (300 MHz, mixture of stereoisomers, $CDCl_3$): δ = 1.13 (d, *J* = 5.4 Hz), 3.23–4.12 (m), 4.33–4.64 (m), 4.67–4.99 (m) ppm.

^{13}C{^{1}H} NMR (100 MHz, mixture of stereoisomers, $CDCl_3$): δ = 16.87–17.36 (CH_3), 66.09–66.58 (CH_2), 68.31–68.56 (CH_2), 72.84–73.60 (CH_2), 74.75–75.77 (CH), 76.17–76.38 (CH), 79.66–79.99 (CH), 154.97 (C=O) ppm.

IR (ATR): $\tilde{\nu}$ = 2972 (w), 2870 (w), 1792 (vs), 1455 (w), 1374 (m), 1343 (w), 1301 (w), 1259 (w), 1163 (m), 1085 (s, br), 1014 (m), 926 (w), 861 (w), 848 (w), 773 (m), 767 (w), 713 (w) cm^{-1}.

MS (EI, 70 eV): *m/z* (%) = 217 (8) [$C_{10}H_{17}O_5^+$], 207 (17), 203 (1) [$C_9H_{15}O_5^+$], 193 (2), 177 (2), 173 (1), 159 (3) [$C_7H_{11}O_4^+$], 151 (1), 149 (1), 147 (1), 145 (1), 135 (2), 101 (4) [$C_4H_5O_3^+$], 87 (8) [$C_3H_3O_3^+$], 73 (10), 57 (17), 44 (100).

HRMS (ESI): *m/z* calc. for $C_{26}H_{46}O_{13}Na$: 589.2831; found: 589.2839 [M^+(*n*= 6) + Na]. *m/z* calc. for $C_{29}H_{52}O_{14}Na$: 647.3249; found: 647.3254 [M^+(*n*= 7) + Na]. *m/z* calc. for $C_{32}H_{58}O_{15}Na$: 705.3668; found: 705.3675 [M^+(*n*= 8) + Na]. *m/z* calc. for $C_{35}H_{64}O_{16}Na$: 763.4087; found: 763.4092 [M^+(*n*= 9) + Na].

PPG-GC$_2$ 468 (50j)[111]

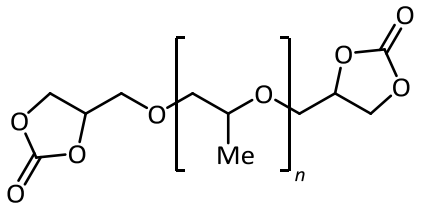

According to **GP-II**, polypropylene glycol diglycidyl ether 380 (**49j**, 3.44 g, 10.00 mmol), 2-hydroxyethyl-tributylammonium iodide (**45a**, 72 mg, 0.20 mmol) and CO_2 were converted for 14 h. The reaction mixture was filtered on silica with CH_2Cl_2 and volatiles were removed under reduced pressure. The product **50j** was obtained as a yellow oil (4.26 g, 9.85 mmol, 98%).

^{1}H NMR (300 MHz, mixture of stereoisomers, $CDCl_3$): δ = 1.11–1.14 (m), 3.41–3.75 (m), 4.39–4.53 (m), 4.78–4.85 (m) ppm.

^{13}C{^{1}H} NMR (100 MHz, mixture of stereoisomers, $CDCl_3$): δ = 16.58–16.97 (CH_3), 43.46–44.13 (CH_2), 66.03–66.34 (CH_2), 68.06–70.31 (CH_2), 72.84–73.49 (CH_2), 74.94–75.38 (CH), 75.89–76.14 (CH), 79.37–79.84 (CH), 154.94 (C=O) ppm.

IR (ATR): $\tilde{\nu}$ = 2974 (w), 2873 (w), 1785 (vs), 1487 (w), 1459 (m), 1393 (w), 1376 (w), 1338 (w), 1305 (w), 1260 (w), 1166 (m), 1099 (s), 1048 (vs), 954 (w), 925 (w), 847 (w), 772 (m), 713 (m) cm^{-1}.

MS (EI, 70 eV): *m/z* (%) = 217 (3) [$C_{10}H_{17}O_5^+$], 207 (19), 203 (7) [$C_9H_{15}O_5^+$], 193 (2), 177 (2), 173 (1), 159 (3) [$C_7H_{11}O_4^+$], 151 (1), 149 (1), 147 (1), 145 (1), 135 (2), 101 (4) [$C_4H_5O_3^+$], 87 (6) [$C_3H_3O_3^+$], 73 (10), 57 (17), 44 (100).

HRMS (ESI): *m/z* calc. for $C_{11}H_{16}O_8Na$: 299.0737; found: 299.0736 [M^+(*n*= 1) + Na]. *m/z* calc. for $C_{14}H_{22}O_9Na$: 357.1156; found: 357.1160 [M^+(*n*= 2) + Na]. *m/z* calc. for $C_{17}H_{28}O_{10}Na$: 415.1575.; found: 415.1570 [M^+(*n*= 3) + Na].

PEG-GC$_2$ 588 (50k)[111]

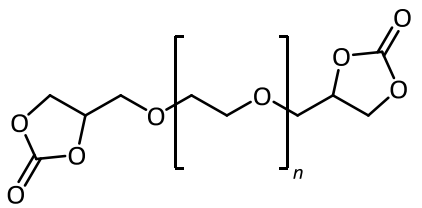

According to **GP-II**, polyethylene glycol diglycidyl ether 500 (**49k**, 5.01 g, 10.0 mmol), 2-hydroxyethyl-tributylammonium iodide (**45a**, 72 mg, 0.20 mmol) and CO_2 were

converted for 14 h. The reaction mixture was filtered on silica with CH_2Cl_2 and volatiles were removed under reduced pressure. The product **50k** was obtained as a yellow oil (5.82 g, 9.90 mmol, 99%).

^{1}H NMR (300 MHz, mixture of stereoisomers, $CDCl_3$): δ = 3.47–4.05 (m), 4.34–4.62 (m), 4.73–5.00 (m) ppm.

^{13}C{^{1}H} NMR (100 MHz, mixture of stereoisomers, $CDCl_3$): δ = 66.10–16.29 (CH_2), 70.16 (CH_2), 70.47 (CH_2), 70.96 (CH_2), 70.84 (CH_2), 71.23 (CH_2), 75.04–76.16 (CH), 154.95 (C=O) ppm.

IR (ATR): $\tilde{\nu}$ = 2868 (m, br), 1787 (vs), 1476 (w), 1457 (w), 1395 (w), 1351 (m), 1299 (w), 1251 (w), 1169 (s), 1086 (vs), 1047 (vs), 949 (m), 872 (w), 847 (m), 773 (m), 712 (w) cm^{-1}.

MS (EI, 70 eV): *m/z* (%) = 263 (1) [$C_{11}H_{19}O_7^+$], 253 (2), 251 (2), 233 (3) [$C_{10}H_{17}O_6^+$], 217 (3), 207 (16), 193 (2), 189 (12) [$C_8H_{13}O_5^+$], 177 (2), 173 (1), 159 (1) 144 (19), 133 (3), 115 (4), 121 (3), 115 (1), 113 (2), 101 (15), 87 (14), 73 (18), 57 (64), 44 (100).

HRMS (ESI): *m/z* calc. for $C_{22}H_{38}O_{14}Na$: 549.2154; found: 549.2159 [M^+(*n*= 7) + Na]. *m/z* calc. for $C_{24}H_{42}O_{15}Na$: 593.2416; found: 593.2422 [M^+(*n*= 8) + Na]. *m/z* calc. for $C_{26}H_{46}O_{16}$: 637.2678.; found: 637.2683 [M^+(*n*= 9) + Na].

Linear NIPU (64a)[82]

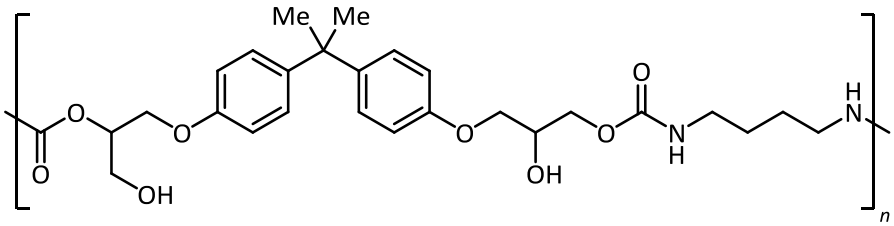

According to **GP-III**, 4,4'-(((propane-2,2-diylbis(4,1-phenylene))bis(oxy))bis(methylene))bis (1,3-dioxolan-2-one) (**50d**, 1.29 g, 3.00 mmol) and 1,4-butylamine (**62f**, 265 mg, 3.00 mmol) solved in DMSO (3 mL) were converted to the desired polymer. The reaction mixture was poured in water (30 mL) and the precipitate was washed with water (200 mL). All volatiles were removed under reduced pressure. The product **64a** was obtained as a yellow solid (1.30 g, 2.52 mmol, 84%).

^{1}H NMR (300 MHz, DMSO-d_6): δ = 1.30–1.35 (m, $NHCH_2CH_2$), 1.55 (s, CCH_3), 2.87–3.00 (m, $CONHCH_2$), 3.54–3.58 (m, CH_2OH), 3.82–4.06 (m, $OCHCH_2O$, OCH_2CHCH_2O), 4.81–4.87

(m, *CH*CH_2OH). 4.81–4.87 (m, *CH*CH_2OH), 4.93 (s, CH_2*OH*), 5.22 (s, CH*OH*), 6.81 (d, *J* = 8.4 Hz, OC*CH*CHC), 7.08 (d, *J* = 8.4 Hz, OCCH*CH*C), 7.11–7.22 (m, OCO*NH*CH_2) ppm.

$^{13}C\{^1H\}$ NMR (75 MHz, DMSO-d_6): δ = 26.76 (CH_2), 30.75 (CH_3), 39.97 (CH_2), 41.17 (C), 59.78 (CH_2), 65.02 (CH_2), 66.55 (CH_2), 67.26 (CH), 69.18 (CH_2), 72.45 (CH), 113.86 (CH), 127.45 (CH), 142.72 (C), 156.21 (C), 156.28 (C=O) ppm.

IR (ATR): $\tilde{\nu}$ = 3330 (m, br) 2960 (w), 2869 (w), 1694 (s), 1606 (w), 1536 (vs), 1508 (m), 1458 (m), 1182 (m), 1146 (m), 1107 (m), 1034 (vs), 929 (m), 830 (w), 745 (w) cm^{-1}.

GPC (DMF, 1 mL·min^{-1}, 50 °C): M_n = 11940 g·mol^{-1}, M_w = 26880 g·mol^{-1}, $Đ$ = 2.25.

DSC: T_g = 6.57 °C (onset), 15.55 °C (middle point).

TGA: $T_{d\,5\%}$ = 225 °C.

According to **GP-IV**, 2,2'-(((propane-2,2-diylbis(4,1-phenylene))bis(oxy))bis(methylene)) bis(oxirane) (**49d**, 1.02 g, 3.00 mmol), Tri-*n*-butyl-(2-hydroxyethyl)ammonium iodide (**45a**, 21.4 mg, 0.06 mmol) and CO_2 were converted to the desired carbonate. Then, 1,4-butylamine (**62f**, 265 mg, 3.00 mmol) and DMSO (3 mL) were added and converted to the desired polymer. The reaction mixture was poured in water (30 mL) and the precipitate was washed with water (200 mL). All volatiles were removed under reduced pressure. The product **64a** was obtained as yellow solid (1.26 g, 2.44 mmol, 81%).

^1H NMR (300 MHz, DMSO-d_6): δ = 1.30–1.36 (m, $NHCH_2CH_2$), 1.55 (s, CCH_3), 2.87–3.00 (m, $CONHCH_2$), 3.54–3.58 (m, CH_2OH), 3.82–4.08 (m, $OCHCH_2O$, OCH_2CHCH_2O), 4.81–4.87 (m, *CH*CH_2OH). 4.81–4.87 (m, *CH*CH_2OH), 4.94 (s, CH_2*OH*), 5.22 (s, CH*OH*), 6.81 (d, *J* = 8.4 Hz, OC*CH*CHC), 7.08 (d, *J* = 8.4 Hz, OCCH*CH*C), 7.12–7.21 (m, OCO*NH*CH_2) ppm.

$^{13}C\{^1H\}$ NMR (75 MHz, DMSO-d_6): δ = 26.80 (CH_2), 30.79 (CH_3), 39.97 (CH_2), 41.23 (C), 59.78 (CH_2), 65.07 (CH_2), 66.55 (CH_2), 67.3 (CH), 69.21 (CH_2), 72.45 (CH), 113.90 (CH), 127.49 (CH), 142.77 (C), 156.27 (C), 156.32 (C=O) ppm.

IR (ATR): $\tilde{\nu}$ = 3312 (m, br) 2933 (w), 2871 (w), 1695 (s), 1606 (w), 1508 (m), 1458 (m), 1232 (vs), 1182 (m), 1144 (m), 1106 (m), 1014 (vs), 950 (m), 830 (w), 772 (w) cm^{-1}.

GPC (DMF, 1 mL·min^{-1}, 50 °C): M_n = 11500 g·mol^{-1}, M_w = 27400 g·mol^{-1}, $Đ$ = 2.38.

DSC: T_g = 22.69 °C (onset), 29.40 °C (middle point).

TGA: $T_{d\,5\%}$ = 169 °C.

Cross-linked NIPU (82)[87]

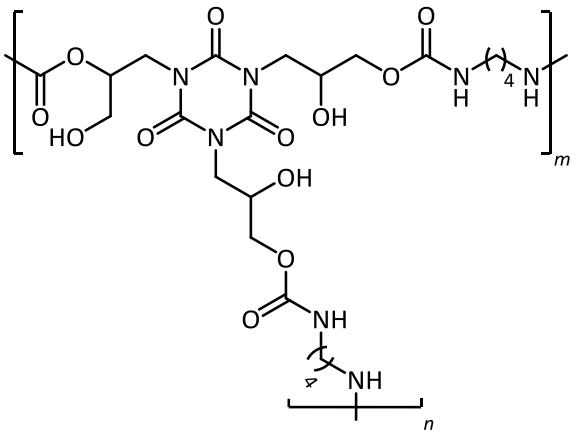

According to **GP-III**, 1,3,5-tris((2-oxo-1,3-dioxolan-4-yl)methyl)-1,3,5-triazinane-2,4,6-trione (**57**, 1.29 g, 3.00 mmol) and 1,4-butylamine (**62f**, 399 mg, 4.50 mmol) solved in DMSO (3 mL) were converted to the desired polymer. The reaction mixture was poured in 30 mL water and the precipitate was washed with DMSO (200 mL) and water (200 mL). All volatiles were removed under reduced pressure. The product **82** was obtained as a yellow solid (1.75 g, 2.84 mmol, 95%).

IR (ATR): $\tilde{\nu}$ = 3320 (m, br), 2944 (w), 2872 (w), 1674 (vs), 1528 (m), 1454 (vs), 1240 (w), 1090 (m), 1025 (m), 858 (w), 764 (m), 717 (m) cm^{-1}.

DSC: T_g = 99.52 °C (onset), 104.41 °C (middle point).

TGA: $T_{d\,5\%}$ = 231 °C.

According to **GP-IV**, 1,3,5-tris(oxiran-2-ylmethyl)-1,3,5-triazinane-2,4,6-trione (**56**, 892 mg, 3.00 mmol), Tri-*n*-butyl-(2-hydroxyethyl)ammonium iodide (**45a**, 22.5 mg, 0.06 mmol) solved in DMSO (1 mL) were converted to the desired carbonate under CO_2 pressure. Then, 1,4-butylamine (**62f**, 397 mg, 4.5 mmol) and DMSO (2 mL) was added and converted to the desired polymer. The reaction mixture was poured in water (30 mL) and the precipitate was washed with DMSO (200 mL) and water (200 mL). All volatiles were removed under reduced pressure. The product **82** was obtained as a yellow solid (1.72 g, 2.77 mmol, 92%).

IR (ATR): $\tilde{\nu}$ = 3290 (m, br), 2943 (w), 2871 (s), 1682 (vs), 1534 (m), 1458 (s), 1312 (w), 1143 (w), 1015 (s), 951 (m), 767 (m), 702 (m), 666 (m) cm^{-1}.

DSC: T_g = 66.68 °C (onset), 78.80 °C (middle point).

TGA: $T_{d\,5\%}$ = 106 °C.

Polycarbonate (71)

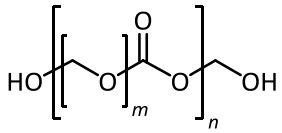

According to **GP-V**, PFA (**68**, 1.00 g), IPr · HCl (**84a**, 100 mg, 10 wt%), TBD (**83**, 100 mg), THF (5 mL) and CO_2 were converted to the desired polycarbonate after 16 h. The product **71** was obtained as a brown oil (1.016 g).

^{1}H NMR (500 MHz, DMSO-d_6): δ = 0.95–1.48 (m), 1.81–2.42 (m), 3.00–3.64 (m), 3.76–5.06 (m) ppm.

^{13}C{^{1}H} NMR (126 MHz, DMSO-d_6, 50 °C): δ = 20.22, 20.94, 22.33, 22.96, 23.79, 24.25, 28.46, 28.62, 30.63, 35.56, 37.23, 46.05, 49.22, 50.83, 59.58, 60.24, 62.69, 63.01, 63.86, 64.32, 68.10, 68.24, 71.52, 74.03, 124.41, 124.58, 125.71, 126.05, 129.07, 129.93, 131.66, 131.81, 139.22, 144.66, 144.81, 146.07, 150.99, 162.13, 171.76 (C=O), 174.59 (C=O), 176.64 (C=O) ppm.

IR (ATR): $\tilde{\nu}$ = 3294 (m, br) 2931 (m), 2871 (m), 1708 (m), 1653 (s), 1439 (m), 1385 (s), 1322 (m), 1094 (m), 1062 (s), 1041 (s), 928 (w), 881 (w), 758 (w) cm^{-1}.

GPC (DMF, 1 mL·min^{-1}, 50 °C): M_n = 480 g·mol^{-1}, M_w = 2350 g·mol^{-1}, $Đ$ = 4.90.

DSC: T_g = –31.22 °C (onset), –15.49 °C (middle point).

TGA: $T_{d\ 5\%}$ = 127 °C.

End group protected polycarbonate (101a)

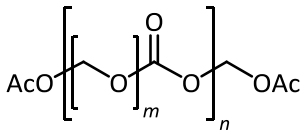

According to **GP-IX**, PFA (**68**, 1.00 g), IPr · HCl (**84a**, 100 mg, 10 wt%), TBD (**83**, 100 mg, 10 wt%) and THF (5 mL) were stirred for 16 h under a CO_2 atmosphere. Subsequently, pyridine (**100**, 5 mL) and acetic anhydride (**99**, 3 mL) were added and stirred for 12 h. The reaction mixture was poured into ice water (20 mL) and the precipitate was filtered off and washed with water (40 mL). The product **101a** was obtained as a brown solid (0.355 g).

^{1}H NMR (300 MHz, DMSO-d_6): δ = 0.87–1.45 (m), 1.57–2.41 (m), 2.95–3.65 (m), 3.81–4.59 (m) ppm.

^{13}C{^{1}H} NMR (126 MHz, DMSO-d_6, 50 °C): δ = 20.00, 20.04, 21.00, 22.32, 24.82, 28.54, 30.63, 32.14, 35.81, 45.68, 48.54, 49.34, 52.71, 57.63, 60.15, 62.72, 63.65, 64.06, 67.71, 71.22, 73.13, 73,78, 74.35, 75.56, 75.66, 123.11, 123.93, 126.41, 129.01, 130.82, 131.49, 139.29, 144.83, 146.97, 151.90, 154.44, 157.82, 158.4, 162.05, 172.06 (C=O), 173.16 (C=O), 174.74 (C=O) ppm.

IR (ATR): $\tilde{\nu}$ = 2934 (w, br) 2874 (w), 1738 (vs), 1631 (m), 1511 (w), 1434 (m), 1369 (s), 1203 (vs), 1040 (vs), 887 (w), 807 (w), 732 (w) cm^{-1}.

GPC (DMF, 1 mL·min^{-1}, 50 °C): M_n = 960 g·mol^{-1}, M_w = 3540 g·mol^{-1}, $Đ$ = 3.69.

DSC: T_g = 3.42 °C (onset), 20.02 °C (middle point).

TGA: $T_{d\ 5\%}$ = 157 °C.

Terpolymer (98)

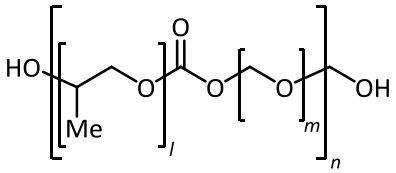

According to **GP-VIII**, PFA (**68**, 1.00 g), IPr · HCl (**84a**, 21.4 mg, 0.06 mmol), TBD (**83**, 100 mg), PPG-1000 (**97**, 2 wt%), THF (5 mL) and CO_2 were converted to the desired polycarbonate after 16 h. The product **98** was obtained as a brown oil (1.014 g).

^{1}H NMR (300 MHz, DMSO-d_6): δ = 0.88–1.34 (m), 1.67–2.42 (m), 3.06–4.44 (m) ppm.

^{13}C{^{1}H} NMR (75 MHz, DMSO-d_6): δ = 20.39, 20.81, 22.56, 21.25, 22.56, 23.13, 24.14, 24.53, 28.68, 30.82, 33,26, 35.84, 37.38, 46.19, 60.32, 62.93, 68.14, 74.38, 77.36, 124.67, 124.83, 126.23, 130.07, 132.06, 144.86, 145.00, 150.98, 151.28, 162.40, 164.82, 172.23 (C=O), 174.92 (C=O) 177.04 (C=O) ppm.

IR (ATR): $\tilde{\nu}$ = 3339 (w, br), 2930 (m), 2873 (w), 1716 (w), 1655 (s), 1542 (w), 1504 (w), 1437 (m), 1408 (m), 1385 (s), 1324 (m), 1254 (m), 1091 (s), 1061 (s), 866 (w) cm^{-1}.

GPC (DMF, 1 mL·min^{-1}, 50 °C): M_n = 1800 g·mol^{-1}, M_w = 9380 g·mol^{-1}, $Đ$ = 5.21.

DSC: T_g = –29.87 °C (onset), –17.32 °C (middle point).

TGA: $T_{d\ 5\%}$ = 120 °C.

End group protected Terpolymer (102)

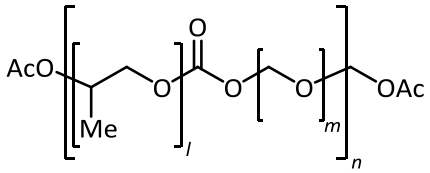

According to **GP-X**, PFA (**68**, 1.00 g), IPr · HCl (**84a**, 100 mg, 10 wt%), TBD (**83**, 100 mg, 10 wt%), PPG-1000 (**97**, 2 wt%) and THF (5 mL) were stirred for 16 h under a CO_2 atmosphere. Subsequently, pyridine (**100**, 5 mL) and acetic anhydride (**99**, 3 mL) were added and stirred for 12 h. The reaction mixture was poured into ice water (20 mL) and the precipitate was filtered off and washed with water (40 mL). The product **102** was obtained as a brown solid (0.367 g).

^{1}H NMR (300 MHz, DMSO-d_6): δ = 0.61–1.46 (m), 1.54–2.52 (m), 2.60–4.63 (m) ppm.

^{13}C{^{1}H} NMR (75 MHz, DMSO-d_6): δ = 20.53, 21.09, 22.87, 23.12, 24.13, 28.35, 28.67, 30.80, 35.82, 124.66, 126.21, 127.15, 130.06, 131.91, 144.85, 162.37, 172.08 (C=O) ppm.

IR (ATR): $\tilde{\nu}$ = 2965 (w) 2932 (w), 2872 (w), 1737 (vs), 1661 (vs), 1506 (w), 1436 (m), 1370 (s), 1198 (vs), 1093 (s), 1041 (s), 908 (m), 807 (w), 757 (w) cm^{-1}.

GPC (DMF, 1 mL·min^{-1}, 50 °C): M_n = 860 g·mol^{-1}, M_w = 5600 g·mol^{-1}, $Đ$ = 6.51.

DSC: T_g = 10.51 °C (onset), 35.30 °C (middle point).

TGA: $T_{d\ 5\%}$ = 113 °C.

6.6 List of Synthesized Compounds

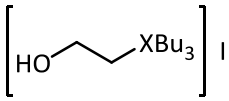

45a X = N
46a X = P

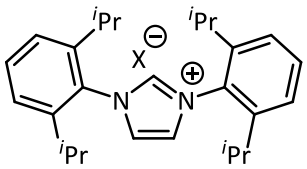

84a X = I

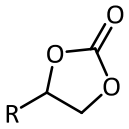

11d R = 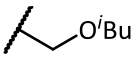 **11e** R = 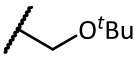 **11f** R = 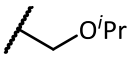

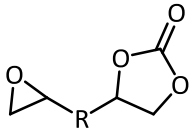

77a R = 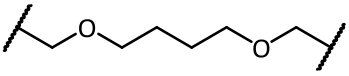 **77b** R = 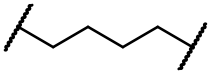

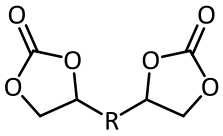

50a R = 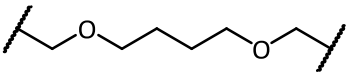 **50b** R = 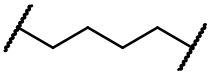

50c R = 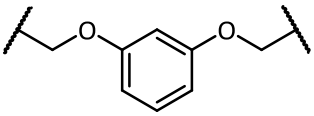

50f R = 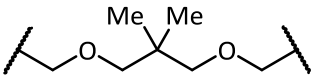

50d R = 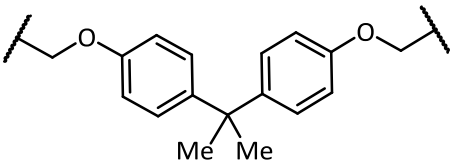

50h R = 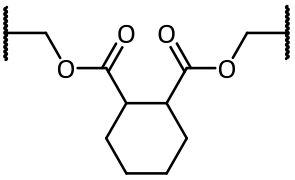

50i R = 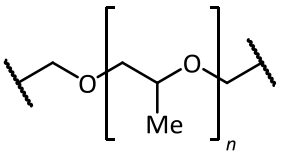

$M_n \approx 728\ g \cdot mol^{-1}$

50k R = 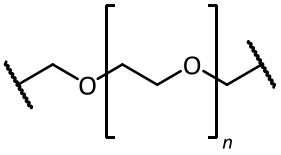

$M_n \approx 588\ g \cdot mol^{-1}$

50j R = 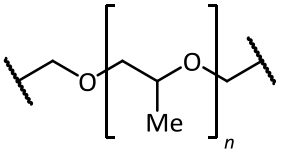

$M_n \approx 468\ g \cdot mol^{-1}$

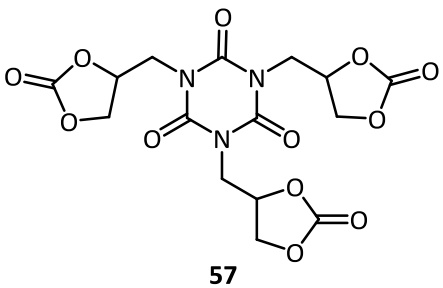

57

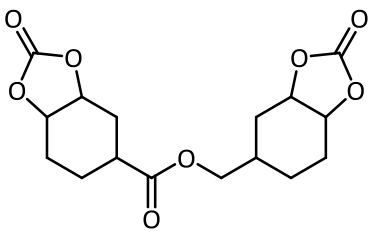

79

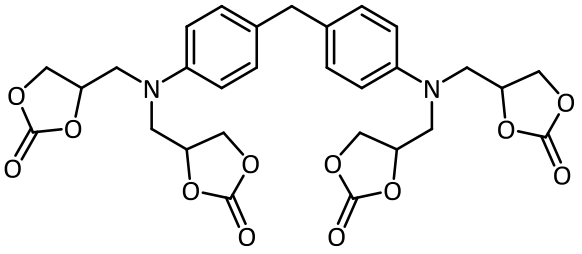

81

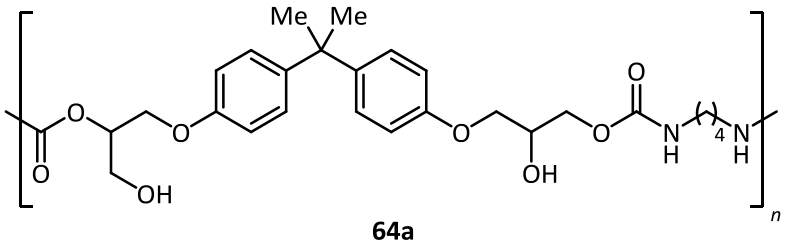

64a

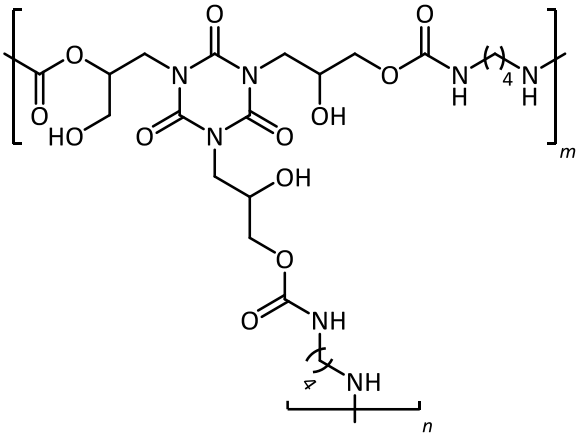

82

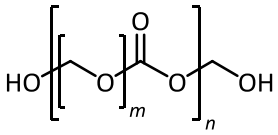

71

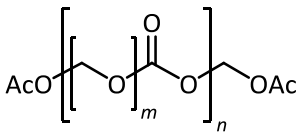

101a

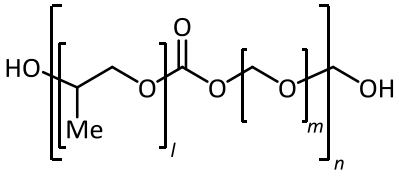

98

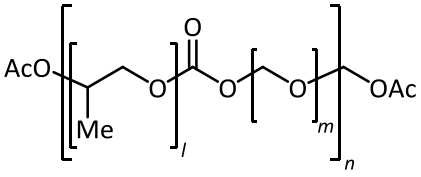

102

7 SPECTRA AND DIAGRAMS

7.1 Epoxide Content of Oligomeric Substrates

The epoxide content of the oligomeric epoxides **49i–49k** was determined by ^{1}H NMR using mesitylene as a standard (Figure 31).

$$n_2 = \frac{n_1 * Int_2 * \frac{H_1}{H_2}}{Int_1} * x$$

n_1 = Amount of standard
n_2 = Amount of epoxide
Int_1 = Integral of standard
Int_2 = Integral of epoxide
H_1 = Number of protons standard
H_2 = Number of protons epoxide
x = Number of epoxide groups

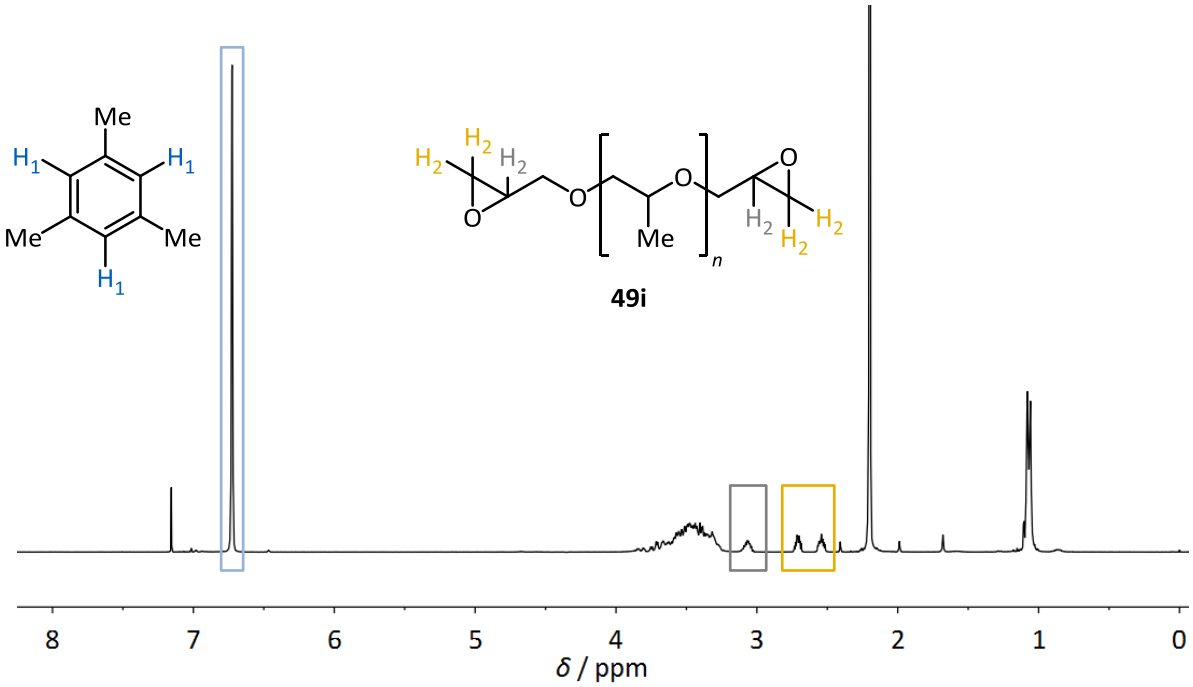

Figure 31. Determination of the epoxide content of the oligomer **49i** using ^{1}H NMR.

For the calculation the proton signal belonging to the secondary carbons (δ = 2.50–2.75 ppm, H_2 in equation; yellow in Figure 31) or the tertiary carbons of the epoxide (δ = 3.08–3.11 ppm, H_2 in equation; grey in Figure 31) were used. Furthermore, the

signals belonging to the tertiary carbons of the standard were used (δ = 6.72 ppm, H_1 in equation; blue in Figure 31).

Table 37. Calculated epoxide content of the oligomers **49i–49k**.

Entry	Substrate		Producer M_n / g·mol^{-1}	mmol (Epoxide)· g^{-1} (Substrate)[a]	g (Substrate)· mol^{-1} (Epoxide)[a]
1	PPG-DGE 640	**49i**	640	3.234	309.25
2	PPG-DGE 380	**49j**	380	5.800	172.24
3	PEG-DGE 500	**49k**	500	3.996	250.25

[a] Determined by ^{1}H NMR using mesitylene as the standard.

The calculated mol (epoxide) / g (reactant) did not differ much from the value M_n which was stated by the producer (Table 37). For PPG-DGE 640 **49i** calculations resulted in 3.234 mmol (epoxide)·g^{-1} (substrate). For PPG-DGE 380 **49j** 5.800 mmol (epoxide)·g^{-1} (substrate) was calculated and for PEG-DGE 500 **49k** a value of 3.996 mmol (epoxide)·g^{-1} (substrate) was measured.

7.2 IR Spectra of Linear NIPU and Reactant

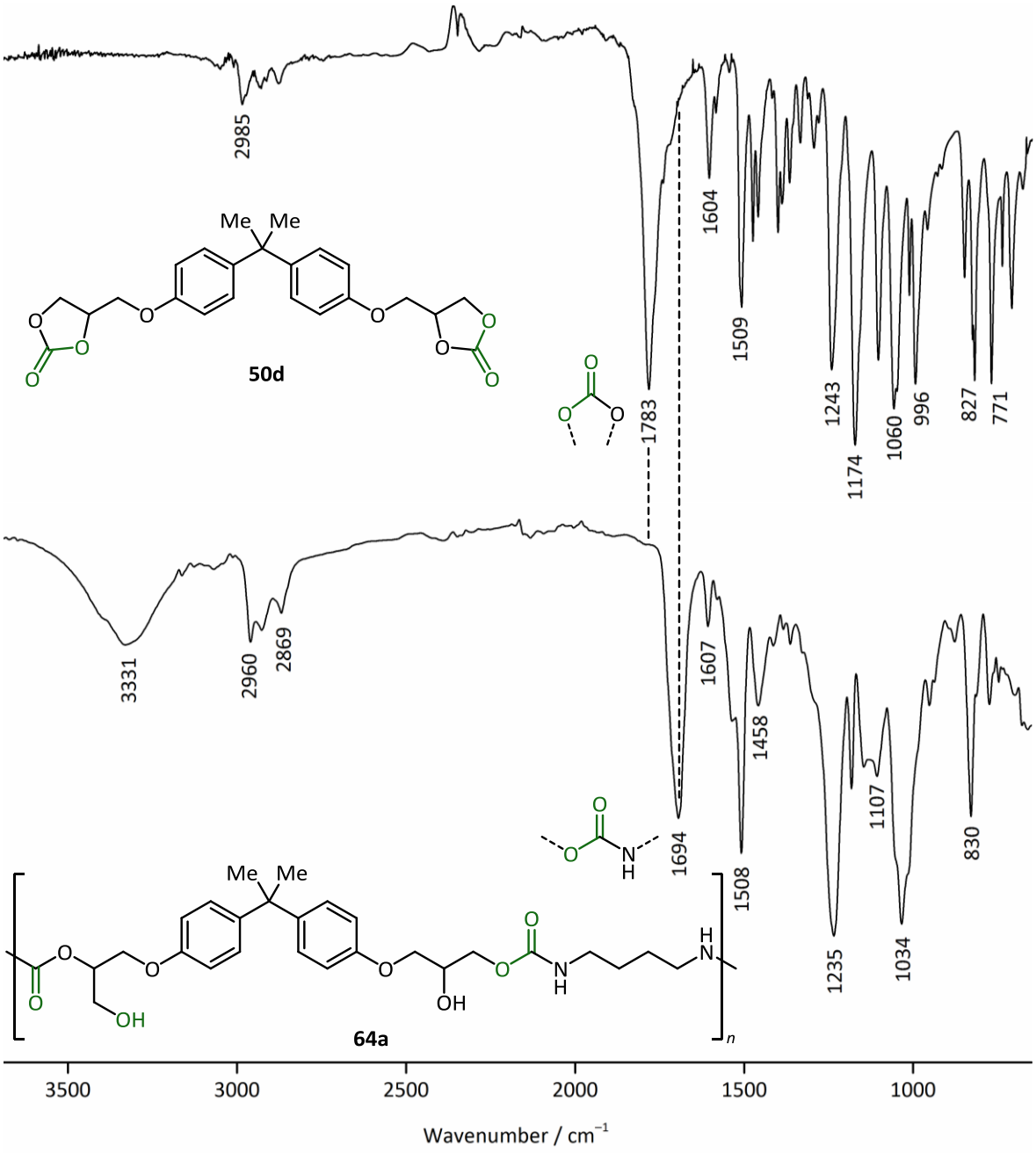

Figure 32. IR of the cyclic dicarbonate **50d** (top) and the obtained NIPU **64a** (bottom).

7.3 IR Spectra of Cross-Linked NIPU and Reactant

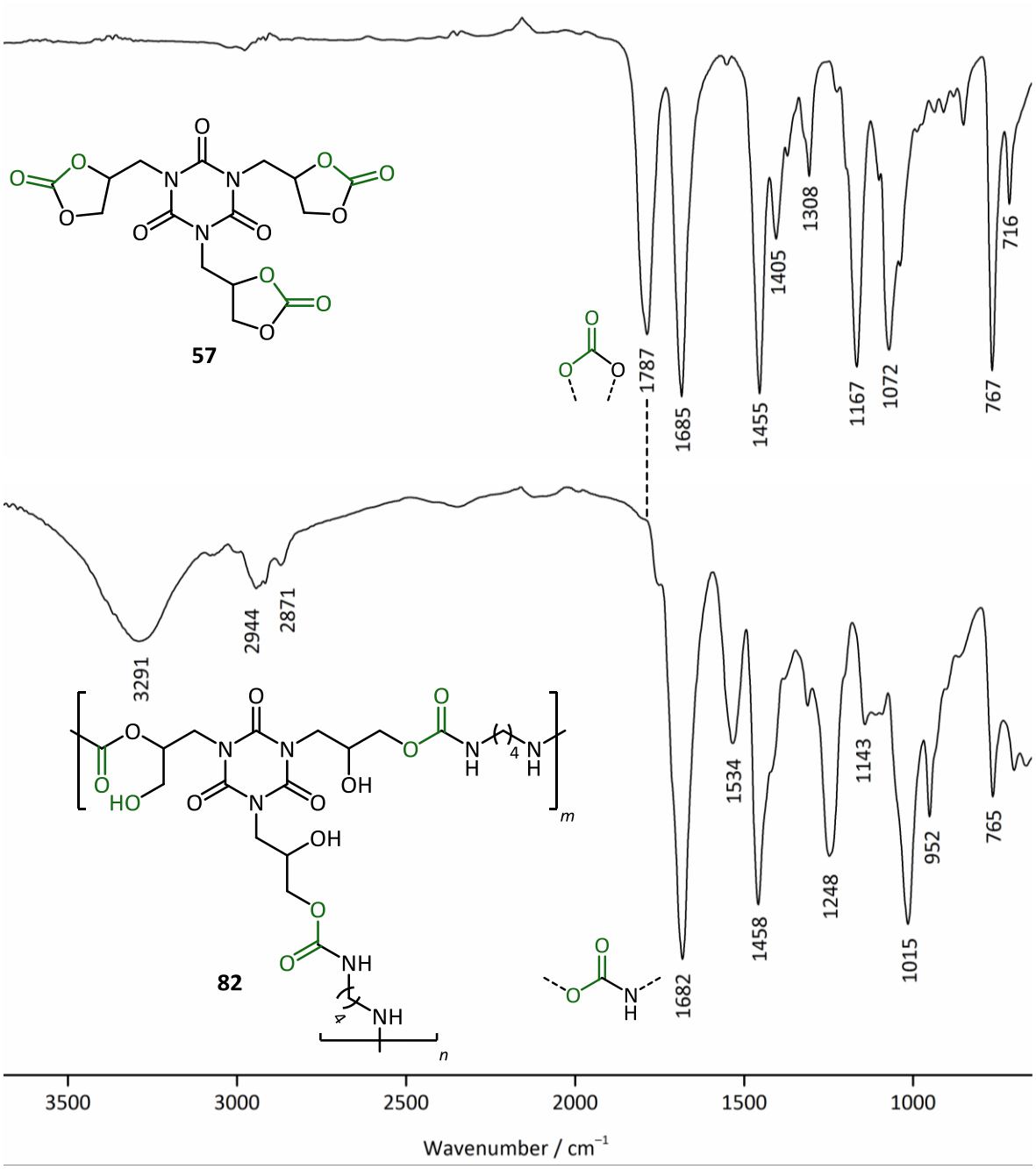

Figure 33. IR of the cyclic tricarbonate **57** and obtained cross linked-NIPU **82**.

7.4 DSC Measurements of NIPUs

For each sample, one full heating and cooling cycle was measured prior to the actual measurements. All samples were analyzed by using a constant heating and cooling rate of 10 K·min^{-1}.

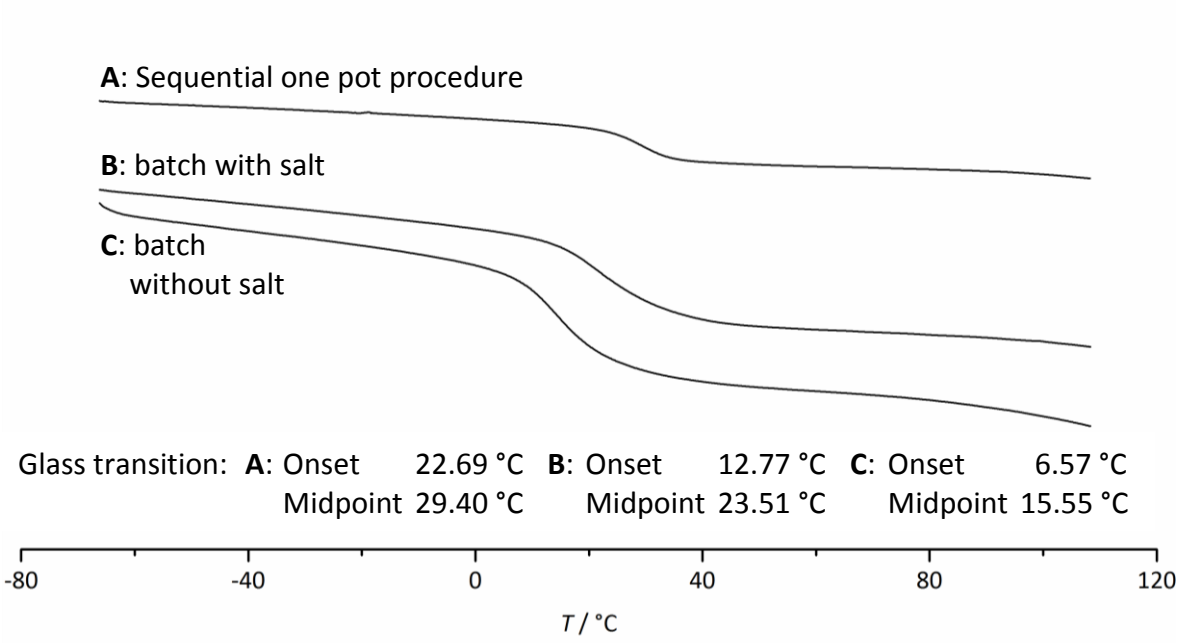

Figure 34. DSC measuremnts of linear NIPU **64a** obtained through different procedures.

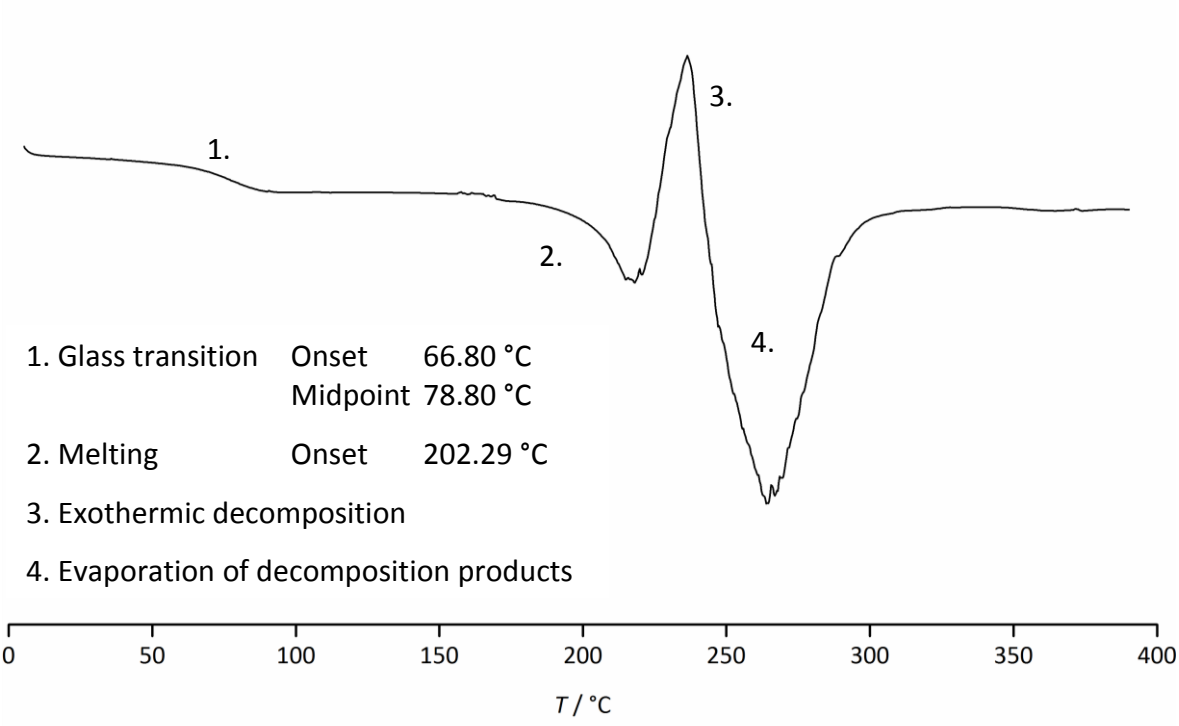

Figure 35. DSC curves of cross-linked NIPU **82** obtained through the sequ. one pot procedure.

7.5 Formaldehyde Concentration

The *Schlosser* solution was produced by codistillation of THF and paraformaldehyde (PFA, **68**). ^{1}H NMR-measurements (*Bruker AV 300*) revealed concentrations of FA **67** in the range of 0.2–0.5 mol·L^{-1}.

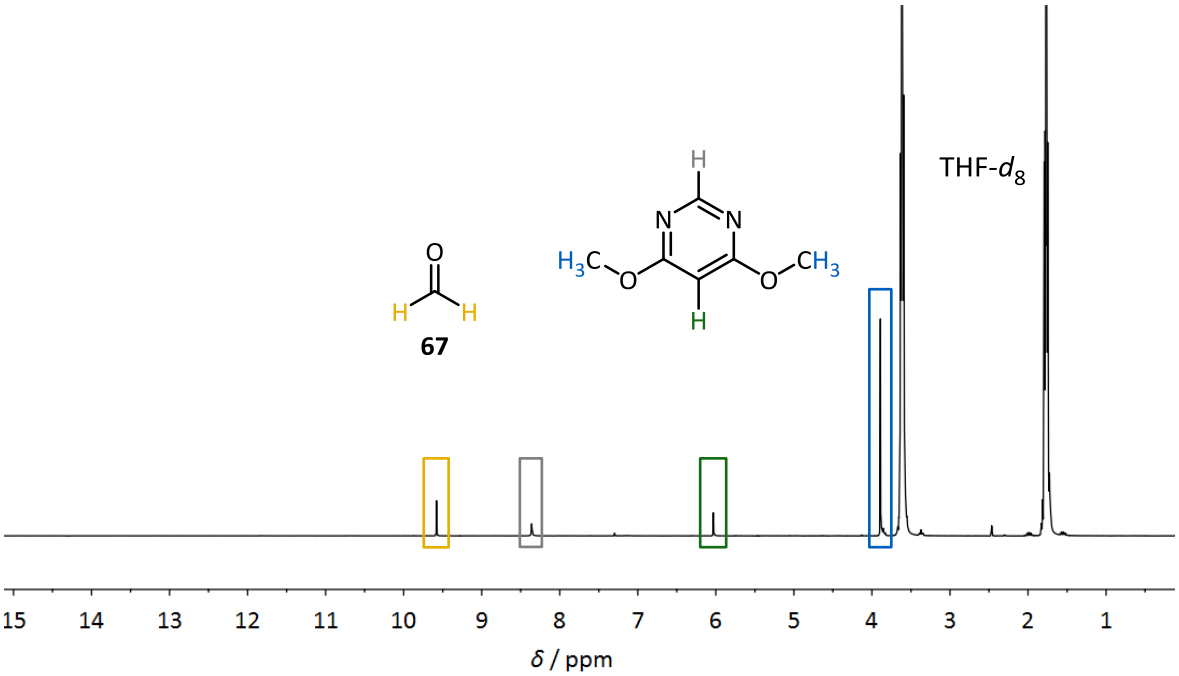

Figure 36. ^{1}H NMR of the *Schlosser* solution **67**·THF with standard.

7.6 IR of DMAP Catalyzed Polymerization

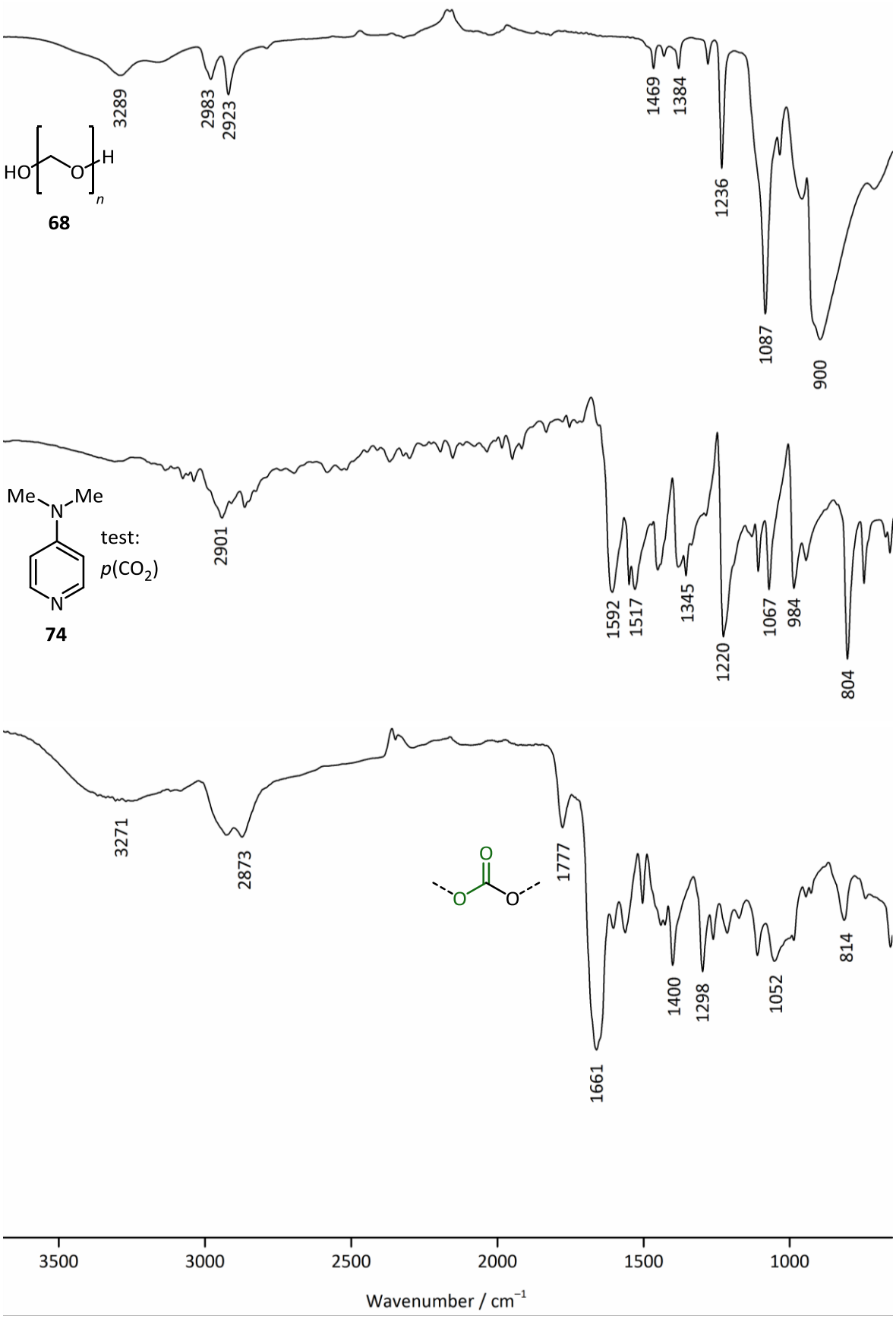

Figure 37. IR of DMAP **74** catalyzed reaction (bottom), PFA **68** (middle), DMAP **74** (top).

7.7 Parameter Screening Utilizing IPR · HCl

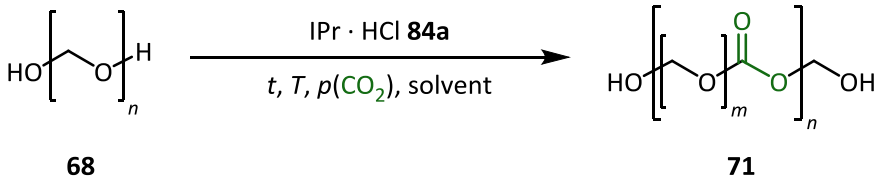

68 **71**

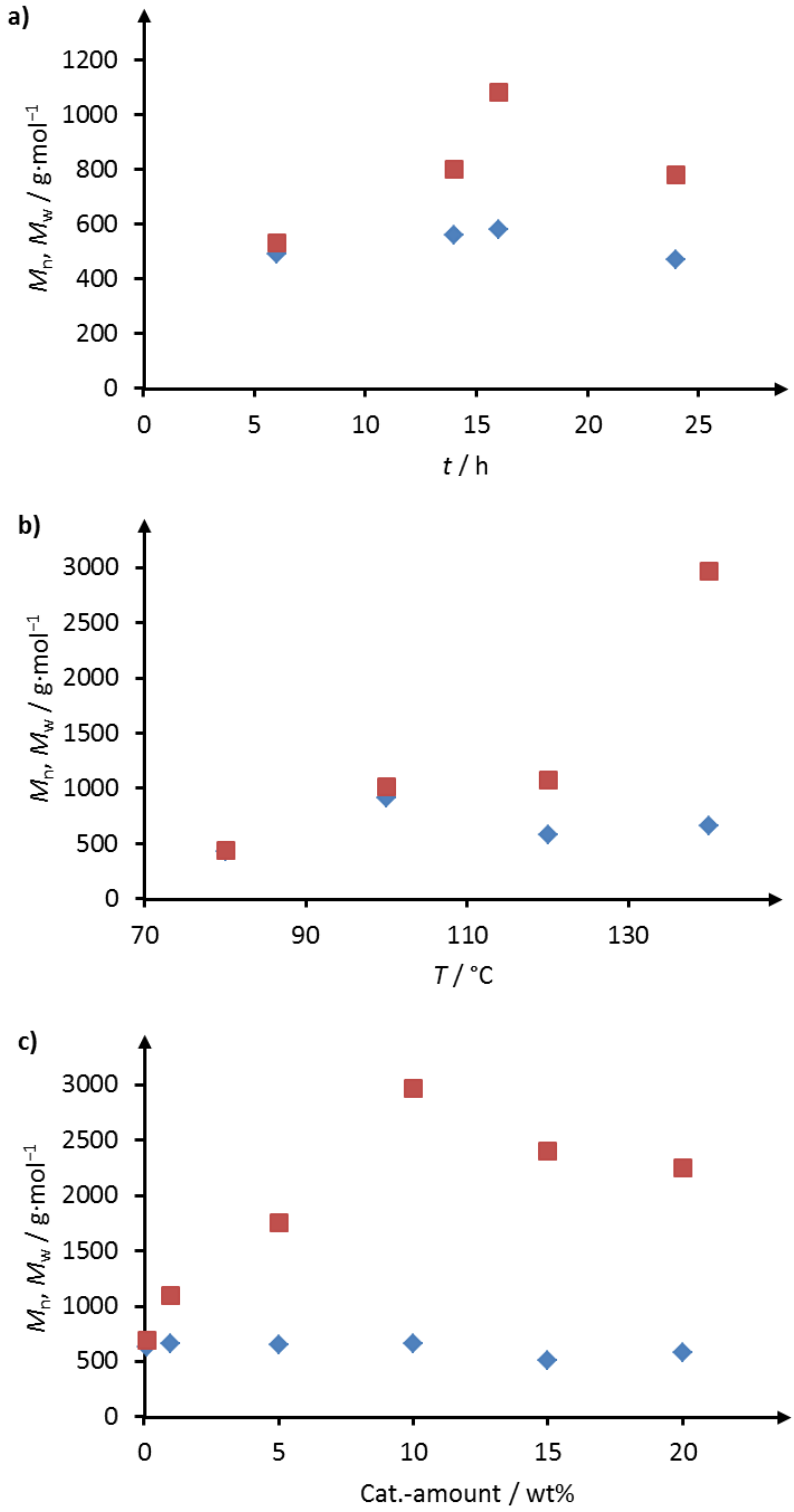

Figure 38. Screening: a) time, b) temperature, c) cat.-amount, d) CO_2 pressure and e) solvent.

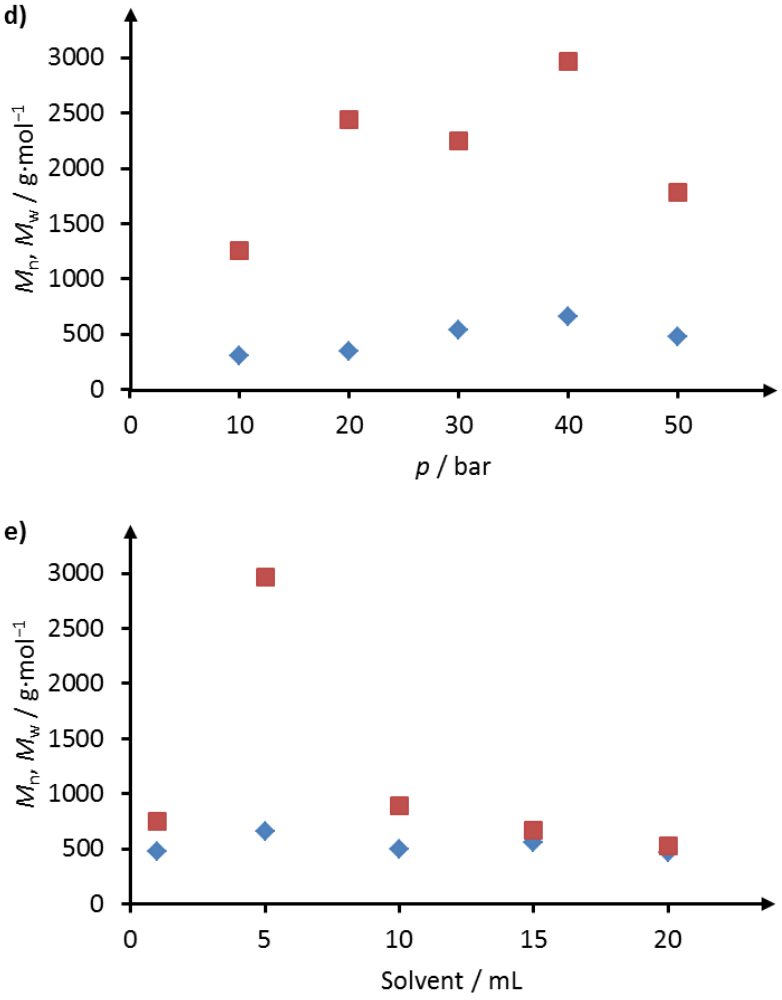

Figure 38. Continued.

7.8 TGA-MS of FA/CO_2-Copolymer

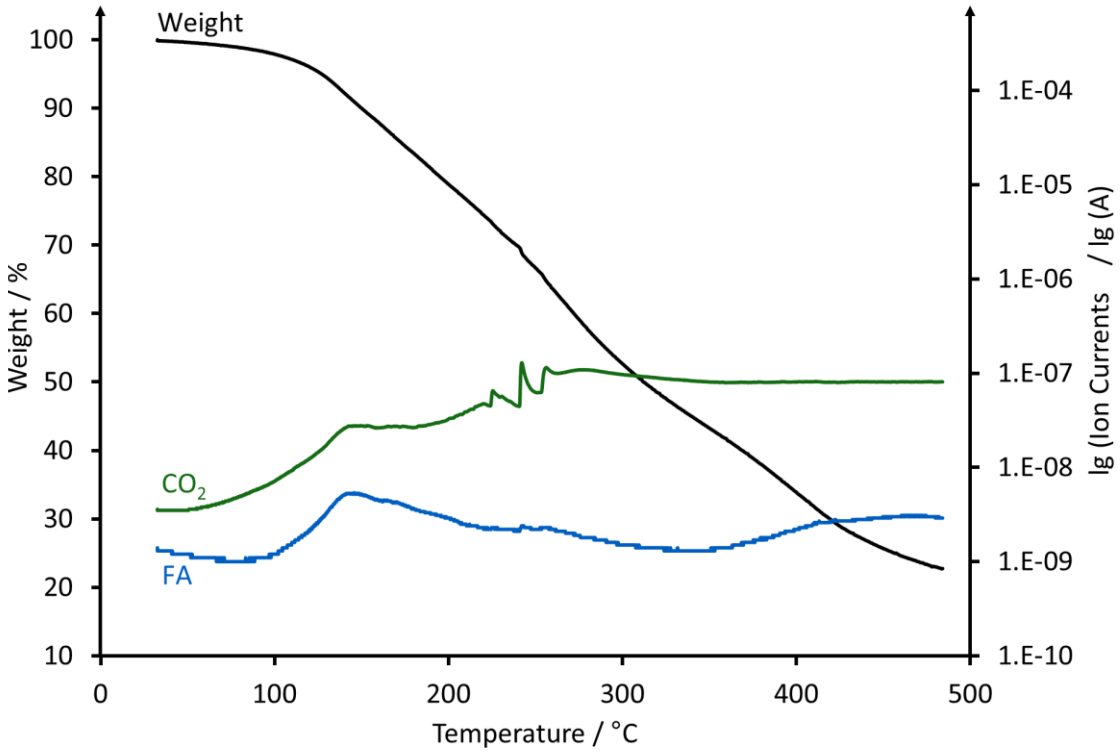

Figure 39. TGA-MS: Loss of mass and decomposition of **71**.

8 REFERENCES

[1] a) D. J. Darensbourg, in *CO_2 Chemistry, Vol. 66* (Eds.: M. Aresta, R. V. Eldik), Elsevier Inc., San Diego, **2014**, 1–23; b) International Energy Agency (IEA), *Key World Energy Statistics 2014*, IEA Publishing, **2014**; c) International Energy Agency (IEA), *World Energy Outlook 2013*, IEA Publishing, **2013**.

[2] a) World Energy Council (WEC), *World Energy Resources*, WEC Publishing, **2013**; b) R. J. Andres, J. S. Gregg, L. Losey, G. Marland, T. A. Boden, *Tellus B* **2011**, *63*, 309–327.

[3] a) F. D. Meylan, V. Moreau, S. Erkman, *J. CO_2 Util.* **2015**, doi:10.1016/j.jcou.2015.05.003; b) C. Le Quéré, G. P. Peters, R. J. Andres, R. M. Andrew, T. Boden, P. Ciais, P. Friedlingstein, R. A. Houghton, G. Marland, R. Moriarty, S. Sitch, P. Tans, A. Arneth, A. Arvanitis, D. C. E. Bakker, L. Bopp, J. G. Canadell, L. P. Chini, S. C. Doney, A. Harper, I. Harris, J. I. House, A. K. Jain, S. D. Jones, E. Kato, R. F. Keeling, K. Klein Goldewijk, A. Körtzinger, C. Koven, N. Lefèvre, A. Omar, T. Ono, G. H. Park, B. Pfeil, B. Poulter, M. R. Raupach, P. Regnier, C. Rödenbeck, S. Saito, J. Schwinger, J. Segschneider, B. D. Stocker, B. Tilbrook, S. van Heuven, N. Viovy, R. Wanninkhof, A. Wiltshire, S. Zaehle, C. Yue, *Earth Syst. Sci. Data Discuss.* **2013**, *6*, 689–760; c) R. K. Pachauri, A. Reisinger, *Climate change 2007: Synthesis Report*, IPPC, Geneva, **2007**; d) W. S. Broecker, *Science* **1997**, *378*, 1582–1588; e) G. A. Meehl, W. M. Washington, *Nature* **1996**, *382*, 56–60.

[4] a) O. Coulembier, S. Moins, V. Lemaur, R. Lazzaroni, P. Dubois, *J. CO_2 Util.* **2015**, *10*, 7–11; b) B. M. Bhanage, *Transformation and Utilization of Carbon Dioxide*, Springer-Verlag, Heidelberg, **2014**.

[5] Organisation for Economic Cooperation and Development (OECD), *Development Co-operation Report 2012*, OECD Publishing, **2012**.

[6] a) G. A. Olah, G. K. S. Prakash, A. Goeppert, *J. Am. Chem. Soc.* **2011**, *133*, 12881–12898; b) Verband der Chemischen Industrie e. V. (VCI), Gesellschaft für Chemische Technik und Biotechnologie e. V. (DECHEMA), **2009**; c) P. T. Anastas, *Green Chem.* **2003**, *5*, 29–34.

[7] a) M. Peters, B. Köhler, W. Kuckshinrichs, W. Leitner, P. Markewitz, T. E. Müller, *ChemSusChem* **2011**, *4*, 1216–1240; b) A. J. Hunt, E. H. K. Sin, R. Marriott, J. H. Clark, *ChemSusChem* **2010**, *3*, 306–322.

[8] a) B.-H. Xu, J.-Q. Wang, J. Sun, Y. Huang, J.-P. Zhang, X.-P. Zhang, S.-J. Zhang, *Green Chem.* **2015**, *17*, 108–122; b) A. Bazzanella, D. Krämer, M. Peters, *Nachr. Chem.* **2010**, *58*, 1226–1230; c) T. Sakakura, K. Kohno, *Chem. Commun.* **2009**, 1312–1330; d) M. Aresta, A. Dibenedetto, *Dalton Trans.* **2007**, 2975–2992.

[9] a) C. M. Mömming, E. Otten, G. Kehr, R. Fröhlich, S. Grimme, D. W. Stephan, G. Erker, *Angew. Chem.* **2009**, *121*, 6770–6773; *Angew. Chem. Int. Ed.* **2009**, *48*, 6643–6646; b) P. G. Jessop, F. Joó, C.-C. Tai, *Coord. Chem. Rev.* **2004**, *248*, 2425–2442; c) X. Yin, J. R. Moss, *Coord. Chem. Rev.* **1999**, *181*, 27–59; d) D. R. Lide, *Handbook of Chemistry and Physics*, 74th ed., CRC Press Inc., Boca Raton, FL, USA, **1993**.

[10] A. Behr, *Angewandte homogene Katalyse*, Wiley-VCH, Weinheim, **2008**.

[11] G. Centi, S. Perathoner, *Catal. Today* **2008**, *138*, 69–76.

[12] a) Q. He, J. W. O'Brien, K. A. Kitselman, L. E. Tompkins, G. C. T. Curtis, F. M. Kerton, *Catal. Sci. Technol.* **2014**, *4*, 1513–1528; b) A. Monassier, V. D'Elia, M. Cokoja, H. Dong, J. D. A. Pelletier, J.-M. Basset, F. E. Kühn, *ChemCatChem* **2013**, *5*, 1321–1324; c) R. H. Crabtree, *Energy Production and Storage: Inorganic Chemical Strategies for a Warming World*, John Wiley & Sons Ltd., Chichester, **2010**.

[13] G. Fiorani, W. Guo, A. W. Kleij, *Green Chem.* **2015**, *17*, 1375–1389.

[14] D. W. C. MacMillan, *Nature* **2008**, *455*, 304–308.

[15] a) Z. Wu, H. Xie, X. Yu, E. Liu, *ChemCatChem* **2013**, *5*, 1328–1333; b) P. Anastas, J. Warner, *Green Chemistry: Theory and Practice*, Oxford University Press, **1998**.
[16] a) H. Mutlu, J. Ruiz, S. C. Solleder, M. A. R. Meier, *Green Chem.* **2012**, *14*, 1728–1735; b) F. S. Pereira, E. R. de Azevedo, E. F. da Silva, T. J. Bonagamba, D. L. da Silva Agostíni, A. Magalhães, A. E. Job, E. R. Pérez González, *Tetrahedron* **2008**, *64*, 10097–10106.
[17] N. Marion, S. Díez-González, S. P. Nolan, *Angew. Chem.* **2007**, *119*, 3046–3058; *Angew. Chem. Int. Ed.* **2007**, *46*, 2988–3000.
[18] M. Alves, B. Grignard, S. Gennen, C. Detrembleur, C. Jerome, T. Tassaing, *RSC Adv.* **2015**, *5*, 53629–53636.
[19] P. Coupillaud, J. Pinaud, N. Guidolin, J. Vignolle, M. Fèvre, E. Veaudecrenne, D. Mecerreyes, D. Taton, *J. Polym. Sci., Part A: Polym. Chem.* **2013**, *51*, 4530–4540.
[20] M. E. Wilhelm, M. H. Anthofer, M. Cokoja, I. I. E. Markovits, W. A. Herrmann, F. E. Kühn, *ChemSusChem* **2014**, *7*, 1357–1360.
[21] Q. Liu, L. Wu, R. Jackstell, M. Beller, *Nat. Commun.* **2015**, *6*.
[22] G. W. Coates, D. R. Moore, *Angew. Chem.* **2004**, *116*, 6784–6806; *Angew. Chem. Int. Ed.* **2004**, *43*, 6618–6639.
[23] J. Sun, S.-i. Fujita, M. Arai, *J. Organomet. Chem.* **2005**, *690*, 3490–3497.
[24] M. S. Kathalewar, P. B. Joshi, A. S. Sabnis, V. C. Malshe, *RSC Advances* **2013**, *3*, 4110–4129.
[25] S. P. Meching, *New successes for Bayer's research*, Bayer MaterialScience, http://news.bayer.de, (retrieved June 29, 2015).
[26] Federal Ministry of Education and Research (BMBF), *Technologies for Sustainability and Climate Protection - Chemical Processes and Use of CO_2*, **2014**.
[27] H. Wolf, H. Haken, *Molecular Physics and Elements of Quantum Chemistry*, Springer-Verlag, Berlin/Heidelberg, Germany, **1995**.
[28] G. M. Schneider, *Chem. Ing. Tech.* **1977**, *49*, 594.
[29] Y. Suehiro, M. Nakajima, K. Yamada, M. Uematsu, *J. Chem. Thermodyn.* **1996**, *28*, 1153–1164.
[30] D. Schuller, *Thermodynamik: Methode zur Beschreibung stofflicher Systeme Lehrbuch für Naturwissenschaftler*, Springer-Verlag, Braunschweig, **1973**.
[31] a) H.-J. Wernicke, L. Plass, F. Schmidt, in *Methanol: The Basic Chemical and Energy Feedstock of the Future*, Springer, Heidelberg, **2014**, 51–301; b) P. J. Linstrom, W. G. Mallard, NIST Chemistry WebBook, NIST Standard Reference Database Number 69, National Institute of Standards and Technology, Gaithersburg MD, http://webbook.nist.gov, (retrieved April 2, 2015).
[32] T. Sakakura, J.-C. Choi, H. Yasuda, *Chem. Rev.* **2007**, *107*, 2365–2387.
[33] P. Markewitz, W. Kuckshinrichs, W. Leitner, J. Linssen, P. Zapp, R. Bongartz, A. Schreiber, T. E. Müller, *Energy Environ. Sci.* **2012**, *5*, 7281–7305.
[34] S. N. Riduan, Y. Zhang, *Dalton Trans.* **2010**, *39*, 3347–3357.
[35] a) R. Srivastava, D. Srinivas, P. Ratnasamy, *Tetrahedron Lett.* **2006**, *47*, 4213–4217; b) R. Srivastava, D. Srinivas, P. Ratnasamy, *J. Catal.* **2005**, *233*, 1–15; c) C.-C. Tai, M. J. Huck, E. P. McKoon, T. Woo, P. G. Jessop, *J. Org. Chem.* **2002**, *67*, 9070–9072.
[36] W. D. McGhee, D. P. Riley, *Organometallics* **1992**, *11*, 900–907.
[37] a) A. W. Miller, S. T. Nguyen, *Org. Lett.* **2004**, *6*, 2301–2304; b) A. Sudo, Y. Morioka, F. Sanda, T. Endo, *Tetrahedron Lett.* **2004**, *45*, 1363–1365; c) A. Sudo, Y. Morioka, E. Koizumi, F. Sanda, T. Endo, *Tetrahedron Lett.* **2003**, *44*, 7889–7891.
[38] a) R. H. Heyn, I. Jacobs, R. H. Carr, *Adv. Inorg. Chem.* **2014**, *66*, 83–115; b) O. Ihata, Y. Kayaki, T. Ikariya, *Chem. Commun.* **2005**, 2268–2270.
[39] S. Moret, P. J. Dyson, G. Laurenczy, *Nat. Commun.* **2014**, *5*.
[40] E. M. Wilcox, G. W. Roberts, J. J. Spivey, *Catal. Today* **2003**, *88*, 83–90.
[41] a) M. Aoki, M. Kaneko, S. Izumi, K. Ukai, N. Iwasawa, *Chem. Commun.* **2004**, 2568–2569; b) M. Takimoto, M. Mori, *J. Am. Chem. Soc.* **2001**, *123*, 2895–2896; c) H. Kolbe, *J. prakt. Chem.* **1874**, *10*, 89–112.

[42] S. Wesselbaum, V. Moha, M. Meuresch, S. Brosinski, K. M. Thenert, J. Kothe, T. v. Stein, U. Englert, M. Holscher, J. Klankermayer, W. Leitner, *Chem. Sci.* **2015**, *6*, 693–704.
[43] K.-i. Tominaga, *Catal. Today* **2006**, *115*, 70–72.
[44] L. Wu, Q. Liu, I. Fleischer, R. Jackstell, M. Beller, *Nat. Commun.* **2014**, *5*, 1–15.
[45] D. Ballivet-Tkatchenko, O. Douteau, S. Stutzmann, *Organometallics* **2000**, *19*, 4563–4567.
[46] Market Study Urea, Ceresana.com (retrieved April 2, 2015).
[47] C. J. A. Mota, R. S. Monteiro, E. B. V. Maia, A. F. Pimentel, J. L. Miranda, R. M. B. Alves, P. L. A. Coutinho, *Rev. Virtual Quim.* **2014**, *6*, 44–59.
[48] O. Kreye, H. Mutlu, M. A. R. Meier, *Green Chem.* **2013**, *15*, 1431–1455.
[49] a) M. Guo, Y. Zhang, Y. Zheng (SABIC Global Technologies B.V.), WO2015036941A1, **2015**; b) R. A. Pyles, J. M. Lorenzo, J. M. Ranalli (Bayer Materialscience LLC), WO2015048211A1, **2015**; c) X. Jiang (New District Jiahe Plastic Co. Ltd.), CN104497529A, **2015**; d) F. Bressan, M. De Nardi (K-Holding S.p.A.), WO2014184692A1, **2014**; e) D. J. Darensbourg, *Chem. Rev.* **2007**, *107*, 2388–2410.
[50] K. Xu, *Chem. Rev.* **2004**, *104*, 4303–4418.
[51] B. Schäffner, J. Holz, S. P. Verevkin, A. Börner, *ChemSusChem* **2008**, *1*, 249–253.
[52] a) K. Massonne, M. Siemer, W. Mormann, P. Frank, BASF SE, Universität Siegen, EP2532646, **2012**; b) J. H. Clements, *Ind. Eng. Chem. Res.* **2003**, *42*, 663–674.
[53] a) F. Shinsuke, *Non-Phosgene Polycarbonate from CO_2 - Industrialization of Green Chemical Process*, Nova Science Pub Inc, New York, **2011**; b) B. Schäffner, F. Schäffner, S. P. Verevkin, A. Börner, *Chem. Rev.* **2010**, *110*, 4554–4581; c) S. Fukuoka, M. Kawamura, K. Komiya, M. Tojo, H. Hachiya, K. Hasegawa, M. Aminaka, H. Okamoto, I. Fukawa, S. Konno, *Green Chem.* **2003**, *5*, 497–507.
[54] C. Bismuth, S. W. Borron, F. J. Baud, P. Barriot, *Toxicol. Lett.* **2004**, *149*, 11–18.
[55] K. M. K. Yu, I. Curcic, J. Gabriel, H. Morganstewart, S. C. Tsang, *J. Phys. Chem. A* **2009**, *114*, 3863–3872.
[56] W. Cheng, Q. Su, J. Wang, J. Sun, F. Ng, *Catalysts* **2013**, *3*, 878–901.
[57] a) S. Foltran, R. Mereau, T. Tassaing, *Catal. Sci. Technol.* **2014**, *4*, 1585–1597; b) J.-Q. Wang, K. Dong, W.-G. Cheng, J. Sun, S.-J. Zhang, *Catal. Sci. Technol.* **2012**, *2*, 1480–1484.
[58] M. North, R. Pasquale, *Angew. Chem.* **2009**, *121*, 2990–2992; *Angew. Chem. Int. Ed.* **2009**, *48*, 2946–2948.
[59] a) P. Yan, X. Tan, H. Jing, S. Duan, X. Wang, Z. Liu, *J. Org. Chem.* **2011**, *76*, 2459–2464; b) R. L. Paddock, S. T. Nguyen, *J. Am. Chem. Soc.* **2001**, *123*, 11498–11499.
[60] J. W. Comerford, I. D. V. Ingram, M. North, X. Wu, *Green Chem.* **2015**, *17*, 1966–1987.
[61] V. Caló, A. Nacci, A. Monopoli, A. Fanizzi, *Org. Lett.* **2002**, *4*, 2561–2563.
[62] a) C. J. Whiteoak, N. Kielland, V. Laserna, F. Castro-Gómez, E. Martin, E. C. Escudero-Adán, C. Bo, A. W. Kleij, *Chem. Eur. J.* **2014**, *20*, 2264–2275; b) C. Beattie, M. North, P. Villuendas, C. Young, *J. Org. Chem* **2013**, *78*, 419–426; c) M. R. Kember, A. Buchard, C. K. Williams, *Chem. Commun.* **2011**, *47*, 141–163.
[63] a) W. Cheng, Z. Fu, J. Wang, J. Sun, S. Zhang, *Synth. Commun.* **2012**, *42*, 2564–2573; b) M. North, C. Young, *ChemSusChem* **2011**, *4*, 1685–1693.
[64] a) S. Enthaler, X.-F. Wu, *Zinc Catalysis: Applications in Organic Synthesis*, John Wiley & Sons, Weinheim, **2015**; b) Y. Yang, Y. Hayashi, Y. Fujii, T. Nagano, Y. Kita, T. Ohshima, J. Okuda, K. Mashima, *Catal. Sci. Technol.* **2012**, *2*, 509–513; c) S.-S. Wu, X.-W. Zhang, W.-L. Dai, S.-F. Yin, W.-S. Li, Y.-Q. Ren, C.-T. Au, *Appl. Catal. A* **2008**, *341*, 106–111.
[65] T. Ema, Y. Miyazaki, S. Koyama, Y. Yano, T. Sakai, *Chem. Commun.* **2012**, *48*, 4489–4491.
[66] T. M. Letcher, J. L. Scott, *Materials for a Sustainable Future*, Royal Society of Chemistry, Cambridge, **2012**.
[67] N. Takeda, S. Inoue, *Bull. Chem. Soc. Jpn.* **1978**, *51*, 3564–3567.
[68] C. J. Whiteoak, E. Martin, M. M. Belmonte, J. Benet-Buchholz, A. W. Kleij, *Adv. Synth. Catal.* **2012**, *354*, 469–476.
[69] a) M. North, P. Villuendas, C. Young, *Tetrahedron Lett.* **2012**, *53*, 2736–2740; b) J. Melendez, M. North, P. Villuendas, C. Young, *Dalton Trans.* **2011**, *40*, 3885–3902.

[70] M. J. Go, K. M. Lee, C. H. Oh, Y. Y. Kang, S. H. Kim, H. R. Park, Y. Kim, J. Lee, *Organometallics* **2013**, *32*, 4452–4455.
[71] K. Kossev, N. Koseva, K. Troev, *J. Mol. Catal. A: Chem.* **2003**, *194*, 29–37.
[72] a) S. Liang, H. Liu, T. Jiang, J. Song, G. Yang, B. Han, *Chem. Commun.* **2011**, *47*, 2131–2133; b) G.-Q. Yuan, Y.-J. Shan, H.-F. Jiang, C.-R. Qi, *Chin. J. Chem.* **2008**, *26*, 947–951; c) J. Song, Z. Zhang, B. Han, S. Hu, W. Li, Y. Xie, *Green Chem.* **2008**, *10*, 1337–1341.
[73] a) T. Werner, N. Tenhumberg, H. Buettner, *ChemCatChem* **2014**, *6*, 3493–3500; b) T. Werner, N. Tenhumberg, *J. CO_2 Util.* **2014**, *7*, 39–45.
[74] a) J. Tharun, Y. Hwang, R. Roshan, S. Ahn, A. C. Kathalikkattil, D.-W. Park, *Catal. Sci. Technol.* **2012**, *2*, 1674–1680; b) J. Ma, J. Song, H. Liu, J. Liu, Z. Zhang, T. Jiang, H. Fan, B. Han, *Green Chem.* **2012**, *14*, 1743–1748; c) Y. Zhou, S. Hu, X. Ma, S. Liang, T. Jiang, B. Han, *J. Mol. Catal. A Chem.* **2008**, *284*, 52–57; d) T. Takahashi, T. Watahiki, S. Kitazume, H. Yasuda, T. Sakakura, *Chem. Commun.* **2006**, 1664–1666.
[75] J. Ma, J. Liu, Z. Zhang, B. Han, *Green Chem.* **2012**, *14*, 2410–2420.
[76] a) M. North, *New and Future Developments in Catalysis: Activation of CO_2*, Elsevier, London, **2013**; b) X.-B. Lu, D. J. Darensbourg, *Chem. Soc. Rev.* **2012**, *41*, 1462–1484.
[77] J. F. Cooper, M. Lichtenwalter (Jefferson Chem Co Inc), US2773070 A, **1956**.
[78] H. Buettner, K. Lau, A. Spannenberg, T. Werner, *ChemCatChem* **2015**, *7*, 459–467.
[79] T. Werner, H. Buettner, *ChemSusChem* **2014**, *7*, 3268–3271.
[80] J. Sun, S. Zhang, W. Cheng, J. Ren, *Tetrahedron Lett.* **2008**, *49*, 3588–3591.
[81] a) Y.-M. Shen, W.-L. Duan, M. Shi, *Adv. Synth. Catal.* **2003**, *345*, 337–340; b) J.-W. Huang, M. Shi, *J. Org. Chem.* **2003**, *68*, 6705–6709.
[82] N. Kihara, T. Endo, *J. Polym. Sci., Part A: Polym. Chem.* **1993**, *31*, 2765–2773.
[83] Y. Xie, T.-T. Wang, R.-X. Yang, N.-Y. Huang, K. Zou, W.-Q. Deng, *ChemSusChem* **2014**, *7*, 2110–2114.
[84] C. J. Whiteoak, N. Kielland, V. Laserna, E. C. Escudero-Adán, E. Martin, A. W. Kleij, *J. Am. Chem. Soc.* **2013**, *135*, 1228–1231.
[85] A. Steblyanko, W. Choi, F. Sanda, T. Endo, *J. Polym. Sci., Part A: Polym. Chem.* **2000**, *38*, 2375–2380.
[86] N. Aoyagi, Y. Furusho, T. Endo, *J. Polym. Sci., Part A: Polym. Chem.* **2013**, *51*, 1230–1242.
[87] A. Suzuki, D. Nagai, B. Ochiai, T. Endo, *J. Polym. Sci., Part A: Polym. Chem.* **2004**, *42*, 5983–5989.
[88] B. Tamami, S. Sohn, G. L. Wilkes, *J. Appl. Polym. Sci.* **2004**, *92*, 883–891.
[89] a) M. Bahr, R. Mulhaupt, *Green Chem.* **2012**, *14*, 483–489; b) M. Bahr, A. Bitto, R. Mulhaupt, *Green Chem.* **2012**, *14*, 1447–1454.
[90] R. Wei, X. Zhang, B. Du, Z. Fan, G. Qi, *R. Soc. Chem. Adv.* **2013**, *3*, 17307–17313.
[91] X. Sheng, G. Ren, Y. Qin, X. Chen, X. Wang, F. Wang, *Green Chem.* **2015**, *17*, 373–379.
[92] L. Poussard, J. Mariage, B. Grignard, C. Detrembleur, C. Jérôme, C. Calberg, B. Heinrichs, J. De Winter, P. Gerbaux, J. M. Raquez, L. Bonnaud, P. Dubois, *Macromolecules* **2016**, *49*, 2162–2171.
[93] O. Bayer, *Angew. Chem.* **1947**, *59*, 257–272.
[94] H. Sardon, A. C. Engler, J. M. W. Chan, J. M. García, D. J. Coady, A. Pascual, D. Mecerreyes, G. O. Jones, J. E. Rice, H. W. Horn, J. L. Hedrick, *J. Am. Chem. Soc.* **2013**, *135*, 16235–16241.
[95] H.-W. Engels, H.-G. Pirkl, R. Albers, R. W. Albach, J. Krause, A. Hoffmann, H. Casselmann, J. Dormish, *Angew. Chem.* **2013**, *125*, 9596–9616; *Angew. Chem. Int. Ed.* **2013**, *52*, 9422–9441.
[96] a) H. Sardon, A. Pascual, D. Mecerreyes, D. Taton, H. Cramail, J. L. Hedrick, *Macromolecules* **2015**, *48*, 3153–3165; b) D. K. Chattopadhyay, D. C. Webster, *Prog. Polym. Sci.* **2009**, *34*, 1068–1133.
[97] a) P. Deepa, M. Jayakannan, *J. Polym. Sci., Part A: Polym. Chem.* **2008**, *46*, 2445–2458; b) D. C. Allport, D.S. Gilbert, S. M. Outterside, *MDI and TDI: Safety, Health and the Environment: A Source Book and practical Guide*, John Wiley & Sons Ltd, Chichester, **2003**.
[98] G. J. Verheugen, *J. Eur. Union* **2009**, L164/167.

[99] E. Delebecq, J.-P. Pascault, B. Boutevin, F. Ganachaud, *Chem. Rev.* **2013**, *113*, 80–118.
[100] B. Nohra, L. Candy, J.-F. Blanco, C. Guerin, Y. Raoul, Z. Mouloungui, *Macromolecules* **2013**, *46*, 3771–3792.
[101] a) W. C. Pan, C.-H. Lin, S. A. Dai, *J. Polym. Sci., Part A: Polym. Chem.* **2014**, *52*, 2781–2790; b) H. Sardon, A. C. Engler, J. M. W. Chan, D. J. Coady, J. M. O'Brien, D. Mecerreyes, Y. Y. Yang, J. L. Hedrick, *Green Chem.* **2013**, *15*, 1121–1126; c) D. Tang, D.-J. Mulder, B. A. J. Noordover, C. E. Koning, *Macromol. Rapid Commun.* **2011**, *32*, 1379–1385.
[102] M. Unverferth, O. Kreye, A. Prohammer, M. A. R. Meier, *Macromol. Rapid Commun.* **2013**, *34*, 1569–1574.
[103] a) J. Kušan, H. Keul, H. Höcker, *Macromolecules* **2001**, *34*, 389–395; b) S. Neffgen, H. Keul, H. Höcker, *Macromol. Rapid Commun.* **1996**, *17*, 373–382.
[104] M. Helou, J.-F. Carpentier, S. M. Guillaume, *Green Chem.* **2011**, *13*, 266–271.
[105] H. Tomita, F. Sanda, T. Endo, *Macromolecules* **2001**, *34*, 7601–7607.
[106] O. L. Figovsky, L. D. Shapovalov, *Macromol. Symp.* **2002**, *187*, 325–332.
[107] H. Tomita, F. Sanda, T. Endo, *J. Polym. Sci., Part A: Polym. Chem.* **2001**, *39*, 851–859.
[108] O. Lamarzelle, P.-L. Durand, A.-L. Wirotius, G. Chollet, E. Grau, H. Cramail, *Polym. Chem.* **2016**, *7*, 1439–1451.
[109] K. Fryauf, V. Strehmel, M. Fedtke, *Polym. Bull. (Berlin)* **1993**, *31*, 183–190.
[110] B. Ochiai, S. Inoue, T. Endo, *J. Polym. Sci., Part A: Polym. Chem.* **2005**, *43*, 6282–6286.
[111] L. Annunziata, A. K. Diallo, S. Fouquay, G. Michaud, F. Simon, J.-M. Brusson, J.-F. Carpentier, S. M. Guillaume, *Green Chem.* **2014**, *16*, 1947–1956.
[112] R. H. Lambeth, T. J. Henderson, *Polymer* **2013**, *54*, 5568–5573.
[113] F.N. Olang (Owens Corning Intellectual Capital), US20120059076 A1, **2012**.
[114] D. C. Webster, A. L. Crain, *Prog. Org. Coat.* **2000**, *40*, 275–282.
[115] O. Figovsky, L. Shapovalov, F. Buslov, *Surf. Coat. Int., Part B: Coat. Trans.* **2005**, *88*, 67–71.
[116] W. Jilani, N. Mzabi, N. Fourati, C. Zerrouki, O. Gallot-Lavallée, R. Zerrouki, H. Guermazi, *Polymer* **2015**, *79*, 73–81.
[117] O. Figovsky, L. Shapovalov, A. Leykin, O. Birukova, R. Potashnikova, *PU Magazine Int.* **2013**, *10*, 256–263.
[118] H. Schnell, L. Bottenbruch, *Naturwissenschaften* **1967**, *54*, 306–313.
[119] D. Walton, P. Lorimer, *Polymers*, Oxford University Press, Oxford, **2000**.
[120] D. C. Clagett, S. J. Shafer, *Comprehensive Polymer Science and Supplements*, Pergamon, Amsterdam, **1989**.
[121] a) H. Sugimoto, H. Ohtsuka, S. Inoue, *J. Polym. Sci., Part A: Polym. Chem.* **2005**, *43*, 4172–4186; b) K. Nozaki, K. Nakano, T. Hiyama, *J. Am. Chem. Soc.* **1999**, *121*, 11008–11009.
[122] a) J. Langanke, A. Wolf, *Org. Process Res. Dev.* **2014**, *19*, 735–739; b) D. Darensbourg, S. J. Wilson, *Green Chem.* **2012**, *14*, 2665–2671.
[123] J. Langanke, A. Wolf, J. Hofmann, K. Bohm, M. A. Subhani, T. E. Müller, W. Leitner, C. Gürtler, *Green Chem.* **2014**, *16*, 1865–1870.
[124] M. Peters, C. Guertler, A. Wolf, *Chem. Eng.* **2011**, *837*, 38–39.
[125] a) J. Hofmann, C. Guertler, H. Nefzger, N. Hahn, K. Lorenz, T. E. Mueller (Bayer MaterialScience AG), WO2012080192A1, **2012**; b) T. E. Mueller, C. Guertler, A. Kermagoret, Y. Dienes, I. Busygin, B. Koehler, W. Leitner (Bayer MaterialScience AG), WO2012059550A1, **2012**.
[126] a) Bayer AG, Annual Report 2014, **2014**, 78; b) Bayer AG, Annual Report 2012, **2012**, 15.
[127] S. P. Meching, *Carbon dioxide – a new raw material*, Covestro, http://www.covestro.de/en/Projects-and-Cooperations/CO_2-Project, (retrieved February 01, 2016).
[128] D. Kahlich, U. Wiechern, J. Lindner, in *Ullmann's Encyclopedia of Industrial Chemistry*, Wiley-VCH Verlag GmbH & Co. KGaA, Weinheim, **2000**.
[129] a) N. Ullrich, B. Kolbe, N. Bredemeyer, *ThyssenKrupp techforum* **2007**, 38–43; b) H. P. Wulff, F. Wattimena, US 4021454, **1976**.
[130] N. von der Assen, A. Bardow, *Green Chem.* **2014**, *16*, 3272–3280.

[131] a) F. Hugo, H. Sperber (Badische Anilin- & Soda-Fabrik AG), US3637751A, **1972**; b) C. E. Schweitzer, R. N. Macdonald, J. O. Punderson, *J. Appl. Polym. Sci.* **1959**, *1*, 158–163.
[132] J. F. Walker, A. F. Chadwick, *Ind. Eng. Chem.* **1947**, *39*, 974–977.
[133] M. Schlosser, T. Jenny, Y. Guggisberg, *Synlett* **1990**, 704.
[134] *Technologies for Sustainability and Climate Protection - Chemical Processes and Use of CO_2*, Federal Ministry of Education and Research (BMBF), Bonn, **2014**.
[135] P. P. Pescarmona, M. Taherimehr, *Catal. Sci. Technol.* **2012**, *2*, 2169–2187.
[136] a) G. A. Olah, A. Goeppert, G. K. S. Prakash, in *Beyond Oil and Gas: The Methanol Economy*, Wiley-VCH Verlag GmbH & Co. KGaA, Weinheim, **2009**, 179–184; b) V. Phillips, P. Takahashi, *Environ. Sci. Technol.* **1990**, *24*, 1136–1137.
[137] T. E. Mueller, C. Guertler, W. Leitner, H. Vogt, G. Barath (Bayer MaterialScience AG), WO2014095679A1, **2014**.
[138] J. Langanke, J. Hofmann, C. Guertler, A. Wolf, *J. Polym. Sci., Part A: Polym. Chem.* **2015**, 2071–2074.
[139] a) J. Hofmann, H.-G. Pirkl, K. Laemmerhold, H. Nefzger, M. Wohak, S. Braun, C. Guertler, A. Wolf, J. Langanke (Bayer MaterialScience AG), WO2015059068A1, **2015**; b) T. E. Mueller, C. Guertler, M. A. Subhani, B. Koehler (Bayer MaterialScience AG), WO2015039981A1, **2015**; c) T. E. Mueller, C. Guertler, W. Leitner, H. Vogt, G. Barath, M. Krautschick (Bayer MaterialScience AG), WO2014198689A1, **2014**; d) C. Guertler, T. E. Mueller, A. Kermagoret, Y. Dienes, J. Barruet, A. Wolf, S. Grasser (Bayer Intellectual Property GmbH), EP2604641A1, **2013**; e) J. Hofmann, C. Guertler, S. Grasser, A. Wolf (Bayer MaterialScience AG), EP2548908A1, **2013**; f) T. E. Mueller, C. Guertler, A. Subhani (Bayer Intellectual Property GmbH), EP2604642A1, **2013**.
[140] R. K. Sharma, E. S. Olson, *Abstr. Pap. Am. Chem. Soc.* **2000**, *45*, 676–680.
[141] W.-Y. Chiang, *Tatung Institue of Technology* **1978**, *9*, 255–265.
[142] T. E. Mueller, C. Guertler, H. Vogt, M. Krautschick, W. Leitner (Bayer MaterialScience AG), WO2014095861A2, **2014**.
[143] a) H. Liu, R. Zeng, R. Hua, *Int. J. Mol. Sci.* **2014**, *15*, 9945–9951; b) G. Brahmachari, *Green Synthetic Approaches for Biologically Relevant Heterocycles*, Elsevier, Amsterdam, **2014**; c) Z.-Z. Yang, L.-N. He, C.-X. Miao, S. Chanfreau, *Adv. Synth. Catal.* **2010**, *352*, 2233–2240.
[144] E. Broughton, *Environmental Health: A Global Access Science Source* **2005**, *4*, 6.
[145] B. Ochiai, J.-i. Nakayama, M. Mashiko, Y. Kaneko, T. Nagasawa, T. Endo, *J. Polym. Sci., Part A: Polym. Chem.* **2005**, *43*, 5899–5905.
[146] a) V. M. Lombardo, E. A. Dhulst, E. K. Leitsch, N. Wilmot, W. H. Heath, A. P. Gies, M. D. Miller, J. M. Torkelson, K. A. Scheidt, *Eur. J. Org. Chem.* **2015**, 2791–2795; b) N. Kihara, T. Endo, *Makromol. Chem.* **1992**, *193*, 1481–1492.
[147] H. Tomita, F. Sanda, T. Endo, *J. Polym. Sci., Part A: Polym. Chem.* **2001**, *39*, 860–867.
[148] D. Schapel, U. Gizycki (Bayer AG), US4129697 A, **1978**.
[149] Dr. M. Wagner, *Thermal Analysis in Practice*, Mettler Toledo, **2009**.
[150] H. Tomita, F. Sanda, T. Endo, *J. Polym. Sci., Part A: Polym. Chem.* **2001**, *39*, 4091–4100.
[151] B. Ochiai, T. Endo, *Prog. Polym. Sci.* **2005**, *30*, 183–215.
[152] M. Kathalewar, A. Sabnis, D. D'Mello, *Eur. Polym. J.* **2014**, *57*, 99–108.
[153] C. Gürtler et al., *Abschlussbericht: Dream Polymers – Nachhaltige Wege zu neuen Polymeren*, **2014**.
[154] M. Morton, *Anionic Polymerization: Principles and Practice*, Academic Press Inc., New York, **1983**.
[155] H. Günzler, H.-U. Gremlich, *IR Spectroscopy*, Wiley-VCH, Weinheim, **2002**.
[156] a) C. Villiers, J.-P. Dognon, R. Pollet, P. Thuéry, M. Ephritikhine, *Angew. Chem.* **2010**, *122*, 3543–3546; *Angew. Chem. Int. Ed.* **2010**, *49*, 3465–3468; b) J. Ma, X. Zhang, N. Zhao, A. S. N. Al-Arifi, T. Aouak, Z. A. Al-Othman, F. Xiao, W. Wei, Y. Sun, *J. Mol. Catal. A: Chem.* **2010**, *315*, 76–81.

[157] a) R. Lo, B. Ganguly, *New J. Chem.* **2012**, *36*, 2549–2554; b) Z.-Z. Yang, L.-N. He, Y.-N. Zhao, B. Li, B. Yu, *Energy Environ. Sci.* **2011**, *4*, 3971–3975; c) K. Nakamura, T. Kamikawa (Sumitomo Chemical Co), DE10244973A1, **2003**.

[158] a) C. Das Neves Gomes, O. Jacquet, C. Villiers, P. Thuéry, M. Ephritikhine, T. Cantat, *Angew. Chem.* **2012**, *124*, 191–194; *Angew. Chem. Int. Ed.* **2012**, *51*, 187–190; b) V. K. Aggarwal, I. Emme, S. Y. Fulford, *J. Org. Chem.* **2003**, *68*, 692–700.

[159] a) D. Kopetzki, M. Antonietti, *New J. Chem.* **2011**, *35*, 1787–1794; b) T. Matsumoto, H. Yamamoto, S. Inoue, *J. Am. Chem. Soc.* **1984**, *106*, 4829–4832.

[160] C. Gibard, H. Ibrahim, A. Gautier, F. Cisnetti, *Organometallics* **2013**, *32*, 4279–4283.

[161] a) B. R. Van Ausdall, J. L. Glass, K. M. Wiggins, A. M. Aarif, J. Louie, *J. Org. Chem.* **2009**, *74*, 7935–7942; b) H. Zhou, W.-Z. Zhang, C.-H. Liu, J.-P. Qu, X.-B. Lu, *J. Org. Chem.* **2008**, *73*, 8039–8044; c) H. A. Duong, T. N. Tekavec, A. M. Arif, J. Louie, *Chem. Commun.* **2004**, 112–113.

[162] N. Kuhl, F. Glorius, *Chem. Commun.* **2011**, *47*, 573–575.

[163] N. E. Jacobsen, *NMR Spectroscopy Explained*, Wiley-VCH, New Jersey, **2007**.

[164] a) G. Reuss, W. Disteldorf, A. O. Gamer, A. Hilt, in *Ullmann's Encyclopedia of Industrial Chemistry*, Wiley-VCH Verlag GmbH & Co. KGaA, **2000**; b) E. S. Ebers, H. H. Nielsen, *J. Chem. Phys.* **1937**, *5*, 822–827.

[165] H. G. O. Becker, W. Berger, G. Domschke, *Organikum*, J. A. Barth, Leipzig, **1996**.

[166] W. L. F. Armarego, C. L. L. Chai, *Purification of Laboratory Chemicals*, Elsevier, Amsterdam, **2003**.

[167] Z.-Z. Yang, Y.-N. Zhao, L.-N. He, J. Gao, Z.-S. Yin, *Green Chem.* **2012**, *14*, 519–527.

[168] C. Martin, C. J. Whiteoak, E. Martin, M. Martinez Belmonte, E. C. Escudero-Adan, A. W. Kleij, *Catal. Sci. Technol.* **2014**, *4*, 1615–1621.

[169] J. Tharun, G. Mathai, A. C. Kathalikkattil, R. Roshan, J.-Y. Kwak, D.-W. Park, *Green Chem.* **2013**, *15*, 1673–1677.

[170] Y. H. Cho, B. K. Kim, *J. Appl. Polym. Sci.* **2001**, *81*, 2744–2753.

9 ACKNOWLEDGEMENT

I want to thank Dr. Thomas Werner for the possibility to work in his junior research group and for the interesting topic of this thesis. Many thanks also to Prof. Dr. Matthias Beller for the possibility to work for my PhD at the Leibniz Institute for Catalysis.

Without the work of the analytical department of the LIKAT this thesis would not have been possible. Therefore, a special thanks goes to Dr. Wolfgang Baumann, Dr. Christine Fischer, Dr. Dirk Michalik, Ms. Christine Rautenberg and Ms. Astrid Lehmann.

Furthermore, I want to express my appreciation for my colleagues Hendrik Büttner, Dr. Willi Desens, Dr. Sunetra Patil Deshmukh, Johannes Diebler, Juliane Epping, Christoph Grimmer, Dr. Marcel Hoffmann, Stefan Joop, Dr. Juliane Koch, Jana Modenbach, Anna Perechodjuk, Annika Pommeres, Luis Schirmer, Dr. Heiko Schramm, Johannes Steinbauer Dr. Nils Tenhumberg and Christoph Wulf for the good atmosphere and discussions.

For the thoroughly correction of this work I want to thank Johannes Steinbauer, Marie-Luis Schirmer, Dr. Willi Desens, and Hendrik Büttner.

Special thanks for the lively discussions about chemistry and other topics over lunch with Michael Sebek, Dr. Patrick Loos, Dr. Hannes Alex, Antonio Ricci, Dr. Baramov Todor, Dr. Stefan Ahlers, Dr. Philip Jungk, Dr. Jaqueline Priebe, Dr. Nico Weding, Dr. Claudia Berger-Karin, Dr. Sandra Hübner, Dr. Jens Baumgard, Prof. Dr. Marko Hapke, Dr. Willi Desens, Dr. Indre Thiel and Dr. Nils Tenhumberg.

I also want to thank Antonio Ricci, Dr. Patrick Loos, Johannes Steinbauer and Michael Sebek for many great evenings battling over various board games and thereby maintaining my work life balance. It was real fun with you guys. My time in Rostock was made enjoyable in large part due to the many friends and groups that became a part of my life and helped me in many ways to strive towards my goal. I am grateful for time spent with roommates and friends, for the time with the volleyball team SV Fortuna e. V. and for many other people and memories.

A special thank you goes therefore to Simon Cremer who never got tired to discuss with me all kind of topics and helped me to find answers beside chemistry.

I would like to thank my family for all their love and encouragement. For my parents who raised me with love and supported me in all my pursuits. Lastly, I would like to express appreciation for my beloved girlfriend Sandra Meese who always supported me. I feel that we both got even closer during that time.

Thank you!